
Analysis and Evaluation of the Dexterity, Grasping, and Manipulation Capabilities of Human and Robot Hands

Nathan Elangovan



A thesis submitted in fulfilment of the requirements for the degree of
Doctor of Philosophy in Mechanical Engineering,
The University of Auckland, 2022.

Abstract

Over the last decades, a lot of research studies have dealt with the notion of dexterity, focusing either on the human arm-hand system or on various technical devices such as robot manipulators, robot hands, grippers, etc. The term “dexterity” was approached in many different ways and various definitions have been provided. Nowadays there is still a lack of a clear pathway to improve the dexterity of a specific gripper or hand. This thesis focuses on the analysis and evaluation of the dexterity of human and robot hands, focusing on the grasping and dexterous manipulation capabilities. To accomplish that, it first investigates the boundaries of the term dexterity by analyzing, evaluating, and classifying the proposed classes and metrics. Based on this analysis and evaluation, a new modular, affordable, accessible open-source dexterity test is proposed that enables replicable research using standardized objects, benchmarking protocols, and scoring methodology for evaluating the dexterity of humans and robots alike. Following this, we analyze, quantify, and model the different aspects of human dexterity through extensive experimentation. The current capabilities of various grippers are benchmarked against human performances to identify the limitations of the designs. We further derive insights for the selection of successful task execution strategies employed by humans with the purpose of translating them into skills for robotic end-effectors. Furthermore, new dexterity classes and metrics have been proposed based on this benchmarking and analysis of the unique strategies utilized by human hands in the successful execution of complex tasks. The proposed metrics are used in the formulation of a design optimization framework that facilitates the design, modelling, and development of a new generation of dexterous artificial hands. The efficiency of the optimization framework is demonstrated by creating a multimodal robotic gripper with reconfigurable finger bases and lockable joints that exhibits improved manipulation capabilities without sacrificing grasping performance. We also proposed a complete methodology for exploiting the post contact reconfiguration of adaptive robot grippers and hands (that is due to the structural compliance and underactuation of the designs) to improve their dexterous manipulation capabilities by predicting the forces exerted based on their reconfiguration profile. The insights from the research

work conducted in this PhD thesis can be employed for the development of new, highly efficient adaptive robotic grippers and hands that perform on par with humans.

Dedicated to my ma, my parents, and my wife
for always being there for me.

Acknowledgements

I would like to express my deepest gratitude to my supervisor, Dr. Minas Liarokapis, who has guided and encouraged me through out my PhD. His constant support during the entire duration of my PhD was invaluable and helped me overcome the hardships I faced on personal and academic front. This thesis would not have taken shape if it hadn't been for his consistent motivation, enthusiasm, and productive feedback.

I would like to thank the departmental staff and technicians for their support and technical assistance.

I wish to express my gratitude to all the students of the New Dexterity research group (Che-Ming Chang, Geng Gao, Mojtaba Shahmohammadi, Joao Buzzatto, Jayden Chapman, Gal Gorjup, Anany Dwivedi, Lucas Gerez, Alex Hayashi, and Bonnie Guan) for their love, support, and friendship. I cherish all the conversations and fun we had working at the labs, lunch, and trips.

I am grateful to my friends and family for accompanying me on this adventure. I thank Manju Nandhi for the valuable conversations, being a constant source of support, and the unconditional love. I thank Sherine for listening patiently, being understanding, and helping me get through the bad days. I am grateful to my pals Bhavna, Sivakumar, Narrendar, Akhil, and Mei, for all the wonderful memories and adventure. I am extremely grateful to my parents for believing in me and supporting me in all my endeavours. Words cannot express how grateful I am to my wife Shalini for her constant support and the sacrifices she has made for me to achieve my dream.

Contents

ABSTRACT	i
DEDICATION	iii
ACKNOWLEDGEMENTS	v
CONTENTS	vii
LIST OF FIGURES	xiii
LIST OF TABLES	xxi
ABBREVIATIONS	xxiii
I Introduction	1
1 BACKGROUND AND MOTIVATION	3
1.1 Background	3
1.2 Motivation	4
2 THESIS OBJECTIVE AND THESIS STRUCTURE	7
2.1 Objectives	7
2.2 Ethics Approval	8
2.3 Thesis Layout	8
3 APPARATUS	11
3.1 Motion Capture System	11
3.1.1 <i>Fiducial Markers</i>	11
3.2 Force Measurement Devices	12
3.3 Robotic Grippers and Hands	13

3.3.1	<i>Parallel Jaw Gripper</i>	13
3.3.2	<i>NDX-A</i>	14
3.3.3	<i>Multi-Modal Gripper with a Rotary Module</i>	15
3.4	Robot Interfaces	15
3.4.1	<i>Palm Mounted Interface</i>	16
3.4.2	<i>Forearm Mounted Interface</i>	16
II	Related Work on Defining and Evaluating Dexterity	19
4	DEFINITIONS AND TAXONOMIES OF DEXTERITY	21
4.1	Introduction	21
4.2	Human Dexterity	22
4.3	Human Hand Anatomy	22
4.3.1	<i>Anatomical Features of Human Hand</i>	22
4.3.2	<i>Degrees of Freedom (DOF)</i>	24
4.3.3	<i>Range of Motion</i>	25
4.4	Robot Dexterity	25
4.5	Grasping and Manipulation	26
4.5.1	<i>Grasping</i>	27
4.5.2	<i>Manipulation</i>	28
4.6	Conclusion	30
5	METRICS AND MEASURES FOR EVALUATION OF DEXTERITY	33
5.1	Introduction	33
5.2	Benchmarking	35
5.2.1	<i>Benchmarking Standardized Objects</i>	35
5.2.2	<i>Benchmarking Learning and Control Algorithms</i>	37
5.2.3	<i>Robotic Competitions</i>	38
5.2.4	<i>Human Dexterity Tests for Robotic Evaluation</i>	40
5.3	Metrics and Measures	42
5.3.1	<i>Metrics based on Jacobian and Manipulability</i>	42
5.3.2	<i>Metric Based on Workspace</i>	47
5.3.3	<i>Other Performance Metrics</i>	50
5.4	Comparison and Discussion of Benchmarks and Metrics	52
5.5	Conclusion	55

III Analysis, Evaluation, and Comparison of Human and Robot Dexterity	57
6 AN ACCESSIBLE, OPEN-SOURCE DEXTERITY TEST	59
6.1 Introduction	59
6.2 Related Work	62
6.3 Design of Dexterity Board	66
6.3.1 Dexterity Rig Development	66
6.3.2 Objects	68
6.3.3 Manipulation Tasks	68
6.4 Dexterity Metrics	71
6.4.1 Successful Completion Score	71
6.4.2 Time Required Score	73
6.4.3 Total Dexterity Score	74
6.4.4 Dexterity Ranks and Grades	74
6.5 Validation of Protocols and Baseline Score of Human Trials	75
6.5.1 Results and Discussion	78
6.6 Conclusion	81
7 COMPARING HUMAN AND ROBOT PERFORMANCE IN THE EXECUTION OF KITCHEN TASKS	85
7.1 Introduction	85
7.2 Related Work	87
7.3 Data Collection Setup	88
7.3.1 Human Data Collection Setup	89
7.3.2 Robotic Grippers Data Collection Setup	90
7.4 Dataset Analysis and Taxonomy Identification	91
7.4.1 Analysis Based on Existing Taxonomies	91
7.4.2 Considerations for Robot Task Execution	94
7.5 Evaluating Robotic Grippers	94
7.5.1 Kitchen Task Specific Taxonomy	97
7.5.2 Summary	99
7.5.3 Data Availability and Dedicated Website	99
7.6 Discussion from Initial Analysis	99
7.7 Further Expansion and Evaluation of Kitchen Dataset	100
7.8 Dataset Analysis using Clustering Techniques	101
7.9 Data Processing	102

7.10	Clustering Algorithms	104
7.10.1	<i>K-means Clustering Algorithm</i>	104
7.10.2	<i>DBSCAN Clustering Algorithm</i>	105
7.11	Cluster Validation, Analysis, and Results	105
7.12	Inter-subject Variability of Grasping and Manipulation Strategies	108
7.13	Conclusion and Future Directions	112
IV	Design Guidelines for Adaptive Robot Hands and Grippers	115
8	EXPLOITING POST CONTACT RECONFIGURATION OF ADAPTIVE ROBOT GRIPPERS AND HANDS	117
8.1	Introduction	117
8.2	Contact Force Estimation Methods	119
8.3	Experimental Setup	120
8.3.1	<i>IMU Based Joint Angles Data Collection</i>	123
8.3.2	<i>Vision Based Joint Angles Data Collection</i>	124
8.4	Results and Discussion	124
8.5	Conclusion and Future Directions	127
9	DESIGN OPTIMIZATION FRAMEWORK FOR MAXIMIZING DEXTEROUS MANIPULATION CAPABILITIES	129
9.1	Introduction	129
9.2	Related Work	130
9.3	Manipulation Workspace Analysis	133
9.3.1	<i>Design Variables and Manipulation Considerations</i>	133
9.3.2	<i>Problem Formulation</i>	134
9.3.3	<i>Manipulation Workspace Generation</i>	136
9.3.4	<i>Manipulation Workspace Implications</i>	136
9.4	Design	142
9.5	Results and Discussion	144
9.6	Conclusion	150
V	Conclusion and Future Directions	151
10	DISCUSSION AND CONCLUSION	153
10.1	Conclusion	153

10.2 Major Contributions	155
10.3 Future Directions	156
VI Appendices	159
A THESIS OUTCOMES	161
A.1 Awards	161
A.2 Journal Publications	161
A.3 Conference Publications	162
B ANNOTATION GUIDE FOR GRASPING AND MANIPULATION TASKS EXE- CUTED IN KITCHEN ENVIRONMENTS	165
B.1 Instructions for Annotating Each Video	165
<i>B.1.1 Object Attributes</i>	166
<i>B.1.2 Grasp Attributes</i>	168
<i>B.1.3 Manipulation attributes</i>	170
B.2 Guideline Annotation Sheet	173
B.3 Clarification on common grasps	174
REFERENCES	177

List of Figures

3.1	Examples of aruco markers being used to: a) locate the origin, b) track the hand motion, and c) determine the joint configurations of fingers.	12
3.2	Force measurement setup containing a SS25LA dynamometer plugged into CH1 electrode channel of a Biopac MP36 data acquisition unit.	13
3.3	A simple parallel jaw gripper controlled by a single actuator.	14
3.4	The new dexterity adaptive, human-like robot hand was used for analysing dexterity of anthropomorphic grippers.	14
3.5	A multimodal gripper containing a simple 2-fingered parallel jaw module and a 3-fingered rotary module.	15
3.6	A palm mounted interface equipped with a T-42 gripper. The interface allows easy control of grippers using four linear potentiometer sliders controlled by the four fingers, a bidirectional joystick, and a press button controlled by the thumb.	16
3.7	A forearm mounted interface equipped with a multimodal gripper. The interface allows easy operation of heavy robot grippers or hands such as the NDX-A and the multimodal gripper over a long duration of time.	17
5.1	This figure presents some of the commonly available object sets for benchmarking grasping and manipulation in literature. The image shows objects proposed in the: a) YCB object set [84], ACRV picking benchmark [85], Robocup@home [86], Amazon shelf picking challenge [87] and Modular, Sensorized objects [88].	36

5.2	A number of robotic competitions were organized over the years to evaluate and standardize robotic grasping and manipulation capabilities. This figure presents the experimental set-up for: a) DARPA robotic challenge [101], b) ASTM grasping dexterity test [102], c) Manufacturing track of grasping and manipulation competition IEEE IROS 2019 [43], d) Robocup @ home [86], e) Amazon picking challenge [87], and f) World robot challenge (WRC) partner robot challenge track [103].	39
5.3	The figure presents the various dexterity tests used for manual dexterity evaluation in humans presented in [113, 114]. More precisely, the tests are: a) Functional dexterity test, b) Purdue pegboard test, c) Tweezers dexterity test d) Grooved pegboard test, e) Minnesota manual dexterity test, f) Roeder manipulative aptitude test, and g) Hand-tool dexterity test.	41
5.4	Subfigure a) presents the manipulability ellipsoid that defines the directional position and orientation variability of the end effector for a given configuration of the gripper. Subfigure b) presents the force manipulability ellipsoid on the other hand that defines directions with a maximum efficiency in terms of input/output forces	43
5.5	Subfigure a) presents the 2-dimensional joint velocity spaces overlapped with jacobian row vectors and subfigure b) presents the corresponding manipulability ellipsoid E_m and manipulability polytope P_m in the task space	45
5.6	Capability map is formed by discretizing the workspace into a number of cubes, sampling each cube and allotting a sphere whose diameter is the same as the dimension on the cube, discretizing the surface of the sphere with points N , and calculating the inverse kinematics feasibility R	49
6.1	Prototype of the proposed dexterity test board that is equipped with a rotating base mechanism. The board is developed using plastic parts that are 3D printed and acrylic parts that are fabricated using laser cutting.	60
6.2	A prototype of the initial version of the dexterity board.	67
6.3	Exploded view of the proposed dynamic dexterity test board.	67
6.4	Manipulation regions/areas grouped based on the object being manipulated on: a) the horizontal rig (HA1 - HA9) and b) the vertical rig (VA1 - VA3).	68
6.5	A subject performing experiments executing tasks of the dexterity test. The subfigures show: a) the initial position of the hand and objects, b) a placing task, c) a tool task, and d) a puzzle task. As shown in the images the orientation of the dexterity board constantly changes requiring the arm-hand system to adapt to various orientations to complete the tasks successfully.	69

6.6	The time taken by 10 subjects to complete various manipulation tasks across 3 trials with and without gloves is presented.	76
6.7	Percentage change in manipulation time with gloves on for the various task category: Pick & Place (PP), Reorientation (RO), Fine Component Manipulation (FC), Tool Task (TT), Puzzle Task (PT), and Total Time (TT).	77
6.8	Subfigure a) presents a comparison of the time taken by the subjects to complete various task categories in seconds when the rig was static and in motion (rotating). Subfigure b) presents the percentage increase in completion time for the various task category when the rig was in motion. The task categories are: Pick & Place (PP), Re-Orientation (RO), Fine Component Manipulation (FC), Tool Task (TT), Puzzle Task (PT), and Total Time (TT).	77
6.9	A subject performing the experiments on the dexterity test board with a palm mounted interface to control a multi-modal parallel jaw gripper, performing: a) a placing task of a medium cylinder, b) a placing task of a large square, and c) a re-orientation task of a grooved peg.	78
6.10	The comparison of time taken by the multi-modal parallel jaw gripper to complete tasks for objects of varying shapes and sizes, is presented. C, S, and P stand for Cylinders, Squares, and Pegs respectively. The subscripts s, m, l, g, denote small, medium, large, and grooved parts respectively.	79
6.11	This pie chart presents a comparison of the time taken by the robotic grippers for executing tasks with objects of varying shapes and sizes when compared against the human hands. C, S, and P stand for Cylinders, Squares, and Pegs respectively. The Subscripts s,m,l, and g denote small, medium, large, and grooved objects respectively.	79
7.1	User wearing a vest mounted human machine interface for controlling a parallel jaw gripper. The gripper and the robot hand used in the experiments are also depicted.	86

7.2	Subfigure a) presents the data collection setup at a user's home kitchen. Subfigure b) presents the side camera view. Subfigure c) presents the central main camera view. Subfigure d) shows the helmet camera. Subfigure e) shows a user loading the dishwasher using an anthropomorphic gripper operated by a human machine interface. The figure is annotated as follows: [1] Helmet camera configuration, [2] three GoPro cameras are mounted on a lightweight helmet. The central main camera faces downwards to capture hand motion and interactions during ADL in a kitchen environment, as shown in Fig. c). Supplementary cameras, e.g., [3] an iPad, are placed elsewhere in the environment to capture the operator's whole-body motion and provide side-on views of grasps, as shown in Fig. b). [4] shows an overhead camera rig, [5] a Birds Eye D435I Camera, [6] the interface on the vest, [7] daily objects, [8] a dishwasher, [9] a dishwasher rack, [10] the data recording platform, [11] the live streams from sensors, and [12] the mobile trolley used to carry the data collection PC.	89
7.3	Frequency of grasp and manipulation types for each of the ten kitchen tasks. There is heterogeneity in the grasp types used for each task. Most tasks involved object movement with fixed contact points (C P M NW NA) type of manipulation.	92
7.4	Frequency of grasp and manipulation types for each category of kitchen tasks is presented. Representative images for the various types of grasps can be seen in the legend on the left and the manipulation types are listed on the right. The radar charts show the frequencies of the power, precision, intermediate, and unknown grasps, as indicated in the legend at the bottom left of the figure. The human subjects employed up to 21 different grasps for the completion of kitchen tasks. The large diameter is one of the most commonly used grasps, usually associated with picking up containers and large objects. It is noted that few intermediate or unknown grasps were used. For all four task categories, there is a high prevalence of prehensile contact, manipulation with motion, not within the hand, and no motion at contact (C P M NW NA) type of manipulation. This represents the manipulation where the contact points are fixed during object motion.	93

7.5	The capability map compares the current capabilities of the robotic grippers to execute the set of 2000 activities performed by the humans for the completion of kitchen tasks. The activities are classified into three main classes based on robotic grippers capability: 1- successfully execute the task every time, 0.5 - multiple attempts or very high duration required to complete the task, 0 - cannot perform the tasks with current capability.	96
7.6	The figure compares the percent of time taken by humans to complete the same set of kitchen tasks performed by robotic grippers.	97
7.7	Some of the manipulation strategies employed by humans in the execution of kitchen tasks are presented in this figure: a) parallel task execution manipulation, b) bimanual stabilized manipulation, c) in-hand stabilized manipulation, d) compound manipulation, and e) grasp conversion manipulation. . .	98
7.8	The process of analyzing the dataset using clustering algorithms.	102
7.9	The various encoding methods used for converting the "Grasp Classification" categorical variable to a binary/numerical variable are presented in this image. The binary values for each of the categorical values generated by one-hot encoding and dummy encoding as well as the numerical values generated by the label encoding methods can be seen in the figure.	103
7.10	The figure presents the "Grasp Classification" attribute in the dataset being converted using the one-hot encoding from categorical to binary values. . .	104
7.11	The clusters generated for all the activities of the kitchen dataset using a k-means clustering algorithm.	107
7.12	The inter-subject variability in the a) grasp classification, b) grasp types, and c) manipulation strategies employed for the completion of the various kitchen tasks are calculated from the 2D dimensionality reduced projection of each subject.	110
7.13	The inter-subject variability mapped along with average task execution time for: a) grasp type (fridge task), and b) manipulation type (unloading dishwasher). In such cases, the fastest task execution time would allow us to select the strategies employed by one subject over the other.	111

8.1	The figure illustrates the experimental setup used for IMU-based data collection. A dynamometer was used to measure the contact force applied by the finger, while the IMUs were used to measure the Metacarpophalangeal (MCP) and Proximal Interphalangeal (PIP) joints. This experiment was conducted for 10 different finger angles from 0° to 90° in 10° steps. The motor, the finger and the dynamometer were connected to bases that were fixed to an acrylic plate. The experiments were repeated for 10 trials for every experimental condition.	121
8.2	The experimental setup for vision based joint angles data collection. The camera was positioned at a distance to capture the ArUco markers for estimating the PIP and MCP joint angles of the robot finger. This experiment was conducted for 10 different dynamometer (force-sensor) angles ranging from 0° to 90° in 10° steps. The angle change was achieved by a modular setup that allows a fast adjustment of the dynamometer angle. The experiments conducted involved 10 different trials for every experimental condition (dynamometer angle).	122
8.3	Comparison of IMU (left) and ArUco (right) data for MCP and PIP joint angles for the experimental condition of 30° dynamometer angle.	122
8.4	The graph shows the variation of the MCP joint angle, the variation of the PIP joint angle, the variation of the actual fingertip forces measured by the dynamometer, and the RF methodology based machine learning model estimations for both ArUcos and IMUs during one experiment (for 10° dynamometer angle).	123
8.5	Comparison of the feature variable importances for contact force prediction based on: a) IMU data (subfigure a) and b) ArUco data (subfigure b). The importance scores are obtained using the inherent RF feature variable importance calculation procedure. The results have been normalized over the results of the 10-fold cross-validation method.	126
9.1	The proposed multi-modal gripper that is equipped with reconfigurable finger bases to improve dexterous manipulation without sacrificing grasping quality.	131
9.2	Kinematic structure of a gripper model with two phalanges (left model) and a gripper model with three phalanges (right model). B is the distance between the finger bases and $L_{pml}, L_{mid}, L_{dtl}, R_{pml}, R_{mid}$, and R_{dtl} represent the left proximal, left middle, left distal, right proximal, right middle, and right distal phalanges, respectively.	134

9.3	Workspace comparison results for symmetric grippers with two phalanges per finger and different object diameters. Inter-finger distance was: i) optimized (B_{opt}), ii) half the object diameter (B_h), and iii) equal to the full object diameter (B_f).	137
9.4	Workspace comparison results for asymmetric grippers with two phalanges per finger and different object diameters. Inter-finger distance was: i) optimized (B_{opt}), ii) half the object diameter (B_h), and iii) equal to the full object diameter (B_f).	138
9.5	Workspace comparison results for symmetric gripper with three phalanges per finger and different object diameters. Inter-finger distance was: i) optimized (B_{opt}), ii) half the object diameter (B_h), and iii) equal to the full object diameter (B_f).	140
9.6	Workspace comparison results for asymmetric gripper with three phalanges per finger and different object diameters. Inter-finger distance was: i) optimized (B_{opt}), ii) half the object diameter (B_h), and iii) equal to the full object diameter (B_f).	141
9.7	The assembled and exploded views of the proposed multi-modal robotic gripper.	142
9.8	The workspace generated by the gripper was examined for objects of varying diameter that include: a marble (diameter: 16 mm), a golf ball (diameter: 42.7 mm), a racquetball (diameter: 55.3 mm), a baseball (diameter: 73.3 mm), and a softball (diameter: 96 mm).	143
9.9	Dexterous manipulation of a racquetball when the inter-finger distances are: a) 0 mm, b) 30 mm, c) 70 mm, and d) 110 mm.	144
9.10	Comparison for different types of grasps that are executed with the proposed gripper.	145
9.11	Results for the multi-modal robotic gripper with reconfigurable finger bases. Comparison of workspace achieved for spherical objects presented in Figure 9.8 that have different diameters and separated by base width: $B_w = 0$ mm, 30 mm, 70 mm, and 110 mm.	146
9.12	Comparison of the workspaces achieved by the multi-modal gripper, the Barrett hand, the T42 gripper, and the Robotiq 3-fingered adaptive robotic gripper for the spherical objects presented in figure 9.8 that have different diameters.	148
9.13	Demonstration of a vertical and horizontal manipulation capability of the multi-modal gripper while performing a peg in hole task.	149

B.1	Grasp Taxonomy used to classify the various grasps employed by the human hand adapted from [38].	169
B.2	Demonstration of differences between: a) tripod, b) thumb 2-fingered, and c) lateral tripod.	173
B.3	Demonstration of differences between: a)lateral pinch, b) extension type, and c) palmar.	174
B.4	Demonstration of differences between: a) power sphere, b) precision sphere, and c) precision disc.	175
B.5	Demonstration of odd grasps executed by humans is shown. Subfigure a) presents a non-prehensile grasp, subfigure b) presents a multi-object grasp, while subfigure c) presents partial grasps.	175

List of Tables

4.1	Definitions of human dexterity commonly presented in literature and related attributes are presented in this table.	23
4.2	Normal range of motion for the human hand	25
4.3	The most commonly used definitions of dexterity with respect to robotic grippers and hands are presented in this table. The attributes of the end-effectors that contribute towards the respective definitions of dexterity have also been identified.	26
5.1	Summary of the various commonly employed metrics to evaluate manipulation is presented along with the advantages and limitations.	52
6.1	Dexterity test board components, regions, and task description grouped according to the five task categories and annotated with different colours. . . .	72
6.2	Table presenting the baseline scores for the dexterity tests performed by a human with a glove and without a glove	73
6.3	Grading system for the grippers based on successful task completion in a given task category.	75
6.4	Table comparing the test environment, object sets, and features being evaluated across various dexterity tests proposed in recent literature. The task categories are abbreviated as PP - Pick & Place, RO - Re-Orientation, FM - Fine Manipulation, TT - Tool Task, PM - Puzzle Manipulation.	83
7.1	The table presents the detailed analysis of the grasping and manipulation strategies employed by humans for the execution of kitchen tasks.	91
7.2	The table presents the validation scores for the K-means and DBSCAN clustering algorithm for the current dataset.	106

7.3	The table presents the analysis of the clusters generated by k-means clustering. The distribution of the task types, number of grasps, manipulation strategies, and kitchen task categories that contribute towards a majority of each cluster (greater than 2/3 of the cluster) are presented in the table. . . .	108
7.4	The table presents the inter-subject variability of the various grasp classification, grasp types, and manipulation types employed for the completion of the various kitchen tasks. The variability is calculated as the area of the polygon formed by the dimensionality reduced projection of the strategies of individual subjects for a given task.	109
8.1	Motion estimation results for different dynamometer angles	125
9.1	Manipulation capability results for various types of grippers and varying object diameters.	136
9.2	Grasping (G) and Manipulation (M) capabilities of the multi-modal gripper for five different spheres employing the adaptive gripper mode (at base widths: 0 mm, 30 mm, 70 mm, and 110 mm) and the parallel jaw mode. . .	143
9.3	Results of the multi-modal robotic gripper with reconfigurable finger bases. The ratio of optimized workspace (WS_{opt}) to the union of all the workspaces ($\bigcup_{i=1}^n WS_i$) generated for spherical objects of varying object diameter at base width $B_w = 0$ mm, 30 mm, 70 mm, and 110 mm.	147
9.4	Workspace comparison of the multi-modal gripper with the Barrett hand, the T42 gripper, and the Robotiq 3-fingered adaptive robotic gripper.	147

Abbreviations

ABS	Acrylonitrile Butadiene Styrene
ADL	Activities of Daily Living
APC	Amazon Picking Challenge
CAD	Computer Aided Design
DBSCAN	Density-Based Spatial Clustering of Applications with Noise
DOF	Degrees of Freedom
DIP	Distal interphalangeal
DRC	Darpa Robotic Challenge
EMG	Electromyography
FDT	Functional Dexterity Test
GUI	Graphical User Interface
HD	High Definition
HDM	Hybrid Deposition Manufacturing
IMU	Inertial Measurement Unit
IP	Inrerphalangeal
IROS	Intelligent Robots and Systems
MCP	Metacarpophalangeal
NIST	National Institute on Standards and Technology
PCA	Principal Component Analysis
PIP	Proximal interphalangeal
PLA	Polylactic Acid
ROM	Range of Motion
ROS	Robot Operating System
STL	Stereolithography
t-SNE	t-distributed Stochastic Neighbor Embedding
UAHPEC	University of Auckland Human Participants Ethics Committee
YCB	Yale-CMU-Berkeley

Part I

Introduction

Chapter 1

Background and Motivation

1.1 Background

The human hand has enabled us to successfully explore and interact with a plethora of unstructured and dynamic environments exhibiting a level of skillfulness that cannot be found in other primates. This can be attributed to the sensory and motor capabilities that endow the human hand with unique manipulation capabilities and a degree of specialization that is not found in other human body parts [1]. These properties of the human hand allows it to successfully manipulate a wide range of objects irrespectively of changes to environment/external disturbances making it Nature's most dexterous and versatile end-effector. It has also been debated whether the increased dexterity of the human hand resulted in the development of a superior human brain or vice versa [2]. While some studies explain that the exploration and interaction of the human hand with the environment has resulted in the co-evolution of human dexterity and superior brain [3, 4], other studies recognize the development of the superior human brain as a result of the mechanical dexterity of human hand [5]. The mechanical dexterity of the human hand can be attributed to the opposable thumb and the ability of the carpo-metacarpal bones to rotate and preposition the finger base frames enabling it to manipulate objects with one hand [6, 7]. This presents the human hand with as many controllable degrees of freedom as all the arms, wrists and legs combined [8]. Furthermore, the human hand is the end-effector of a highly dexterous and versatile system, the human arm. These redundancies in the human hand system coupled with the redundancy in the arm space provide the human hand-arm system with a high degree of versatility and dexterity.

Owing to these features the human hand has always been an inspiration for the development of robotic hands and grippers that vary from simple two-fingered parallel jaw grippers to dexterous human-like hands with complex sensing and control mech-

anisms. Anthropomorphic grippers with high degrees of freedom are considered to be of paramount value in achieving robust grasping and manipulation capabilities and a number of five-fingered hands with varying degrees of anthropomorphism have been developed [9, 10, 11, 12, 13]. However, the increased number of actuators, transmission components, and sensing modules required to achieve the increased degrees of freedom are difficult to incorporate and make control computationally expensive and difficult [14, 15]. In recent times, a new class of adaptive underactuated grippers have shown promise in offering robust grasping as well as improved manipulation capabilities with simple actuation and lack of complicated sensing [16, 17, 18]. However, the compliance in the finger joints and the underactuation of these designs introduce a reconfiguration of the fingers post contact with the objects resulting in variations and a reduction of the contact forces exerted during this phase [19, 20]. Owing to these limitations, the roboticists have found it extremely difficult to emulate the level of dexterity and functionality demonstrated by the human hands despite the plethora of robotic grippers being developed [21].

1.2 Motivation

The notion of dexterity as defined and utilized across various studies is substantially different from one another and there is no clear means of implementing dexterity in a particular robotic gripper or hand [21, 8]. The numerous definitions proposed in the literature with respect to human dexterity [22, 23, 24] and dexterity of robotic end-effectors [5, 25, 26] attribute dexterity to various features. Most human dexterity studies define dexterity as a measure of functionality and task completion capabilities but do not consider the workspace or kinematic dexterity [27, 28]. On the other hand, the robotic studies ascribe the dexterity in terms of kinematic redundancies and workspace maximization considerations among others [29, 30]. These disparities have resulted in numerous methods, metrics, and tools being introduced to quantify robot dexterity and made comparison against human counterparts complicated and subjective. Though numerous performance measures have been employed for a long time by roboticists for the design, synthesis, and evaluation of robotic manipulators, researchers cannot agree on a commonly accepted measure owing to the limitations of dimensions, scale, order, and bounds of the various approaches [31].

Research efforts involving anthropomorphic hands have focused on quantifying robot dexterity and anthropomorphism through optimization of the spatial correspondences between the human and the robot systems, minimizing structural dissimilarities, achieving

human-like compliance, kinematics, and force exertion capabilities but without really evaluating or optimizing the degree of dexterity of the robot mechanisms [32, 33, 34]. Similarly the performance analysis of the mechanical characteristics and limits of prosthetic hands performed by Belter et al concluded that these measures vary with patient needs and characteristics such as level of amputation, desired activities of daily living, and specific uses of the devices among others [35]. Other studies have tried to compare the robot performance against humans by evaluating the mechanical complexity and functional potential of the end-effectors [36]. For this purpose, the grippers were evaluated to determine the range of achievable grasps [37, 38], manipulation motions achieved [8], and thumb dexterity [39]. While a number of benchmarking systems have also been proposed to compare the performance of grippers and human hands, there is an increasing difficulty in comparing their performance owing to the lack of standardized benchmarks, metrics, and reproducible experimental setups [40].

This thesis focuses on the systematic analysis, assessment, and evaluation of the dexterity of human and robotic hands in the execution of robust grasping and dexterous, in-hand manipulation tasks. To do so, we will first collect, evaluate, and classify the pre-existing dexterity and grasp quality metrics. In particular, we create a comprehensive taxonomy of the various dexterity classes using these metrics. Subsequently, we focus on analyzing, quantifying, and modeling the different aspects of human dexterity through extensive experimentation. The experiments that are conducted include multiple trials with human subjects performing grasping and dexterous manipulation tasks with various model and everyday life objects under a range of uncertainties (e.g., object pose or perception uncertainties) while blocking certain types of feedback (e.g., vision feedback, tactile feedback etc.). Such experiments help us identify any meaningful correlations between higher-level synergistic organizations of the brain and muscle activities (e.g., motor strategies) and human dexterity.

By performing these studies that will focus on the human hand, we are able to extend our knowledge of human dexterity and propose new dexterity classes and metrics. The derived metrics are then used in the formulation of a design optimization framework for the development of new robotic and grippers and hands that are as dexterous and efficient as possible but also intuitive and simple to control.

Chapter 2

Thesis Objective and Thesis Structure

2.1 Objectives

The main goal of this thesis is to analyse and evaluate the dexterity and the grasping and dexterous manipulation capabilities of human and robot hands, deriving design inputs for the development of new classes of robotic grippers and hands that exhibit the same level of dexterity as the human hands. To do this, we first clearly define the term dexterity with respect to human hands and robotic end-effectors. We derive the various attributes and characteristics that contribute towards the increased human dexterity and propose methods to translate these attributes to robotic grippers and hands. The main objectives of this work are:

1. Investigate the boundaries of the term dexterity, analysing, evaluating, and classifying the proposed classes and metrics, formulating new taxonomies.
2. Analyze, quantify, and model the different aspects of human dexterity through extensive experimentation.
3. Benchmark the current capabilities of the robotic end-effectors against human hands and identify the factors that contribute towards dexterity shortcomings in robot grippers and hands.
4. Propose new dexterity classes and metrics based on analysis and benchmarking.
5. Employ the proposed metrics in the formulation of design optimization frameworks that will lead to a new generation of dexterous artificial hands that are lightweight, affordable, simple to control and intuitive to operate.

2.2 Ethics Approval

All the experiments conducted for the completion of this thesis have received the approval of the University of Auckland Human Participants Ethics Committee (UAHPEC) with the reference number #019043. Prior to the study, all subjects provided written and informed consent to the experimental procedures.

2.3 Thesis Layout

This thesis is divided into five main parts: Introduction (Part I), Related Work on Defining and Evaluating Dexterity (Part II), Analysis, Evaluation, and Comparison of Human and Robot Dexterity (part III), Improving the Design of Adaptive Robot Hands and Grippers (Part IV), and Conclusion and Future Directions (Part V).

The chapters of Part I are organized as follows:

- Chapter 2 discusses the main objectives of this thesis.
- Chapter 3 presents the equipment and apparatus used to conduct experiments to test and validate the proposed frameworks.

The chapters of Part II are organized as follows:

- Chapter 4 presents an overview of the human hand, Nature's most effective end effector. The terms dexterity, grasping, and manipulation are explored with respect to human hands, robot hands, and grippers.
- Chapter 5 examines the state of the art dexterity measures, benchmarking tools, and metrics that are used to evaluate human and robot dexterity.

The chapters of Part III are organized as follows:

- Chapter 6 presents a new open-source dexterity test that can be used for benchmarking the dexterity, grasping, and manipulation capabilities of humans and robots alike. A standardised scoring methodology and a dexterity metric to quantify the benchmarking results are also proposed.
- Chapter 7 discusses a kitchen activities specific dexterity comparison between humans and robotic end-effectors, as an initial study focusing on the promising field of household robots. The unique attributes of human grasping and manipulation

strategies are classified in a taxonomy that can be used for developing alternate strategies using existing robot designs as well as for the development of new classes of robotic grippers and hands. New metrics for designing efficient data collection processes and protocols focusing on the most critical / valuable data are also proposed.

The chapters of Part IV are organized as follows:

- Chapter 8 presents a methodology that exploits the "parasitic" post-contact reconfiguration of adaptive fingers with compliant joints to predict the forces exerted by the adaptive robotic fingers.
- Chapter 9 presents a design optimization framework for improving the dexterous manipulation capabilities of robotic grippers without sacrificing their grasping efficiency. The results of the optimization are used to develop multi-modal robotic grippers with reconfigurable finger bases that have significantly increased manipulation capabilities and dexterous manipulation workspaces.

Finally:

- Chapter 10 concludes the thesis by highlighting the major contributions of this work and providing future directions for research.

Chapter 3

Apparatus

This chapter introduces the robotic equipment used throughout this thesis. This includes:

- Motion capture systems used for tracking human and robot motions.
- Force measurement devices to capture the output forces exerted by the grippers and hands.
- Robotic grippers and hands developed by the New Dexterity research group.
- Interfaces employed to control the robotic grippers for the performance of various tasks.

3.1 Motion Capture System

3.1.1 Fiducial Markers

We employed fiducial marker based motion tracking for real time pose estimation. In this study, we employed the ArUco class of fiducial markers [41]. A webcam was used to track appropriately designed square fiducial markers generated from the 7 by 7 ArUco library. This computer vision processing library enables the detection of square fiducial markers. Relative positional data such as the angles and the Cartesian coordinates for each marker were extracted using the OpenCV [42] implementation. Figure 3.1a shows a base ArUco marker used as the origin. The initial pose and trajectory of the gripper are calculated relative to this marker using a secondary marker placed on the interface as shown in Figure 3.1b. The markers are tracked during the operation of the gripper using a birds eye camera (Intel RealSense T265) mounted 60 cm above the origin marker to ensure all markers are within the field of view. Figure 3.1c shows another example where

a 4k web camera tracks ArUco markers attached to the finger structure to obtain relative positional data like each marker's angles and cartesian coordinates.

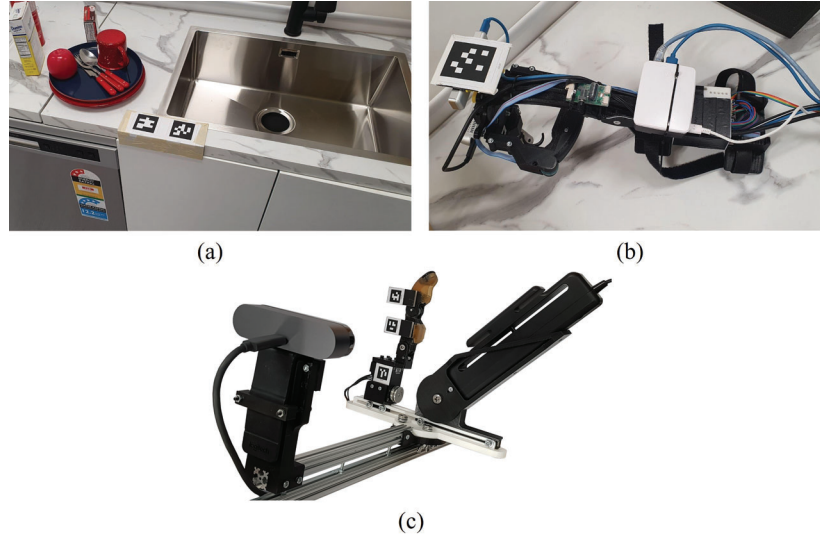


Figure 3.1: Examples of aruco markers being used to: a) locate the origin, b) track the hand motion, and c) determine the joint configurations of fingers.

3.2 Force Measurement Devices

A Biopac MP36 data acquisition unit (Biopac Systems, Inc., Goleta, California) equipped with the SS25LA dynamometer was used to collect force measurements. The SS25LA dynamometer is a lightweight, ergonomic force measurement unit that can record forces in the range of 0-50 kgf (Kilogram-force). It is equipped with a 3 metre long cable that allows the easy movement and positioning of the force sensor away from the recording unit. The dynamometer can be connected easily to one of the four electrode channels (CH input channels) located on the front of MP36 unit. The transducer can provide direct output in pounds or kilograms and only requires a very simple calibration. The MP36 can record inputs from the transducer at a sampling rate of 100 KHz with 24-bit A/D sampling resolution. Figure 3.2 shows the data acquisition unit and the dynamometer.



Figure 3.2: Force measurement setup containing a SS25LA dynamometer plugged into CH1 electrode channel of a Biopac MP36 data acquisition unit.

3.3 Robotic Grippers and Hands

A number of robotic grippers and hands were used for collecting robotic data as well as for comparison against human grasping and manipulation capabilities. These grippers and hands are discussed in this section.

3.3.1 Parallel Jaw Gripper

A simple parallel jaw gripper as seen in Figure 3.3 containing two fingers that are driven linearly utilising a rack and pinion system was designed within the New Dexterity Research group. It is operated by a single Dynamixel XM-430-W350-R that opens and closes the grippers along the linear rails for enabling simple grasps. Each finger is equipped with compliant finger pads that can conform to objects of various shapes to enable robust grasping. This simple gripper with one DOF serves as the baseline robot gripper mechanism for comparison against other grippers and hands.



Figure 3.3: A simple parallel jaw gripper controlled by a single actuator.

3.3.2 NDX-A

Experimental protocols involving anthropomorphic hands were performed using the New Dexterity, adaptive, human-like robot hand [12] developed within the New Dexterity research group . This underactuated hand shown in Figure 3.4 is tendon-driven and utilises 5 actuators (Dynamixel XM430-W350) to control 15 degrees of freedom. One actuator is employed to control the flexion of each finger, except for the ring and pinky fingers that are coupled together using a differential mechanism. An additional Faulhaber DC motor and a non-backdrivable gearbox are used to control thumb opposition. The hand also features compliant fingerpads and palm to facilitate object grasping and manipulation.



Figure 3.4: The new dexterity adaptive, human-like robot hand was used for analysing dexterity of anthropomorphic grippers.

3.3.3 Multi-Modal Gripper with a Rotary Module

This multimodal gripper developed by Geng Gao in the New Dexterity research group combines a parallel-jaw element with a 3-fingered rotary module allowing the gripper to perform a) pinch, b) extension, and c) rotation primitives in the execution of manufacturing tasks [43]. The gripper presented in Figure 3.5 is controlled using three actuators (two Dynamixel XM-430-W350-R, and one Dynamixel XL-320). The parallel jaw module is comprised of a pair of modular fingers with compliant finger pads. It utilises a rack and pinion mechanism to perform the pinch (Eg. picking objects for insertion tasks) and extension (eg. extending a belt with the back of the fingers) grasping tasks. The 3-fingered rotary module on the other hand can perform grasping and rotation of the grasped objects using a scroll wheel mechanism. The potential errors encountered during the use of rotary tool is compensated by implementing mechanical compliance along the axis of rotation of the rotary module.

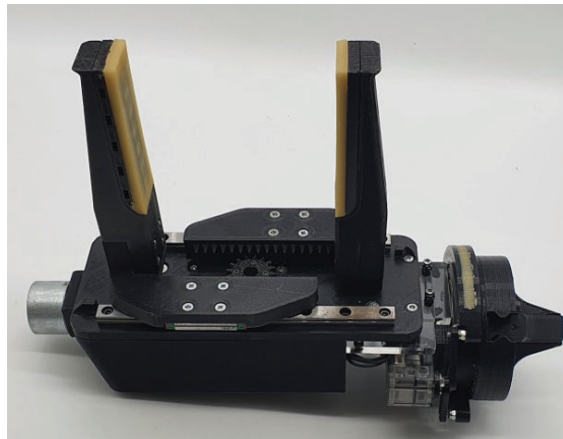


Figure 3.5: A multimodal gripper containing a simple 2-fingered parallel jaw module and a 3-fingered rotary module.

3.4 Robot Interfaces

A number of interfaces were employed to control the robotic grippers in the performance of various tasks. These interfaces can be mounted with various grippers and are equipped with control interfaces such as sliders, trigger controls, selection button etc for real time programming of the end-effectors. The mounting modules designed to accommodate several cameras can be used for recording videos of grasping and manipulation strategies performed by the grippers for analysis and evaluation.

3.4.1 Palm Mounted Interface

The palm mounted interface seen in Figure 3.6 was designed by Jayden Chapman in the New Dexterity research group [44]. This compact interface can be constrained in the palm of the user by the ergonomic palm rest. The device is held in place by an adjustable, elastic strap that allows holding the device in place without requiring support from any fingers. The interface allows easy control of grippers with up to six actuators using a) four linear potentiometer sliders controlled by the four fingers, b) a bidirectional joystick, and c) a press button controlled by the thumb. The device is efficient in controlling lightweight devices, and for shorter operation times. The interface can be customized for both right and left-handed users, using a customizable palm pad and a trigger switch that reconfigures the controls for the different handed users. The interface can accommodate two RGBD cameras. The information that can be recorded using the interface includes the camera feeds, control module outputs, and actuator data (position, velocity etc.).

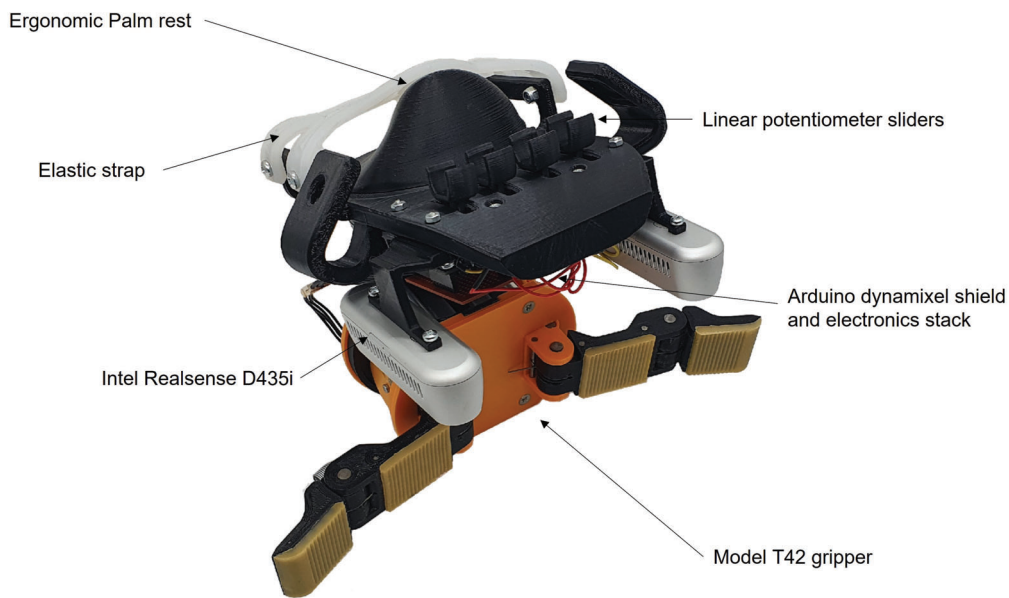


Figure 3.6: A palm mounted interface equipped with a T-42 gripper. The interface allows easy control of grippers using four linear potentiometer sliders controlled by the four fingers, a bidirectional joystick, and a press button controlled by the thumb.

3.4.2 Forearm Mounted Interface

The forearm stabilized interface was designed by Che-ming chang within the New Dexterity research group and is presented in Figure 3.7 [44]. The arm module padded with

clothed sponges supports the interface on the forearm of the user and can be secured in place using Velcro straps. The ergonomic grip also contains three control modules: a) an incremental encoder, a rotary potentiometer, and a push-button. These modules can be used to control a maximum of six actuators individually or in parallel. The 3D printed design of the interchangeable arm module (of different lengths) is customizable for individual users. The entire interface can be supported by a passive, iso-elastic arm mounted onto the waist structure. Hence, this interface can help overcome fatigue while operating heavy grippers over a long period of time. The camera mounting plate on the interface can accommodate a maximum of two cameras at different angles. The motor/gripper data is parsed by an Arduino and get transmitted to the computer via encoded serial communication. The modular mechanical system and electronics allow the gripper to be adapted to various grippers, actuators, and applications.

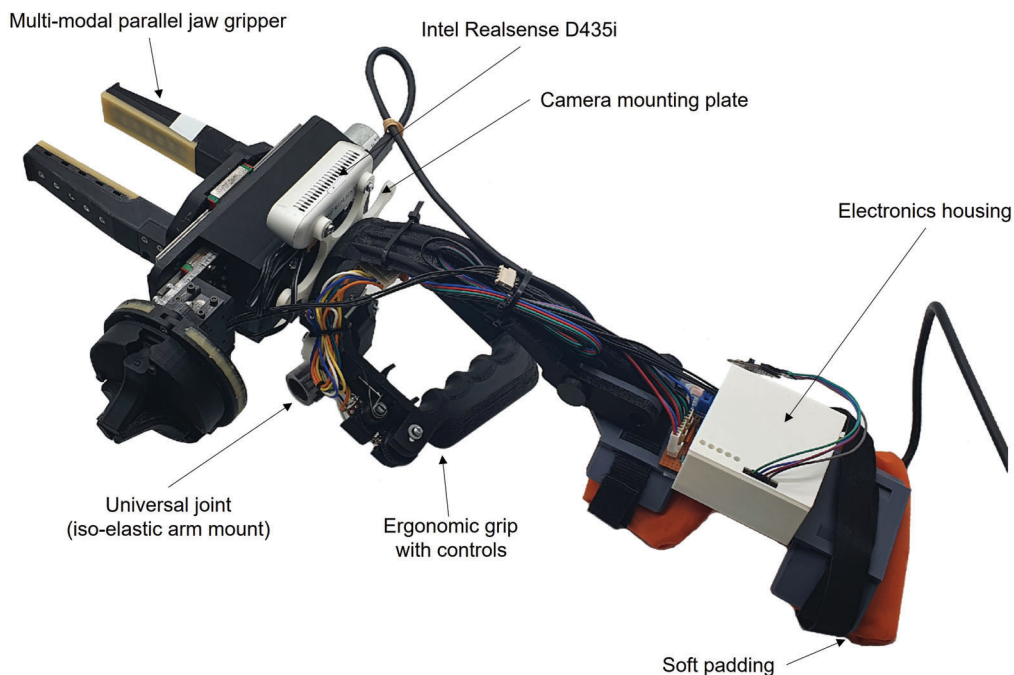


Figure 3.7: A forearm mounted interface equipped with a multimodal gripper. The interface allows easy operation of heavy robot grippers or hands such as the NDX-A and the multimodal gripper over a long duration of time.

Part II

Related Work on Defining and Evaluating Dexterity

Chapter 4

Definitions and Taxonomies of Dexterity

4.1 Introduction

Dexterity and dexterous hands are the most common terms associated with studies involving robotic grippers and hands. The objective of most of these studies is to develop a robotic end-effector with improved overall dexterous capability or task specific dexterity. However, there has been very little understanding about the means to impart dexterity to a specific set of grippers [45]. This might be attributed to the fact that many researchers assume and attribute dexterity to highly functional, human-like hands with high DOF [32]. Owing to this reason many researchers characterize their end-effectors as dexterous without assessing the actual level of dexterity and/or benchmarking them against similar devices and humans. Hence it is important to properly define the term dexterity, identify the boundaries of the term, and attributes that directly contribute towards improving it. In this chapter, we provide the commonly accepted definitions for the term dexterity with respect to humans and robots. We also identify the attributes that are responsible for the specific classes of dexterity. The rest of the chapter is organized as follows: Section 4.2 discusses the various attributes of human dexterity and defines the term. The unique features of the human hand anatomy that contribute heavily to its high dexterity are presented in section 4.3. The various definitions and attributes of robot dexterity presented in the literature are discussed in section 4.4. Grasping and Manipulation strategies employed by the human and robot hands are discussed in section 4.5.1 and 4.5.2 respectively. Section 4.6 concludes the chapter.

4.2 Human Dexterity

The human hand is considered the most dexterous end-effector as it is capable of performing a diverse set of tasks across various environments and settings, serving as a general purpose manipulator [45]. The range of objects that can be manipulated by a human hand varies over a huge range of sizes, shapes, and other object properties. The level of precision obtainable by the human hand and the ease with which they are performed are also impressive [27, 23]. This range of tasks and precision is obtained by a combination of gross and fine voluntary movements executed by the human hand. All these skills of the human hand can be improved through training, learning, and experience, enabling them to perform the tasks with further ease in a shorter duration of time [22]. Some of the most commonly used definitions of human dexterity are presented in Table 4.1. As shown in the table, most human studies consider dexterity as a measure of functionality and task completion capability of the human hands. Owing to this, human dexterity measures are used to measure the degree of improvement or deterioration of functionality in rehabilitation post injuries or stroke [46]. They have also been used to evaluate manual dexterity in workers required to perform specific industrial tasks like assembly, packing, and operating specific machines, and also for surgeons who require a high level of dexterity and precision. Deriving from these studies, we define human dexterity as "The ability of the hand to perform with ease a diverse set of complex tasks that require increased skillfulness and that involve objects of varying properties irrespectively of changes in the environment and other external conditions and disturbances."

4.3 Human Hand Anatomy

The human hand is considered to be Nature's most dexterous end-effector and owes many of its capabilities to its anatomical design. Like any good design, the human hand has undergone numerous iterations of evolution over millions of years and has been optimized by nature. The key features of the human hand anatomy detailing its kinematic structure, the available degrees of freedom, and the range of motion of each joint are presented here.

4.3.1 Anatomical Features of Human Hand

One of the key features of the human hand that separates it from the hands of other organisms is the robust long thumb relative to the length of the fingers. The human hand is made up of 27 bones. Each finger(except the thumb) consists of 3 phalanges: the proximal, middle, and distal phalanx. The distal phalanges form the tips of the finger and

Table 4.1: Definitions of human dexterity commonly presented in literature and related attributes are presented in this table.

Study	Definitions of Dexterity	Attributes
Poirier, 1988 [22]	"Manual ability requiring rapid coordination of gross and fine voluntary movement, based on a certain number of capacities that are developed through learning, training, and experience."	Functionality, Gross & Fine motor Control
Backman et al, 1992 [27]	"fine, voluntary movements used to manipulate small objects during a specific task, as measured by time required to complete the task."	Functionality, Task completion capability, Fine motor control
Latash et al, 1994 [23]	"The ability to adequately solve any motor task... precisely, quickly, rationally and deftly."	Functionality, Task completion capability
Canning et al, 2000 [24]	"Skill and ease in use of the hands, but is also defined as adroitness and competency in use of the limbs and body generally, especially in the performance of a task."	Functionality, Task completion capability
Lawrence et al, 2014 [47]	"The sensorimotor capability to dynamically regulate fingertip force vectors and motions to stabilize an unstable object."	Force modulation, Motion modulation, Sensory feedback
Yong et al, 2020 [28]	"the co-ordination of voluntary movement to accomplish an actual or simulated functional goal/task accurately, quickly, resourcefully and adapting to environment or change."	Motor control, Task completion capability

have prominent broad apical tufts that facilitate better manipulative control. The proximal phalanges are located closer to the palm. All the fingers except the thumb have a middle phalange in between the distal and proximal phalanges. The phalanges are attached to each other by hinge joints. These joints are called the proximal interphalangeal (PIP) joint and the distal interphalangeal (DIP) joint. The thumb has only one joint which is called the interphalangeal (IP) joint. The fingers are connected to the base of the wrist through the long and slender metacarpal bones that are attached to the proximal phalanges by the metacarpophalangeal joint (MCP). The I metacarpal bone connects the thumb, the II metacarpal connects the index, the III metacarpal connects the middle finger, and so on. The head of the metacarpals is attached to the proximal phalanges through a condyloid(oval) joint that helps articulate the finger bases. These condyloid joints allow 360-degree motion of the fingers at their bases. The articulation of the metacarpals enables the folding, stretching, and compressing of the palm. The wrist is made up of a set of 8 carpal bones that are arranged in two rows of four each. The metacarpal bones are attached to the carpal bones in the distal row by the carpometacarpal ligaments. The fifth carpometacarpal joint is saddle-shaped, allowing the metacarpal bone of the little finger to rotate towards the thumb. On the palmar side, the carpus is concave, forming a canal known as the carpal tunnel. The nerves, tendons, and ligaments extend into the palm from the forearm and wrist through the carpal tunnel. The proximal row of the carpal

bones is rounded and forms a flexible wrist joint with the bones of the forearm - ulna and radial. The rotation of these bones about the proximal radioulnar joint at the elbow results in the pronation and supination of the forearm. The muscles in the forearm enable the movement of the bones of the forearm and wrist. They also facilitate the flexion and extension of the phalanges by pulling on long tendons that run through to the fingers via the wrist and hand.

4.3.2 Degrees of Freedom (DOF)

The sophisticated anatomy of the human hand has endowed it with 29 degrees of freedom (DOF). Each finger (except the thumb) has four DOF. Three of these are flexion/extension at the MCP joint, PIP joint, and DIP joint respectively, and the fourth DOF is the adduction/abduction at the MCP joint. The thumb owing to its complex joints at the base has 5 DOF. Two for flexion/extension at the MCP and IP joints. The saddle joint at the base of the thumb accounts for 3 DOF: one for flexion/extension, one for adduction/abduction, and one for lateral and medial rotation. The metacarpal bones (II through V) of the palm are also endowed with two degrees of freedom each. One each for flexion/extension and one each for adduction/abduction. These extra DOFs enable the repositioning of the finger base frames and the thumb to oppose the other fingers. The opposable thumb and repositionable finger base frames are unique features that provide the human hand with the ability to perform pinch grasps with high precision. This allows the human hand to perform in-hand manipulation over an incredible range of objects. These are the key components that contribute toward rendering the human hand as Nature's most dexterous end-effector.

4.3.3 Range of Motion

The normal range of motion observed for each joint of the human hand as presented in the electronic textbook of hand surgery [48] is presented in Table 4.2.

Table 4.2: Normal range of motion for the human hand

Range of Motion for Human hand DOF		
Joints	DOF	Range (degrees)
DIP joints	Extension/Flexion	0/80
PIP joints	Extension/Flexion	0/100
MCP joints	HyperExtension/Flexion	0-30/90
Thumb IP joint	HyperExtension/Flexion	15/80
Thumb MCP joint	HyperExtension/Flexion	10/55
Thumb Basal joint	Palmar Adduction/Abduction	Contact/45
	Radial Adduction/ Abduction	Contact/60
Wrist	Extension/Flexion	70/75
	Radial/Ulnar	20/35

4.4 Dexterity of Robotic Grippers and Hands

There are numerous definitions of dexterity put forth and applied across the various robotics research studies. Some of the most commonly utilized definitions are presented in Table 4.3. Some of these definitions provide a very general statement like "the skill in the use of hands" [26] and do not provide any insights as to how it can be achieved. And some defined dexterity with respect to specific task environments. For example, Hollerbach defined dexterity as "a feature that would make assembly lines more adaptive and flexible, reducing the need for custom fixtures in each assembly task" [49]. Most studies associate dexterity with kinematic redundancy [29] and consider it a necessity for the robot fingers to reach arbitrary orientation and exert forces across a given workspace [50]. A majority of the robotics research defines dexterity as an object-centered task execution capability. They define dexterity as a characteristic of the robotic gripper that would allow it to grasp and manipulate the objects between multiple configurations [51]. The most commonly applied definition, as described by Bicchi et al is "The capability of a robot hand to change the position and orientation of the manipulated object, from a reference configuration to a different arbitrary chosen configuration, within the hand workspace" [5]. Recent studies have shown that interactivity among the robotic fingers is an important attribute that contributes towards object manipulation. Along these lines, robotic dexterity can be defined as the capability of a given end-effector to effectively

coordinate multiple manipulators or fingers to grasp and manipulate objects without losing contact with the object for the execution of tasks [25, 52, 30]. Deriving from these studies we define robot hand dexterity as "The combination of robust grasping and in-hand manipulation capabilities of a robotic gripper or hand that allow it to successfully relocate and reorient objects of varying properties from a given configuration to a target configuration for the successful execution of complex tasks, irrespectively of changes in the environment and other external conditions and disturbances."

Table 4.3: The most commonly used definitions of dexterity with respect to robotic grippers and hands are presented in this table. The attributes of the end-effectors that contribute towards the respective definitions of dexterity have also been identified.

Study	Definitions of Dexterity	Attributes
Hollerbach, 1982 [49]	"A feature that would make assembly lines more adaptive and flexible, reducing the need for custom fixtures in each assembly task."	Functionality, Task completion capability, Kinematic dexterity
Klein et al, 1987 [29]	"The kinematic extent over which a manipulator can reach all possible orientations."	Kinematic dexterity, Optimized Workspace
Li et al, 1989 [51]	"The process of manipulating an object from one grasp configuration to another."	Kinematic dexterity
Sturges et al, 1990 [26]	"The skill in the use of hands."	Functionality, Task completion capability
Park et al, 1994 [50]	"Ability to move and apply forces in arbitrary directions as easily as possible."	Force modulation, Kinematic dexterity, Optimized workspace
Bicchi, 2000 [5]	"The capability of a robot hand to change the position and orientation of the manipulated object, from a reference configuration to a different arbitrary chosen configuration, within the hand workspace."	Kinematic dexterity, Optimized workspace
Okamura et al, 2000 [25]	"The cooperation between multiple manipulators or fingers, to grasp and manipulate objects."	Interactivity of fingers
Bicchi et al, 2002 [52]	"The ability of a hand to relocate and reorient an object being manipulated among its fingers, without losing the grasp."	Interactivity of fingers, kinematic dexterity
Suarez et al, 2006 [30]	"A grasp is dexterous if the hand can move the object in a task-specific way, or for the general case that the task specifications are not provided when it is able to move the object in any arbitrary direction."	Kinematic dexterity, Optimized Workspace, Task completion capability

4.5 Grasping and Manipulation

Each study approaches the dexterity of robotic grippers differently and characterizes dexterity to different attributes. In general, dexterous manipulation could be considered as a sequence of events to be performed by a robot for the accomplishment of a task. This includes the planning and execution of establishing the contact points on the object, exerting forces on these contact points for restricting the object's motion, and motion of the robot fingers/arms to enable the movement of the object from the current configuration to a desired target configuration for the successful task execution [25]. In simple

terms, dexterity is a combination of robust grasping and effective manipulation. Hence, a number of research has been done to classify the grasping and manipulation strategies with the intention to derive the optimal approaches for robots [5, 53, 54]. These studies have analyzed grasping and manipulation providing us with object-centric [55], force-centric [56], hand-centric [38], and motion-centric [8] classification. A brief explanation of the characteristics of grasping and manipulation strategies employed by the robotics community is presented here.

4.5.1 Grasping

Grasping can be defined as the act of restraining an object's motion using the hand configuration and force/torque modulation [57]. Feix et al defined "A grasp is every static hand posture with which an object can be held securely with one hand, irrespective of the hand orientation" [38]. This definition of grasp has been used to classify the various postures of the hand based on a) the nature of grasp (power or precision), b) Thumb position, c) Opposition types, and d) functional units of fingers (Virtual Fingers).

The nature of grasp is determined based on the activity to be performed with the grasped object and has been classified into three main categories: power, precision, and intermediate. The power grasp establishes a rigid hand-object relation that restricts the object motion completely, and any movement needs to be imparted from the arm [58]. Contrarily, the precision grip enables the object motion through intrinsic finger movements [58]. And one of the most commonly used taxonomies established by cutkosky classified the grasps into one of these categories [37]. However, some of the grasps observed did not fit into either of these categories and a third category called intermediate grasp has been introduced [59]. The intermediate grasp exhibits equal characteristics of power and precision grasp. Further classification has been proposed based on the position of the thumb. There are two main categories in this classification: abduction and adduction. Abduction is when the thumb moves out of the plane from the palm and opposes the fingertips. During adduction, the thumb remains in the same plane as the palm and can apply forces to the side of the fingers.

Another main feature used for categorization classifies the grasps based on three basic directions of force exertion on the object [60]. In the first category, called the palm opposition, the forces are exerted between the surfaces of the hand and palm (generally perpendicular to the palm) like holding a large bottle, hammer etc. In pad opposition, the forces are exerted between the volar surfaces of the fingers and thumb like holding a pen, small object etc. If the opposition occurs between the side surfaces of the hand transverse to the palm, it can be classified as side opposition. Examples include holding a

key between the side of the finger and thumb. Furthermore, the fingers, thumb, and palm often perform in combination with each other, called functional units. Each of these functional units has been described as a virtual finger (VF) made up of a number of fingers (one or more) exerting forces in a similar direction in unison [61]. For example, if an object is being held against the palm by the four fingers, the palm acts as VF1 and the four fingers act as a single functional unit VF2. The object is stabilized between these two functional units. Such grasps, where the object can be stabilized by the forces exerted by the hand alone, are often termed prehensile and require a minimum of two VFs. On the other hand, the grasps where objects are stabilized using one VF (or more) and external conditions (like gravity) are classified as non-prehensile. Examples include holding a plate with an open palm where the plate is stabilized using one VF and gravity.

A number of grasp taxonomies have been proposed in the literature that classifies grasping based on one or a combination of the categories described above. The most commonly used taxonomy in the field of robotics was the one proposed by cutkosky, which presented a hierarchical classification of 15 different grasps [37] and has been commonly employed by various robotic hands for design/evaluation. More recently, Feix et al had compared over 22 taxonomies, identified the similarities between the various classifications, and presented a new systematic categorization of the grasps in a new taxonomy [38]. The comprehensive taxonomy captured 33 different prehensile grasps in which the objects can be secured solely based on hand posture. Apart from this, humans also employ a number of non-prehensile and dynamic grasps for stabilizing objects for the purpose of restriction and motion. These taxonomies have been used to compare the gripper capabilities by classifying grippers that can successfully execute more number of grasps as more dexterous [36]. However, despite this variation in the types of grasp, humans only employ a small fraction of grasps during daily work activities. It was identified that the humans employed only five grasps during household and ten grasps during machine shops for the completion of 80% of the tasks [62]. This provides valuable insight for the design of robotic end-effectors that a majority of the tasks performed by humans can be executed successfully with the limited number of grasps specifically designed for a given task category. And the number of grasps that a gripper can successfully execute can no longer be an indication of its dexterity.

4.5.2 Manipulation

Manipulation can be defined as the process of moving an object from one configuration to another using the motion of robotic fingers, hands, or arms. In most situations, task completion requires an object to be translated and/or rotated about a predefined axis

while being restricted by a robot hand. Studies have decomposed the tasks into a set of primitive actions that the gripper needs to execute in sequence [63, 64]. These could include the free motion of the robotic hand to posture the fingers, establishing a stable grasp, lifting the grasped object, rotating the object about an axis, and redistribution of forces to enable in-hand manipulation etc [65, 66]. The ambiguity in these manipulation actions being effected by the "hands" as opposed to the manipulator "arm" has been a topic of discussion in the field of dexterous robotic manipulation [21]. In most cases, a simple gripper capable of stably grasping a number of objects can accomplish a wide range of tasks using arm dexterity [21]. Even in cases where the object is grasped in a different orientation owing to restricted environment/space, the desired end configuration can be obtained through a sequence of grasping-regrasping strategies [67].

However, hand dexterity where the object motion is a result of the reconfiguration of the hand/fingers can increase the workspace of the arm-hand system, especially at arm singularities and obstacles. The energy required to accomplish a task within the hand is much lower compared to tasks requiring arm motions. Hence, some level of hand dexterity is preferable for finer movements. And a combination of the arm (for large-scale positioning, higher force-torque exertion) and hand (for finer positioning, precision handling) is necessary for obtaining optimal manipulation capabilities. Some of the commonly observed in-hand manipulation techniques include: a) regrasping- where an object is released and regrasped to change the orientation of the grasp [67], b) in-grasp reorientation - where fine changes in finger configuration enable change in object orientation using redundancy in finger space, c) finger gaiting - replacing fingers that have reached joint limits with free fingers to extend the kinematic limitation [68], d) finger pivoting - where an axis of rotation is determined by two-point contacts (fingers) and a free finger rotates the object about this axis [69], e) slipping - where the object is manipulated by using controlled slip [70], and f) rolling - easily achievable non-prehensile manipulation that can be achieved for certain object geometries [71].

A number of taxonomies have classified manipulation behaviours for the purpose of transferring the classified characteristics to robot hands [72, 73]. The classification has been approached from an object-centric [63], force-centric [56], and hand-centric view [74, 75]. These approaches help determine the tasks differently enabling the robots to formulate strategies for the completion of the task. For example, an object-centric classification would define the activity of opening a bottle cap as the rotation of the cap along the axis of the bottle and lifting it upwards. However, the same can be defined from a hand-centric view in multiple ways. One approach could be turning the object using in-hand manipulation of fingers, while another could be grasping the cap firmly

and performing the action using a manipulator arm. One of the most widely employed taxonomies proposed by Bullock et al involves the hand-centric and motion-centric classification of tasks that help identify the manipulation strategies [8].

This hierarchical categorization is based on contact condition, grasp category, object motion, and hand-motion relationship. The manipulation is said to have established contact if the hand or any parts of it touches an external object. Actions such as hand movements, sign making etc are classified under no contact while all tasks require the hand to establish contact with the object for manipulation. The type of contact established is classified into prehensile and non-prehensile categories as defined in the grasp taxonomy. Once this has been established, the manipulation further evaluates if the object is in motion with respect to the world frame. While most manipulation requires object movement, certain tasks require the objects to be stabilized before manipulating a part of the object. Examples could include stabilizing a bottle with one hand prior to opening the bottle cap. If the object is in motion, we determine if the motion occurs within the hand or external to the hand. Thus, a set of 15 manipulation strategies are defined in the taxonomy to represent the various classes of hand-centric and motion-centric manipulation.

This taxonomy has been employed by studies to identify the manipulation strategy employed by humans and mimic them with a robotic end-effector for specific tasks [76]. And since the classification is not anthropometric, it can be used to analyze the manipulation strategies employed by the general arm-hand system of robotic grippers and hands. Though the taxonomy helps classify the high-level taxonomy for task execution, additional categorizations and inputs need to be derived from other classification taxonomies to compensate for the finer details such as objects being interacted with or the hand configuration etc. And often times, the manipulation strategy employed by humans is personal choices obtained through practice, ease of use, or habitual. Hence, the tasks could be completed by the robotic end-effectors by employing alternate strategies.

4.6 Conclusion

In this chapter, we address the ambiguity associated with the term dexterity and the lack of standardized methods to quantify, compare, and impart dexterity to various grippers. The various definitions and attributes of the human hand that make it the nature's most versatile and dexterous end-effector are identified. The human dexterity can be defined as "The ability of the hand to perform with ease a diverse set of complex tasks that require increased skillfulness and that involve objects of varying properties irrespective of changes in the environment and other external conditions and disturbances". The

anatomical and kinematic features of the human hand that contribute towards achieving this high level of functionality are detailed. We also analyzed the various definitions of robot dexterity put forth in the literature and the qualities it is attributed to. Based on this, we propose that the dexterity of a robotic end-effector can be described as "The combination of robust grasping and in-hand manipulation capabilities of a robotic gripper or hand that allow it to successfully relocate and reorient objects of varying properties from a given configuration to a target configuration for the successful execution of complex tasks, irrespectively of changes in the environment and other external conditions and disturbances". Hence, the dexterity of a gripper is a cumulative outcome of its ability to establish contact points on the object, exert forces to restrict object motion and move the object to a target configuration using the motion of fingers/arms. This could be simplified as robust grasping and effective manipulation. The most commonly employed taxonomies and classification methods used to analyze the grasping and manipulation strategies of humans and robots are also presented. We have utilized these taxonomies to analyze the current human/robot performance as well as map the performance capabilities of humans to robots in this study.

Chapter 5

Comparison of Benchmarking Tools, Dexterity Measures, and Metrics

5.1 Introduction

Over the last decade, a lot of research effort has been put into the development of dexterous robotic grippers and hands. However, the lack of common metrics, benchmarks, and scores prevents quantification and comparison of robot dexterity. One of the primary reasons for this is the diverse design features available for robotic grippers that can be varied to create a plethora of robotic end-effectors ranging from simple parallel-jaw grippers to anthropomorphic hands. Even among grippers of a specific design structure, the grasping and manipulation strategies depend on a wide number of parameters such as actuation methods, sensing capabilities, control algorithms etc. Hence there is a need to quantify dexterity based on standardized dexterity metrics and/or a scoring system that encompasses all sets of robotic grippers irrespective of their design parameters. The need for such a quantification framework has been identified and listed by the US National Institute of Standards and Technology (NIST) in a roadmap that discusses the progress of measurement science in robotic dexterity [77].

The dexterity of a robotic gripper is the cumulative effect of two major components: i) The hardware components and ii) the perceptive system. The gripper's physical properties such as the mechanical design, the force exertion capabilities, available degrees of freedom, frictional properties etc., are determined by the hardware components that make up the hand and directly affect the gripper performance. The planning and control of the

robotic system are attributed to the effectiveness of its perception system that captures and analyzes the data captured from the robot's surroundings/environment. The comparison of the effectiveness and efficiency of various grippers requires standardized testing platforms and tasks that are reproducible and scalable to multiple platforms[78]. This standardization can be implemented in the hardware, software, object sets, and/ or tasks used for the benchmarking. The critical requirement of these tests is measurable metrics and replicable results, enabling the comparison effective. These performance metrics allow us to compare the functional and task execution capabilities of the grippers [79].

A number of such benchmarking systems have already been proposed and involve the execution of a variety of tasks under varying circumstances. These can be broadly classified into component benchmarking and system benchmarking. While component benchmarking tries to evaluate a particular component of the robotic gripper, the system benchmarking tests evaluate a robotic system as a whole, taking into consideration the interactions between the components including the robot design, perception, and control among others. A benchmarking system usually defines a structured/randomized test environment, standardized object sets that cover an extensive range of shapes and sizes, initial and final object configurations, the procedure to be followed for the completion of a task and a success metric used to evaluate the performance [80]. Benchmarking scores are usually expressed in terms of i) probability of success and ii) time taken for task completion. The computed benchmarking scores can be used to compare the task completion capability of a given gripper against established standard tasks and time frames. Hence, a comprehensive benchmarking system with diverse environmental conditions is necessary to evaluate a wide range of grippers and their ability to perform different grasping and manipulation tasks. For example, the YCB benchmarking system provides a comprehensive list of daily living objects of varying size, shape, weight, and texture as well as a number of grasping and manipulation tests have been established using this set of objects [81].

Apart from these benchmarking measures, a number of performance indices have also been proposed in the literature to optimize the designs and dexterity analysis of robotic grippers/hands. These indices are used to measure the performance, accuracy, and success rate of the robotic systems. Some commonly used kinematic measures like the manipulability ellipsoids, condition number, isotropy etc., are based primarily on the jacobian matrix. The most widely used index among these is the manipulability ellipsoid, which provides the ability to perform motion in any arbitrary task direction and the correlation between the joint velocities and the end-effector velocity. Another similar index called the manipulability force ellipsoid, evaluates the force/torque transmission

from the joints to the end-effector using the jacobian. There have also been more recent and complex metrics such as the capability map and task completion metric that are independent of the jacobian but can be used to analyze and quantify dexterity.

In this chapter, we present the various metrics and benchmarking assessments available for the evaluation of robotic grippers along with the advantages and disadvantages of each. The remaining of this chapter is organized as follows: Section 5.2 presents the various commonly used benchmarking methods and the various metrics used for analyzing dexterity are presented in section 5.3. The comparison of these metrics, advantages, and disadvantages is discussed in section 5.4, and the conclusion is presented in section 5.5.

5.2 Benchmarking

While the evaluation of robotic grippers lacks a commonly accepted dexterity metric, a number of benchmarking assessments that evaluates the execution of a variety of tasks under varying circumstances are available. These evaluation tests can be broadly classified into component benchmarking and system benchmarking. In component benchmarking, the goal is to evaluate a specific capability of the gripper like perception, control strategy, sensing capability, and force exertion capability among others. System benchmarking, on the other hand evaluates the robotic system as a whole, taking into consideration the interactions between the components including the robot design, hardware, and/or software capabilities in the successful execution of a task. In this section, we discuss some of the benchmarking tests and environments that are most commonly used for the evaluation of robotic grippers.

5.2.1 Benchmarking Standardized Objects

In order to successfully evaluate the manipulative dexterity of robotic hands, it is necessary not only to execute a number of dexterous manipulation tasks but also to examine a plethora of different object shapes and sizes. However, most of the manipulated objects have been generally found to share similar characteristics [82]. Feix et al. had corroborated this fact based on an analysis of video data of daily activities that were executed by household workers and machinists. Most of the objects manipulated by these workers had a weight of less than 500 grams and required a grasp width of less than 70 mm[83]. Hence, the objects used for benchmarking framework may be limited in size and shape adhering to these standards.



Figure 5.1: This figure presents some of the commonly available object sets for benchmarking grasping and manipulation in literature. The image shows objects proposed in the: a) YCB object set [84], ACRV picking benchmark [85], Robocup@home [86], Amazon shelf picking challenge [87] and Modular, Sensorized objects [88].

One of the most prominent benchmarks used for the evaluation of robotic grasping and manipulation is the YCB benchmarking system that has provided an extensive set of standardized objects as shown in figure 5.1a and associated models to facilitate replicable research and evaluation [81]. A benchmarking protocol can be developed using a subset/all of these standardized objects. A number of evaluation protocols and benchmarks have been proposed using the YCB object set to evaluate various grasping and manipulation capabilities of robotic hands and grippers [89, 90]. Robotic competitions

and benchmarks have also proposed standardized objects specific to the features of evaluation protocols. The Amazon Picking Challenge[91] presented the participants with a physical object set that needed to be used for shelf-picking tasks as shown in figure 5.1d. Similarly, the ACRV benchmarking defined a set of 42 commonly available objects shown in 5.1b for shelf-picking tasks deriving from the first Amazon Picking Challenge [85]. On the other hand, Robocup @ home competition that involves object recognition and manipulation in home environments had 30 objects as shown in figure 5.1c categorized into predefined categories that included tableware, cutlery, bags, Disks/books, can be poured, tiny, heavy, and fragile objects among others [86]. Each object is located in a location based on the object category. For example, the cutlery and tableware are located on the kitchen table and the disks/books in a bookshelf, and the tasks involve recognizing and manipulating the objects successfully.

Gao et al. presented a set of modular, sensorized objects equipped with various motion capture markers or sensors that facilitated object motion tracking for the assessment of dexterous, in-hand manipulation capabilities as shown in figure 5.1e [88]. The key feature of this object set is the modular objects can be used to develop variants of soft and rigid objects with cavities that allow for the mounting of markers as well as the variation of the object weight. This allows the test conditions to be varied across different contact conditions and weighted objects while the sensors allow pose tracking of the objects during the execution of the tasks. This provides an insight into the ranges of motion, repeatability, and drift of the system.

5.2.2 Benchmarking Learning and Control Algorithms

A number of open-source simulation suites are available to compare the control strategies and learning algorithms irrespective of their environments. Examples of such suites include the Gazebo, ALE (Arcade learning environment), openAI gym etc. They enable evaluation and comparison of various learning strategies and control algorithms independently of any physical restrictions [92, 93, 94]. Gazebo is capable of reproducing an accurate model of the gripper along with the environments it may encounter using virtual sensors such as tactile sensor, force/torque sensor, and Kinect among others. Many studies have simulated manipulator designs and evaluated their task planning and execution capabilities in gazebo [95]. Similarly, the openAI gym provides a diverse collection of benchmarking tasks and environments with a common interface to compare algorithms. The users can also compare the performance of their algorithms against other algorithms through the openAI website. SURREAL is another open-source scalable framework that includes a manipulation specific simulation suite called the SURREAL Robotics suite

[96]. The suite allows importing new robot models and environments while providing a standard set of robot manipulation tasks with varying levels of complexity that can be used for benchmarking and reproducible robotics research. PyRobot is another open-source benchmarking system that supports Gazebo simulation primarily focusing on hardware-independent APIs for robotic manipulation [97]. Another such toolkit that enables the design, implementation, and deployment of robots to perform everyday manipulation activities is the CRAM (Cognitive Robot Abstract Machine) [98]. Some studies (ROBEL, REPLAB etc.) have also focused on developing a standardized hardware system for the evaluation of control strategies and learning algorithms irrespective of hardware limitations [99, 100]. These benchmarking platforms save valuable time required for the design and build of physical robots and enable evaluating the learning and control algorithms required for robotic manipulation in parallel.

5.2.3 Robotic Competitions

A number of robotic competitions have also been organized in recent years with the intent to evaluate different robotic platforms holistically on their ability to perform a set of tasks sequentially in a given, fixed environment. For instance, 4 out of the 8 tasks evaluated during the DARPA robotic challenge (DRC) involved manipulation as a key element [104]. Figure 5.2a shows the course that evaluated the manipulation capabilities of the robots from their performance of the door task, valve task, wall task, and a surprise task that involved operating a button, electrical breaker switch etc., located within a box [101]. The grasping dexterity test presented by ASTM international evaluates a manipulator's dexterity based on its ability to remove various blocks from an alcove composed of 3 shelves [102]. These objects, not necessarily configured for the manipulator are placed in different orientations as shown in figure 5.2b and the speed with which the blocks are removed determines the overall ability of the manipulator. Another significant grasping and manipulation competition that focuses on evaluating the dexterity of robot grippers and hands based on benchmarking tasks is the Robotic Grasping and Manipulation Competition of the IEEE/RSJ International Conference on Intelligent Robots and Systems. The particular competition is being continuously organized since 2016 [105, 106]. These tasks are performed on a dedicated task board that incorporates four representative classes of industrial assembly tasks [107]. Figure 5.2c shows the task board of the manufacturing track of the robotic grasping and manipulation competition at IEEE IROS 2019 (Macau, China) comprising of the four classes of manipulation tasks: fastener threading, insertions, wire routing, and belt threading & tensioning [43].

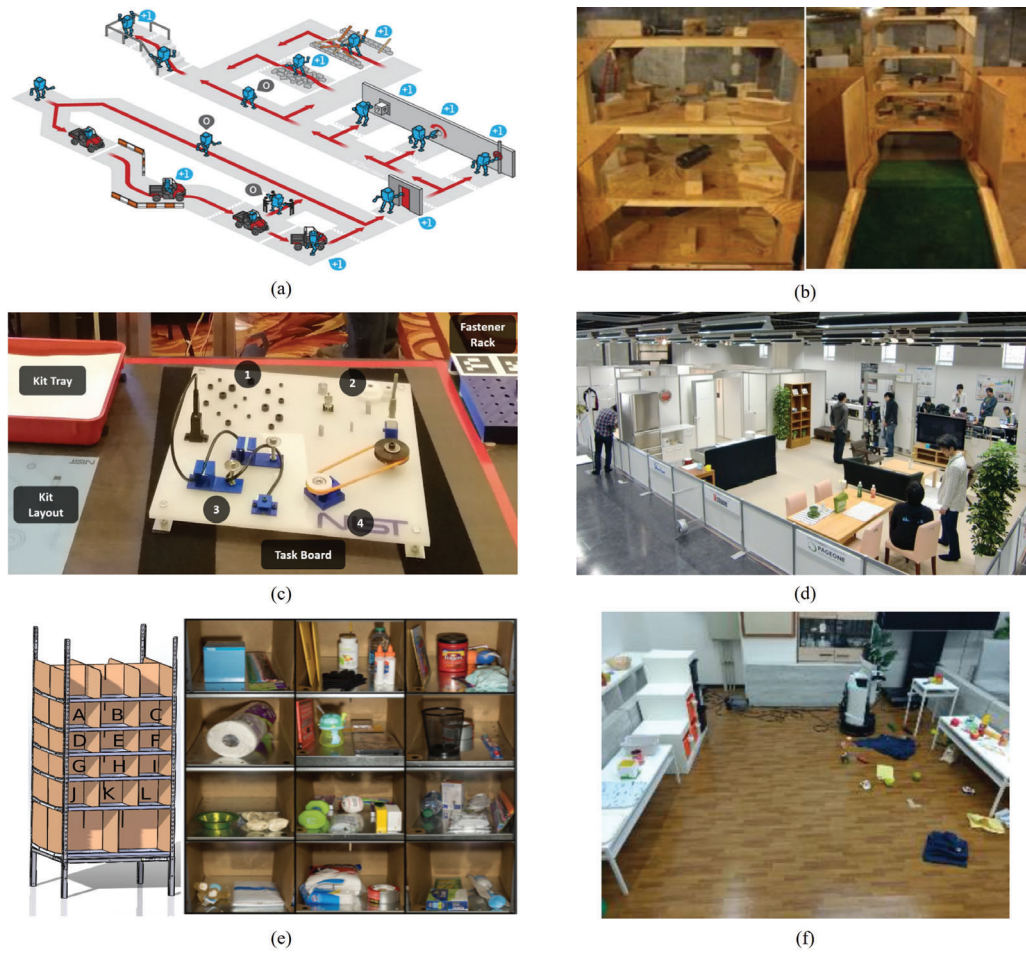


Figure 5.2: A number of robotic competitions were organized over the years to evaluate and standardize robotic grasping and manipulation capabilities. This figure presents the experimental set-up for: a) DARPA robotic challenge [101], b) ASTM grasping dexterity test [102], c) Manufacturing track of grasping and manipulation competition IEEE IROS 2019 [43], d) Robocup @ home [86], e) Amazon picking challenge [87], and f) World robot challenge (WRC) partner robot challenge track [103].

Competitions are also being organized to evaluate the performance of the robots to navigate and interact with a home environment by manipulating household objects. For example, Robocup @ home competition that is organized by the Robocup initiative employs a set of benchmark tests to evaluate robot abilities and performance in manipulation and human-interaction among others in non-standardized home environments that included a bedroom, dining room, living room, and kitchen as shown in figure 5.2d [108]. The tasks varied widely and required the robots to perform a number of manipulation tasks that involved moving tiny and heavy objects, pouring milk without spilling, load-

ing dishes from a table into dishwasher etc [109]. Another competition that focuses on the performance of robots in a domestic environment is the partner robot challenge (Real Space) that is organized as part of the world robot summit[110]. Similar to the Robocup competition, this challenge requires the robots to operate in a living room and dining room set up to manipulate cluttered objects such as clothes, toys, plastic bottles, etc to tidy up the room.

The Amazon Picking Challenge evaluated the shelf-picking capabilities of a robotic gripper from a warehouse shelf. The task involved picking target objects from one of the 12 bins of the shelf stuffed with varied objects as shown in figure 5.2e and placing them in a storage container within a fixed amount of time [87]. Similar to this, the Amazon Robotic Challenge (ARC) evaluates the capabilities of robotic grippers to pick and stock objects in a semi-structured environment representative of the shelves in an Amazon warehouse[111]. The effectiveness of the benchmarking competitions relies on the experiments being carried out following identical experimental conditions and protocols. While this may be organized at physical competitions, it is not possible for all labs to achieve exact experimental conditions. The lighting, space, and environment of the setup might vary across each lab. This might result in slight variations of outcomes. Leitner et al proposed the easily replicable ACRV picking benchmark to overcome this limitation. The test environment consists of a commonly available shelf, an object set, and a detailed protocol that defines the position and orientation of the object placement determined by stencils [85]. Other research challenges and progress with respect to recent robotic grasping and manipulation competitions have been summarised in [112].

5.2.4 Human Dexterity Tests for Robotic Evaluation

The design parameters of the anthropomorphic design are limited to a certain extent as they are designed to resemble the human hand. A plethora of well documented functional and dexterity tests are available to assess the human hands [115]. Hence, a set of standard manual dexterity and functional tests for human hands used in the medical and industrial setups can be used to obtain comparative dexterity measures of anthropomorphic robot hands[116, 117]. Quispe et al adopted these tests for robotic dexterity and classified these benchmark tests into three levels of complexity: physical, dexterity, and functional [40]. These evaluation tests require objects of specific shapes and sizes to be grasped/manipulated by the gripper hands to efficiently complete a set of tasks with speed and accuracy for the evaluation of these tests. This helps evaluate the placing, turning, and assembly capabilities of the gripper.

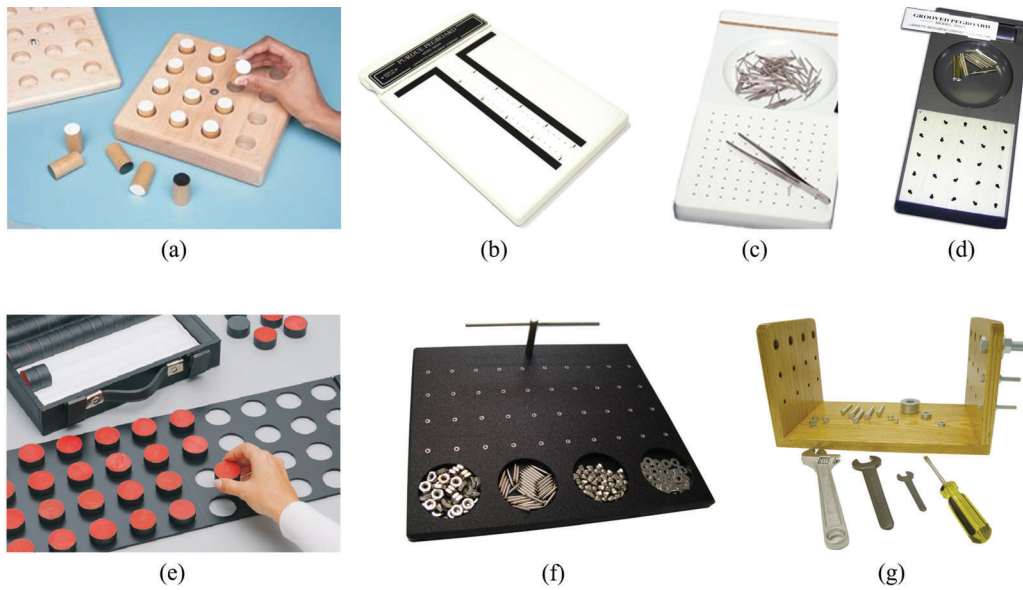


Figure 5.3: The figure presents the various dexterity tests used for manual dexterity evaluation in humans presented in [113, 114]. More precisely, the tests are: a) Functional dexterity test, b) Purdue pegboard test, c) Tweezers dexterity test d) Grooved pegboard test, e) Minnesota manual dexterity test, f) Roeder manipulative aptitude test, and g) Hand-tool dexterity test.

The simplest and most common assessment is the functional dexterity test (FDT), also known as the peg board test. FDT consists of a peg board containing cylindrical pegs arranged in holes. The speed and accuracy with which a hand can pick, reverse, and place the pegs in the holes define its functional dexterity [118]. Variations of the peg board tests require the gripper/hand to pick, manipulate, and place cylindrical pegs of sizes varying from cylindrical pins (Tweezers dexterity test) to large cylindrical wooden pegs (Purdue peg board test, Minnesota manual dexterity test) [119, 120, 121, 122]. Another variation of the pegboard test, the grooved pegboard test involves grooved metal pegs that need to be oriented along key shaped holes dispersed across the board in multiple orientations prior to insertion [122]. Roeder manipulative aptitude test is another dexterity test that focuses on finger dexterity and speed in manipulating four fine components: rods, caps, bolts, and washers [123, 124]. The first phase of the test involves screwing a rod onto the board followed by screwing a cap onto the rod within a fixed time period. The next phase of the test requires adding a bolt and washer alternatively to the T-bar mounted on the board. The score is calculated based on the number of tasks completed across both the evaluation tasks. Furthermore, the hand-tool dexterity test can be used to evaluate the hands' ability to use tools such as wrenches and screwdrivers [125]. The apparatus

consists of two upright walls with one wall mounted with nuts, bolts, and washers. The time required by the subject to successfully move these components from one given wall to the other determines the tool dexterity score. Figure 5.3 presents the various dexterity tests used to evaluate and benchmark manual dexterity in humans that have been adapted for the evaluation of anthropomorphic grippers.

5.3 Metrics and Measures

In robotic manipulation, the ability of the robot to reach optimal points, configurations, and poses within the workspace of the robot determines its manipulative capabilities. A robot capable of performing a task at these ideal points avoiding singularities and degenerative is considered more dexterous. A number of metrics have been proposed to quantify the manipulative capability based on the Jacobian, eigen values, eigen vectors, and transformations of the manipulator. This section summarises such efforts to quantify dexterity.

5.3.1 Metrics based on Jacobian and Manipulability

5.3.1.1 Manipulability Ellipsoid

The manipulability ellipsoid is the most commonly used and widely accepted metric used for robotic dexterity. Though a number of dexterity metrics based on eigen values, eigen vectors, similarity transformations, singular-value decompositions, and the Moore-Penrose inverse of the manipulator Jacobian have been proposed in various literature [126], the most common metric used to measure the manipulation capability of an end effector is the manipulability measure proposed by Yoshikawa [127]. It can be defined as the "capacity of change in position and orientation of the end-effector given a joint configuration". It can be used to calculate the end-effectors' ability to perform a motion in a given task direction and the velocity transmission from joint to task space in a given direction. This measure indicates the distance to singular configuration and can be written as shown in equation 5.1.

$$\mu = \sqrt{\det(J(q)J(q)^T)} = \sigma_1 \sigma_2 \sigma_3 \dots \sigma_n \quad (5.1)$$

where J and J^T are the jacobian and transpose of the jacobian at joint configuration q . The equation shows that the measure can be written as the product of singular values $\sigma_1, \sigma_2, \dots, \sigma_n$. This measure provides a manipulability ellipsoid that is spanned by the singular values of the jacobian and the resultant measure is proportional to the volume of

the ellipsoid [128]. Hence, this measure can be used to determine the ideal postures for robotic hands and fingers that are further away from singular configurations. Figure 5.4 shows the directional position and orientation variability of the end-effector for a given joint configuration of the gripper. There are two common forms of manipulability ellipsoids. The velocity ellipsoid is a measure/relationship of how the linear/angular velocity is transmitted from the joints to the end-effector [127]. And the force ellipsoid measures the transmission of force/torque from the joints to the end-effector [126].

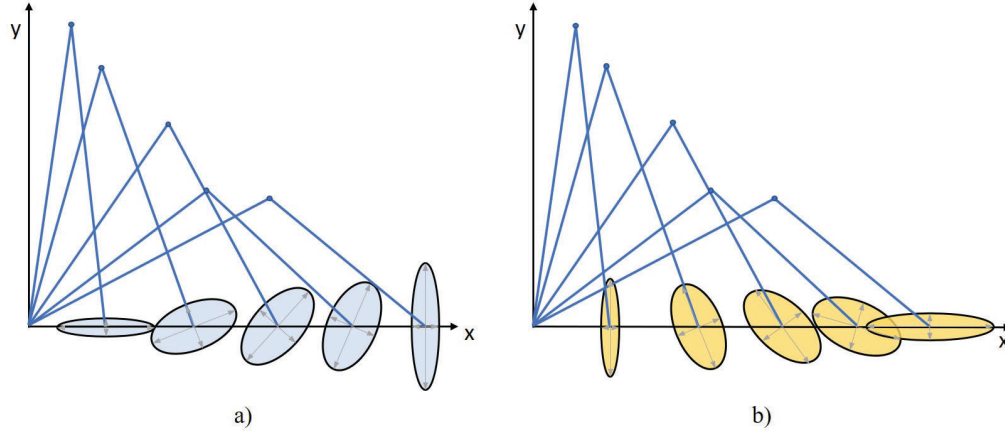


Figure 5.4: Subfigure a) presents the manipulability ellipsoid that defines the directional position and orientation variability of the end effector for a given configuration of the gripper. Subfigure b) presents the force manipulability ellipsoid on the other hand that defines directions with a maximum efficiency in terms of input/output forces

5.3.1.2 Condition Number

In [129], Togai had applied singular value decomposition and perturbation analysis to the jacobian and introduced two new measures, "manipulability" and "sensitivity" based on the condition number of the jacobian. The condition number can be computed using the formula

$$c = \text{cond}(J) = |J| |J^{-1}| \quad (5.2)$$

The term c in equation 5.2 provides manipulability of the gripper that is independent of any scaling factors or the size of J and provides "nearness" to singularities. Equation 5.3 gives the function written in terms of singularities.

$$c = \frac{\sigma_{\max}}{\sigma_{\min}} \quad (5.3)$$

where σ_{max} and σ_{min} are the absolute maximum and minimum singular values. Hence, the conditioning number is greatest when σ_{min} is close to zero and the best manipulability occurs when $c = cond(J) = 1$. The study also introduced another measure called the velocity sensitivity s_q^{ws} given by equation 5.4 which can be defined as the ratio of velocity variation in the workspace to the velocity variation in the joint co-ordinates.

$$s_q^{ws} = \frac{(\text{relative velocity change in workspace})}{(\text{relative velocity change in joint co-ordinates})} \quad (5.4)$$

This measure is determined by the condition number of jacobian c , which determines how the error in joint configuration is translated to the workspace. More precisely, the inverse of the manipulability gives the lower bound of kinematic sensitivity given by equation 5.5.

$$s_q^{ws} \leq \frac{1}{cond(J)} \quad (5.5)$$

5.3.1.3 Isotropic Indices of Jacobian

The isotropic indices measure is based on the manipulability ellipsoids and is the inverse of the condition number. Even for a configuration of a gripper that results in a manipulability ellipsoid with high volume, the velocity/force is not uniformly distributed along all directions. For such conditions, the uniformity/isotropy of the ellipsoid provides more insight into the capability of the gripper than the ellipsoid volume [130]. This quantification is based on the singular value decomposition of the jacobian and is the inverse of condition number as presented in equation 5.6.

$$\Gamma_{iso} = \frac{\sigma_{min}}{\sigma_{max}} \quad (5.6)$$

where σ_{max} and σ_{min} are the absolute maximum and minimum singular values of the jacobian. The best isotropic index is obtained when Γ_{iso} is close to unity signifying the manipulator can transmit velocity uniformly along all directions. Hence, this measure seems more significant compared to the volume of manipulability ellipsoids in determining the performance of a manipulator.

5.3.1.4 Manipulability Polytope

An alternate to the manipulability ellipsoid is the manipulability polytope that transforms the polytope of the range of velocity space to a polytope in task space [131]. Unlike the ellipsoids, the polytope is capable of transforming the joint constraints into task space by

vector addition. If $v_{i,j} = 1, 2, \dots, N_v$ represents the vertex of a polytope in n -dimensional task space with N_v vertex, these vertices form a cone cell. The volume of the i^{th} cone cell is defined in equation 5.7.

$$K_i = \frac{1}{d_n} |\det([v_{k1} \ v_{k2} \dots v_{kn}])| \quad (5.7)$$

where d_n is a constant determined by the dimension of the task space and $[v_{k1} \ v_{k2} \dots v_{kn}]$ is a $n \times n$ matrix and the volume of the manipulability polytope can be calculated using equation 5.8.

$$\omega_p = \sum K_i \quad (5.8)$$

The two dimensional joint velocity spaces overlapped with jacobian row vectors and their corresponding translation to the manipulability ellipsoid and polytope in the task space is presented in figure 5.5.

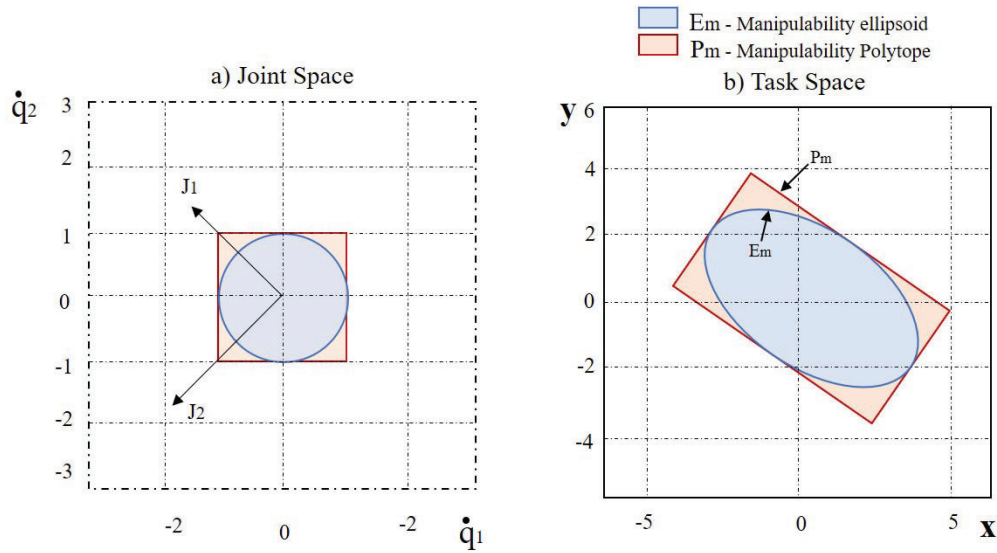


Figure 5.5: Subfigure a) presents the 2-dimensional joint velocity spaces overlapped with jacobian row vectors and subfigure b) presents the corresponding manipulability ellipsoid E_m and manipulability polytope P_m in the task space

5.3.1.5 Dynamic Manipulability Ellipsoid

The dynamic manipulability ellipsoid allows the calculation of end-effector acceleration by taking into account the dynamic parameters of the gripper [126]. Taking into account the arm dynamics under a given constraint, the ability of a gripper in positioning and

orienting the end effector can be calculated by the ellipsoid formed by taking into account the set of all realizable end-effector acceleration. Unlike the simple manipulability measure (μ) that measures the kinematic performance of the end-effector, dynamic manipulability measures its ability to generate acceleration from the joint driving force. The calculation of the dynamic manipulability is shown in equation 5.9.

$$\mu_d = \sqrt{\det[J(M.M^T)^{-1}J^T]} \quad (5.9)$$

where μ_d is the dynamic manipulability measure, J is the Jacobian, and M is the inertia matrix.

5.3.1.6 Power Manipulability Ellipsoid

The above mentioned measures employ kinetostatic indices for the measurement of manipulability and are reliable for grippers that employ only rotational or translational joints. However, the manipulability, condition number, or jacobian matrix indices may not be employable in mechanisms made up of both translational and rotational degrees of freedom due to the dimensional inconsistency among its elements. To overcome these shortcomings, a new measure based on power has been suggested in [132] through a power quadrivector expression given in equation 5.10.

$$\vec{S}_i = \begin{bmatrix} P_i \\ \vec{Q}_i \end{bmatrix} \quad (5.10)$$

where P_i represents the real power component and \vec{Q}_i is a vector comprised of 3 components of reactive power. This expression has been extended to calculate the total apparent power of a mechanism that depends only on the power vector p as shown in equation 5.11.

$$S = \sum_k S_k = p^T \left(\sum_k \sum_{i=1}^4 [\Phi_{i,k} \Phi_{i,k}^T] \right) p \quad (5.11)$$

where S is the total apparent power, the term $[\Phi_{i,k} \Phi_{i,k}^T]$ is positive definite ensuring S is always positive. The performance index can be formulated from this equation as follows.

$$p^T \left(\sum_k \sum_{i=1}^4 [\Phi_{i,k} \Phi_{i,k}^T] \right) p \leq 1 \quad (5.12)$$

Equation 5.12 is the equation of an ellipsoid in power p space. The isotropy of this ellipsoid constitutes the power isotropy performance and its volume, the power volume

performance index. This vectorial representation of power takes into account the orientation of the articulation wrench along with kinematic transmission and states that the articulation wrench needs to be oriented along the articulation axis for better manipulability.

5.3.1.7 Normalised Manipulability Index

One of the key limitations of the manipulability measure is its unbounded nature. It provides the relative measure of the manipulator conditioning at a given point compared to the other points in the workspace. Hence, the maximum manipulability index in the workspace needs to be known in order to evaluate the value of a measure at any given point. To overcome this limitation and make the manipulability index a bounded parameter, the normalized manipulability index (μ_n) as shown in equation 5.13 has been proposed [31].

$$\mu_n = \frac{\mu_i}{\max(\mu_1 \mu_2 \mu_3 \dots \mu_n)} \quad (5.13)$$

where μ_i is the manipulability index as a given point i , and the term $\max(\mu_1 \mu_2 \mu_3 \dots \mu_n)$ calculates the maximum manipulability index among all the points in the workspace.

5.3.2 Metric Based on Workspace

5.3.2.1 Workspace Index

One of the most commonly employed measures of a manipulator's efficiency is the workspace and a number of studies have focused on quantifying manipulator performance based on the workspace [133, 134, 135]. The workspace of a robotic end-effector is calculated primarily based on the kinematic structure, link lengths, and DOF. And this provides vital information regarding the workspace boundaries, optimal placements to avoid singularities, voids, holes etc that can be used for the analysis, design, and optimization of the manipulator performance [133, 136]. Hence, in order to improve a gripper performance it needs to have a well conditioned and dexterous workspace. The manipulator performance varies across the workspace and is not uniformly distributed. This has led to the classification of the workspace volume into two main categories: the reachable workspace and the dexterous workspace.

The reachable workspace is the set of points that can be reached by the end-effector with at least one orientation while the dexterous workspace is composed of a set of points that can be approached from multiple orientations. The dexterous workspace is a subset of the reachable workspace. While the most common metric used to quantify the

workspace is the volume (area for planar manipulators) generated by the set of reachable workspace points, there have also been other measures such as the workspace index used to quantify the workspace. In simple terms, the workspace index is a quantification of the number of workspace points attainable by the manipulator without exceeding physical limitations on the joints [137] and can be calculated using the equation 5.14.

$$WSI = \frac{n_{ws}}{n_G} \in [0, 1] \quad (5.14)$$

where WSI is the workspace index, n_{ws} is the number of feasible workspace points (without exceeding physical limitations), and n_G is the total number of points in the objective workspace. This bounded index varies between 0 and 1, providing us with the percentage of workspace dexterously achievable by the gripper.

5.3.2.2 Dexterity Index

Dexterity index is another performance measure that calculates the dexterity at a given point within the workspace based on its ability to achieve varying orientations at the point [138]. For a given point in the workspace, the manipulator orientation can be defined as shown in equation 5.15.

$$R_{xyz} = R_{x,\gamma} R_{y,\beta} R_{z,\alpha} \quad (5.15)$$

where α, β, γ are the yaw, pitch, and roll angles respectively and vary between $0 - 2\pi$. The range of possible yaw ($\Delta\alpha$), pitch ($\Delta\beta$), and roll ($\Delta\gamma$) angles about a given point determines the dexterity indices about the particular axes. The dexterity index presented in equation 5.16 is the summation of the dexterity indices about each of the axes.

$$D = \frac{1}{3} \left(\frac{\Delta\gamma}{2\pi} + \frac{\Delta\beta}{2\pi} + \frac{\Delta\alpha}{2\pi} \right) \quad (5.16)$$

This can be rewritten as given in equation 5.17.

$$D = \frac{1}{3} (d_x + d_y + d_z) \in [0, 1] \quad (5.17)$$

where d_x, d_y , and d_z are the dexterity indices about the X, Y, and Z axes respectively. This bounded index shows that the points that can be approached from multiple orientations have a higher dexterity index as opposed to points with unique solutions. A dexterity index of 1 at a given point indicates that the end-effector is fully dexterous at the point. Similarly, if one of the dexterity indices d_x or d_y is unity, the gripper can be considered to

be X-dexterous or Y-dexterous respectively at the given point. Similarly, the mean dexterity over a given region of a workspace with N points can be calculated using equation 5.18.

$$D_{Mean} = \frac{\sum D}{N} \quad (5.18)$$

where D_{Mean} is the mean dexterity over the region with N points.

5.3.2.3 Capability Map

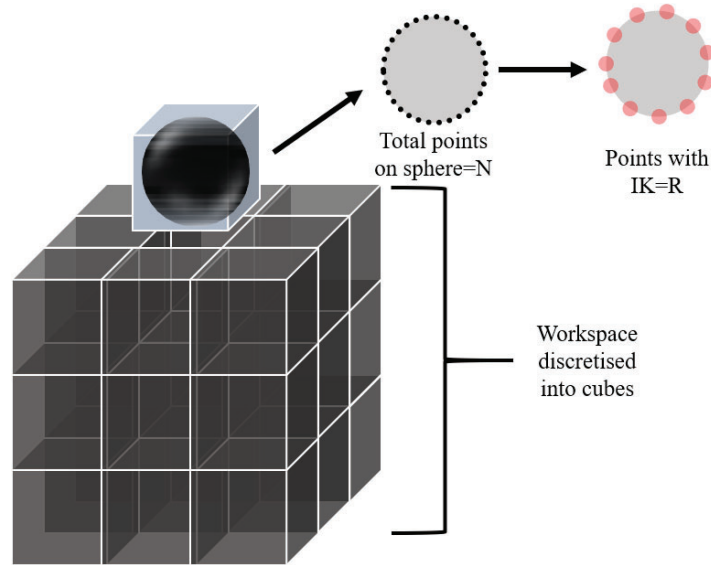


Figure 5.6: Capability map is formed by discretizing the workspace into a number of cubes, sampling each cube and allotting a sphere whose diameter is the same as the dimension on the cube, discretizing the surface of the sphere with points N , and calculating the inverse kinematics feasibility R

The ability of a human hand to grasp and manipulate objects depends heavily on its posture, and the region of workspace where the object is located. These maps/models are developed intrinsically by humans and are used in the successful grasp and manipulation of objects by determining the location of the object on the map, the direction of grasp approach, and the best posture for the task. Similar to this, the capabilities of a manipulator in the robot's workspace were shown to be structured and captured in a map called the Capability map in [139]. This map is anchored to the arm base and indicates the subspace within the workspace where versatile grasping and/or re-grasping is feasible, thereby extending the manipulative capabilities of the gripper. It also helps determine the direction of the grasp approach and path planning for a given task. This is achieved by

discretizing the workspace into multiple cubes for task planning, randomized sampling the configuration space, inscribing a sphere into each cube with N sampling points, and calculating the inverse kinematics as shown in figure 5.6. Once this is achieved, the percentage of the sphere with an inverse kinematic solution is calculated using the formula given in equation 5.19.

$$I_r = \frac{R}{N} \cdot 100 \quad (5.19)$$

where I_r is the reachability index, R is the number of points on the sphere with inverse kinematic solution, and N is the total number of points on the sphere. These spheres are then colored based on the reachability index to create the Capability map based on shape primitives. This map can be used to solve the positioning of the robot base, approach, path planning, grasp/re-grasp, and effective manipulation resulting in dexterous manipulation.

5.3.3 Other Performance Metrics

5.3.3.1 Metric Based on Cartesian Pose Control Error

This metric is a kinematic measure used to quantify the in-hand manipulation capability of a gripper. The metric calculates the control error between the desired and measured object pose in the Cartesian space over a time varying trajectory. The resulting control error is used to define the in-hand manipulation efficacy of the gripper [140]. Only the pose of the object is used as a control variable and other dependencies such as finger configuration and contact positions are not considered. The grasped Cartesian pose of the object at initial time t_0 is given by $r_c(t_0) \in \mathbb{R}^{6 \times 1}$. The hand is then required to manipulate the object along as many of the 6 independent axes along a desired Cartesian trajectory $r_{cd} \in \mathbb{R}^{6 \times 1}$ which is given by equation 5.20.

$$r_{cd} = [x, y, z, \gamma, \beta, \alpha] \quad (5.20)$$

where x, y, z are translations and γ, β, α are the rotations about the X, Y, and Z axes respectively. The object needs to be translated and rotated along each axis in both the positive and negative direction from the initial condition. An example of the desired time varying cartesian trajectory is given in equation 5.21.

$$r_{cd,i}(t) = A \sin(2\pi f t) + r_{c,i}(t_0) \quad (5.21)$$

for $i = 1, 2, \dots, 6$

where A is the magnitude of motion and f is the frequency expressed in motion cycles per second, and t is the time in seconds. The total error e_{total} given by equation 5.22

calculates the error between the desired pose and the actual pose of the object over time for the duration of the test.

$$e_{total} = r_{cd} - r_c \quad (5.22)$$

The Root Mean Square error of e_{total} , $RMSE_{e_{total}}$ gives the measure of the manipulation efficacy of the gripper. The lower the value of this measure, the better the in-hand manipulation capability of the gripper.

5.3.3.2 Metric Based on Task Completion

One of the most commonly used measures based on tasks is the stability and Mean picks per hour (MPPH). These picks are characterized by three R's: rate, reliability, and range (class of objects) [80]. This has been written mathematically in equation 5.23.

$$E(\rho) = v * q(\text{mean over } N \text{ grasp attempts}) \quad (5.23)$$

where $E(\rho)$ is the mean picks per hour (MPPH), v is the mean grasp rate, and q is the probability of success for given grasp attempts. And the mean grasp rate which is dependent on the time taken for robot sensing (r_s), computation(r_c), and motion(r_m) can be written as shown in equation 5.24.

$$v = \frac{1}{(r_s + r_c + r_m)} \quad (5.24)$$

However, these metrics do not encompass the quality and success of the final task completion which is the primary goal of robotic manipulation. Along these lines, Ortenzi et al had proposed a new metric that can adjudge the quality of the manipulation task by embedding not just the features of grasping necessary for successful manipulation but also dependent on the manipulation task [141] as shown in equation 5.25.

$$\rho = f(t) \times g(f_g, u_g, y_g, l_g | t) \quad (5.25)$$

where t is the task, $f(t)$ is a boolean function that returns either 0(task failed) or 1(task successful) based on task completion. f_g is the grasping force, u_g is the grasp velocity, y_g is the grasp type and l_g is the grasp location. The term $g(f_g, u_g, y_g, l_g | t)$ returns a value between 0 to 1 based on how good the grasp contributes towards the outcome of the task t . The function g is determined based on the output requirements of task t . For a task that requires speed over accuracy, then the speed term u_g will contribute more towards the metric. This metric not only helps determine the quality of grasps/manipulation but also helps in grasp selection that will benefit the manipulation task.

Table 5.1: Summary of the various commonly employed metrics to evaluate manipulation is presented along with the advantages and limitations.

Metric	Based on Jacobian	Description	Advantages and/ Limitations
Manipulability Ellipsoid	✓	Arbitrary change in end-effector position and orientation calculated for a given joint configuration. Can be used to calculate postures further away from singularity.	Capable of transforming i) linear/angular velocity (velocity ellipsoid) ii) force/torque (Force ellipsoid) from joints to end-effector. Joint constraints not taken into account.
Condition number of Jacobian	✓	Provides manipulability of gripper based on the conditioning number of Jacobian (J). Also, captures how the error in joint configuration is translated to workspace (sensitivity).	Provides manipulability and kinematic sensitivity independent of scaling factors of Jacobian.
Isotropic indices of Jacobian	✓	Calculates the uniformity/isotropy of ellipsoids based on SVD of Jacobians. Shows how uniformly the gripper can transmit velocity/force within the ellipsoids.	Provides more insight into the capability of the gripper than the volume of ellipsoid.
Manipulability polytope	✓	Transforms range of polytope in velocity space to a polytope in task space.	Capable of transforming joint constraints into task space by vector addition.
Dynamic Manipulability Ellipsoid	✓	Ellipsoid formed by set of all realizable end-effector acceleration is used to determine the ability of a gripper in positioning and orienting the end effector.	Takes dynamic parameters of the gripper into account to calculate the end-effector acceleration.
Power Manipulability Ellipsoid	✗	A power quadrivector is used to compute the ellipsoid in power space. This ellipsoid is constituted of the power isotropy performance and power volume performance index.	Can be used in mechanisms composed of a combination of translational and rotational degrees of freedom overcoming dimensional inconsistency.
Normalised Manipulability Index	✓	Normalizes the manipulability of an end-effector across all the points in the workspace.	Converts manipulability into a bounded measure.
Workspace Index	✗	Quantification of number of workspace points attainable without exceeding physical limitations of manipulator.	Bounded index that provides percentage of dexterous workspace.
Dexterity Index	✗	Calculates the dexterity of points in the workspace based on the orientation angle range that can attain the specific points.	Can be used to calculate the dexterity over a region of workspace based on dexterity indices about individual axis.
Capability Map	✗	Structured grasping and manipulation capabilities in a robot's workspace is captured in a map. By discretizing workspace into multiple cubes, inscribing spheres into each cube with sampling points and calculating inverse kinematic solutions for each point.	This map indicates subspace within the workspace where versatile grasping/ re-grasping is feasible. Also helps solve direction of grasp approach and path planning.
Metric based on Cartesian pose control error	✗	Control error between the desired and measured object pose in the Cartesian space over a time varying trajectory is calculated. The resulting control error is used to define the in-hand manipulation efficacy.	Manipulation efficacy of gripper is calculated using object pose as control variable. Independent of dependencies like finger configuration and contact positions.
Metric based on task completion	✗	A function based on the grippers grasping force, speed, grasp type, and grasp location is used to determine the ideal grasp for a given manipulation task.	Can be used not only in grasp evaluation but also in grasp synthesis for any given task thereby increasing the probability of success for a manipulation task.

5.4 Comparison and Discussion of Benchmarks and Metrics

The efficiency of a benchmarking system to compare various grippers relies on standardization and reproducibility of i) Test environment/platform, ii) Object sets, iii) Task execution description, iv) Evaluation measures/scoring methodology. Most robotic competitions and functional evaluation tests ensure standardized test environments by providing a rig/platform on which the task is to be executed. While this ensures the reproducibility in

terms of environment, the resulting benchmark restricts the object to a well-defined final orientation that remains constant across all trials. And almost all of these test boards/rigs are stationary. Thus the performance of the grippers on these platforms might not be an indicator of real-life scenarios where the orientation of the object changes continuously. Moving obstacles are also a major component in an industrial setting that has not been replicated in these test environments. Exact environmental conditions such as lighting, space etc., can not be replicated across all labs. While this might result in slight variations of outcomes, the robotic grippers need to be ultimately able to perform tasks across various platforms and environments.

Most benchmarking systems provide standardized object sets and associated models that can be replicated efficiently. However, most evaluation tests are specific to a limited range of object shapes and sizes. Benchmarking protocols must include a wide range of objects shapes and sizes associated with everyday living and industrial settings to enable a comprehensive benchmarking system. Incorporating objects with sensors as proposed in [88] would allow pose tracking throughout the task execution allowing comparison of repeatability and drift. The Task description must provide sufficient details regarding the initial and final position/orientation of the objects, task execution methods, and limitations if any to be followed during the task execution. For example, the task description must include if the initial condition is structured/ random, followed by the target final position/orientation, the sequence in which the test needs to be carried out, and limitations like the workspace within which the task is to be completed. In order to ensure the effectiveness of the benchmarking system, a set of standard operating and evaluation procedures need to be provided. The evaluation protocol must detail what constitutes a successful task completion and the scores that need to be awarded for complete/partial task execution, the penalty for mistakes during task execution etc., The evaluation methodology and scoring sheets must be provided to ensure the tests are organized and scored under sufficiently similar conditions. Given the extensive variety of robotic grippers and hands, there is a need for a common benchmarking platform to quantify dexterity irrespective of the design parameters. Such a benchmarking platform would allow a comparison of the various grippers and their dexterous manipulation capabilities.

A number of metrics have also been defined in literature to evaluate the grasping and manipulation efficiency of robotic grippers. Kinetostatic performance indices like the jacobian matrix, manipulability ellipsoids, and condition number have been employed in several studies for dexterity analysis, trajectory planning, and design optimization among others. These studies focus on various methods to identify the optimal configuration of the grippers by calculating the task execution capability of a manipulator in a

given configuration and its "nearness" to singularity. Manipulability ellipsoid is the most commonly used index that is used to determine how far a given configuration is from a singularity. Further, the condition number of the jacobian can also be used to calculate the "nearness" to singularity and compute optimal postures for grippers. While the volume of the manipulability ellipsoid provides a scalar value, the isotropic indices provide better insights of the force/velocity transmission of the gripper by calculating the uniformity/isotropy of the ellipsoids as the velocity/force is not uniformly distributed along all directions. A limitation of the manipulability ellipsoid is its inability to transform joint velocity constraints to the task space. This can be overcome by employing a manipulability polytope that adopts a scaled jacobian matrix in place of a conventional jacobian matrix enabling the transformation of joint constraints into task space by vector addition. This also helps avoid the false optimal direction of motion in task space.

The set of all realizable end-effector acceleration is used to calculate the Dynamic manipulability ellipsoid. This measure can help determine the ability of a gripper in positioning and orienting the end effector taking the arm dynamics into account under a given constraint. All of these measures employ kinetostatic indices for measurement and can provide reliable results for grippers employing only rotational or translational joints. To overcome this limitation and obtain meaningful results for mechanisms employing both translational and rotational joints, the power manipulability ellipsoid can be used. This measure employs a power quadrivector to calculate the ellipsoid in power space, thereby overcoming dimensional inconsistencies as power has the same physical unit in translations and rotations. One key limitation of the manipulability based measures is their unbounded nature and the inability to provide an absolute measure. This can be overcome by applying the normalized manipulability index that provides a bounded measure of the end-effector's manipulation capabilities.

The manipulator workspace is another key performance analysis measure used to evaluate manipulator capability. The manipulator workspace provides insights about the optimal placement of the manipulator that can help maximize the workspace volume. Apart from the volume of the workspace, the conditioning of the workspace is important for the efficient manipulation of the objects across all regions of the workspace. This can be calculated from the workspace index that provides a ratio of dexterous workspace points. Further, the ability of the gripper to reach the workspace points from varying orientations can be calculated using the dexterity index. Another metric called the capability map stores the capabilities of the gripper in the various region of its workspace in a structured map and helps successful manipulation by determining the locations of the object on the map, the direction of the grasp approach, and the best posture for the given

task. This map anchored to the arm base provides subspaces where versatile grasp/re-grasp is feasible and can be used to plan the positioning of the robot base, path planning, approach, and manipulation strategies resulting in dexterous manipulation.

Differing from the above kinetostatic measures, a recently introduced kinematic measure based on the control error between the desired and measured object pose in the cartesian space enables the quantification of the in-hand manipulation capability of a gripper. The main advantage of this measure is its use of the pose of the object as the only design variable and dependencies such as finger configuration and contact positions are not considered. Measures based on task completion in general evaluate grippers based on mean picks per hour (MPPH) and the mean grasp rate ignoring the quality and success of the final task completion. However, a recent metric based on grasp features like grasp type, force, velocity, and grasp location taking into account the contribution of the grasp towards the successful completion of a given task has been proposed in the literature. Such a metric helps in grasp selection while also determining the quality of manipulation capabilities in the successful execution of tasks.

5.5 Conclusion

In this chapter, we presented a comprehensive review of the most commonly used benchmarking tools and manipulation metrics for the evaluation of robotic grippers and hands. The benchmarking protocols can be used to evaluate various grippers based on their performance under a standardized i) Test environment/platform, ii) Object set, iii) Standardised task execution, and iv) Evaluation and scoring methodology. This enables a standardized scale for the comparison of various grippers independent of their design parameters. However, most studies are limited by the object range being evaluated and the fixed final orientation of the objects on a stationary rig. This is not representative of real life home/industrial scenarios where there are often moving platforms and obstacles requiring the gripper/hand to grasp/re-grasp and re-orient during the approach to complete the task successfully. Hence, a comprehensive benchmarking system incorporating the features of a wide range of object sets and tasks specifically designed for robotic grippers with a dynamic platform would enable the ideal evaluation and comparison of robotic grippers/hands.

On the other hand, a number of performance indices and measures of robot dexterity such as the manipulability ellipsoids, manipulability polytopes etc., are used to evaluate robotic manipulators. Most of these measures are dependent on kinetostatic measures like the Jacobian matrix, manipulability or condition number. The advantages, limitations, and approaches used to overcome these limitations have also been discussed.

The localised and bounded nature of these measures can be overcome by normalization, employing a scaled jacobian matrix or metrics that are not dependent on the jacobian. Manipulator measures used to evaluate the volume and conditioning of the manipulator workspace can help in the ideal positioning of the bases that can help avoid singularities and maximising the efficiency of the gripper within its workspace. These include metrics like the workspace index, dexterity index, and the capability map, that evaluate the manipulative capabilities of the gripper at specific regions within the workspace. Studies have also focused on adjudging the quality of manipulation tasks by embedding the features of grasping required for successful manipulation in the completion of specific manipulation tasks. Apart from evaluating manipulation capabilities, these metrics and indices are also employed to improve the manipulation capability. These metrics can be used for deciding the ideal posture, trajectory planning, and grasp selection within the workspace of the gripper as well as for dexterity analysis and design optimization resulting in better design parameters.

Part III

Analysis, Evaluation, and Comparison of Human and Robot Dexterity

Chapter 6

An Accessible, Open-Source Dexterity Test: Evaluating the Grasping and Dexterous Manipulation Capabilities of Humans and Robots

6.1 Introduction

Over the last decade, a plethora of studies have focused on the development of dexterous robotic grippers and hands. However, the lack of a standardized definition and methods or tools for assessing and evaluating dexterity has resulted in researchers considering increased adherence to human-likeness to also offer increased dexterity, as discussed in [32]. This can be particularly attributed to the lack of appropriate dexterity metrics that properly define the various aspects of dexterity and quantify how dexterous specific robotic end-effectors are [117]. A tool or method for evaluating dexterity is of paramount necessity not only for designing new highly capable robotic end-effectors but also for evaluating the skillfulness of humans in a variety of settings and application domains. Examples of such applications include post-injury rehabilitation assessment and standard skill assessment for specific professions (e.g., surgeons, pilots, construction workers etc.).

Human hand dexterity is generally defined as the ability of the hand to perform a desired motor task precisely and deftly with ease, and skillfulness [24, 23]. Various func-

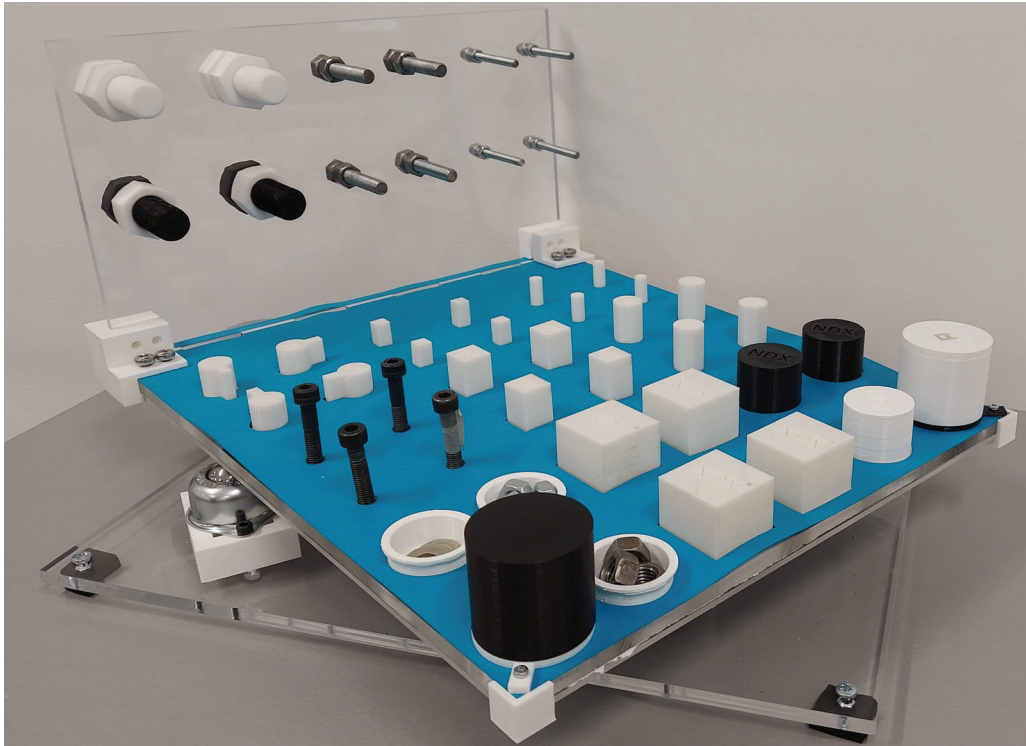


Figure 6.1: Prototype of the proposed dexterity test board that is equipped with a rotating base mechanism. The board is developed using plastic parts that are 3D printed and acrylic parts that are fabricated using laser cutting.

tional evaluation tests have been employed by researchers over the years to assess and evaluate the dexterity of the human hand [22]. These tests can quantify the functional performance of human hands based on the ability of subjects to complete a wide range of tasks and industry specific tests. The outcomes of these dexterity tests can also serve as a valid indication of residual hand function after a severe injury or stroke, in addition to being an evaluation of skillfulness. It is a common practice in industrial settings to use these dexterity tests for the purpose of screening and selection by evaluating the workers' manual dexterity potential. The degree of improvement or the deterioration of hand functions during rehabilitation can also be determined by clinicians and researchers employing such tests [46]. However, each of these tests is limited to a specific object range and task category. Also, most of these tests rely on stationary platforms and require the task to be completed in only one specific orientation. It is evident based on the analysis and discussion of the related work that there are a number of significant hand assessment tests that evaluate specific aspects of dexterity. However, there is a lack of comprehensive, holistic tests that evaluate dexterity as a whole and can be adapted to evaluate the capabilities of both robotic grippers and hands as well as human hands.

Robotic dexterity is generally being defined as the "*capability of changing the position and orientation of the manipulated object from a given reference configuration to a different one*" [5]. The structure of robotic grippers varies widely from simple two-fingered parallel-jaw grippers to highly complex anthropomorphic hands. Even within a class of grippers, the design parameters vary widely. These variations have resulted in the lack of a common evaluation platform, benchmarks, metrics, and scores to evaluate the dexterity of robotic hands. Hence, there is a need for a dexterity assessment test that can evaluate the performance of robotic end-effectors, irrespective of their design parameters. This need has also been identified in a roadmap that discusses the measurement science progress in quantifying robotic dexterity [77].

The various factors that contribute to robot dexterity are: i) the dexterity and skillfulness of robotic hardware components and ii) the effectiveness of the perception and control system employed by the robotic system in the execution of dexterous tasks. The hardware component dexterity takes into account all the physical properties of the robotic gripper or hand, such as the mechanical design, the available degrees of freedom, the force exertion capabilities, the frictional properties etc., that contribute directly towards the grasping and manipulation performance of the system. The perception system on the other hand, encompasses all the data that is captured and analyzed based on the information collected from the environment/ surroundings of the robot, affecting the performance of the planning and control schemes of the robotic hardware system. In general, advanced sensing systems and complex control architectures have been deemed necessary for the execution of robust grasps and for the successful manipulation of a wide range of everyday life objects. However, a number of recent studies have demonstrated dexterous in-hand manipulation capabilities by employing underactuated, adaptive robot hands with minimal sensing and simple control schemes [142, 143]. The lack of commonly accepted methodologies to compare new algorithms and hardware across different robotic platforms is a topic of discussion in various workshops and forums organized by the robotic grasping and manipulation community [40, 144]. Our previous work involved developing a series of tests to evaluate the dexterity of humans and robotic grippers on a static platform [145]. We have expanded the work to include a dynamic environment and more complex manipulation tasks. In particular, in this work, we propose:

- A modular, accessible, open-source dexterity test that consists of a horizontal and vertical rig on which the manipulation tasks are to be performed. The rigs are mounted on a rotating module to simulate assembly task environments that require the tasks to be performed in varying orientations or in dynamic situations with varying obstacle spaces.

- A comprehensive set of tasks that evaluate the grasping and manipulation capabilities, and therefore the dexterity, of human and robotic hands. The proposed tasks range from simple pick and place to complex dexterous manipulation tasks.
- Evaluation protocols that provide quantitative dexterity metrics based on success rates and speed efficiency.
- A baseline score based on the analysis of human trials with and without tactile feedback.

The proposed dexterity test can serve as a valuable evaluation tool for determining the manual dexterity of human hands and for measuring the improvement in human hand function post-injury. It can also evaluate the performance of robotic hands based on their ability to complete a task irrespectively of their individual design parameters, control systems, and sensing capabilities. The proposed dexterity test uses well-defined measures of success (ability to complete a task successfully) and speed efficiency (time taken to perform a set of tasks) [40], to calculate the overall performance of the human hand and robotic grippers¹.

The rest of the chapter is organized as follows: Section 6.2 presents the related work that focuses on benchmarking dexterity, Section 6.3 presents the design of the dexterity test, section 6.4 introduces the dexterity metrics used for the formulation of the benchmarking system, section 6.5 discusses the validation of protocols and the baseline scores generated from human and robot experiments, while section 6.6 concludes the chapter and discusses some potential future directions.

6.2 Related Work

A plethora of dexterity tests have been proposed in the literature to assess the dexterity and functionality of human hands [115]. The development of such tests has helped in the evaluation of manual dexterity and the contribution of various hand anatomy attributes toward functional performance. Each of these dexterity tests requires the human hand to use various strategies for the successful grasping and manipulation of objects of specific shapes and sizes. The most commonly used assessment, the functional dexterity test (FDT) requires the hands to pick up cylindrical pegs placed in holes of a peg board and

¹Majority of the chapter is based on [146], © 2022, Frontiers. Reprinted, with permission, from Nathan Elangovan, Che-ming Chang, Geng Gao, and Minas Liarokapis, An accessible, open-source dexterity test: Evaluating the grasping and dexterous manipulation capabilities of humans and robots, Frontiers in Robotics and AI, 2022

invert them. This evaluates the ability of the user in performing a dynamic 3-jaw chuck prehension [118]. This is a common form of a pegboard test. A number of variations of this test involving a number of test boards and objects have been described in section 5.2.4. These tests evaluate the speed and accuracy with which the hands being evaluated can pick, place, re-orient, and assemble objects of varying shapes for the completion of a task.

Each of these tests is specific to particular object shapes and sizes and hence cannot be accepted as a generic dexterity score. Moreover, all these tests are performed on a stationary board/rig that has a fixed orientation throughout the evaluation. This is far from real world scenarios where the hands will need to adapt to a wide range of orientations. Hence, in order to successfully evaluate the human hand function, tasks presented should require the hand to perform tasks in a wide range of hand configurations or even in a dynamic environment with a dynamic obstacle space. These functionality evaluation tests have been adopted by studies focusing on anthropomorphic robots to quantify the dexterity of robotic grippers, comparing them with their human counterparts [116, 117]. A taxonomy of robotic manipulation benchmarks derived from the aforementioned studies has been proposed by Quisepe et al., classifying robot dexterity tests with three levels of increasing complexity: physical, dexterity, and functional tests [40].

There are also certain evaluation tests developed exclusively for robotic dexterity evaluation that can be broadly classified into component benchmarking and system benchmarking. These tests require the robotic grippers to perform a set of manipulation tasks with a variety of objects under specific circumstances. As the name suggests, component benchmarking focuses on specific components used for robotic grasping like perception, control, mechanical hardware design etc. The system benchmarking on the other hand evaluates the capability of a complete robotic system as a whole to successfully execute tasks and has been the focus of a number of studies. Benchmarking studies pivot around the reproducibility, adaptability, and scalability of the benchmarking environments and procedures to various platforms [78]. Hence, studies have focused on standardizing the testing platforms, objects, environments, and software.

A gripper that can successfully grasp and manipulate a wide range of different objects is generally considered to have a higher dexterity. Hence, a number of studies have proposed a standardized set of objects that range in size, shape, and weight to facilitate replicable benchmarking systems. Section 5.2.1 details the various object sets employed for creating benchmarking protocols by the robotics community. Efforts have also been made to compare the control strategies and learning algorithms irrespective of the physical limitations of the end-effector. Such efforts discussed in section 5.2.2 include

both virtual simulation suites and standardized hardware systems that enable hardware independent performance benchmarking of control and learning strategies proposed by various studies.

In recent years, a number of robotic competitions have been organized with the intent to holistically evaluate different robotic platforms based on their ability to perform a set of tasks sequentially in a given, fixed environment. Each competition aims at comparing and benchmarking the grippers' capabilities in executing specific tasks that are representative of a given environment. For example, the challenge could evaluate the capabilities of robotic grippers in performing a variety of tasks in a warehouse environment [111], home environment [108], a manufacturing board [107] etc. Some of the prominent competitions organized in recent years are discussed in section 5.2.3.

Apart from the above-mentioned studies, a number of recent studies have proposed dexterity tests consisting of various object sets with the objective to evaluate and quantify specific aspects of dexterity. The features of these tests and how they compare with the test proposed in this study are presented in the results section. Gonzalez et al. designed a Variable Dexterity Test (VDT) that consists of 4 subtests, each specifically designed to evaluate a particular type of grasp like the precision, cylinder, spherical, and extended spherical [147]. Another dexterity measurement kit proposed by [148] focuses on the evaluation of pinch grasping capabilities of the fingers based on insertion, twisting, and locking tasks on a spring-loaded wooden box. A simple and fast dexterity test for the evaluation of hand function called the peg test was presented by Noel et al., [149]. More recently a 3D printed platform that combined the features of multiple dexterity tests like the Box and Block test (BBT), Nine-Hole Peg test (NHP), and grooved pegboard tests for the evaluation of fine manipulation and grasping capabilities has been proposed [150].

Despite the plethora of studies focusing on benchmarking dexterity, there is a lack of commonly accepted evaluation systems across the robotics community. Given the increasing interest in the design and development of dexterous robotic grippers and hands, there is a need for a common benchmarking platform to quantify dexterity irrespectively of the design parameters. In our previous work, we had proposed an evaluation system that encompasses and builds upon important characteristics from the various commonly accepted dexterity evaluation methods reviewed [145]. We further expand this work to include more complex manipulation tasks involving a dynamic rig that requires the object orientation to be changed constantly and a new set of objects.

In particular, in this work, we propose a dexterity test that can evaluate the performance of a plethora of end-effectors solely on their task completion ability and speed of execution irrespectively of individual design parameters like the number of fingers,

actuators used, or control systems employed. Hence, it can be used to benchmark different classes and types of grippers and hands. For example, it can be used to evaluate the efficiency of devices such as suction grippers, parallel jaw grippers, two-fingered or three-fingered adaptive end-effectors, and anthropomorphic robot hands among others. The proposed dexterity test is equipped with both horizontal and vertical components that contain regions of specific manipulation tasks and objects that have been designed as described in section 6.3. A key aspect of this test is the ability to rotate, changing the position and orientation of the slots, requiring the hand to re-orient and re-position the objects in order to successfully complete the tasks. This simulates a dynamic assembly environment. The most important characteristic of the various benchmarking systems is a set of standardized objects that is representative of the set of objects encountered in industrial and home environments. However, most of the manipulated objects have been generally found to share similar characteristics [82]. This fact has also been corroborated by Feix et al., using video analysis of daily manipulation activities executed by household workers and machinists. Most of the objects manipulated by these workers had a weight of less than 500 g and required a grasp width of less than 70 mm [83]. Deriving from these insights, a set of standardized objects have been proposed for evaluation as described in section 6.3.2. The types of objects used (sizes, shapes etc.) were chosen from the state of the art dexterity tests that were proposed to evaluate specific aspects of manual/gross dexterity in rehabilitation and industrial settings. These tests provide insights on a subject's ability to perform activities of daily living based on their performance in handling/manipulating simple objects like cylindrical pegs, cuboid blocks etc. For example, the Functional Dexterity Test (FDT) can assess the subject's capability in executing functional daily tasks involving any object that requires 3-jaw chuck prehension based on a simple test performed with cylindrical pegs [118]. Although the simple shapes of the objects may result in simple to secure grasps, the proposed tasks require the objects to be manipulated and assembled onto a rig that could also be moving. This requires the hands to re-orient the objects as they approach the rig. The designated holes for the examined objects have low tolerances during assembly. Thus, the complexity of the task and the dexterity required for its execution are considerable. The complexity increases further during the execution of fine-manipulation tasks like fastening nuts onto bolts when they are in motion or performing thrust and twist motions to screw threaded pins into heat inserts etc., Assembly and disassembly of the puzzle tasks also require the hands to manipulate the outer covers of the puzzle by navigating them through a complex trajectory track on the inner block. Hence, this test can evaluate a wide range of manipulation capabilities using the simple set of objects proposed.

A set of standard operating procedures for task execution during the evaluation tests has been prepared so as to ensure the effectiveness of the benchmarking system. The sequence and conditions in which the test needs to be carried out are presented in section 6.3.3 to ensure that the tests are organized under sufficiently similar conditions. Each set of experiments is repeated 3 times. The results of the three trials are used to examine the effect of familiarity to the tasks and the effect of mastering (over time) the manipulation capabilities. The evaluation method is described in section 6.4 and the scoring sheet is also made available. The proposed evaluation system is validated and baseline scores for the evaluation system are determined based on human evaluation trials and the results are presented in section 6.5. Section 6.6 concludes the chapter.

6.3 Design of Dexterity Board

6.3.1 Dexterity Rig Development

The dexterity rig, as shown in Figure 6.1, is made up of a horizontal plate (450 x 350 mm) that is split into nine manipulation regions (HA1-HA9) and a vertical plate (350 x 200 mm) made up of three manipulation areas (VA1-VA3) shown in Figure 6.4. Each plate has a thickness of 10 mm. Each part of the region is specific to a given set of objects and tests. Corner brackets are used to attach the vertical plate to the horizontal plate. The assembled rig is placed on a flat surface so as for the horizontal plate to be parallel to the surface as shown in Figure 6.2 and to have enough space to the right of the rig where the objects can be dropped. This initial version of the rig was stationary and had a total of 19 different manipulation tasks. This meant that irrespective of the number of trials performed by the human hands or robotic end effectors, the end position and orientation of the objects remain fixed on the board. Hence, the tasks could be completed much faster during repeated trials. However, this was not representative of real life assembly/home environments where the target location/orientation changes every single time and might be dynamic as well. To overcome this limitation, a second version of the rig that is dynamic in nature was designed as shown in Figure 6.3.

For this purpose, the assembled test board is mounted onto a rotating base unit using a gear and lazy Susan mechanism that enables the entire test board to be rotated. The base mechanism is equipped with a Dynamixel XM430-W350 motor with a pinion gear mounted on it to drive the gear attached to the horizontal rig. This allows the test rig to be rotated at varying speeds in either a clockwise or anti-clockwise direction. The base unit is fixed to a base plate that also has three inverted caster wheels supporting the horizontal rig plate, enabling smooth rotation of the rig. The exploded view of the proposed mech-



Figure 6.2: A prototype of the initial version of the dexterity board.

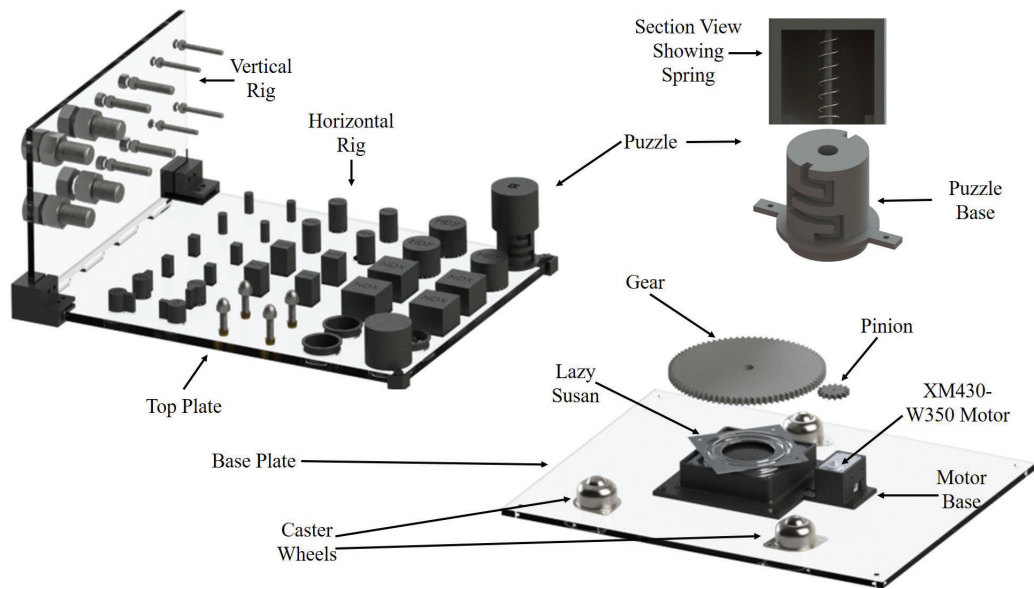


Figure 6.3: Exploded view of the proposed dynamic dexterity test board.

anism showing the various parts comprising the test is shown in Figure 6.3. The various regions of manipulation on the horizontal and vertical plates are presented in Figure 6.4.

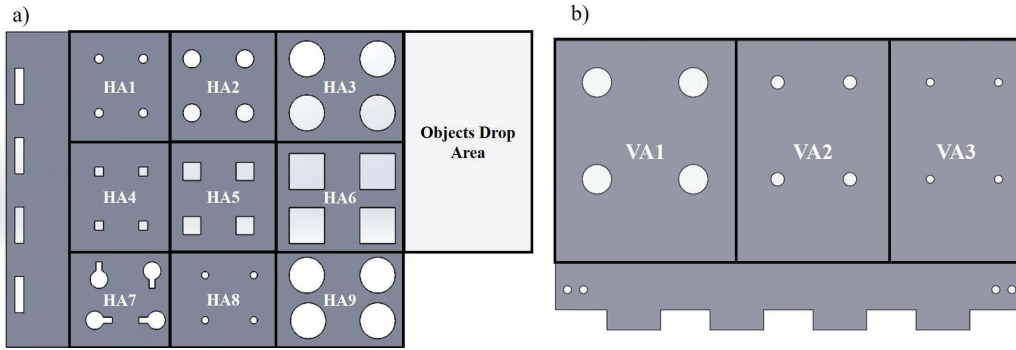


Figure 6.4: Manipulation regions/areas grouped based on the object being manipulated on: a) the horizontal rig (HA1 - HA9) and b) the vertical rig (VA1 - VA3).

6.3.2 Objects

Custom 3D printed objects of varying shapes (cylinders, cuboids, and grooved pegs) and sizes have been designed for tests MT01 – MT13. The engraving on one face indicates the top side and is useful for benchmarking orientation. Tests MT14- MT22 employ standard threaded screws, washers, bolts, and nuts of three sizes (small, medium, and large), providing the range over which the robot hand needs to operate. Custom puzzles consisting of inner and outer puzzles are designed for tests MT23 and MT24. The base of the inner puzzles can be screwed onto the horizontal plates in HA3 and HA9 regions respectively. A compression spring and an extension spring between the inner and outer puzzles are used to examine the capability of the gripper to exert sufficient forces during assembly and disassembly. Robot grippers can plan the grasping and manipulation strategies using the 3D models of the objects that are provided online. Table 6.1 summarizes the list of objects used, their dimensions, the specific manipulation region on the horizontal/vertical plate for the given task, as well as the task number, name, and detailed description.

6.3.3 Manipulation Tasks

Twenty four benchmarking tasks have been broadly classified into 5 manipulation categories. These tasks are numbered MT01-MT24.

These tasks have been adapted from existing dexterity tests as well as challenges designed to provide an insight of the hand efficiency in assembly, packing, tool and machine operation, and other jobs. The tasks are as follows:

- **Simple Manipulation Tasks (MT01, MT03, MT05, MT07, MT09, MT11):** The initial positions and orientations of the objects to be manipulated in both industrial settings and home environments are generally randomized. To render the testing

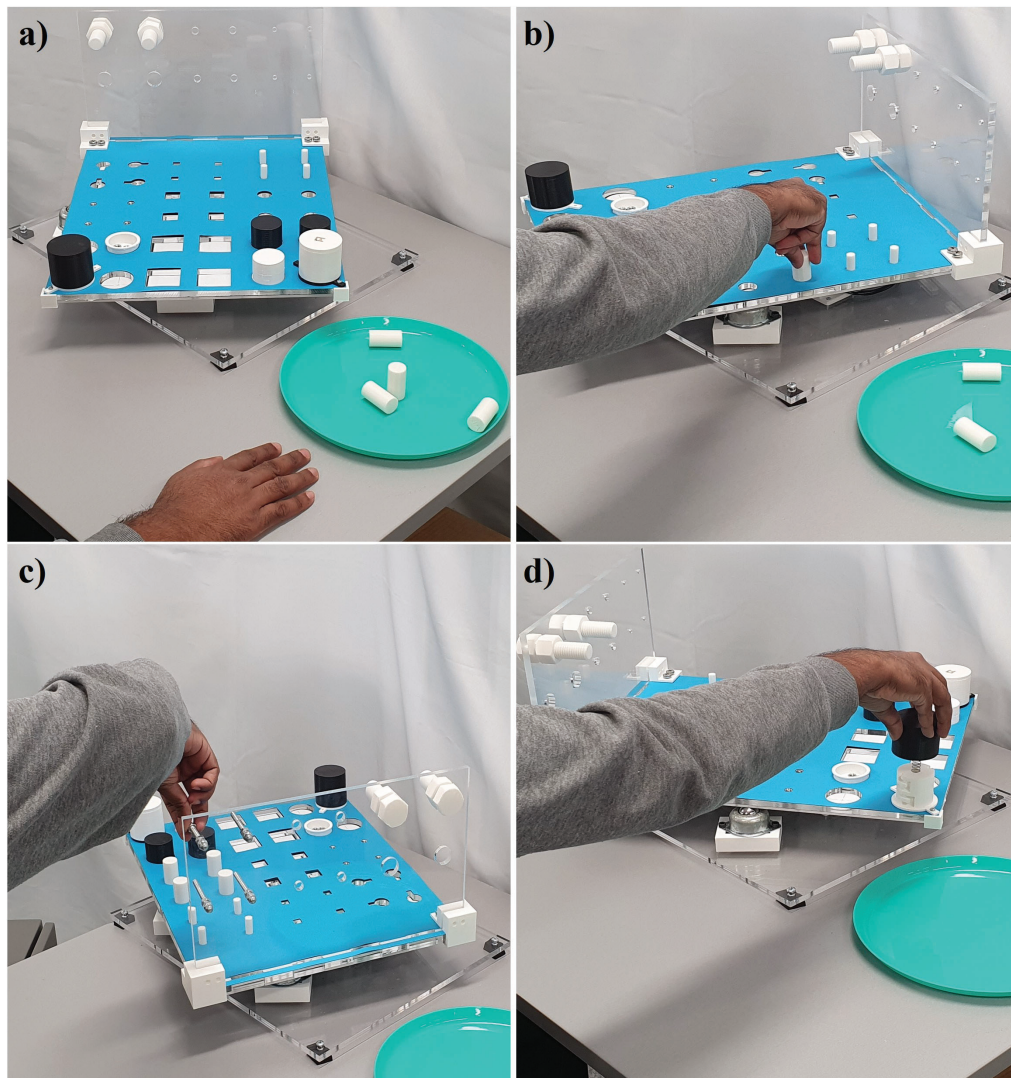


Figure 6.5: A subject performing experiments executing tasks of the dexterity test. The subfigures show: a) the initial position of the hand and objects, b) a placing task, c) a tool task, and d) a puzzle task. As shown in the images the orientation of the dexterity board constantly changes requiring the arm-hand system to adapt to various orientations to complete the tasks successfully.

conditions similar to this, cylindrical and cuboidal objects of varying sizes are cluttered in random initial orientations within the reachable workspace of the robot. The robot gripper or hand then needs to perceive, pick these objects from a random initial pose, position them, and place them in designated holes on the horizontal rig with a specific orientation. Successful execution of these tasks evaluates the gripper's perception capability to identify the initial position and orientation of

the objects, planning the best approach to grasp, orient the objects such that the engraving is on top, and sequentially place them into respective holes.

- **Re-orientation Tasks (MT02, MT04, MT06, MT08, MT10, MT12, MT13):** One of the key manipulative skill of the human hand lies in its ability to re-orient objects along one or more axes within its workspace. The tasks in this category examine the capability of the end-effector to grasp an object from any given orientation, rotate the object along one or more axes, and place the object in designated holes in a very specific final orientation. The robot's ability to successfully complete the tasks serves as a direct indicator of its perception of the position and orientation of the object and target hole during the reach to assemble phase, as they must be aligned before the execution of the insertion task. Cylindrical and cuboidal objects need to be inverted for tasks MT02, MT04, MT06, MT08, MT10, and MT12 while MT13 requires the reorientation and placement of grooved pegs into key shaped holes.
- **Fine Manipulation Tasks (Fine Component Manipulation Tasks - Set A) (MT14, MT15, MT16):** The tasks in this category evaluate fine manipulation capabilities of fingers and hands required for assembly and disassembly of fine components such as washers and nuts. These tasks evaluate the gripper's ability to pick up small components (like nuts, and washers), orient them, and screw/fasten them onto other components to create an assembly. Fine finger movements like thrust and twist, and twist and pull motions are evaluated in tests MT14 and MT15. The threaded pins are placed in random initial orientation in the object drop area. The gripper needs to grasp one threaded pin at a time, orient them onto the designated holes with heat inserts on the horizontal region(HA8), thrust and twist to screw the pins in. The next task requires unscrewing the threaded pins one at a time by twist and pull motions and place them back in the object drop area. The final set of tasks in this category requires the gripper to grasp small components (washers and nuts) placed in small trays in the HA9 region of the board and insert them alternatively onto a screw mounted in the VA3 region of the vertical plate.
- **Tool Tasks (Fine Component Manipulation Tasks - Set B) (MT17 - MT22):** These tasks are an extension of the arm-hand manipulation tasks described above and require finer control of small components to be completed. The tasks in this category evaluate the dexterity associated with picking, precision placement, assembling, disassembling, and fitting together parts without any tools. These are complex tasks that require the end-effector to robustly grasp fine components such

as nuts of varying sizes (small, medium, and large), place them precisely onto tips of screws that are mounted on the vertical rig, and tighten them onto the screws as the rig is rotating. This is followed by disassembling the nuts from the screws and placing them back in the trays located in the HA9 region. The components will have to be grasped robustly, and re-oriented multiple times for the successful completion of the task as the rotation of the rig causes the orientation of the screws to vary continuously. The complexity of tasks in this category requires a high level of dexterity for successful task execution. Hence, the rate of success and completion time for this task category can serve as a valid indicator of the gripper dexterity.

- **Puzzle Manipulation Tasks (MT23 - MT24):** These tasks employ two cylindrical puzzles fixed onto horizontal regions HA3 and HA9. Each puzzle is made up of an inner and outer puzzle component attached to each other with a compression spring (puzzle 1) and extension spring (puzzle 2). Successful completion of the tasks requires the outer component to be grasped and navigated through the puzzle engraved on the inner component by manipulating it clockwise and anti-clockwise, and lifting it all the way up until each puzzle is completely disassembled. This needs to be followed by assembling the puzzle back by guiding the outer component through the puzzle route on the inner component until the puzzle is completely assembled.

6.4 Dexterity Metrics

In this section, we introduce metrics based on the successful task completion (ability) and rate of completion (speed) of the tasks. The total score is then presented as a weighted average of these individual scores. The final part of this section presents a ranking and grading system that would allow easy comparison of grippers and choose the ideal gripper for a particular set of tasks. The metrics are as follows.

6.4.1 Successful Completion Score

Each of the tasks described in section 6.3.3 is repeated with four objects sequentially and a point is awarded for each successful completion. Hence, the score for any given task 'i' can vary between '0' to '4'. And equation 6.1 describes S_s (Successful completion Score), the ability of the gripper to successfully complete all the tasks.

$$S_s = \frac{1}{P_{max}} \sum_{i=1}^n P_i, \quad (6.1)$$

Table 6.1: Dexterity test board components, regions, and task description grouped according to the five task categories and annotated with different colours.

 Pick & Place	 Re-orientation	 Fine Manipulation	 Tool Task	 Puzzle Manipulation	
Objects	Object Dimensions (mm)	Manipulation Region	Task #	Task Name	Task Description
Small Cylinder	10 x 28	HA1	MT01	Placing Task	Perceive, Grasp, Orient (Engraving on top), Position, Place
			MT02	Turning Task	Grasp, Re-orient vertically (z-axis), Engraving on bottom, Place
Medium Cylinder	20 x 38	HA2	MT03	Placing Task	Perceive, Grasp, Orient (Engraving on top), Position, Place
			MT04	Turning Task	Grasp, Re-orient vertically (z-axis) Engraving on bottom, Place
Large Cylinder	40 x 38	HA3	MT05	Placing Task	Perceive, Grasp, Orient (Engraving on top), Position, Place
			MT06	Turning Task	Grasp, Re-orient vertically (z-axis) Engraving on bottom, Place
Small Square	10 x 10 x 28	HA4	MT07	Placing Task	Perceive, Grasp, Orient (Engraving on top), Position, Place
			MT08	Turning Task	Grasp, Re-Orient vertically (z-axis), Engraving on bottom, Place
Medium Square	20 x 20 x 38	HA5	MT09	Placing Task	Perceive, Grasp, Orient (Engraving on top), Position, Place
			MT10	Turning Task	Grasp, Re-Orient vertically (z-axis), Engraving on bottom, Place
Large Square	40 x 40 x 38	HA6	MT11	Placing Task	Perceive, Grasp, Orient (Engraving on top), Position, Place
			MT12	Turning Task	Grasp, Re-Orient vertically (z-axis), Engraving on bottom, Place
Grooved Peg	10 x 28	HA7	MT13	Orienting Task	Perceive, Grasp, Orient (Engraving on top), Perceive, Re-orient (Key groove aligned to key hole), Place
Threaded Pins	M8 1.25 mm thread, 40 mm	HA8	MT14	Thrust & Twist	Perceive, Fine grasp, Orient, Position, Place, Thrust and Twist
			MT15	Twist & Pull	Perceive, Fine grasp, Twist and Pull, Position and Place
Washers and Nuts	M6 or higher	VA3	MT16	Insertion Task	Perceive, Fine grasp, Orient (Concentric to M6 screw), Position, Place
M6 Bolt	M6 1 mm thread, 60 mm	VA3	MT17	Tool Task (Assemble)	Grasp nut (robustly), Orient nut to bolt tip, Manipulate, Re-orient, Manipulate
		VA3	MT8	Tool Task (Disassemble)	Grasp nut (robustly), Orient, Manipulate, Re-orient, Manipulate
M10 Bolt	M10 1.5 mm thread, 60 mm	VA2	MT19	Tool Task (Assemble)	Grasp nut (robustly), Orient nut to bolt tip, Manipulate, Re-orient, Manipulate
		VA2	MT20	Tool Task (Disassemble)	Grasp nut (robustly), Orient, Manipulate, Re-orient, Manipulate
M22 Bolt	M22 2.5 mm thread, 60 mm	VA1	MT21	Tool Task (Assemble)	Grasp nut (robustly), Orient nut to bolt tip, Manipulate, Re-orient, Manipulate
		VA1	MT22	Tool Task (Disassemble)	Grasp tool (robustly), Orient tool tip to nut, Manipulate, Re-orient, Manipulate
Puzzle 1	Puzzle with Compression Spring	HA9	MT23	Disassemble & Assemble	Grasp puzzle, Rotate left/right, Lift (Disassemble), Rotate left/right and Push down (Assemble)
Puzzle 2	Puzzle With Extension Spring	HA3	MT24	Disassemble & Assemble	Grasp puzzle, Rotate left/right, Lift (Disassemble), Rotate left/right and Push down (Assemble)

Table 6.2: Table presenting the baseline scores for the dexterity tests performed by a human with a glove and without a glove

Task category	No Glove			With Glove		
	Average Time (s)	Standard Deviation	Coefficient of Variance	Average Time (s)	Standard Deviation	Coefficient of Variance
Total Time	452.10	57.65	12.67	500.31	64.46	12.72
Pick and Place	63.49	7.04	11.07	68.28	7.41	10.54
Reorientation	62.28	5.05	8.08	71.33	7.64	10.39
Fine Manipulation	51.20	5.61	7.55	66.04	5.84	6.24
Tool	253.51	44.76	17.52	275.21	43.55	15.72
Puzzle	20.72	4.55	21.95	19.44	3.31	14.71

n is the total number of tasks (24) and the term P_{max} denotes the maximum possible score that can be achieved by a gripper completing all the n tasks and can be written as $P_{max} = 4n$. P_i is the number of objects successfully manipulated for the i^{th} set of tasks and can vary between '0' and '4'. The total points achieved by a gripper $\sum_{i=1}^n P_i$ denotes the total score of successful completion and can be replaced by the term P_{total} . Equation 6.1 can now be rewritten as,

$$S_s = \frac{P_{total}}{P_{max}}, \quad (6.2)$$

Equation 6.2 provides us with a Successful completion score S_s that varies between 0 to 1. The lower end of the scale represents a non-dexterous device incapable of executing any tasks and the higher end of the scale represents a highly dexterous device capable of successfully executing all the manipulation tasks.

6.4.2 Time Required Score

The metrics introduced in this section can be used to measure the rate of task completion. Task completion time can vary between each individual task depending on the objects, the initial orientation of the objects, grasp planning, approach, and manipulation strategy employed. Equation 6.3 provides S_t (Time required score), the speed with which the gripper can complete the tasks.

$$S_t = \frac{\log(T_{min})}{\log(\sum_{i=1}^n T_i)}, \quad (6.3)$$

where T_{min} is the minimum time taken for task completion obtained from the human experiments. We consider human performance as the baseline. The time required for completion of i^{th} task is given by T_i . The cumulative time taken for all n tasks is calculated as $\sum_{i=1}^n T_i$ and can be written as T_{total} . Equation 6.3 can now be rewritten as,

$$S_t = \frac{\log(T_{min})}{\log(T_{total})}, \quad (6.4)$$

Equation 6.4 provides us with a time required for task completion score S_t that varies between 0 to 1. A higher time score S_t indicates the ability of the gripper to complete the manipulation tasks at a faster rate and thus signifies better dexterity.

6.4.3 Total Dexterity Score

The total dexterity score S_{total} is calculated from the weighted sum of the successful completion score (S_s) and time required score (S_t). This metric provides us with the combination of gripper's ability and speed in completing the various manipulation tasks. To allow for easy comparison, the total score is presented on a percentage scale ranging from 0 to 100% as shown in equation 6.5.

$$S_{total} = (w_s S_s + w_t S_t) * 100, \quad (6.5)$$

Replacing the values of S_s and S_t , the equation can be rewritten as,

$$S_{total} = \left(w_s \left(\frac{P_{total}}{P_{max}} \right) + w_t \left(\frac{\log(T_{min})}{\log(T_{total})} \right) \right) * 100, \quad (6.6)$$

The weight constants for successful completion (w_s) and time (w_t) are used to vary the importance of individual sub-score. The sum of these constants must be equal to 1 ($w_s + w_t = 1$). If the weights are assigned an equal value (0.5 each) the equation would distribute equal importance to the ability and speed of task completion. In the case of evaluating the gripper's ability to perform certain complex tasks irrespective of the time taken to complete them, a greater value could be assigned to w_s . The results are presented on a scale ranging from 0 (simplistic, non-dexterous system) to 1 (human-like, dexterous system). This score represents the capabilities of a gripper or hand to perform complex grasping and manipulation tasks compared with the human hand, which is considered to be Nature's most effective and dexterous end-effector. If a gripper can perform all the tasks successfully within the baseline time determined by human experiments, the gripper is considered to be highly dexterous exhibiting human-like grasping and manipulation performance.

6.4.4 Dexterity Ranks and Grades

In order to classify and compare the robot grippers amongst each other, a system of ranks and grades is introduced. This grading system helps decide on the ideal gripper

Table 6.3: Grading system for the grippers based on successful task completion in a given task category.

Tasks completed	Grades
No tasks completed	F
Tasks $< 1/3(T_{total})$	D
$1/3(T_{total}) < \text{Tasks} < 2/3(T_{total})$	C
Tasks $> 1/3(T_{total})$	B
All tasks completed	A

for a given set of tasks. The ranks for the robot grippers can vary from "0 stars" to "5 stars" (one star corresponding to each task category). A robot gripper is awarded 1 star on successful completion of all the tasks in a given task category. No star is awarded if the gripper fails in executing any of the tasks. Hence, a robot's dexterity can be easily verified based on the number of stars from '0 stars' (non-dexterous) to '5 stars' (most dexterous). For example, if a hand can accomplish all the tasks in 3 of the 5 task categories, its rank would be '3' stars. To differentiate between hands that are equally ranked, a grading system consisting of 6 grades is provided. If none of the tasks in a task category can be executed, it is graded as an 'F' and an 'A' is awarded for grippers capable of completing all the tasks successfully. The detailed grading system is presented in Table 6.3. This ranking and grading system serves as an indicator of the robot's overall performance as well as its individual capabilities in the successful execution of various task categories. If the requirement is for a simple pick and place task, a '1' star robotic gripper that has graded 'A' for pick and place tasks would be well suited rather than a complex '5' starred gripper. Thus, this ranking and grading system shall help identify grippers suitable for various needs and task categories.

6.5 Validation of Protocols and Baseline Score of Human Trials

The benchmarking protocols detailed in section 6.3 were executed by humans to validate their efficiency and the results were calculated using equations 6.1, 6.3, and 6.6 to obtain a dexterity score. The average of these human hand experimental results is used as a baseline score for comparison and evaluation of human hand dexterity, as well as for comparing the dexterity of other robotic grippers and hands. This study recruited ten healthy subjects whose arm lengths were $76.15 \text{ cm} \pm 4.48 \text{ cm}$. The University of Auckland Human Participants Ethics Committee approved this study, and all participants gave informed consent. The subjects sat in a comfortable position for the entire duration of the

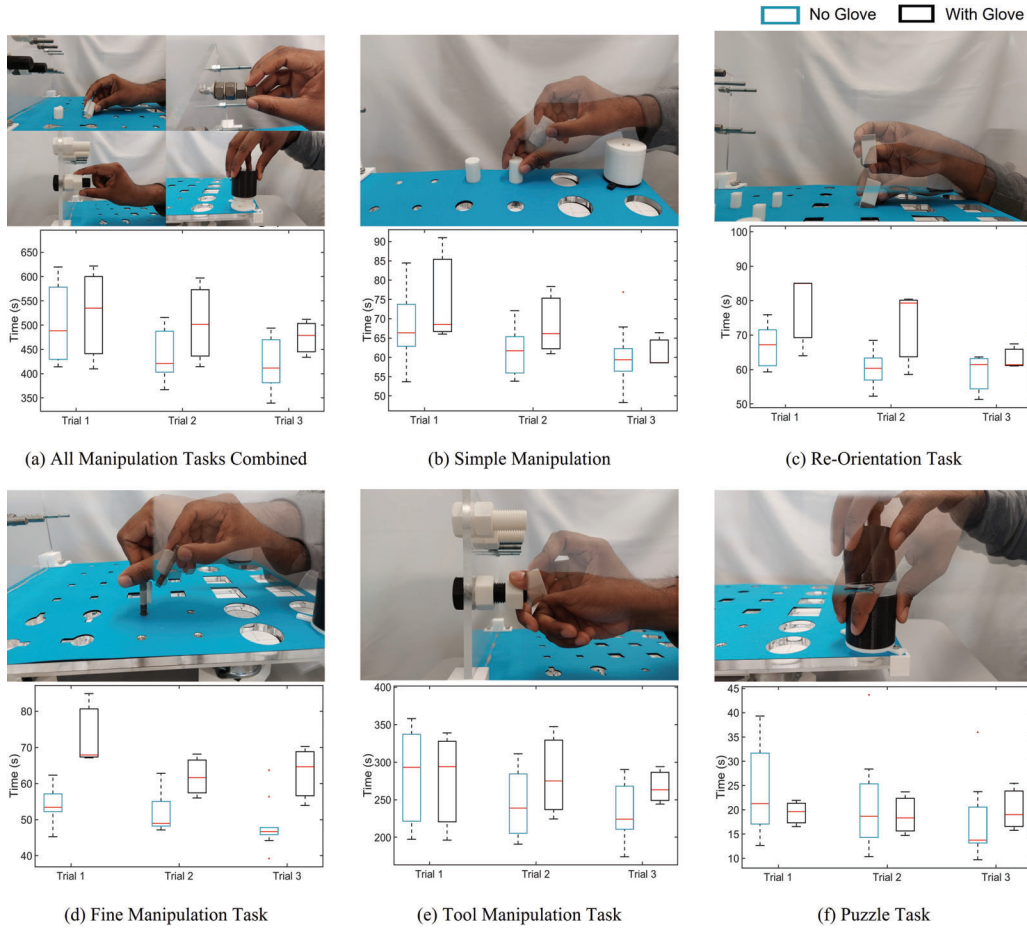


Figure 6.6: The time taken by 10 subjects to complete various manipulation tasks across 3 trials with and without gloves is presented.

experiments, with the forearm placed to the right of the dexterity test as an initial configuration. Three sets of experiments were performed by the subjects as shown in Figure 6.5. Each subject repeated the tasks MT01 - MT24 sequentially for three trials for the first set of experiments without gloves. The experiments were then repeated with a padded palm, high grip glove for three trials to determine the effect of reduced tactile sensing on dexterous manipulation capabilities. For both sets of experiments, the dexterity rig was rotating at a constant speed of 3 RPM to examine the subjects' ability to adapt to a dynamic test environment in terms of perception, planning, and manipulation capability. The third set of experiments involved performing the tasks on a stationary rig for three trials in order to determine the effect of static against dynamic environments on the performance of the participants. The detailed evaluation protocol with explanatory images

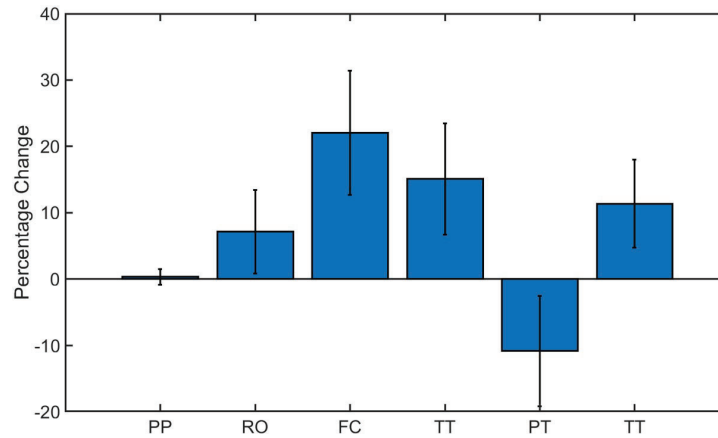


Figure 6.7: Percentage change in manipulation time with gloves on for the various task category: Pick & Place (PP), Reorientation (RO), Fine Component Manipulation (FC), Tool Task (TT), Puzzle Task (PT), and Total Time (TT).

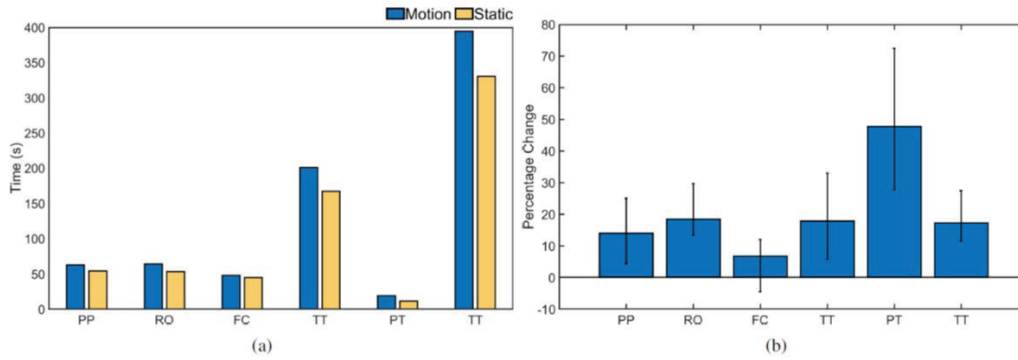


Figure 6.8: Subfigure a) presents a comparison of the time taken by the subjects to complete various task categories in seconds when the rig was static and in motion (rotating). Subfigure b) presents the percentage increase in completion time for the various task category when the rig was in motion. The task categories are: Pick & Place (PP), Re-Orientation (RO), Fine Component Manipulation (FC), Tool Task (TT), Puzzle Task (PT), and Total Time (TT).

and scoring sheets, as well as the open-source CAD files of the proposed dexterity test are provided and can be downloaded from the following website:

<http://www.newdexterity.org/dexteritytest>

The particular website will also serve as a repository of the scores and evaluations of various robotic hands and grippers.

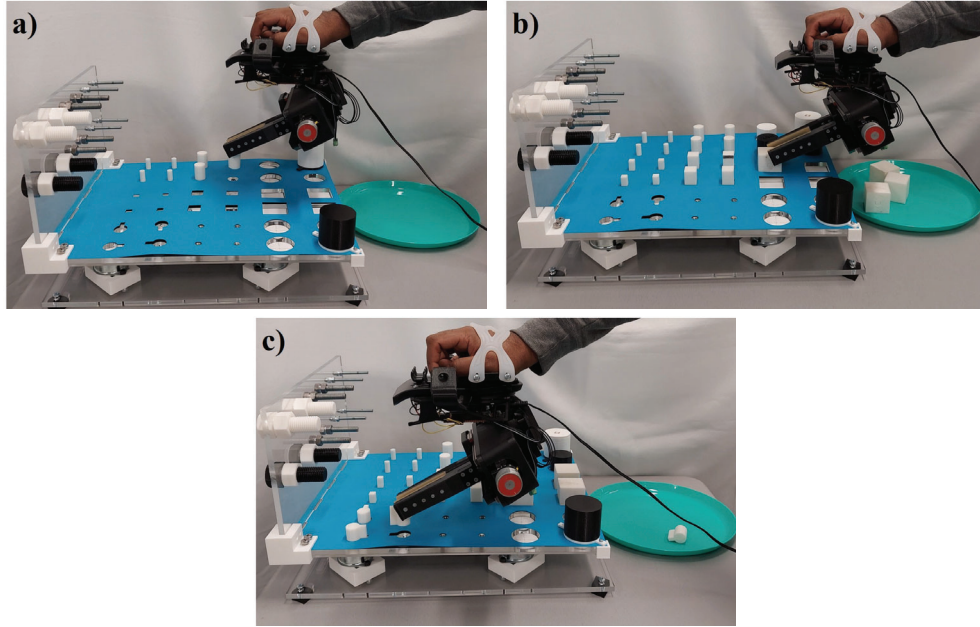


Figure 6.9: A subject performing the experiments on the dexterity test board with a palm mounted interface to control a multi-modal parallel jaw gripper, performing: a) a placing task of a medium cylinder, b) a placing task of a large square, and c) a re-orientation task of a grooved peg.

6.5.1 Results and Discussion

The various features being evaluated in this study and how they compare with other existing dexterity tests is shown in Table 6.4. Figure 6.6 presents a visual representation of the tasks and the results of the experimental trials corresponding to each of the five different task categories. In order to determine the degree of variation, we calculated the percentage coefficient of variation (%CV) for each category's completion time and the overall completion time using

$$\%CV_t = \frac{\sigma_t}{\mu_t} * 100, \quad (6.7)$$

where, σ_t and μ_t are the standard deviation and mean for a given task category t . The $\%CV_t$ for the overall completion time for all the participants across three trials was 13%. The $\%CV$ for all the individual task categories was less than 20%. These values of $\%CV$ signify low dispersion time across various subjects and trials and helps in validating the efficiency of the experimental protocols across various subjects. Hence, the values derived from these experiments could be used as baseline scores for human and robot dexterity evaluation experiments. There was no significant correlation between the arm length of the subjects and the performance for the task categories examined in this study.

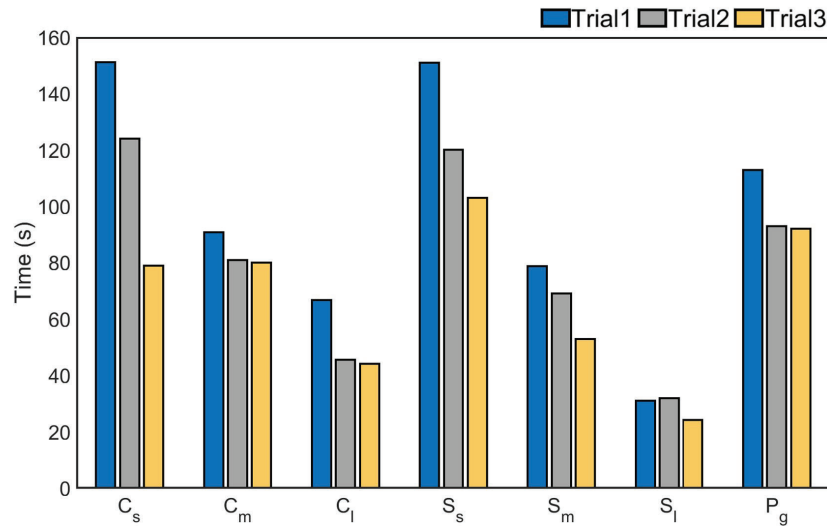


Figure 6.10: The comparison of time taken by the multi-modal parallel jaw gripper to complete tasks for objects of varying shapes and sizes, is presented. C, S, and P stand for Cylinders, Squares, and Pegs respectively. The subscripts s, m, l, g, denote small, medium, large, and grooved parts respectively.

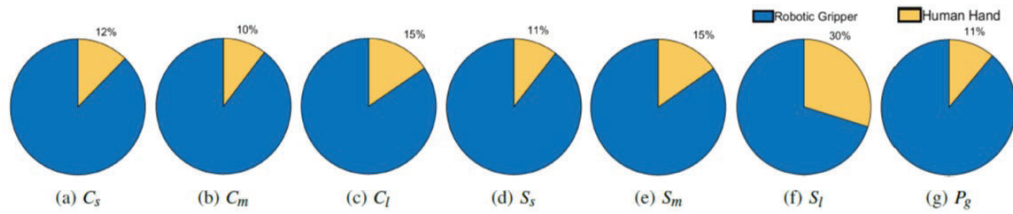


Figure 6.11: This pie chart presents a comparison of the time taken by the robotic grippers for executing tasks with objects of varying shapes and sizes when compared against the human hands. C, S, and P stand for Cylinders, Squares, and Pegs respectively. The Subscripts s,m,l, and g denote small, medium, large, and grooved objects respectively.

It can also be noted from the plots that the average time taken by the subjects to complete the tests in each of the individual task categories was significantly lower than the time taken in the previous trial. The results are validated using ANOVA to determine the statistical significance between the trials. A p-value of 0.013 (less than the alpha value of significance, 0.05) for the total time taken to complete the tasks across the 3 trials indicates that the time taken for successive trials decreases significantly. This could be attributed to the subject's familiarity with the tasks and hence indicates that dexterity improves with repetition. Dexterity could then be considered a learned attribute that can be improved by exercising specific sets of tasks.

In order to determine the effect of tactile sensing on the dexterous manipulation capabilities, the experiments were repeated with gloves on and the results are presented

in Figure 6.6. This had varying effects for various task categories, as shown in Figure 6.7. The time taken to complete the pick and place task category was identical with the gloves on and off. The effect was most pronounced for fine manipulation tasks where the average completion time was higher by 30% when performed with the gloves. On the other hand, the puzzles could be solved 12% faster with gloves on. Similar to the first set of experiments, the tasks were completed faster when the trials were repeated indicating the learning curve is effective in improving dexterous manipulation even with the gloves on. ANOVA resulted in a p-value of 0.0066 which is less than the alpha value of significance (0.05) and one would reject the null hypothesis, as there is strong evidence that the values between trials differ. The percentage coefficient of variation (%CV) for all the individual tasks as well as the combined total time was under 20%. The results obtained from these two sets of human experiments are presented in Table 6.2. These results serve as the baseline scores for the dexterity tests.

Further, the third set of experiments was performed for three trials on a stationary rig to investigate how much dexterous manipulation capability improved on a fixed rig as opposed to when one in motion was used. The coefficient of variation for all the task categories was well under 13% indicating a closer dispersion time across subjects in completing the tasks on a stationary rig. The result of this experiment is presented in Figure 6.8. It is clear from the plots that the task completion time was faster on a stationary rig for all the task categories. This effect was most prominent for the puzzle task which took 40% more time when the rig was moving. As opposed to this the fine manipulation task category was slower only by 7%. As with the previous set of experiments, the task completion time decreased across the trials further confirming the effects of the learning curve on the execution of dexterous manipulation tasks. The experiments were also performed with a multi-modal parallel gripper mounted on a palm interface as shown in Figure 6.9 to determine the dexterous manipulation capabilities of the gripper and to investigate the effect of learning on manipulation capabilities across trials. The gripper was unable to complete all the task categories as it lacked the complex in-hand manipulation capabilities required for successful task completion in these categories. However, task completion time reduced significantly with each consecutive trial for all the tasks that could be successfully completed, as presented in figure 6.10. This further supports the argument that dexterity can be learned and improved by performing a particular set of tasks repeatedly. Figure 6.11 presents the pie chart comparing the percentage of time taken by the human hand to complete the various tasks against the time taken by the robotic gripper. As seen from the pie chart, human hands can complete the tasks in a very small fraction of the time taken by the robotic grippers. This shows that there is a huge room for improvement of robotic devices.

6.6 Conclusion

In this chapter, we proposed a new modular, affordable, accessible open-source dexterity test that evaluates the grasping and manipulation capabilities of humans and robotic hands, and other end effectors by combining the features of multiple human dexterity tests as well as new task categories specifically designed for robots. These tests help quantify the manual dexterity of humans apart from evaluating the human hand function improvement post-injury. The features from many existing hand function tests, along with new features such as the rotating module and the dexterity puzzles make this test one of the most comprehensive dexterity evaluation systems. Apart from this, the test also involves benchmarking tasks that evaluate key robotic manipulation capabilities identified from the literature and robotic challenges. A set of dexterity metrics have also been proposed that quantifies the dexterity of robot grippers and hands by evaluating their ability to complete these tasks on a scale ranging from 0 (simplistic, non-dexterous system) to 1 (human-like, dexterous system). The scores are based on the hands' ability to complete the tasks successfully with accuracy and precision, as well as the speed at which the tasks can be executed. The weighted sum of the successful completion and speed of completion is used to obtain the final dexterity score. Further alternative measures in the form of dexterity ranks and grades enable comparison of various grippers and their manipulation capability in an intuitive manner irrespectively of their individual design parameters. Thus, the proposed dexterity test and metrics provide researchers around the world with benchmarking methods and tools that can be easily replicated to quantify the ability of robotic end-effectors to perform complex tasks effectively, allowing the comparison of their grippers against various classes of grippers. The accompanying website shall serve as an open-access repository of dexterity scores for robot hands and grippers as well as an open-source initiative for the dissemination of the dexterity test designs. The various evaluation methods proposed in the study have been validated using human trials. The output of these trials has been used to quantify dexterity based on the scoring methodology proposed. The importance of tactile feedback in performing these evaluations is also examined by performing the tasks with a padded glove and the results are presented. From the results, it is clearly evident that the task completion time decreases with trials for both sets of experiments, indicating that a clear learning curve exists and that humans perform better after practicing. The subjects took significantly longer to complete the tasks with the padded gloves. This clearly shows the importance of tactile feedback in performing dexterous manipulation. It is also clear from the robot gripper experiments that the human hands can complete the tasks in a very small fraction of the time taken

by the robotic grippers indicating that there is a huge room for improvement of robotic devices.

Table 6.4: Table comparing the test environment, object sets, and features being evaluated across various dexterity tests proposed in recent literature. The task categories are abbreviated as PP - Pick & Place, RO - Re-Orientation, FM - Fine Manipulation, TT - Tool Task, PM - Puzzle Manipulation.

Studies	Designed for		Test Environment	Object set	Task Categories					Obstacle
	Humans	Robots			PP	RO	FM	TT	PT	
Noel et al., 2011	✓		2 vertical planes	Plastic pegs	✓					N/A
Gonzalez et al., 2015	✓		2 wooden boards	Custom made plastic objects (4 sets)	✓					N/A
Darpa Robotic Challenge, 2015		✓	Four sequential courses	Manipulation tasks of varying complexity (4 tasks)		✓	✓			Stationary
Amazon Robotic challenge, 2016 [151]		✓	Shelving unit structured in 12 bins	Objects representative of objects handled in amazon warehouse (39 objects)	✓	✓				Stationary
Saraf and Bisht, 2020	✓		Single holed, spring loaded wooden box	3D printed pegs	✓	✓	✓			N/A
IROS RGMC, 2020 [152]		✓	Dedicated taskboard	Objects representing different classes of Industrial assembly (4 sets)	✓	✓	✓	✓		Stationary
Robocup@home, 2020		✓	Home environment arena with structured rooms	Categorized objects (30 objects)	✓	✓				Stationary
Wilson et al., 2021	✓		3D printed platform	3D printed pegs	✓	✓				Stationary
This study	✓	✓	Dynamic board	3D printable objects and standard bolts/nuts (14 sets)	✓	✓	✓	✓	✓	Dynamic

Chapter 7

Comparing Human and Robot Performance in the Execution of Kitchen Tasks: Evaluating Grasping and Dexterous Manipulation Skills

7.1 Introduction

Essential tasks that need to be performed routinely for safe and good quality of life are described as activities of daily living (ADL) [153]. One of the key subsets of extended ADLs involves the ability of an individual to independently perform kitchen tasks like feeding oneself, making a hot drink/food, carrying the hot drink from one room to another, and washing up [154]. Several assistive robotic arms and grippers have been developed to specifically address the difficulties in executing activities of daily living [155, 156]. A number of studies have also focused primarily on developing of robots for kitchen-specific task execution. For example, a generalized framework for operating the doors and drawers in a kitchen environment has been presented in [157]. Furthermore, the system integration of a daily assistive robot for the successful execution of cooking tasks like cutting, peeling, and transferring was demonstrated using the successful preparation of a salad in [158].

However, there is a wide gap in the focus and the employed approaches of the robotics research and the healthcare community focusing on human-oriented task completion [159]. While robotics research focuses on task executions as a sequence of control strategies and motion types, the healthcare community is more concerned about clini-



Figure 7.1: User wearing a vest mounted human machine interface for controlling a parallel jaw gripper. The gripper and the robot hand used in the experiments are also depicted.

cal assessment. Hence, several robotics researchers have investigated the various grasps and manipulation types employed in completing ADLs from video recordings of task execution in selected environments like homes, machine shops, etc [62]. The various attributes contributing to successful task executions can be captured in a taxonomy. These attributes can then be translated to enable the planning and execution of manipulation tasks by robotic grippers [73].

Hence, there is a need for capability maps and taxonomies capable of mapping the task execution capabilities of both humans and robotic grippers alike. In this study, a vast dataset that includes detailed annotations of the various grasping and manipulation strategies is generated based on the analysis of video recordings of human subjects performing ADLs in a kitchen environment. Based on the analysis, we propose a kitchen task-specific taxonomy that classifies the various features employed to complete activities in a kitchen environment successfully. The same tasks were repeated using robotic grippers/hands mounted on an interface in a kitchen setup prepared in a laboratory setting. The taxonomy proposed is used to compare the grasping and manipulation capabilities of robotic grippers and human hands. The comparison results are presented in a color-coded map highlighting the current abilities and limitations of the robotic grippers in the execution of specific kitchen tasks. These insights can help develop a new class of robotic grippers that can execute the various sets of kitchen tasks on par with human hands.

7.2 Related Work

Unlike a manufacturing setting, the kitchen environment is constantly changing, and the objects being encountered vary widely from cutlery, a variety of food items, appliances, groceries, and trash. The most commonly executed tasks can be categorized into four categories: i) loading and retrieving the groceries from the pantry/fridge, ii) preparing the food, iii) rinsing cutlery, loading and unloading the dishwasher, iv) cleaning the counter, cooktop, sink, and taking out the trash. Each of these task categories requires different grasping and manipulation strategies depending on the properties of the object being manipulated (shape, weight, texture etc.), where they are located (top shelf of the cabinet, lower rack of the dishwasher, on the countertop, etc.) and whether the object surface is wet/dry, and on the person performing the task. Hence, an ideal dataset of kitchen-specific tasks must include all these modalities being performed by subjects in their home kitchen environments.

Currently, several datasets are available that contain observations of grasping and manipulation strategies employed by subjects for performing a specific type of kitchen task like cooking, setting the table, or other similar tasks in an identical environment. The TUM kitchen dataset, for example, is made up of subjects setting the table using the same objects and similar locations in the sensor-equipped TUM kitchen environment [160]. The food preparation dataset presented in [161] on the other hand, was collected from participants following a predetermined task order within a delimited space to prepare a single portion of salad. The GTEA Gaze dataset is comprised of subjects preparing a meal of their choice from 30 different kinds of foods allowing for a varied set of manipulation tasks specific to the meal [162]. However, these tasks and environments are not representative of everyday tasks performed in a kitchen environment. Hence, in this study, the proposed dataset was generated for all of the task categories associated with a home kitchen environment, from stocking the groceries, retrieving them to prepare a meal, cleaning the dishes, cleaning the cooktop, cleaning the counters, and taking out the trash.

Analyzing these datasets helps us determine the patterns of grasps and manipulations executed by the human hands for specific tasks/objects in a kitchen environment. For instance, subjects have been identified to use five to ten specific grasps in a home environment and machine shop, respectively, for the completion of 80% of the tasks [62]. The grasp planning of robotic grippers has been aided by grasp taxonomies defined from grasping data and videos. Common terminology for the classification of the human hand grasp configurations has been identified based on opposition types, thumb position, finger assignments, and grasp types in terms of precision, intermediate, and power grasps

executed [38]. The general manipulation tasks and strategies have been classified in a taxonomy based on the hand-centric and motion-centric attributes of the task. They have been demonstrated to apply to both humans and robots [8]. A taxonomy specifically for the recognition of human manipulation strategies and for transferring them to robotic end-effectors has also been proposed [72]. With respect to kitchen tasks, effective manipulation motions employed in cooking tasks have been classified in a motion taxonomy that captures the attributes of a particular motion as manipulation codes [73]. However, some of the grasping and manipulation behaviors exhibited by humans are not feasible by a robot hand.

There is a lack of a database that captures all the essential tasks performed in a kitchen environment. The robots can complete kitchen tasks using a sequence of simple grasps and manipulation strategies as opposed to the complex strategies employed by humans to manipulate multiple objects in parallel. The efficiency of these simple strategies on successful task completion and their effect on the completion time needs to be analyzed. In this study, three main steps were involved in the formulation of the taxonomy and capabilities maps of robotic grippers for the execution of kitchen specific tasks: i) generating a dataset of grasping and manipulation strategies, ii) classifying the attributes associated with each execution in a taxonomy, and iii) comparing the performance of human hands, robot hands, and grippers¹.

The rest of the chapter is organized as follows: Section 7.3 details the setup used for the collection of kitchen specific grasping and manipulation data from humans and robot grippers, section 7.4 presents the detailed analysis of the human dataset, section 7.5 presents the comparison of the robotic end-effectors against the human hand and proposes a kitchen task specific taxonomy, while section 7.6 discusses the results of the analysis of the initial dataset.

7.3 Data Collection Setup

In this section, we present the detailed experimental setup used for data collection of the grasping and manipulation strategies executed in a kitchen environment by humans and humans directly operating robotic end-effectors.

¹Majority of the chapter (sections 7.1 - 7.6) is based on [163], © 2022, IEEE. Reprinted, with permission, from Nathan Elangovan, Che-ming Chang, Ricardo V. Godoy, Felipe Sanches, Ke Wang, Patrick Jarvis, and Minas Liarokapis, Comparing Human and Robot Performance in the Execution of Kitchen Tasks: Evaluating Grasping and Dexterous Manipulation Skills, in 2022 IEEE-RAS International Conference on Humanoid Robots (Humanoids), IEEE, Okinawa, Japan, 2022.

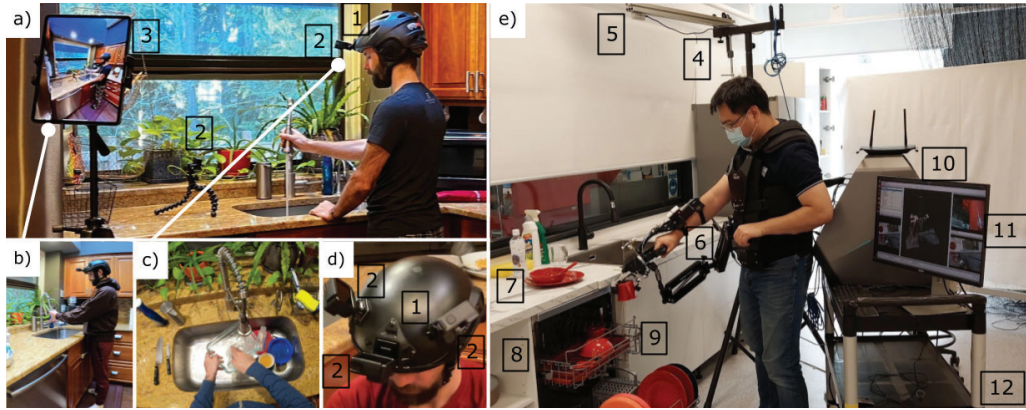


Figure 7.2: Subfigure a) presents the data collection setup at a user's home kitchen. Subfigure b) presents the side camera view. Subfigure c) presents the central main camera view. Subfigure d) shows the helmet camera. Subfigure e) shows a user loading the dishwasher using an anthropomorphic gripper operated by a human machine interface. The figure is annotated as follows: [1] Helmet camera configuration, [2] three GoPro cameras are mounted on a lightweight helmet. The central main camera faces downwards to capture hand motion and interactions during ADL in a kitchen environment, as shown in Fig. c). Supplementary cameras, e.g., [3] an iPad, are placed elsewhere in the environment to capture the operator's whole-body motion and provide side-on views of grasps, as shown in Fig. b). [4] shows an overhead camera rig, [5] a Birds Eye D435I Camera, [6] the interface on the vest, [7] daily objects, [8] a dishwasher, [9] a dishwasher rack, [10] the data recording platform, [11] the live streams from sensors, and [12] the mobile trolley used to carry the data collection PC.

7.3.1 Human Data Collection Setup

The human data were collected from multiple users performing kitchen tasks associated with activities of daily living in their home kitchen environment with the purpose of analyzing them and extracting the frequencies of the grasping and manipulation strategies employed (see Fig. 3).

These activities included a set of 10 tasks categorized into four major categories: i) stocking - pantry and fridge, ii) cooking - breakfast, lunch, dinner, and operating kitchen appliances, iii) dishwasher - loading and unloading, and iv) cleaning - counter, cooktop, and taking out the trash. The setup for the collection of human data is shown in Figure 7.2. The primary data was obtained from a lightweight helmet mounted with three GoPro cameras capturing the grasping and manipulation tasks executed by the subject in a field of view angle. The view from the primary, central camera mounted on the helmet was complemented by two other outward-facing cameras to provide a wider angle of view and overcome the boundary conditions. The second set of cameras mounted on a tripod was placed in the task execution regions to capture the manipulations performed in tight

and occluded spaces like a dishwasher rack, inside a fridge shelf, pantry, etc. Moreover, the third set of cameras provided a side-on view that recorded the overall environment, operator's pose, and shoulder movements. All cameras recorded the various activities performed by the subjects to complete each task. The initial data was collected from four separate households performing the tasks at different instances.

The videos collected were compiled and time synced during the annotation process. The data was then reviewed and annotated based on existing grasp, and manipulation taxonomies [38, 8]. Every individual activity was annotated detailing attributes such as activity duration, number of hands, grasp classification, manipulation type, the direction of object movement, posture, shoulder movement, level of water residue on the object, and an indication of washing hands. The data was collected by AI Data Innovations Corporation and reviewed by two teams of annotators following a detailed guide outlining the annotation process. Subject experts continuously reviewed the annotations to ensure consistency.

7.3.2 Robotic Grippers Data Collection Setup

The data for robotic grippers was collected from users performing manipulation tasks in a kitchen setup at the laboratory as shown in Figure 7.2e. A parallel jaw gripper and the NDX-A anthropomorphic robot hand [12] were operated using a forearm mounted interface to perform various activities in the kitchen environment. The configuration for the forearm mount interface shown in Figure 7.1 is adapted from the setup described in [44]. A Raspberry Pi 4 Model B was used to buffer the onboard Intel Realsense T265 camera data flow, and a desktop computer was placed on a trolley instead of the lightweight back mounted Intel NUC. This was primarily due to weight considerations, bandwidth limitations, and facilitating the collection of larger datasets. The interface allows programmable target positions and preset current limits to each of the motors in the grippers used. The resulting motor positions and trigger motion data are streamed to the desktop computer.

An iso-elastic arm vest with higher payload capacity substitutes the previous lightweight vest and arm. A tripod with an extension arm positioned the birds-eye view camera above the workspace. The bird's eye camera used an Intel Realsense D435I RGBD camera that provides top-down depth information and RGB data for fiducial marker tracking during the data collection process. The birds-eye view camera provides a pose and initial relative position data between the set marker and the forearm mount interface. Since the height from the floor to the bird's eye camera is known, a planar reference can be obtained by placing the fiducial markers on the surface of the benchtop.

The depth data can be used for visualization and telemetry but is heavily affected by occlusions, resolution, and noise. Data from the T265 tracking camera is used as the primary pose and trajectory estimation source during occlusion from the bird's eye camera. All relevant datasets are published onto ROS nodes and recorded for analysis.

Table 7.1: The table presents the detailed analysis of the grasping and manipulation strategies employed by humans for the execution of kitchen tasks.

Task category	Tasks	Hands		Grasp Classification			Thumb Orientation		Average grasps used	Manipulation		
		One	Both	Power	Intermediate	Precision	Abduction	Adduction		Contact fixed	Contact changes	Hold
Stocking	Pantry	79	21	46.9	6.8	46.3	77.2	22.8	9.5	90.2	9.2	0.6
	Fridge	37.5	62.5	62.4	4.3	33.3	79.1	20.9	10.5	71.3	13	15.7
Cooking	Breakfast	39.1	60.9	49.9	9.2	40.9	78.7	21.3	15	67.8	8.2	24
	Lunch	70.5	29.5	36.8	18.5	44.7	85.3	14.7	13.5	91	1.1	7.9
	Dinner	49.4	50.6	39.7	9.7	50.6	76.3	23.7	17	81.7	5.8	12.5
	Appliance	84.6	15.4	64.4	8.9	26.7	66.7	33.3	5.25	88.5	0	11.5
Dishwasher	Loading	73.8	26.2	42.1	15.1	42.8	73	27	13.5	90.7	5.6	3.7
	Unloading	56.3	43.7	43.4	8	48.6	75.2	24.8	13.33	97.7	1.2	1.1
Cleaning	Counter/cooktop	77.1	22.9	34.1	10.5	55.4	70.7	29.3	14.5	82.8	11.5	5.7
	Trash	25.4	74.6	60	32.7	7.3	70.9	29.1	9	70.4	22.2	7.4

7.4 Dataset Analysis and Taxonomy Identification

7.4.1 Analysis Based on Existing Taxonomies

Every activity performed during the completion of the four categories of kitchen tasks was annotated based on the existing grasp and manipulation taxonomies. This resulted in a dataset that included over 2000 individual activities performed by the four subjects in different household settings. Figure 7.4 presents the various grasping and manipulation attributes associated with each of the task categories. It was observed that different subjects employed different grasp and manipulation approaches for the same objects depending on the task category. The way a spoon is grasped varies heavily during a cooking task where it had to be manipulated within hand, while for the dishwashing tasks, a more simple grasp will suffice to pick and place them from the dishwasher. This indicates the effect of manipulation required for a task on grasp planning. All the grasping and manipulation strategies associated with each of the task categories are presented in Figure 7.4 along with the graphical representation of the grasps. The most commonly employed manipulation types are also detailed in the figure. The subjects employed a sum of 33 grasps and 10 manipulation types to complete the various kitchen activities. However, some approaches were more commonly used than others. The frequency at which these various grasps and manipulation are used are presented for each of the individual tasks in Figure 7.3.

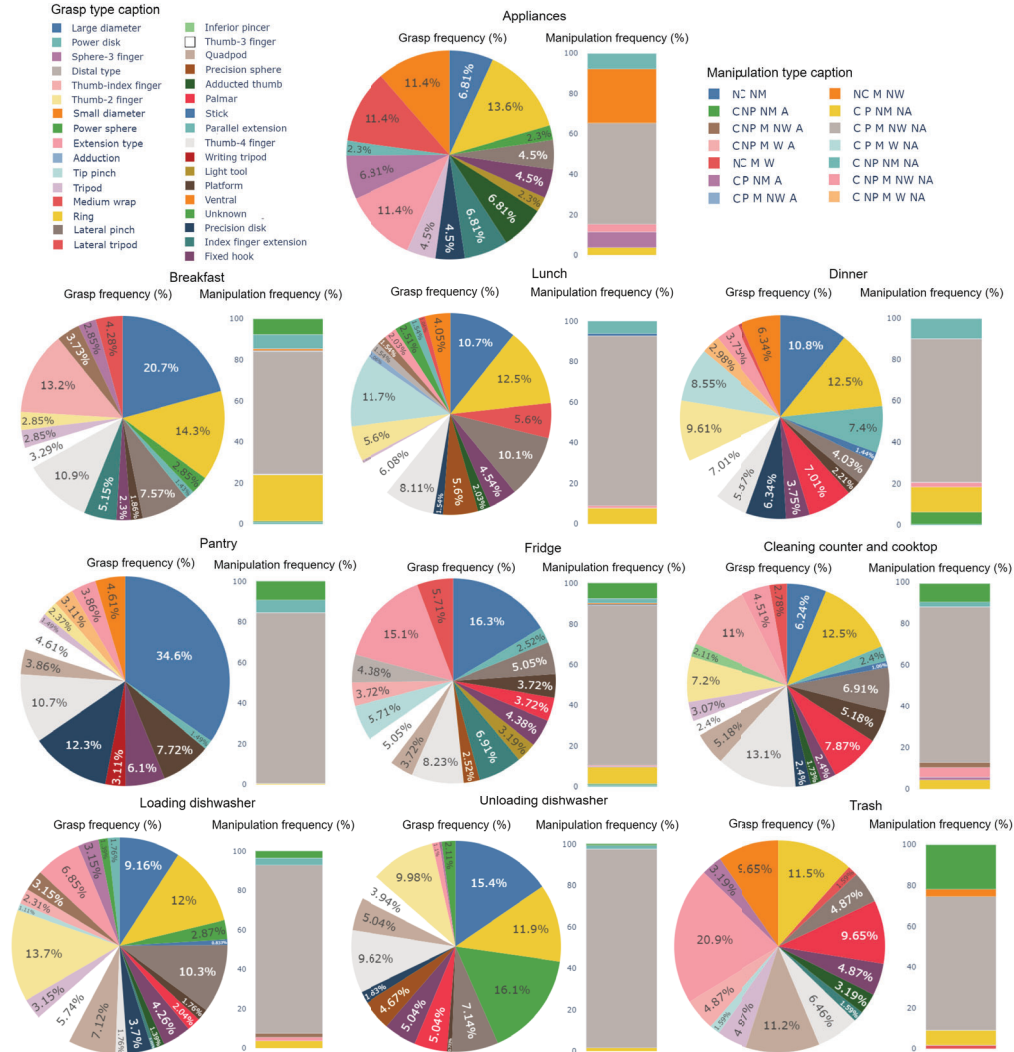
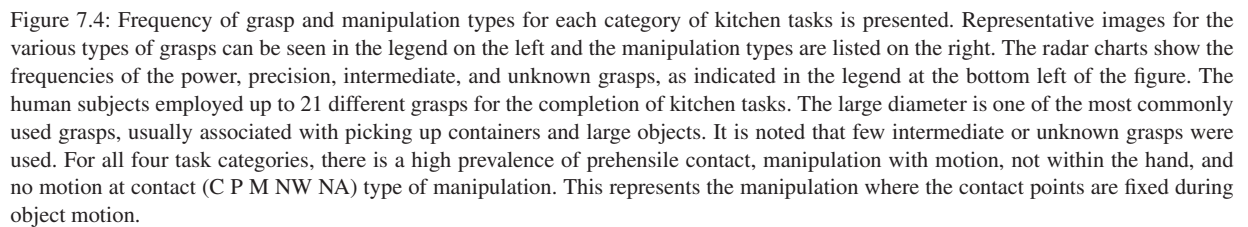


Figure 7.3: Frequency of grasp and manipulation types for each of the ten kitchen tasks. There is heterogeneity in the grasp types used for each task. Most tasks involved object movement with fixed contact points (C P M NW NA) type of manipulation.



7.4.2 Considerations for Robot Task Execution

Table 7.1 summarises the results of the human grasping and manipulation strategies employed for the successful completion of various categories of kitchen activities. This can be used to derive insights for the selection of the minimum attributes required for the completion of specific kitchen tasks. For instance, the stocking of groceries onto a pantry required the use of only one hand for 79% of the time, indicating the lack of need for bi-manual strategies in this category. On the other hand, the preparation of breakfast, lunch, and dinner required both hands to complete more than 50% of the cooking tasks successfully. Similarly, most of the grasps performed during the kitchen activities could be classified under power and precision. These accounted for 87% of the task executions. Every task category required the thumb to be out of the plane from the palm and oppose the fingers for the completion of 75% of the total tasks. The number of unique grasps performed by the subjects during each task category indicates that the cooking tasks required a varied number of grasp types, while the appliances could be operated with the least number of grasps. Also, most of the manipulation tasks could be completed with the contacts fixed on the object during task execution.

This analysis is valuable for the design of robotic grippers and hands. Deriving from these results, an end-effector with a thumb positioned out of plane from the fingers and opposing them will complete a significant quantity of the kitchen tasks. The average unique grasps employed for each category is much lower than the total grasp types identified from the annotations. This indicates alternate grasp types can be used to complete kitchen tasks that require complicated grasps, and the choice of grasp selection was subjective. Hence, a gripper that can only perform a limited number of grasp types can still perform complicated kitchen tasks using alternative approaches. These inferences have been experimentally validated based on the execution of the kitchen tasks using an anthropomorphic robot hand and a two-fingered parallel gripper, and the results are presented in section 7.5.

7.5 Evaluating Robotic Grippers

The ability of the robotic grippers to execute the set of 2000 activities from the human data was analyzed. The output has been grouped into 3 classes: i) the gripper/hand can execute the task efficiently every time, ii) the tasks failed during multiple trials or required extensively long duration to complete, and iii) tasks cannot be performed with the current design of the gripper. The results of this analysis are presented in the dexterity/capability map shown in Figure 7.5. The analysis showed that the gripper could perform 56% of the

tasks performed by the humans efficiently and 35% of the tasks could not be executed as efficiently, as the grippers required multiple attempts to perform these tasks successfully. Certain complex tasks had to be executed by performing multiple steps that resulted in a significantly higher duration to complete. Several factors contributed to this loss of efficiency, varying from the position and orientation of the object, operating in tight spaces or cluttered environments, and the properties of the object being manipulated, among others. For example, the gripper failed to pick small objects like spoons that were placed inside the dishwasher's cutlery basket due to the restricted operation space. The grippers also failed multiple times at picking a plate lying flat on the counter. The gripper was unable to complete 9% of the tasks executed by the humans using the current design restrictions. This included some tasks requiring complex in-hand manipulations that could not be converted to multiple sub-tasks that can be executed sequentially.

In order to further evaluate the performance of the robotic grippers based on the time duration required to complete, a set of 8 kitchen tasks were performed with the grippers mounted on an interface and with humans. The results of this comparison are presented in Figure 7.6. Though the robots could complete the majority of the tasks performed by humans using the limited grasping and manipulation strategies available with the current design, the execution time was significantly higher. The figure shows that humans only require a very small fraction of the time the robotic grippers require to complete all of the evaluated kitchen tasks, leaving tremendous room for improvement. The review of the human and robot task execution data revealed a number of strategies commonly employed by humans in a kitchen environment. These strategies are classified in the following kitchen-oriented task-specific taxonomy.

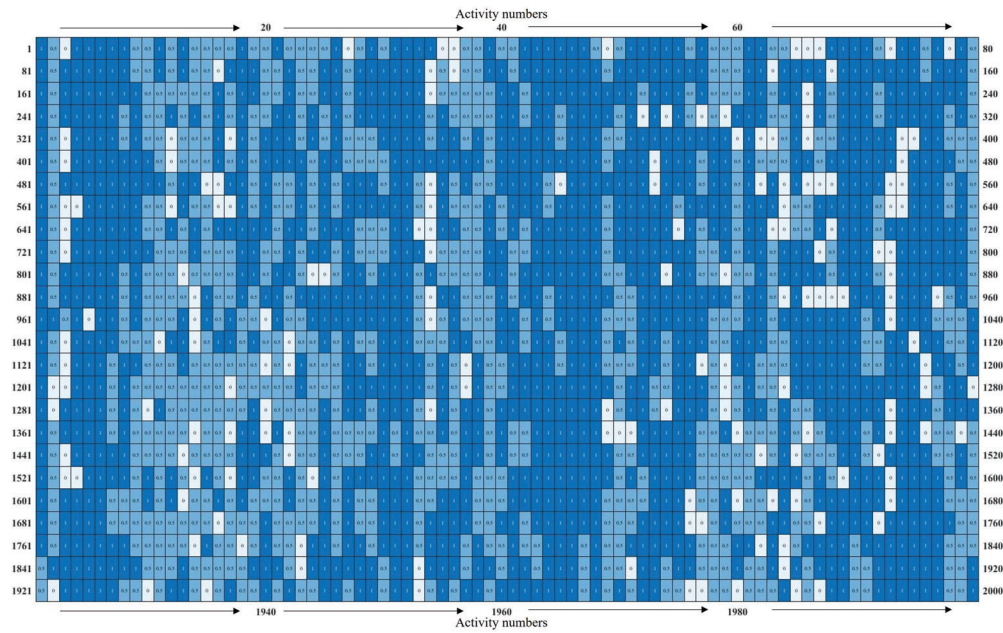


Figure 7.5: The capability map compares the current capabilities of the robotic grippers to execute the set of 2000 activities performed by the humans for the completion of kitchen tasks. The activities are classified into three main classes based on robotic grippers capability: 1- successfully execute the task every time, 0.5 - multiple attempts or very high duration required to complete the task, 0 - cannot perform the tasks with current capability.

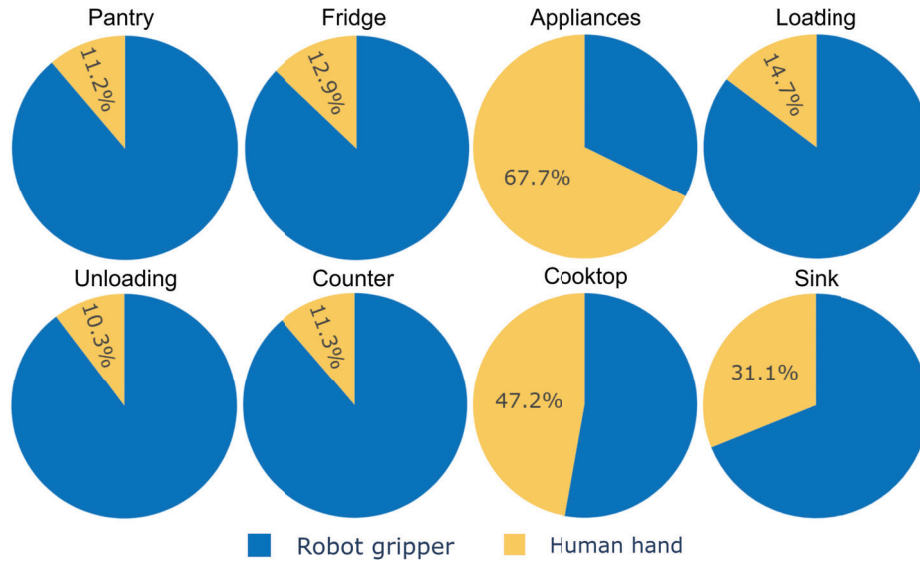


Figure 7.6: The figure compares the percent of time taken by humans to complete the same set of kitchen tasks performed by robotic grippers.

7.5.1 Kitchen Task Specific Taxonomy

Humans employ a variety of complex grasps and manipulation strategies for task execution that decrease the completion time significantly. In this section, we propose a taxonomy of the unique manipulation strategies employed by humans in a kitchen environment as presented in Figure 7.7.

7.5.1.1 Parallel Task Execution Manipulation

Parallel task execution accounts for the majority of the time saved by humans. A complex task is executed by the cumulative effort of individual tasks performed by the hands. Placing a plate in between two plates would require the hand to lift the top plate, move the other plate onto the lower plate, and place the top plate. This complex task executed as a single task by the humans is performed as 3 sequential tasks by the robots, resulting in slower task completion.

7.5.1.2 Bimanual stabilized Manipulation

Bimanual stabilized manipulation tasks require the objects being manipulated to be stabilized by one hand while being manipulated by the other as demonstrated in Figure 7.7b. For example, a salt grinder needs to be held firmly by one hand while the other hand can

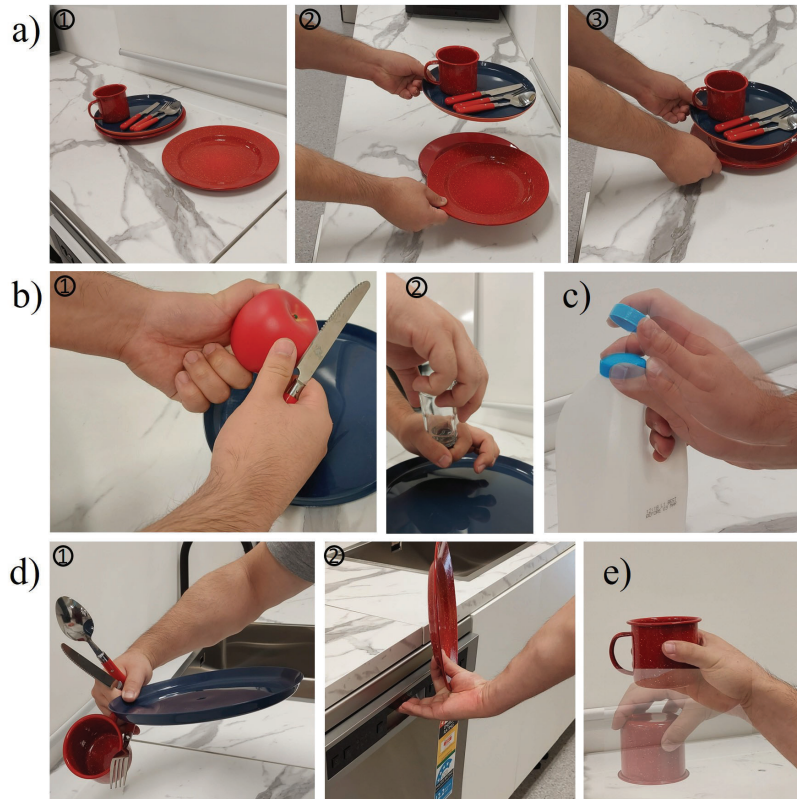


Figure 7.7: Some of the manipulation strategies employed by humans in the execution of kitchen tasks are presented in this figure: a) parallel task execution manipulation, b) bimanual stabilized manipulation, c) in-hand stabilized manipulation, d) compound manipulation, and e) grasp conversion manipulation.

twist it to grind the salt. Another example would be an apple held firmly on a cutting board while another hand can peel the skin off.

Another key manipulation exhibited by the humans involved holding down an object and manipulating a part of the object using the same hand. In-hand stabilized manipulation can be seen in Figure 7.7c where the user stabilizes the milk can by holding its handle while twisting the cap using the index and thumb fingers to open it.

7.5.1.3 Compound Manipulation

The humans demonstrate the ability to grasp and manipulate a wide number of objects of varying shapes and sizes that each require a different grasp type in a single task. In Figure 7.7d, the subject can be seen manipulating a set of cutlery, a plate, and a cup by picking more objects while securely holding on to others and moving them from the counter. This type of task execution is called compound manipulation. This skill is not achievable

by most current robotic grippers due to the complexity of the task and individual control over the joints required to execute them successfully.

7.5.1.4 Grasp Conversion Manipulation

Grasp conversion manipulation refers to the ability of the human hand to move the manipulated object from one grasp type to another during the execution of a task. This is demonstrated by a user moving a cup grasped in a large diameter power grasp type to a precision disk type grasp while picking and placing a cup from the counter onto a dishwasher without losing contact with the manipulated object as shown in Figure 7.7e.

7.5.2 Summary

These five manipulation strategies enable the human hands to complete the kitchen task execution across various categories in a fraction of the time required by the robotic grippers. The inability of the current gripper to perform these complex manipulations limits its task execution and increases the task completion time. The gripper performance can be improved significantly by incorporating these manipulation capabilities.

7.5.3 Data Availability and Dedicated Website

The complete dataset, videos in HD quality, and a dedicated website complementing this study can be found at the following URL:

www.newdexterity.org/kitchendataset

7.6 Discussion from Initial Analysis

In this study, we compared the performance of robotic grippers and humans in the execution of complex kitchen tasks grouped under different categories. A comprehensive dataset containing more than 2000 annotated kitchen activities was created from videos of users performing the tasks in their kitchen environment. A detailed analysis of this dataset was performed to extract the most commonly employed grasping and manipulation strategies in kitchen activities. An anthropomorphic hand and a parallel jaw gripper operated using an arm-mounted human machine interface were used to complete the same set of tasks in a kitchen setup at the lab. We compared the performance of human hands and robotic grippers against each of the activities in the dataset and we presented a color-coded dexterity map that enables us to visualize their current capabilities and limitations in the execution of complex kitchen tasks. The capability map classifies the

activities into tasks that the robots can execute into 3 classes: i) can complete efficiently, ii) require multiple attempts or significantly higher duration, and iii) not achievable with the current design of robots. Further, evaluating the task completion time revealed that the humans only required a fraction of the time taken by the robot counterparts for the successful execution of the kitchen tasks indicating the need for massive improvement of the robotic grippers. We have classified five major manipulation strategies employed uniquely by humans to achieve this efficiency level in a kitchen-oriented task-specific taxonomy. The key insights from the initial analysis is used to create an expanded dataset that includes further essential attributes to the annotation process.

The rest of the chapter is organized as follows: Section 7.7 details the creation of the expanded dataset, section 7.8 introduces clustering for analysis of the data, section 7.9 discusses the various data processing methods employed, section 7.10 presents the various clustering algorithms used in this study, while section 7.11 presents the validation and interpretation of the clusters, section 7.12 discusses the variation in task execution strategies across subjects, and section 7.13 concludes the chapter and discusses some potential future directions.

7.7 Further Expansion and Evaluation of Kitchen Dataset

We further expanded the dataset by annotating the videos recorded from a number of further subjects in their respective kitchen. Certain tasks were also performed under specific protocols to restrict the numerous grasping and manipulation options available to humans and examine the performance under new conditions. Examples include loading the dishwasher one object at a time to directly compare the performance of the robotic grippers and humans performing the exact task. We annotated further detailed features to understand other contributing factors in the improved human task performance. The total number of attributes included in this dataset was increased to 24 (from 13 in the initial dataset). A detailed guide explaining the annotation process starting from the naming convention of the files, each of the attributes being annotated, and guidelines for selecting the pre-established options for classifying each attribute are provided in Chapter VI B. Some critical features added to the annotation include object properties such as shape, size, and weight among others to determine the correlation between the grasp/manipulation selection with respect to certain object classes. Another key addition to this dataset includes the height where the object is located in the environment and how the human hand-arm system approaches the object. This can help determine strategies for the robot arm-hand system to execute the best approach, grasping, and manipulation of objects depending on their location.

Our analysis of the earlier dataset showed that the effectiveness of the robot hands decreased significantly when the objects to be manipulated were buried under other objects or placed in unconventional orientations. This required the robot grippers to determine a sequence of steps to move the objects on top, pick the specified object, and place the other objects back in their original position, causing a significantly increased task completion time. Hence, we captured the orientation of the objects being grasped and manipulated in the expanded dataset to analyze the specific strategies employed by humans in overcoming these instances. We also captured the shoulder movements and posture of the humans during the execution of the task to determine their importance in improving the task execution capabilities. All the options associated with the task attribute were simplified to a single word description of the task. All the possible options for each attribute were provided and could be chosen from a drop down option by the annotators. New options identified for the attributes were added to the pre-established options as and when deemed necessary during the annotation process.

The new dataset was generated from videos of kitchen tasks executed in the home kitchen environment of three subjects over five trials. The tasks and trials were performed over a number of days at different times of the day and were not performed consecutively to avoid fatigue and repetitiveness of the tasks. The dataset comprising of high definition videos (total duration ~7 hours), and detailed annotations including more than 10,000 activities is made available on the following URL:

www.newdexterity.org/kitchendataset

7.8 Dataset Analysis using Clustering Techniques

A multi-dimensional dataset was the result of the annotation process. To detect underlying structures in the data we employed a series of clustering techniques [164]. Unlike the earlier analysis, we did not impose any predefined classes or labels on the dataset entries. The clustering techniques were used to generate clusters from the activity attributes and provide us with patterns among the dataset. The similarities and differences among the clusters were analyzed to provide us with information regarding the attributes associated with them. The cluster analysis procedure followed in this study is presented in Figure 7.8.

The video samples were collected from the kitchen tasks that were executed by all subjects and were annotated during the data labeling phase. The complete annotated dataset was used for the analysis in this work and is presented in detail below.

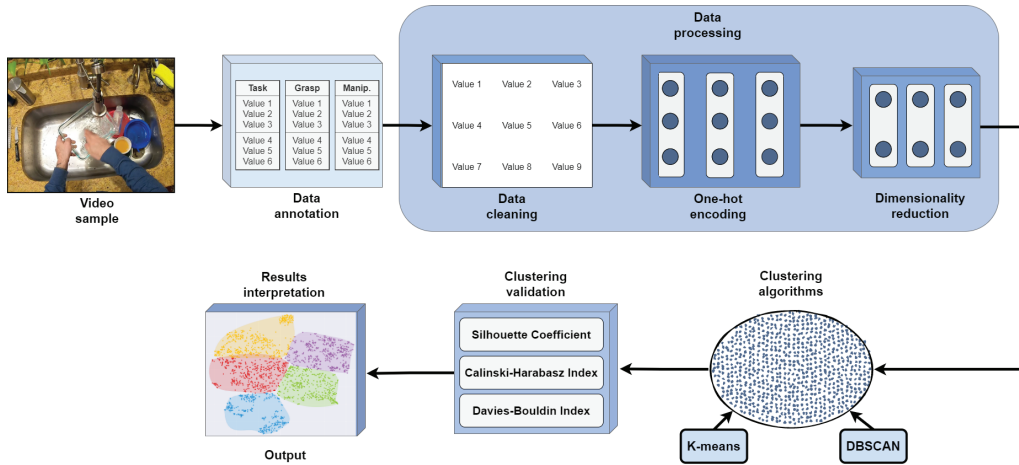


Figure 7.8: The process of analyzing the dataset using clustering algorithms.

7.9 Data Processing

The first step in processing involved data preparation. This step ensured the dataset was continuous and was converted to the necessary structure required for processing. The dataset was checked for empty rows and rows that missed significant information required for the processing. Such entries were removed from the dataset. The dataset was checked for missing values post this step across the various columns and the missing values were replaced by NaN to enable further processing. This was followed by converting the time taken for task completion columns to numerical values and validating the entries based on the start and end times of the tasks. This was performed to ensure the time duration column did not contain any null or negative values that would indicate an error in the annotation or preprocessing stages.

Once this was complete, the "start time" and "end time" columns became redundant and were dropped from the dataset. The attributes were analyzed to identify outliers and the outliers were either associated with existing variables wherever applicable. The values that could not be grouped under the pre-established categories were grouped as "other". Specific attributes in the dataset that were not significant for a given analysis were also dropped. For example, the initial clustering of grasping/manipulation characteristics associated with the object properties and orientation did not depend much on the "Washes hands" column as all entries fell under the same option ("No" washing of hands was recorded). Hence, this column was dropped from the analysis.

As most of the attributes in the dataset were made up of categorical data, they need to be transformed in order to be processed by the clustering algorithm [165]. We employed various encoding methods including one-hot encoding, dummy encoding, and

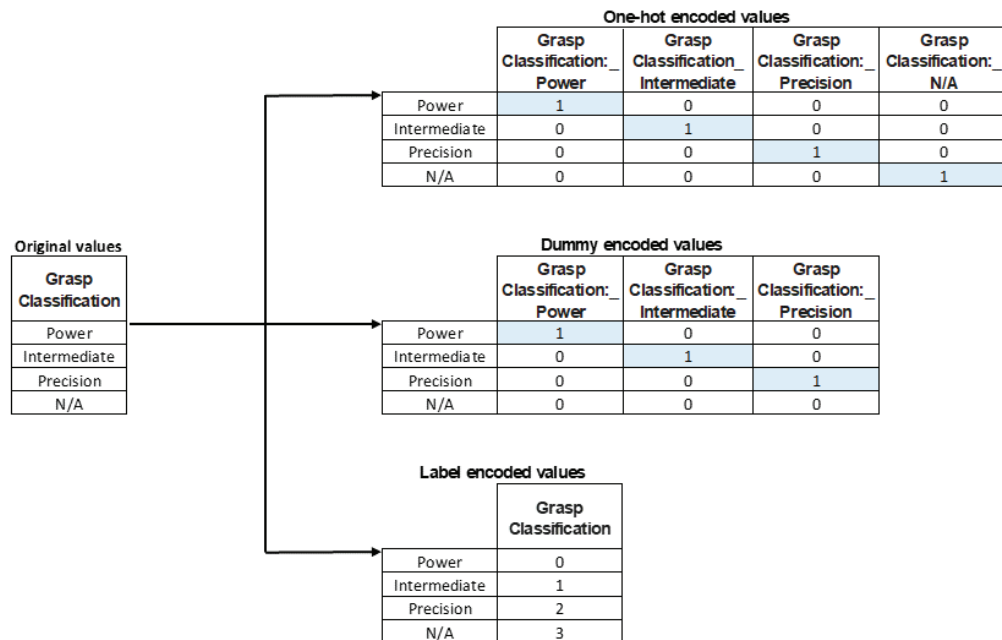


Figure 7.9: The various encoding methods used for converting the "Grasp Classification" categorical variable to a binary/numerical variable are presented in this image. The binary values for each of the categorical values generated by one-hot encoding and dummy encoding as well as the numerical values generated by the label encoding methods can be seen in the figure.

label encoding methods to the categorical values as shown in Figure 7.9. The simple and commonly used label encoding method assigned an integer value to each of the categorical classes. However, it also introduced a false sense of the ordinal relationship. For example, the "precision" class with an integer value of 2 is considered more significant than the "power" class with an integer value of 0. Since the categorical variables in the dataset do not have an ordinal relationship, a one-hot encoding is employed to generate a binary variable for each unique value in the dataset. However, this resulted in N columns for the N unique categorical values. Dummy encoding though similar to the one-hot encoding method, resulted in $N - 1$ columns. Even after dropping some of the columns, the resulting dataset was still in a very high dimension. This makes visualizing the data infeasible while also significantly increasing the computational time and cost. To overcome this limitation, dimensionality reduction techniques were used to process the dataset.

Grasp Classification		Grasp Classification: _Intermediate	Grasp Classification: _N/A	Grasp Classification: _Power	Grasp Classification: _Precision
0	Power	0	0	1	0
1	Power	0	0	1	0
2	Precision	0	0	0	1
3	Precision	0	0	0	1
4	Power	0	0	1	0
...
10014	Power	0	0	1	0
10015	Precision	0	0	0	1
10016	Precision	0	0	0	1
10017	Precision	0	0	0	1
10018	Power	0	0	1	0
10019 rows × 1 columns		10019 rows × 4 columns			
Original Dataset: "Grasp Classification"		One-hot encoded dataset: "Grasp Classification"			

Figure 7.10: The figure presents the "Grasp Classification" attribute in the dataset being converted using the one-hot encoding from categorical to binary values.

We applied dimensionality reduction to project the data onto a lower dimensional space (2D) retaining most of the data variance. The most commonly employed dimensionality reduction technique PCA (Principal Component Analysis), was not effective as it did not retain the non-linear variance of the dataset. Hence, in this study we employed the non-linear dimensionality reduction technique, t-SNE (t-distributed Stochastic Neighbor Embedding) [166]. This algorithm is effective in retaining local variance by retaining the variance of local points and embedding them into lower dimensions by retaining the structure of neighboring points. The PCA was applied only for dimensionality reduction and visualization of the variance across the subjects [167]. The dimension-reduced dataset is provided as the input to the clustering algorithms for further analysis.

7.10 Clustering Algorithms

7.10.1 K-means Clustering Algorithm

K-means is one of the simplest and most popular unsupervised machine learning algorithms used in clustering. It groups the various data points into clusters based on their similarities resulting in patterns of the data. The k-means is a centroid based algorithm that allocates each point in the dataset to one of the "k" centroids of clusters based on distance [168]. We need to provide the number of clusters "k" as input to the algorithm. To identify the optimal value for "k", we employed the elbow method to calculate the distortion score for all clusters for a range of k values [169]. The distortion score is calculated as the sum of squares distances from each point to its respective centroids. The

scores for the various values of k are then plotted and the point of inflection (elbow) in the resultant line chart that resembles an arm is chosen as the best value of k . For our dataset, the optimal value for k was calculated as 5.

7.10.2 DBSCAN Clustering Algorithm

DBSCAN (Density-Based Spatial Clustering of Applications with Noise) [170] is another clustering algorithm that groups high density data into clusters separated by regions of lower density. Unlike the k -means algorithm, DBSCAN does not require the number of clusters to be provided as input beforehand and is capable of identifying outliers in the dataset as noise. The only parameters required by the DBSCAN algorithm are ϵ - the minimum distance between the points for them to be considered neighbors and $minPts$ - the minimum number of points required to form a dense region or cluster [171]. The $minPts$ was calculated as $2 * Data\ dimension$. And the ϵ value was calculated by plotting the distance between each data point to its closest neighbor calculated using *Nearest Neighbours*. The maximum value at the curvature is determined as the ϵ . However, this resulted in more than 30 clusters with enormous overlapping. Hence, the optimal values were chosen empirically based on the silhouette scores obtained for varying ϵ and $minPts$.

7.11 Cluster Validation, Analysis, and Results

The outputs of the clustering algorithm were validated using three measures: the Davies-Bouldin index [172], Silhouette coefficient [173], and Calinski-Harbasz index [174]. The Davies-Bouldin index calculates the average "similarity" between clusters by comparing the distance between the clusters with their respective size. A lower Davies-Bouldin index signifies a model with better separation between the clusters. On the other hand, the silhouette method validates clusters based on two measures: a - the mean distance between a given point and all other points within a cluster and b - the mean distance between the point and all other points in the next neighboring cluster. The two measures provide us with the closeness of points within a given cluster and the distance of points between different clusters. The value of this measure varies from -1 (incorrect) to 0 (overlapping) to 1 (highly dense) clusters. The Calinski-Harbasz index validates clusters based on the ratio of the sum of between-clusters dispersion and inter-cluster dispersion for all clusters. A higher score represents a better clustering performance. The scores for the various measures obtained by the k -means algorithm and DBSCAN algorithm are presented in

Table 7.2. As shown in the table, the current dataset was more efficiently clustered using the k-means algorithm indicated by the higher values for silhouette's co-efficient and Calinski-Harabasz as well as the lower Davies-Bouldin index. These indexes represent a higher similarity between the data points within the k-means cluster as compared to the DBSCAN cluster.

Table 7.2: The table presents the validation scores for the K-means and DBSCAN clustering algorithm for the current dataset.

Cluster Validation Measure	Scores for Algorithm	
	K-means	DBSCAN
Input Parameters	k = 5	$\epsilon = 4.4$ minPts = 9
Number of clusters	5	9
Davies-Bouldin Index	0.8543	1.5072
Silhouette Coefficient	0.3735	-0.2562
Calinski-Harabasz Index	8949.088	592.1351

The clusters obtained from the k-means are presented in Figure 7.11. The optimal value of k provided as input resulted in 5 clusters using the k-means clustering method. In comparison, the DBSCAN algorithm provided 9 clusters for the optimal value of ϵ and $minPts$. The clusters produced by the k-means algorithm had a more uniform distribution. In contrast, the clusters formed by the DBSCAN algorithm are unbalanced owing to the higher density of data across the plane resulting in a huge number of data points being allocated to cluster 1 (8739 points). Also, as indicated by the low silhouette coefficient there is an overlapping of clusters created by DBSCAN. Hence, we only utilized the results from k-means clustering in this study.

In Table 7.3, the distribution of the various vital characteristics among the clusters is presented. The number of elements in each cluster averaged at 2000 and it can be seen from the table that closely related activities are grouped together signifying the cluster efficiency. For example, cluster 0 grouped activities involving the loading and unloading of dishes from a dishwasher that only required four different grasps and manipulating the grasped object without motion at contact for the successful execution of the majority of tasks. On the other hand, cluster 2 and cluster 3 captured the cooking tasks including the preparation of breakfast, lunch, and dinner, and operating the appliances. These clusters required over 9 grasps each to complete a significant part of the tasks. While cluster 4 required the pick & place tasks, the opening and closing of various objects were grouped under cluster 2. The requirement of the MT8 manipulation type shows a number of objects were placed and moved without completely restricting their motions in a grasp (non-prehensile). Cluster 4 had the most number of mixed activities compared to

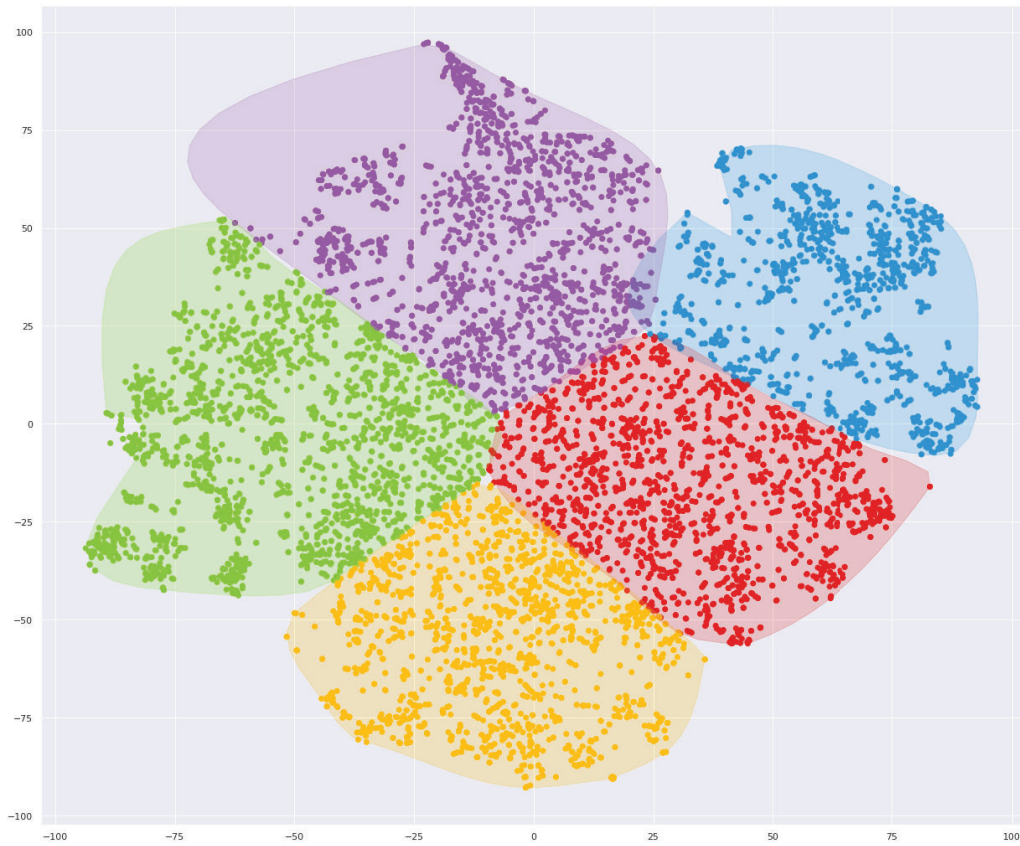


Figure 7.11: The clusters generated for all the activities of the kitchen dataset using a k-means clustering algorithm.

other clusters even though stocking tasks occupied a significant portion of the cluster. The requirement for "carry" tasks along with pick & place correlates to carrying the objects from the counter or shopping bags to the fridge/pantry during the stocking tasks. And the grasp conversion used by humans while picking and placing the objects into a dishwasher can also be seen from the task type and category columns of cluster 4.

It is evident from these observations that the points within each cluster have a high similarity with each other and are well distinct from the points in neighboring clusters. Hence, the unsupervised learning methods employed in this study can successfully group data points into clusters enabling us to visualize the similarities and characteristics of each cluster. Furthermore, these clustering analysis reinforce our earlier inference that a majority of the kitchen tasks can be successfully executed using a limited number of grasps without the need for complex in-hand manipulation tasks. A significant part of the activities performed in the kitchen environment could be classified into simple tasks

Table 7.3: The table presents the analysis of the clusters generated by k-means clustering. The distribution of the task types, number of grasps, manipulation strategies, and kitchen task categories that contribute towards a majority of each cluster (greater than 2/3 of the cluster) are presented in the table.

Cluster Number	Number of entries	Major (>2/3rd) Contribution			
		Task type	Number of Grasps	Manipulation type	Kitchen Task
0	2063	Pick, Place, Hold	4	MT10	Dishwasher
1	2456	Pick, Place	7	MT10	Cleaning (Dinner, Loading Dishwasher)
2	1450	Open, Close	9	MT10	Cooking
3	1930	Pick, Place	10	MT10, MT8	Cooking
4	2120	Hold, Pick, Place, Carry, Convert grasp	6	MT10, MT6	Stocking (Loading Dishwasher, Dinner)

like pick, place, open, close, and hold among others that can be executed by grasping an object and moving it in space without changing the contact points.

7.12 Inter-subject Variability of Grasping and Manipulation Strategies

The dataset was analyzed to derive specific inputs for further data collection and for determining the tasks/strategies that require more focused analysis. The percentage distribution of the various grasping and manipulation strategies employed by individual subjects for each of the ten kitchen tasks was calculated from the dataset. This provided us with the percent usage of over 45 different grasp types and over 15 manipulation types employed by the subjects for the successful task completion stored in a 45 dimension and 15 dimension space respectively. The distribution of the grasp classes (power, intermediate, precision) was also calculated for the task categories. To visualize this data and enable easy computation, principal component analysis (PCA) [167] was employed to reduce the dimensionality of each of these distributions to two dimensions. The resulting visualization shown in Figure 7.12 resulted in 10 data points per subject (annotated as H1, H3, and H5 respectively) corresponding to each of the task categories (represented by specific colors). To calculate the variability in the grasp and manipulation strategies for a given task, a polygon is formed using the projection of each subject for the corresponding task as the vertices. For a given N number of subjects, the inter-subject variability μ is the area of the polygon given by Eq. 7.1.

$$\mu = \frac{1}{2} \sum_{k=1}^N |(x_k y_{k+1} - x_{k+1} y_k)| \quad (7.1)$$

where x and y are the 2D coordinates of each distribution in the dimensionality reduced space. The area of the polygon provides the similarity or variation across the subjects. The results of the variance for each of the task categories are detailed in Table 7.4.

Table 7.4: The table presents the inter-subject variability of the various grasp classification, grasp types, and manipulation types employed for the completion of the various kitchen tasks. The variability is calculated as the area of the polygon formed by the dimensionality reduced projection of the strategies of individual subjects for a given task.

Task Categories	Kitchen Tasks	Inter-subject variability of		
		Grasp classification (Power, Precision, Intermediate)	Grasp type	Manipulation type
Cleaning	Cleaning Counter	0.009176663	0.00250189	0.000225643
	Trash	0.008876194	0.00209437	0.010817924
Cooking	Appliance	3.33941E-05	0.00032804	0.005290514
	Breakfast	0.034791146	0.00685288	0.002827732
	Dinner	0.00902811	0.00016537	8.18402E-05
	Lunch	0.023628928	0.00029364	0.003235945
Dishwasher	Loading Dishwasher	0.011448654	0.00273866	0.000506101
	Unloading Dishwasher	0.006309446	0.00340936	0.011469317
Stocking	Fridge	0.024928724	0.03346606	0.002102952
	Pantry	0.05255976	0.02292499	0.000307737

The variability is higher if the area of the polygon is higher indicating that the subjects employed different strategies from each other for the completion of the specific task. It can be noted from the table that a higher variation in the grasp types usually is complemented by a high variance in grasp classification. This could mean that the subjects employ different grasp types classified under different categories (power, precision, intermediate) for successful completion. While the first subject might employ a rigid power grasp, the following subject might use a precision grasp to restrict the motion of a given object. This difference in grasp strategies might stem from a personal preference as well as environmental conditions such as the location of the object. Irrespective of the cause, these tasks require attention during the further data collection stages to determine the ideal strategies to be transferred to robot grippers and hands. Another common observation is that the grasping and manipulation strategies vary inversely with each other in most cases. For example, the stocking of the pantry and fridge had a high variability of grasp types across the subjects. This can be attributed to the different objects/groceries being stocked in each kitchen requiring a different grasping strategy. However, these tasks only involved picking up the groceries and placing them on the pantry/fridge shelf. Hence the manipulation strategy used by all the subjects is identical resulting in a low variance. On the other hand, all subjects used similar grasping strategies for unloading a

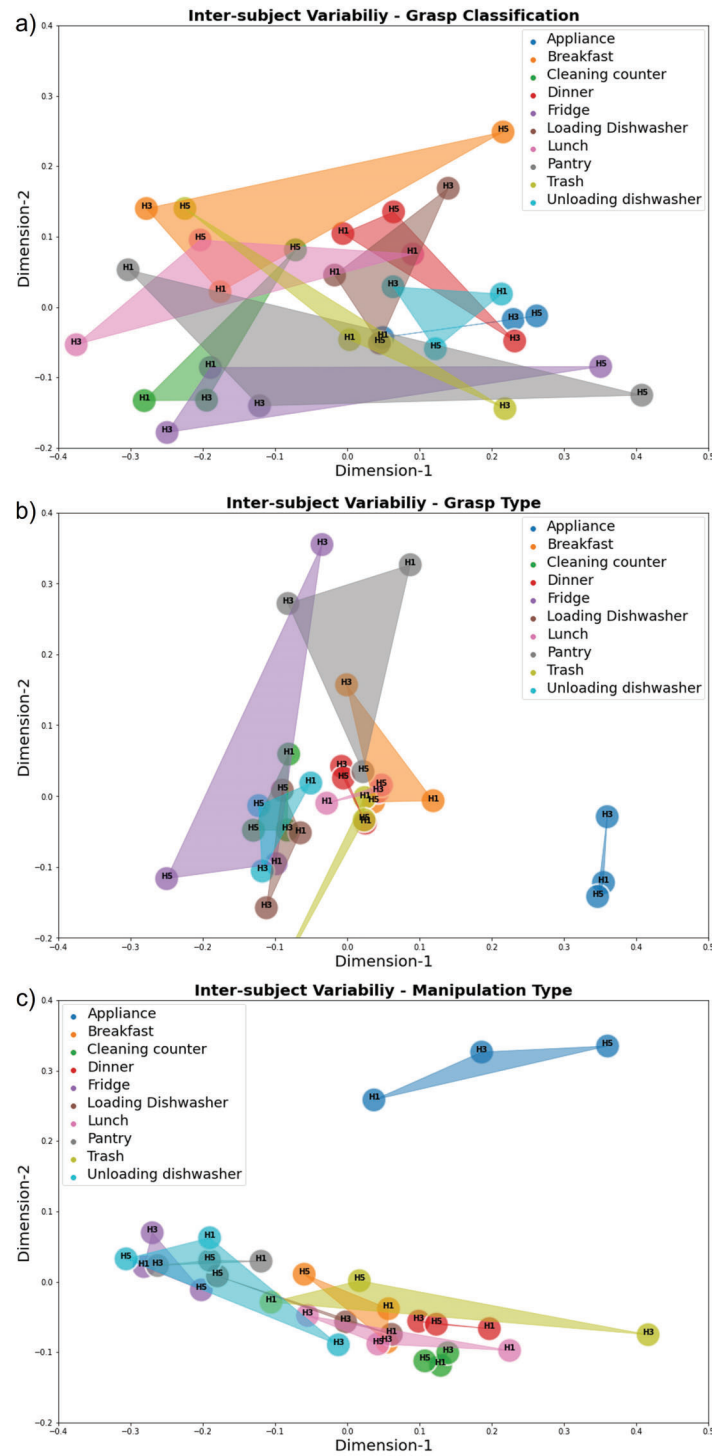


Figure 7.12: The inter-subject variability in the a) grasp classification, b) grasp types, and c) manipulation strategies employed for the completion of the various kitchen tasks are calculated from the 2D dimensionality reduced projection of each subject.

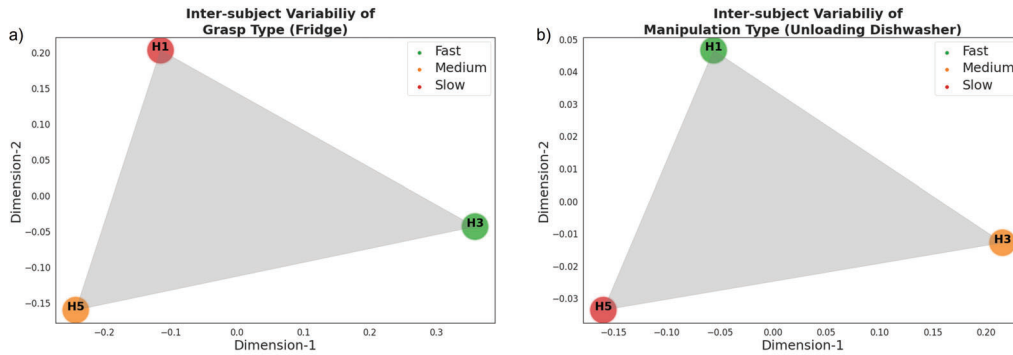


Figure 7.13: The inter-subject variability mapped along with average task execution time for: a) grasp type (fridge task), and b) manipulation type (unloading dishwasher). In such cases, the fastest task execution time would allow us to select the strategies employed by one subject over the other.

dishwasher but the manipulation strategies varied widely. Similar variation can also be observed in the clearing of trash where the object to be grasped remained identical with different manipulation strategies being employed.

The primary focus of this data collection and analysis is to identify the key skills employed by humans for the successful execution of various task categories in a kitchen environment. This would enable the identification and transfer of key skills for the development of robotic grippers and hands that can perform on par with humans as well as collaborate with humans. The tasks with a low variance indicate a standard strategy being employed by all subjects and are directly transferable to robots. Tasks such as cleaning the counters and loading a dishwasher have a very small variance across the subjects and the grasping/manipulation strategies employed for these tasks can be used by the robotic end-effectors. On the other hand, the tasks with a high inter-subject variance such as cooking require data collection from a number of subjects to determine the ideal strategy. And determining the cause for the variation across subjects can also provide insights for the selection of optimal grasping and manipulation strategies by considering other parameters such as the speed of execution and accuracy. For example, if each of the subjects uses a different set of strategies for identical objects placed in similar conditions owing to personal preference, the strategy that enables the fastest task execution and higher accuracy can be chosen over others.

Figure 7.13 presents the inter-subject variability for grasp type and manipulation type for a given task color-coded based on average task completion time. Subject 3 employed a "Large diameter grasp" for a majority of the fridge loading task as opposed to subject 1 and subject 5 who performed most of the tasks using the "precision sphere" grasp type. It can be seen from Figure 7.13a that subject 3 had the fastest execution time indicating

the effectiveness of the "Large diameter" grasp type in loading the fridge. Similarly in Figure 7.13b, subject 1 completed unloading the dishwasher faster than other subjects by combining manipulation of grasped objects (with fixed contacts), non-prehensile manipulation of objects (pushing or moving the objects without grasping), and grasp conversion manipulation. While subject 2 and subject 3 were slower as they did not employ non-prehensile manipulation of the objects resulting in a slower completion time. Hence, it is beneficial to impart non-prehensile manipulation strategies to robots to achieve faster task execution.

Thus, the analysis helps select the optimal strategies employed by the various subjects. It also provides directions for the specific data to be collected and key attributes that require focus during data collection to improve the skill transfer and collaboration between humans and robots.

7.13 Conclusion and Future Directions

In this study, We further expanded the initial kitchen dataset by annotating videos recorded from a number of further subjects that included tasks being performed under specific constraints. Over 24 attributes were annotated for each activity and a comprehensive dataset containing more than 10,000 kitchen activities was created from videos of users performing the tasks in their kitchen environment. The multi-dimensional dataset created from this process was analyzed using clustering, an unsupervised classification method. The preliminary results show that the clustering algorithm can utilize the input data feature space to define and address the proposed goal of analyzing and finding patterns in the dataset. The generated clusters reinforced our earlier inferences by grouping, for example, activities involving loading and unloading dishes from a dishwasher together (cluster 0). And a majority of the tasks in each category can be completed using a limited number of grasp and manipulation types. Hence, given new input data, our trained clustering algorithms would be able to extract information and predict to which clustering group this data belongs. This relationship knowledge can direct and optimize future applications by focusing on the desired feature space and cluster group. Further data from multiple subjects need to be recorded to improve efficiency and validate the clustering algorithms further.

The primary focus of the dataset is to determine the strategies employed by humans for the execution of kitchen tasks and transfer the necessary skills to a robotic end-effector enabling it to complete the tasks autonomously or collaborate with humans. The percent distribution of the various grasping and manipulation strategies was presented in

a dimensionality-reduced space. We analyzed the inter-subject variability for the different task categories in this space to determine the commonly employed strategies that can be directly transferred to the robots. For example, all subjects employ identical skills for cleaning the counters and loading a dishwasher and these can be transferred more directly to a robotic end-effector. The tasks with high inter-subject variability require further data collection to determine the ideal strategies and form conclusive results. The current analysis shows a high variation in grasping strategies for stocking the fridge and pantry. The manipulation strategies vary highly during unloading the dishwasher and clearing the trash. Hence, attention needs to be paid to the data collection of the above-mentioned tasks across many subjects to determine the ideal grasp/manipulation strategies. In case of high variance across subjects, further input parameters such as speed of task execution and accuracy can help select subjects that employ the ideal strategies. Further constraints such as a limited number of grasps, fingers etc could be added during the data collection to eliminate the subject bias generated by individual preference and limit the grasp choices. This will also make the skill transfer to robotic grippers/hands more effective as they are usually capable of executing a limited number of grasps. The insights from this work can be used to develop new classes of robotic grippers and hands capable of performing on par with human hands.

Part IV

Design Guidelines for Adaptive Robot Hands and Grippers

Chapter 8

Exploiting Post Contact Reconfiguration of Adaptive Robot Grippers and Hands

8.1 Introduction

Adaptive robot hands have received an increased interest over the last decade due to their simplicity and intuitiveness of operation, their cost effectiveness, and their paramount efficiency in executing robust grasping and dexterous, in-hand manipulation tasks. This new class of hands uses the concept of underactuation (less actuators than the available degrees of freedom) and structural compliance that allow them to conform to the object geometry and improve their performance [175, 143]. In particular, adaptive robot hands offer an increased performance in extracting stable, precise grasps and full / power grasps, being able to efficiently replace complex, heavy, and expensive robot hands in different activities of daily living (ADLs) [15, 176]. Moreover, recent studies have also demonstrated their efficiency in executing dexterous, in-hand manipulation tasks [177]. Adaptive hands have also been of key interest in the development of prosthetic hands owing to their increased functionality at reduced size and weight [178]. The Open Bionics hands[179], the SDM hand[180] and the ISR-SoftHand[181] are some examples of underactuated, adaptive prosthetic hands with compliant joints. However, adaptive hands also suffer from certain shortcomings and limitations. For instance, the forces distribution in underactuated fingers is predetermined by their mechanical design and cannot be easily controlled [182]. Furthermore, reconfiguration reduces the effective grasping force at the robot fingertips during pinch grasps and could lead to the deterioration of

the grasping capabilities or to failure to maintain the desired object positions and orientations. The post-contact reconfiguration experienced in adaptive fingers is commonly caused by the compliance of the joints, the non-rigid parts that compose their structure and the underactuation of the mechanisms [19]. This reconfiguration causes the contact points between the object and the finger to change until an equilibrium configuration is reached. Hence the force exertion required to reach an equilibrium depends on the configuration of the individual phalanges, the joint compliance, and the contact area during reconfiguration [183]. Thus, there is a need to predict the actual force exerted by adaptive hands during grasping in order to guarantee the execution of stable grasps.

Regarding previous works, a number of studies have tried to determine the relationship between the finger configuration and the forces exerted. Two main matrices are commonly used to determine the effects of joint configuration on force exertion capabilities [184]. The first is the Jacobian of the finger that transforms the torque at each of the finger joints to the contact force the finger generates. The second one is the transmission matrix, that uses the types of transmission systems (e.g., linkages, gears, tendons) as a function to determine the force output. In [185], the authors determine the output forces based on the configuration of the differential as well as the open and closed configurations of the fingers and the thumb. In [186], the authors present a method to predict the contact forces exerted by an underactuated robotic gripper using adaptive neuro-fuzzy estimation. In [187], the authors propose an observer-based recurrent neural network (RNNOB) to estimate the non-contact forces during highly dynamic motions. In [188], authors try to reduce the post-contact reconfiguration based on a data-driven optimization of underactuated hands.

Additional sensors such as tactile / FSR (Force Sensing Resistor) sensors that can provide force feedback or a flex sensor that determines the joint angles would increase the cost, the complexity, and the size of the system. Moreover, the integration of force and flex sensors in adaptive hands that use flexure joints is extremely challenging from a cable routing perspective. Hence, in this study we use IMU sensors that are already used for posture recognition in adaptive hands such as the Pisa/IIT SoftHand [189, 190] and commercial prosthetic hands such as the i-limb hand[191] and ArUco markers that provide a vision based estimation of the hand kinematics. The data from these sensors are then processed to train a machine learning regression model.

In this study, we exploit motion capture systems on adaptive robot hands to estimate the contact forces exerted by adaptive robot hands during fingertip/pinch grasps by taking advantage of their post-contact reconfiguration profile. As these systems are highly nonlinear, it is difficult to obtain an accurate mathematical model to predict the

forces analytically[186]. This study uses a machine learning algorithm (Random Forests regression) to predict the contact forces exerted by an adaptive robot finger (output of the model) based on reconfiguration data (input to the model). The reconfiguration data consists of inertial measurement unit (IMU) data collected from appropriate IMU sensors and vision-based data collected from a set of ArUco markers [41]. All markers and sensors were fixed on the different phalanges of the examined adaptive robot finger. The forces exerted by the adaptive finger were measured by a dynamometer (force sensor) unit. A wide range of experiments was conducted in order to validate the efficiency of the proposed methods. During the different experimental conditions the pose and the distance of the finger from the force sensor were varied, as it leads to different post-contact, reconfiguration motions¹.

The rest of the chapter is organized as follows: Section 8.2 introduces the force estimation methods proposed, section 8.3 details the experimental setup, section 8.4 discusses the results, while section 8.5 concludes the chapter and discusses some possible future directions.

8.2 Contact Force Estimation Methods

The contact forces exerted by the adaptive robot finger are estimated based on the post-contact reconfiguration profile. This is achieved by using a machine learning algorithm (Random Forests) in order to formulate a regression problem.

In order to successfully estimate the force exerted by the robot finger, we need to solve a regression problem that maps the reconfiguration profile of the finger (motor current, motor position, angle of proximal and distal phalanges w.r.t. the relaxed finger position) to the force exerted at the fingertip. We choose to use a machine learning approach because of analytical modelling:

- does not take into account some hard to model phenomena like the deformation of the fingerpads and the friction in the finger's tendon routing system
- depends on parameters that are hard to measure with accuracies like the motor load and the tendon tension

¹Majority of the chapter is based on [192], © 2019, IEEE. Reprinted, with permission, from Nathan Elangovan, Anany Dwivedi, Lucas Gerez, Che-ming Chang, and Minas Liarokapis, Employing imu and aruco marker based tracking to decode the contact forces exerted by adaptive hands, IEEE-RAS 19th International Conference on Humanoid Robots (Humanoids), 2019.

For solving the regression problem, we compare the performance of three different models: i) a Multiple Linear Regression model, ii) a Support Vector Machine regressor with Radial Basis Function (RBF) kernel, and iii) a Random Forest regressor.

Multiple Linear Regression (MLR) models the relationship between two or more explanatory variables (input feature vector) and a response variable. Support Vector Machines (SVM) is a popular machine learning tool for classification and regression that was first proposed by Vladimir Vapnik [193]. SVM based regression is considered a non-parametric technique because it relies on kernel functions. SVM is a powerful tool, but the computational and storage requirements increase rapidly when the dimensionality of the training problem increases. Random Forest (RF) is a supervised learning algorithm and was originally proposed by Tin Kam Ho of Bell Labs [194] and Leo Breiman [195]. It is an ensemble learning method that consists of many decision trees and it can be used for both classification and regression. The final output of the RF model is the most popular class among all the trees in case of classification or the average of the output of all the trees in case of regression. Since the final output of RF is an average of all the trees, the output is regularized and is not prone to phenomena like overfitting.

A few other advantages of an RF based learning scheme over others are that it is able to work efficiently with small as well as large databases, it is fast, and it can solve multi-dimensional problems. To create an RF model, the trees are grown using the training set. To do this, the dataset and the feature set are randomly divided by a process called Bootstrap Aggregation (Bagging). This is a process of random selection with replacement. Typically, $2/3$ of the dataset is selected by bagging, and on this newly selected dataset Attribute Bagging is performed. Attribute Bagging is done to select 'm' features from the 'M' features of the dataset. For example, for 10 different selected values of m, 10 different trees are grown. These trees are tested on the remaining $1/3$ of out-of-bag data and the tree with the best performance is selected. The process is repeated 'T' different times to grow 'T' such trees. This approach is also used to calculate the importance of the feature variables as reported in Fig. 8.5. The raw importance score for each feature variable is computed as the average importance score of all trees of the RF. During the model validation phase, we use the 10-fold cross validation procedure to validate all three types of models that we compare.

8.3 Experimental Setup

In order to validate the efficiency of the proposed methods, we conducted two different types of experiments involving the collection of IMU data and vision based data of the

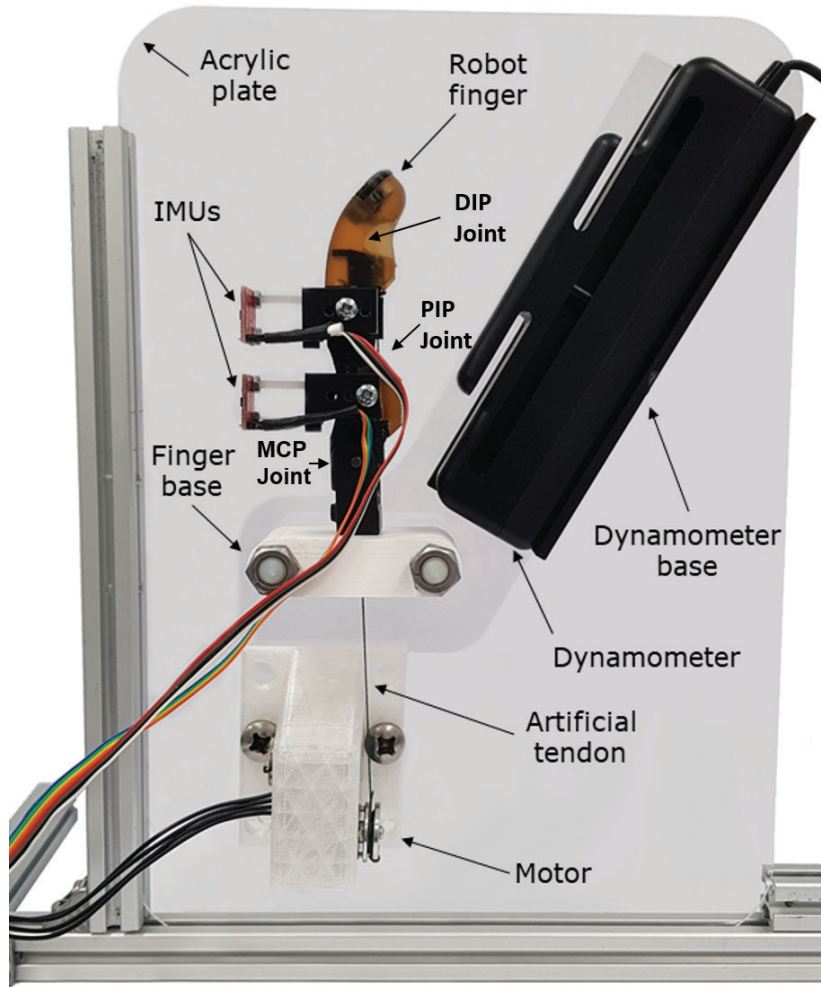


Figure 8.1: The figure illustrates the experimental setup used for IMU-based data collection. A dynamometer was used to measure the contact force applied by the finger, while the IMUs were used to measure the Metacarpophalangeal (MCP) and Proximal Interphalangeal (PIP) joints. This experiment was conducted for 10 different finger angles from 0° to 90° in 10° steps. The motor, the finger and the dynamometer were connected to bases that were fixed to an acrylic plate. The experiments were repeated for 10 trials for every experimental condition.

reconfiguration profiles of the system for different experimental conditions. For both experiments, an anthropomorphic, adaptive, robot finger was used. It consists of a base, a proximal phalanx, and a second link that combines the middle and distal phalanges. The adaptive finger has two spring loaded pin joints. The joints have limited range of operation between 0° to 90° for θ_1 and 0° to 90° for θ_2 . The finger structure consists of a combination of Polylactic Acid (PLA) plastic links and a polyurethane elastomer (urethane rubber Smooth On PMC-780) that is used on the fingerpads to increase the friction

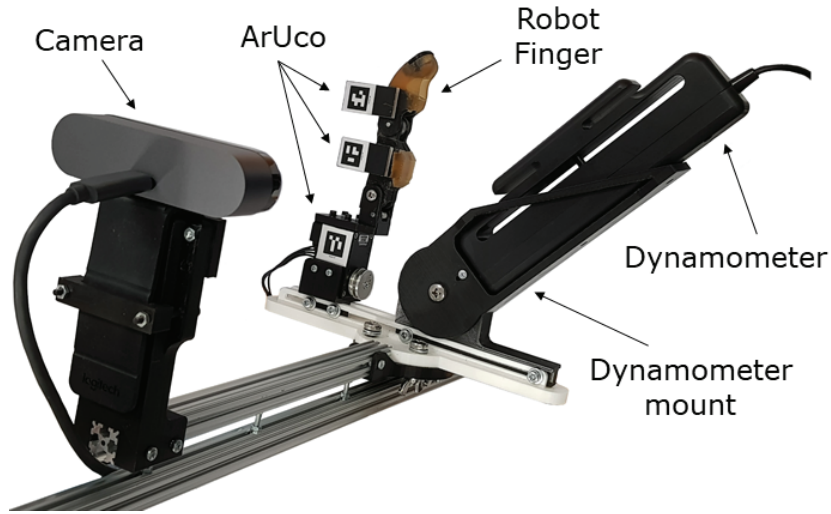


Figure 8.2: The experimental setup for vision based joint angles data collection. The camera was positioned at a distance to capture the ArUco markers for estimating the PIP and MCP joint angles of the robot finger. This experiment was conducted for 10 different dynamometer (force-sensor) angles ranging from 0° to 90° in 10° steps. The angle change was achieved by a modular setup that allows a fast adjustment of the dynamometer angle. The experiments conducted involved 10 different trials for every experimental condition (dynamometer angle).

between the finger and the object during object handling, while the elastomer at the distal end of the finger acts like a distal interphalangeal joint (DIP) that has limited mobility and offers only conformability to the object surface. The robotic finger was designed with a hllwell-known, tendon-driven actuation system for adaptive and underactuated grippers [196, 197, 198].

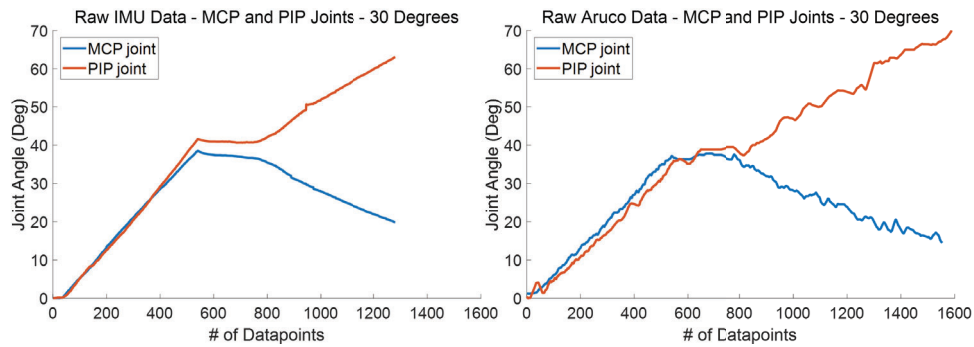


Figure 8.3: Comparison of IMU (left) and ArUco (right) data for MCP and PIP joint angles for the experimental condition of 30° dynamometer angle.

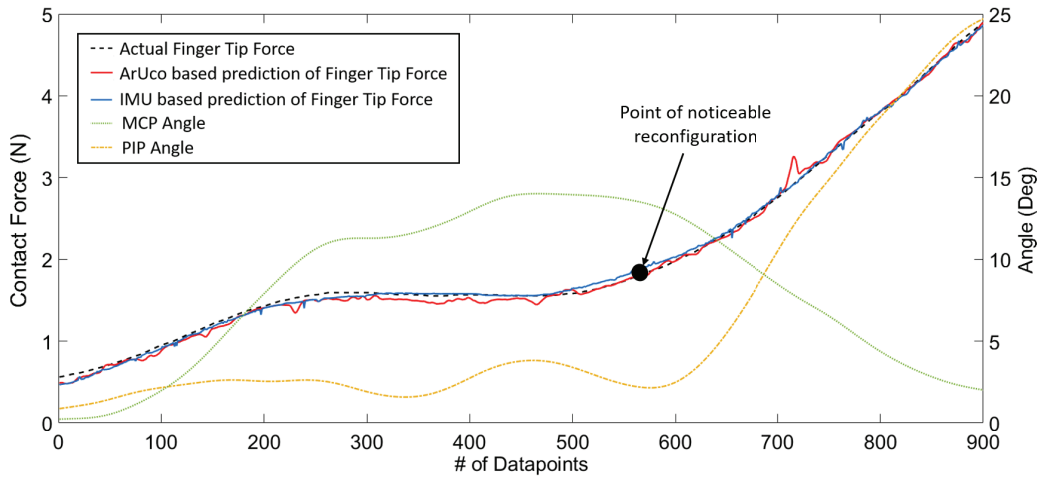


Figure 8.4: The graph shows the variation of the MCP joint angle, the variation of the PIP joint angle, the variation of the actual fingertip forces measured by the dynamometer, and the RF methodology based machine learning model estimations for both ArUcos and IMUs during one experiment (for 10° dynamometer angle).

8.3.1 IMU Based Joint Angles Data Collection

The finger was mounted onto a test structure with detachable mounts that allows us to vary the distance between the finger and the sensor as well as the angular parameters. The experimental setup is shown in Fig. 8.1 with the dynamometer mounted with a 30° angle on the acrylic plate. Customized, non-conductive mounts were prepared for the IMU sensors (MPU-9250) to be attached to the finger structure without interfering with the fingertips and the phalanges reconfiguration. The Biopac MP36 data acquisition unit (Biopac Systems, Inc., Goleta, California) was equipped with the SS25LA dynamometer and it was used to collect the contact force measurements. The motor (Dynamixel XM-430-W350-R) and the finger were mounted on a custom acrylic plate while the dynamometer was attached to offset acrylic plates that had an angle different between 0° and 90° . The experiments were repeated for 10 trials for every experimental condition. The IMU data, the motor positions, and the contact forces exerted on the dynamometer were recorded from the initial position of the finger through to the stop of the reconfiguration motion of the examined adaptive robot finger. It must be noted that in certain cases it was observed that the finger continued to exert forces after the reconfiguration stopping point, establishing contact with the fingernail. Such trials were neglected due to the different materials (fingernail is made out of tough resin) and types of physical interaction involved and they were not included in the examined dataset.

8.3.2 Vision Based Joint Angles Data Collection

A second optical setup was created using a 4k web camera and a set of ArUco markers (see Fig. 8.2). The markers were attached on the finger phalanges instead of the IMU sensors. ArUco is a computer vision processing library developed by Rafael Muñoz and Sergio Garrido [41] and it allows the detection of appropriately designed square fiducial markers, providing relative positional data such as the angles and the Cartesian coordinates for each marker. Two markers were attached onto the finger structure (on the two different phalanges) and the dynamometer was mounted on a pivot locking mechanism with angular slots the orientation of which could range from 0° to 90° in 10° steps. A pin was used to lock the base of the dynamometer into predefined 10° interval angles and the motor was used to actuate the adaptive robot finger from a resting position to the surface of the dynamometer, where forces were exerted. The motor position, the contact forces exerted and the angular position measurements of the adaptive robot finger joints were recorded. The experiments were conducted for a total of 10 trials for every experimental condition examined (different angles / prepositioning of the employed dynamometer).

8.4 Results and Discussion

Results of the IMU based and ArUco based angle measurements exhibit similar characteristics and trends but the ArUco data had higher noise (see Fig. 8.3). The IMU data was more consistent and the measurements were able to account for small angle changes during finger reconfiguration. The noise included in the ArUco datasets was likely caused by ambient lighting and occlusions or shadows created during the finger motion. The efficiency of the trained model was assessed by using the percentage of the Normalized Mean Square Error (NMSE) for accuracy obtained using Eq. 8.1, to compare the predicted and the actual object motion. The NMSE value of 0% implies a bad fit whereas the NMSE value of 100% implies that the two trajectories are identical. The NMSE value is defined as,

$$NMSE(\%) = 100 * \left(1 - \frac{\|x_r - x_p\|^2}{\|x_r - \text{mean}(x_r)\|^2} \right) \quad (8.1)$$

where, $\|\cdot\|$ indicates the 2-norm of a vector, x_r is the actual reference motion and x_p refers to the predicted motion. Estimation results for the three models examined are presented in Table 8.1 for all the different configurations of the dynamometer. The three different techniques that were considered were MLR, RF, and SVR models. The examined RF based models were trained with 100 trees. For the SVM regressor, we used a non-linear

RBF kernel. It can be noted that the RF based models had the best performance for all the dynamometer configurations for both ArUcos and IMUs. Fig. 8.4 compares the actual fingertip force measured with the contact force predicted using the RF model trained with the ArUco and IMU data. The features used for the model training were the joint angles, the motor position, and the motor load (current). The Random Forests model takes into account the joint angle measurements from the IMU sensors and the ArUco markers throughout the reaching, contact, and post-contact reconfiguration phases, achieving a significant accuracy for the contact force predictions up to 96.1% for the ArUco data and 95.3% for the IMU data.

Table 8.1: Motion estimation results for different dynamometer angles

Model	Initial Angle		0°	10°	20°	30°	40°	50°	60°	70°	80°	90°	Avg
MLR	ArUco	Accuracy (%)	84.9	89.9	81.0	86.9	88.2	68.8	80.7	89.3	84.8	80.2	83.5
		Standard Deviation (%)	2.4	2.6	0.8	1.2	3.1	9.2	5.6	1.0	1.2	2.9	3.0
	IMU	Accuracy (%)	88.6	87.3	84.6	75.2	67.0	85.3	82.9	85.8	91.3	88.9	83.7
		Standard Deviation (%)	3.1	2.7	6.3	22.1	9.7	5.0	5.5	2.6	1.5	8.9	6.7
SVM	ArUco	Accuracy (%)	90.9	93.4	94.8	89.8	89.7	70.3	85.3	91.1	91.9	88.0	88.5
		Standard Deviation (%)	2.2	3.8	2.3	2.3	3.5	9.4	8.8	1.3	2.6	9.3	4.5
	IMU	Accuracy (%)	90.3	89.7	87.7	81.7	68.7	88.2	87.3	90.2	92.1	84.8	86.1
		Standard Deviation (%)	3.4	3.2	5.8	10.9	16.5	5.7	5.1	2.6	2.1	8.2	6.3
RF	ArUco	Accuracy (%)	96.1	93.9	95.4	90.1	90.4	72.6	89.8	94.6	94.7	91.2	90.8
		Standard Deviation (%)	1.69	2.75	1.57	1.70	3.16	8.20	3.53	1.20	1.26	4.31	2.93
	IMU	Accuracy (%)	91.2	90.5	87.7	84.5	68.5	88.2	87.1	90.8	95.3	90.7	87.4
		Standard Deviation (%)	3.67	2.96	6.35	6.74	9.66	6.41	6.55	3.07	1.01	4.66	5.10

In Fig. 8.5, we present the importance plots for each feature variable for both the IMU and the ArUco based RF models, derived by the RF inherent feature variables importance calculation procedure. It is evident that the motor position was overall the most important feature that was used for the contact force prediction. The MCP and PIP joint angles follow in importance, while the motor load (current) was the least important feature examined.

The importance of the features is similar for the two types of motion capture systems. The variation of the MCP and PIP joint angles during the reaching phase, contact, and post-contact reconfiguration is presented in Fig. 8.4. It must be noted that the bending profile of the finger prior to establishing contact with the dynamometer (reaching phase) remains constant for all the examined experimental conditions. As the finger approaches

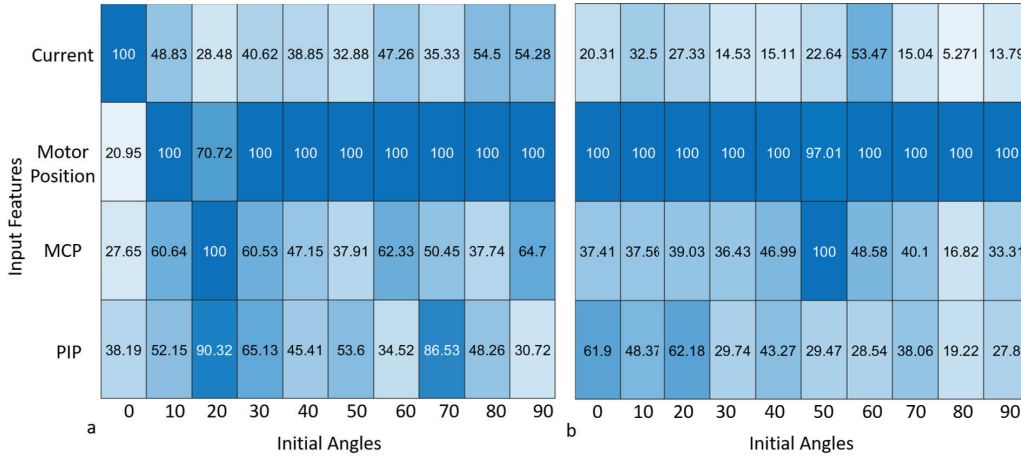


Figure 8.5: Comparison of the feature variable importances for contact force prediction based on: a) IMU data (subfigure a) and b) ArUco data (subfigure b). The importance scores are obtained using the inherent RF feature variable importance calculation procedure. The results have been normalized over the results of the 10-fold cross-validation method.

the object, the MCP joint angle increases while the PIP joint remains unchanged until contact is established. Once the contact is made, the contact force exertion begins and the force increases gradually. During the post-contact reconfiguration phase, the distal phalanx keeps bending causing the PIP joint angle to increase while the proximal phalanx starts reconfiguring backward decreasing the MCP joint angle. The post contact reconfiguration of the finger varied widely for different angular orientations of the dynamometer with respect to the finger base. The force exertion continued to increase throughout the reconfiguration. Regarding the accuracies comparison, as it can be noticed in Table 8.1, the estimation accuracies for the RF model trained with the ArUco data were slightly better than the accuracies of the model trained with the IMU data for all the dynamometer configurations examined. This can be attributed to the high resolution of the 4K web camera used for the ArUco markers tracking as well as to the noise in the ArUco training set that led to the creation of a more efficient regression model. However the difference between the ArUco and the IMU based models was marginal and for a robust implementation IMU sensors integrated into the finger phalanges would be more practical than ArUco markers that suffer from calibration, occlusion, and lighting condition errors. Furthermore, the ArUco markers require an external camera that needs to be positioned with a significant offset from the robot hand, making the setup bulkier and imposing new collision constraints in cases that the gripper is attached on a robot arm. The IMU sensors on the other hand can be integrated into the finger phalanges by

design without restricting the motion of the system.

8.5 Conclusion and Future Directions

In this study, we proposed a methodology that combines Random Forest regression models and motion capture systems to predict the contact forces exerted by an adaptive robot finger in pinch grasps, using its post-contact reconfiguration profile. Three different types of models were compared: i) Multiple Linear Regression model, ii) a Support Vector Machine regressor with RBF kernel and iii) a Random Forest regressor. Each model was trained with either IMU or ArUco data and the efficiency of the different models in estimating the exerted contact forces were compared. The experimental validation was conducted for a wide range of conditions involving different prepositioning of the dynamometer with respect to the examined finger. The experimental results demonstrate that the Random Forest models trained with the IMU or ArUco data can efficiently predict the robot finger contact forces, achieving high accuracies (up to 96.1%), independently of the examined experimental condition. The difference in accuracy between the IMU and ArUco based models is negligible. However, the IMU sensors provide a more practical implementation, as they can be integrated within the fingers without affecting the overall performance of the system (imposing new collision constraints). ArUco markers require a camera, a camera mount, and a significant offset between the camera and the finger, making the solution much bulkier. Many adaptive hands currently use IMU sensors for posture recognition that could also be exploited to determine the contact forces without incurring further costs. Though the model is finger specific, it can easily be retrained for other adaptive fingers. Regarding future directions, we plan to extend the models for use in five fingered adaptive robot hands and to create a complete framework for integrated systems to perform complex and dexterous tasks.

Chapter 9

Design Optimization

9.1 Introduction

Robotic hands and grippers are employed as end-effectors of robotic platforms to facilitate their interaction with the environments surrounding them (e.g., grasp an object, push buttons, open a door). The versatility and ability of the grippers to manipulate a wide range of objects across many use cases and scenarios from service tasks [199] to industrial tasks [200] as well as their effectiveness in completing these tasks can be used as an indicator of their dexterity [196]. Traditionally, such complex tasks are executed by employing fully actuated, expensive, rigid robotic hands that require advanced sensing elements [201, 202]. However, the sophisticated control laws and schemes required by these hands to operate efficiently complicate their operation. The relatively new class of adaptive (underactuated and compliant) robotic grippers and hands aims to address these shortcomings, offering task execution robustness with simplified control. These devices demonstrate excellent performance in the execution of robust grasping and dexterous manipulation tasks [45, 143], without requiring sophisticated learning and control schemes [203]. The superior grasping performance of adaptive hands is typically attributed to the introduction of structural compliance combined with underactuation that make control simpler and more intuitive [142]. These characteristics have led to a surge in the number of studies that focus on adaptive end-effectors. However, the structural compliance and underactuation compromise the pinch grasping capabilities of the gripper, introducing a post-contact parasitic reconfiguration of the gripper-object system [177] that affects grasping stability. The optimization of the gripper link lengths is vital for the minimization of reconfiguration and maximization of the grasping quality achieved by such an end-effector. Finally, the distance between the finger base frames highly af-

fects the grasping and manipulation capabilities of the gripper as well as the post-contact reconfiguration of the gripper-object system.

In this study, we propose a framework that improves the dexterous manipulation capabilities of two fingered grippers by optimizing the finger link dimensions and analyzing the effect of finger symmetry and the distance between the finger base frames on their manipulation workspaces. The results of this analysis are used to design a new, improved, multi-modal robotic gripper that performs significantly better than other grippers in the execution of dexterous manipulation tasks without compromising grasping efficiency. To solve the optimization problem, we employed a parallel multi-start search algorithm. The optimal link lengths were used to investigate how the inter-finger distance, the design symmetry, and the object size affect the manipulation workspace. The results demonstrate that different inter-finger distances lead to completely different dexterous manipulation workspace shapes and volumes and that the area of the union of all workspaces is always larger than the area of any single "optimized" workspace. Motivated by these results, we designed a two fingered, multi-modal gripper with reconfigurable finger base frames and lockable joints. This ensures that the gripper can cover the union of workspaces rather than a single optimal workspace. The proposed gripper is considered multi-modal as it has a locking function implemented with solenoids that allows it to transition between an adaptive grasping configuration and a parallel-jaw gripper configuration as shown in Figure 9.1. The contributions of this research work are: i) an optimization scheme for improving the dexterous manipulation capabilities of robotic grippers and hands and ii) a novel, multi-modal gripper design with reconfigurable finger bases and lockable joints that exhibit improved manipulation capabilities without sacrificing grasping performance.

9.2 Related Work

A number of studies have focused on optimizing the design parameters of underactuated and passively adaptive robotic hands so as to achieve increased performance over a large set of objects and grasping tasks [204, 205, 206]. The design characteristics of individual fingers determine their ability to interact with other fingers and the environment as well as to robustly grasp and manipulate various objects. More specifically, the two most important parameters that contribute to the effectiveness of a robotic gripper or hand are the link dimensions and the palm width (distance between the finger bases) [207, 208, 209, 210]. Both of these parameters directly affect the range of objects that can be grasped and manipulated (different sizes and shapes). Design optimization of underactuated robotic

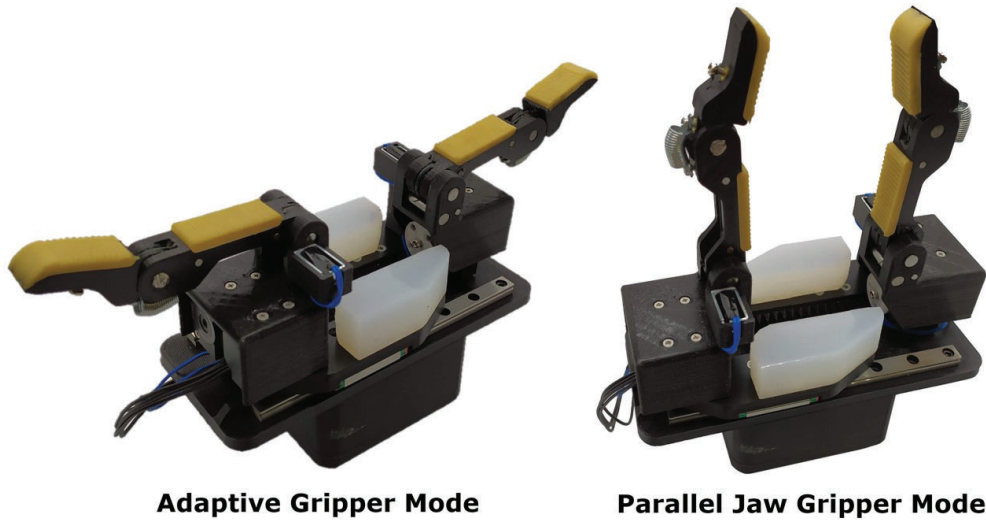


Figure 9.1: The proposed multi-modal gripper that is equipped with reconfigurable finger bases to improve dexterous manipulation without sacrificing grasping quality.

gripper parameters has been employed in a number of studies to offer increased dexterity despite the small number of controllable degrees of freedom that is used in such devices. The main parameters that are optimized in these studies are the link dimensions of the fingers. Previous work has focused on the effect of gripper dimensions on contact force distribution [207]. Six of the seven design variables that were optimized using the teaching-learning based optimization algorithm in this study were the dimensions of the gripper. Dong *et al* employed a genetic algorithm to find the ideal gripper dimensions as well as the most appropriate tendon routing solution, which would optimize the grasping performance of an underactuated robotic gripper [208]. Datta *et al* employed a multi-objective evolutionary algorithm to find the optimal link lengths as well as the joint angles of a robot gripper [209].

Once the optimal finger dimensions of a gripper have been determined, the ideal inter-finger distance needs to be calculated as it directly affects the functionality and dexterous manipulation performance of the system. In particular, the dexterity of a gripper or hand is mainly attributed to its fingers' ability to impart large object motions and forces during precision grasps, perturbing the object pose [211]. Studies have also proposed performance indices to quantify this interaction that leads to in-hand manipulation. You *et al* have quantified the ability of the fingers to interact with each other, using a performance index called "interactivity of fingers (IF)" and they employed this index so as to optimize the Saddle joint's position and orientation [212]. The relation between the manipulation workspace and the kinematic design parameters (i.e., linkage ratio and

base width among others) and the differences between the manipulation workspace and the actual usable workspace have been studied for linkage-based fingers [213]. One of the key design parameters associated with the design of stable robotic grippers that are optimized for precision grasps is the palm width as proposed by Leddy et al [214]. This study also suggests that grasp stability is optimized in underactuated hand and gripper designs when the palm width and the finger length are equal. Bircher *et al* examined the caging ability of underactuated hands and concluded that the palm width should be "just right" (not too small or too large) to allow for effective caging grasps [215]. For example, if the palm width is too small, larger objects come in contact with the proximal phalanges first and are pushed out while the fingers close. This indicates that a variable base width would be ideal for different objects.

The range of object sizes that need to be grasped and manipulated also determines the ideal link dimensions and inter-finger distance. Liarokapis and Dollar investigated the relationship between the object sizes and manipulation range of motion [177], showing that a given hand can have different manipulation capabilities for different object sizes and shapes. Hence, the object set to be grasped and manipulated plays a vital role in determining the dexterous manipulation capabilities of a gripper or hand and should be considered while optimizing the design parameters. Ciocarlie et al. optimized the link dimensions to extend the size range of objects a gripper can kinematically enclose/entrap, through a combination of random search and gradient descent with numerical gradient computation [196]. Finally, the optimal joint coupling for a wide range of object sizes and positions has been identified to optimize gripper performance [210].

Although all the aforementioned studies optimized one or more kinematic parameters of robotic grippers, the objective function varied widely focusing on different characteristics, such as: i) the grasping performance [208], ii) the gripping forces [207, 206], iii) the grasping and manipulation workspace [213], iv) the dexterous manipulation performance [177] among others. Moreover, all these optimization studies were limited to specific robotic gripper designs, and specific task and application conditions, and considered only specific and limited object sets. From the examined related work, it is evident that the link dimensions, palm width, and the interaction between the fingers are the key parameters that contribute towards the manipulation capabilities of a robotic hand or gripper. These parameters depend on the object set that needs to be manipulated. Also, it can be noted that there cannot be a one-size-fits-all gripper for all object sizes. All the grippers in the aforementioned studies had a fixed pre-determined finger-base position and inter-finger distance limiting their grasping and manipulation capabilities to a particular object size range. The multi-modal gripper proposed in this study on the other hand

has reconfigurable finger base frames and can operate in both an adaptive grasping configuration and a parallel-jaw gripper configuration. This enables the gripper to choose the right configuration and vary the inter-finger distance, grasping and manipulating objects of varying sizes¹.

The rest of the chapter is organized as follows: Section 9.3 details the dexterous manipulation workspace analysis, the outcomes of the analysis, and their implications, section 9.4 presents the design of the proposed multi-modal robotic gripper, section 9.5 presents the results of the grasping and manipulation experiments that have been conducted with the proposed robotic gripper, while section 9.6 concludes the chapter and discusses some possible future directions.

9.3 Manipulation Workspace Analysis

The workspace analysis of the various two-fingered robotic gripper designs is defined as a constrained multi-parametric optimization problem. We employ a parallel multi-start search algorithm to solve this problem. The objective is to find the ideal link lengths and inter-finger distance of a two fingered gripper that maximizes its manipulation capability for a set of different object sizes.

Four different categories of two-fingered grippers are analyzed: i) symmetric fingers with two phalanges, ii) asymmetric fingers with two phalanges, iii) symmetric fingers with three phalanges, and iv) asymmetric fingers with three phalanges.

9.3.1 Design Variables and Manipulation Considerations

A kinematic model is created for each of the grippers with the link lengths and base width as variables. The kinematics models of symmetrical grippers with two and three phalanges are presented in Figure 9.2. Each Degree of Freedom (DoF) can be actuated independently of the other DoFs as the models are considered to be fully actuated. The five variables for the robotic grippers with the two phalanges per finger are: i) the four-link dimensions of the proximal and distal phalanges of the two fingers and ii) the distance between the finger base frames. The seven variables for the robotic grippers with the three phalanges are: i) the six link dimensions of the proximal, middle, and distal phalanges of the two fingers, and ii) the distance between the finger base frames. The object length is added as a constraint. In order to limit the design space that needs to be explored and

¹Majority of the chapter is based on [216], © 2021, IEEE. Reprinted, with permission, from Nathan Elangovan, Lucas Gerez, Geng Gao, and Minas Liarokapis, Improving Robotic Manipulation Without Sacrificing Grasping Efficiency: A Multi-Modal, Adaptive Gripper With Reconfigurable Finger Bases, IEEE Access, 2021.

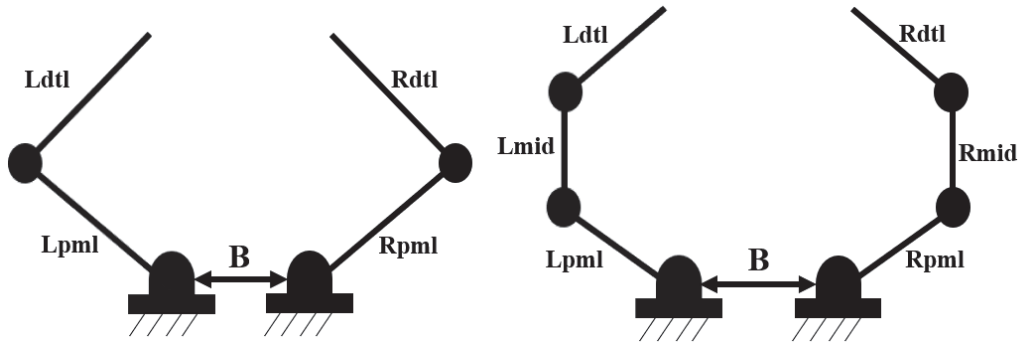


Figure 9.2: Kinematic structure of a gripper model with two phalanges (left model) and a gripper model with three phalanges (right model). B is the distance between the finger bases and L_{pml} , L_{mid} , L_{dml} , R_{pml} , R_{mid} , and R_{dml} represent the left proximal, left middle, left distal, right proximal, right middle, and right distal phalanges, respectively.

prevent exploring options that are unrealistic or non-feasible, the following were taken into consideration:

- The total length of each finger was constrained to have an upper limit.
- This study only analyses pinch grasps and manipulation motions that can be executed by the fingertips.
- The in-hand manipulation tasks involving the proximal phalanges of the fingers are excluded from this analysis.
- Equilibrium point manipulation was hypothesized that is executed with point contacts in each finger. Rolling contacts and the associated slipping that may occur were hypothesized to be of minimal significance for the purpose of this work. Such phenomena are also hard to model and simulate.
- For the symmetrical designs of robotic grippers with two and three phalanges, symmetry is set as a constraint.
- The object is added as an extra link to one of the fingers. Thus dexterous manipulation is modelled as the inverse kinematics problem of finding the configuration of the finger with the extra object link that can reach the tip of the other finger (if such a configuration exists).

9.3.2 Problem Formulation

The volume of the dexterous manipulation workspace is given by the function $V(\mathbf{x})$ where \mathbf{x} is the vector containing the decision/design variables presented in the previ-

ous section. Thus, the optimization problem to maximize the volume of the manipulation workspace by finding the ideal link lengths and distance between the finger base frames can be written as presented in Eq. (9.1),

$$\begin{aligned} x^* = \underset{x}{\operatorname{argmin}} \quad & -V(x) \\ \text{s.t.} \quad & \end{aligned} \quad (9.1)$$

$$l_b = l_{total} - (l_{max}^l + l_{max}^r)$$

$$\left. \begin{aligned} l_p^l + l_d^l &\leq l_{max}^l \\ l_p^r + l_d^r &\leq l_{max}^r \end{aligned} \right\} \text{if } n_p = 2$$

$$\left. \begin{aligned} l_p^l + l_m^l + l_d^l &\leq l_{max}^l \\ l_p^r + l_m^r + l_d^r &\leq l_{max}^r \end{aligned} \right\} \text{if } n_p = 3$$

where n_p is the number of phalanges and the maximum link dimensions for left (l_{max}^l) and right (l_{max}^r) fingers are limited to the sum of individual finger length and object length and l_b is the distance between the finger bases calculated as the difference between the total link dimensions (including the object length) and finger lengths. The symmetry between the left and right fingers is added as a constraint (when needed). The constraints for the objective function are presented in Eq. (9.2), as follows

$$\begin{aligned} l_{total} &= l_{max}^r + l_{max}^l + l_b \\ l_{max}^l &= l_{max}^r = l_{total} + l_{obj} \\ l_p^l &= l_p^r \\ l_m^l &= l_m^r (\text{for } n_p = 3 \text{ only}) \\ l_d^l &= l_d^r \end{aligned} \quad (9.2)$$

The proposed formulation seeks to identify the ideal link lengths and the distance between the finger base frames that maximize the dexterous manipulation workspace. The gripper model was created using the MATLAB Robotics toolbox [217]. The initial dimensions of the gripper and the range of object sizes are provided as user-defined inputs. An *fmincon* solver is then used to search the optimization space using a non-linear gradient ascent. The optimization speed was optimized using MATLAB's parallel solver by initiating the parallel pool and the multi-start algorithm. The parallel pool employs multiple solvers each initiating from a random start point spread across the search space to solve the optimization problem in parallel. Apart from ensuring that the optimization

Table 9.1: Manipulation capability results for various types of grippers and varying object diameters.

Manipulation Capability Metric	$WS_{opt} / \bigcup_{i=1}^n WS_i$					
Object Length	0 mm	10 mm	20 mm	30 mm	40 mm	50 mm
Symmetric gripper with 2 phalanges per finger	0.9745	0.9302	0.8627	0.7955	0.8975	0.8983
Asymmetric gripper with 2 phalanges per finger	0.8137	0.933	0.8728	0.8429	0.8717	0.8827
Symmetric gripper with 3 phalanges per finger	0.9692	0.4934	0.9169	0.8541	0.7602	0.8415
Asymmetric gripper with 3 phalanges per finger	0.5821	0.4065	0.9537	0.8384	0.932	0.9

does not exit on a local maximum, the multi-start algorithm also increases the optimization speed considerably. Once the function tolerance is reached, the solver exits with a positive flag providing the optimal link lengths for a given object size.

9.3.3 Manipulation Workspace Generation

The dexterous manipulation workspace is calculated as the space occupied by the possible positions that the object's center of mass can attain during in-hand manipulation in the manipulation plane. These positions are derived as a set of points, a point cloud. The bounding volume of the point cloud is calculated using the *alphashape* method, which formalizes the abstract shape of the given set of points using Delaunay triangulation [218].

9.3.4 Manipulation Workspace Implications

The manipulation workspace was significantly influenced by each of the design variables and constraints. The manipulation workspace for the robotic gripper with the three phalanges is higher than the robotic gripper with the two phalanges when they have the same total finger length. This could be attributed to a finer control over the workspace provided by the extra link. The optimal ratio of the lengths of the proximal and distal phalanges for the symmetrical gripper with the two phalanges averaged at 0.61 and 0.39, respectively. For the symmetrical design with the three phalanges, the ratio of the proximal, middle, and distal dimensions averaged at 0.29, 0.34, and 0.36 respectively. When the constraint of symmetry was removed, the right finger ratios changed to 0.38, 0.28, and 0.33 for the proximal, middle, and distal phalanges, while the respective ratios for the left finger averaged at 0.38, 0.31, and 0.32. For the gripper with the two phalanges, the right finger ratio remained identical to the symmetrical gripper averaging at 0.60 and 0.40 for the proximal and distal phalanges respectively, with a standard deviation of 0.06. The left finger dimensions converged to 0.57 and 0.43.

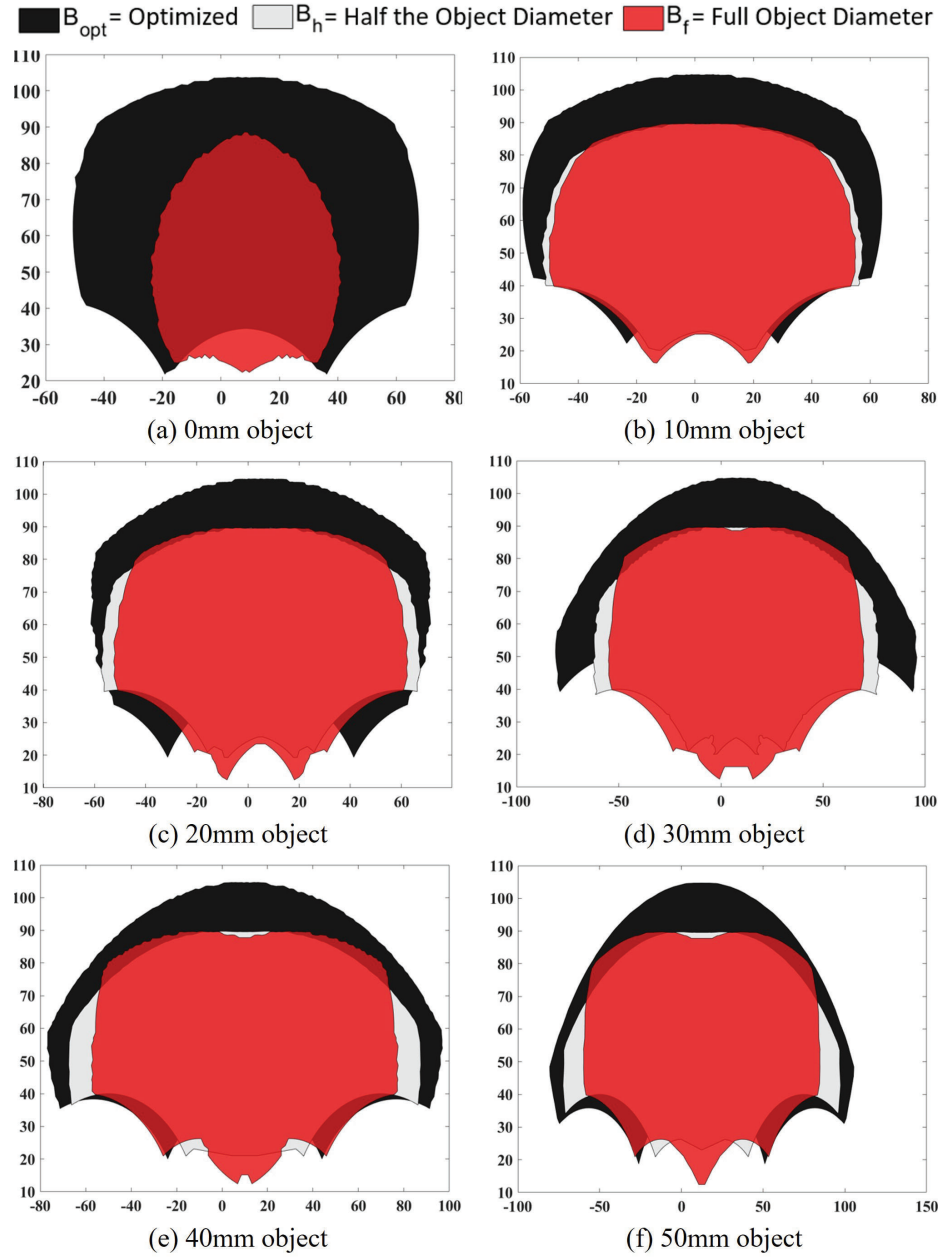


Figure 9.3: Workspace comparison results for symmetric grippers with two phalanges per finger and different object diameters. Inter-finger distance was: i) optimized (B_{opt}), ii) half the object diameter (B_h), and iii) equal to the full object diameter (B_f).

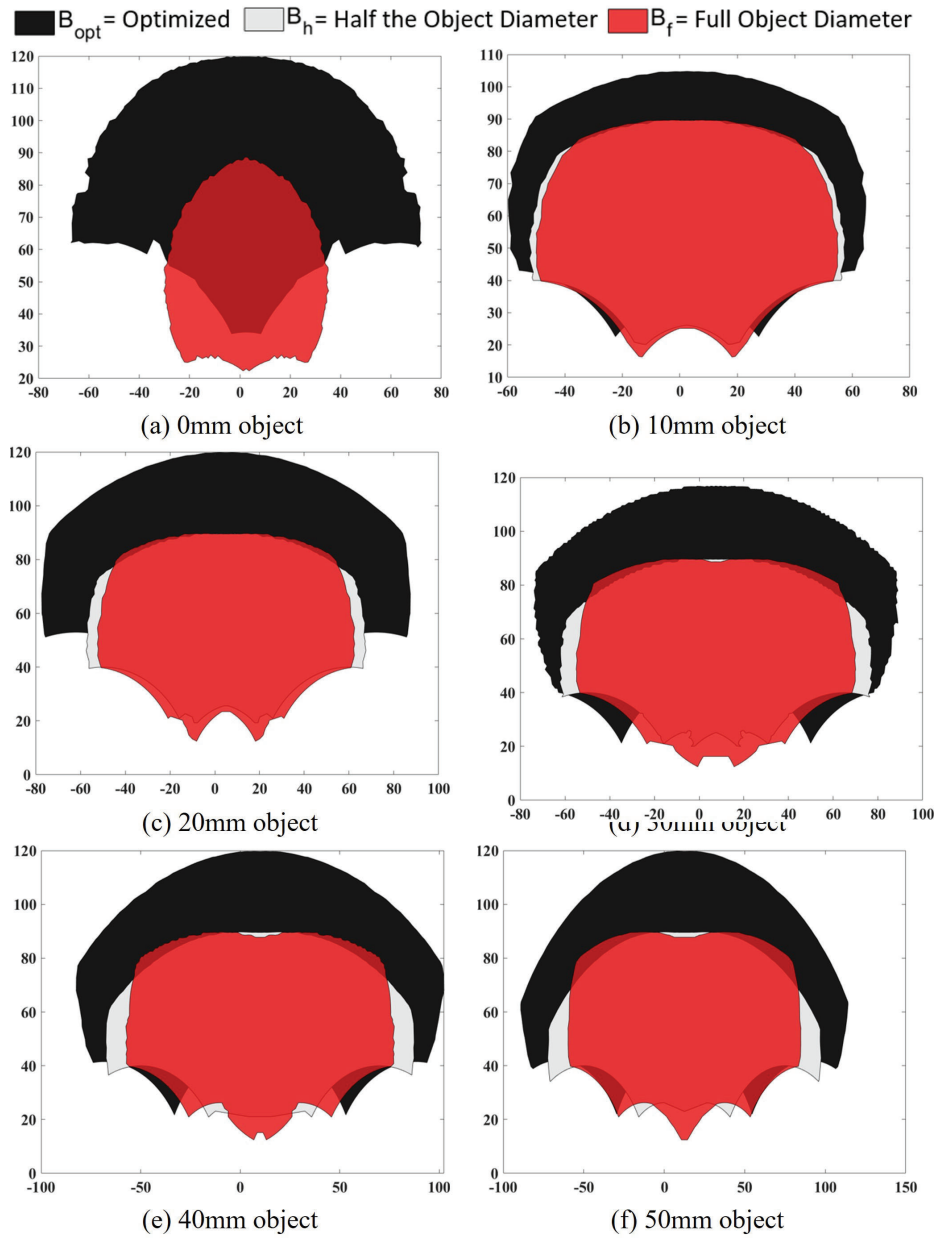


Figure 9.4: Workspace comparison results for asymmetric grippers with two phalanges per finger and different object diameters. Inter-finger distance was: i) optimized (B_{opt}), ii) half the object diameter (B_h), and iii) equal to the full object diameter (B_f).

For all the optimization cases the distance between the finger bases converged to zero. This could indicate that the manipulation capability is inversely proportional to the inter-finger distance. To further investigate this effect, the manipulation workspace for varying inter-finger distance was calculated for the original finger dimension. The results of this computation are presented in Figure 9.3, Figure 9.4, Figure 9.5, and Figure 9.6 showing that halving the inter-finger distance results in improved manipulation workspace volume and causing a change in the workspace shape as well. The shape of the workspace varied not only for the different categories of grippers but also with each object as seen in these plots. This can be attributed to the fact that the grasping configuration changes with the objects as well as with the inter-finger distance. When the base frames are closer, the fingertips can stay in contact for a greater range of configurations, allowing the object to be displaced to a wider range of positions to the left and right of the fingers and resulting in a larger manipulation workspace volume. As the finger bases move further away from each other, this displacement region keeps decreasing. Once the base frames move further than a certain limit the object can only be manipulated in a narrow space between the fingers.

It can also be observed that the workspace generated by the asymmetrical finger configurations is asymmetrical as well. This effect is more evident in fingers with three phalanges. Figure 9.6 presents the workspace generated by fingers with three phalanges under optimal symmetrical and asymmetrical link ratios. It shows how the workspace generated by asymmetrical fingers is askew and irregularly populated, while the symmetrical workspace is uniformly distributed. As the fingers are of different dimensions the center between the fingers is altered making the workspace favour one half over the other, resulting in abnormal workspaces with rough edges. The rough edges that change abruptly throughout also mean that the grasp robustness might be compromised at these regions and the fingers may lose contact with the object as they traverse through such regions owing to sudden jerk motions. Though the volume is comparable to the symmetrical configurations, the asymmetry would make the control difficult and a decision would need to be made on which finger or half of the workspace is to be favoured on a case by case basis. As this seems to cause difficulties under practical conditions, it is better to opt for symmetrical configurations that result in evenly distributed workspaces with smoother edges.

The comparison also shows the maximum workspace volume that was achieved with optimal link ratios and nullified inter-finger distance. It can be noticed that the different achievable workspaces are not always a subset of the optimized workspace. The differences in workspace shapes and sizes mean that the fingers can manipulate the objects in

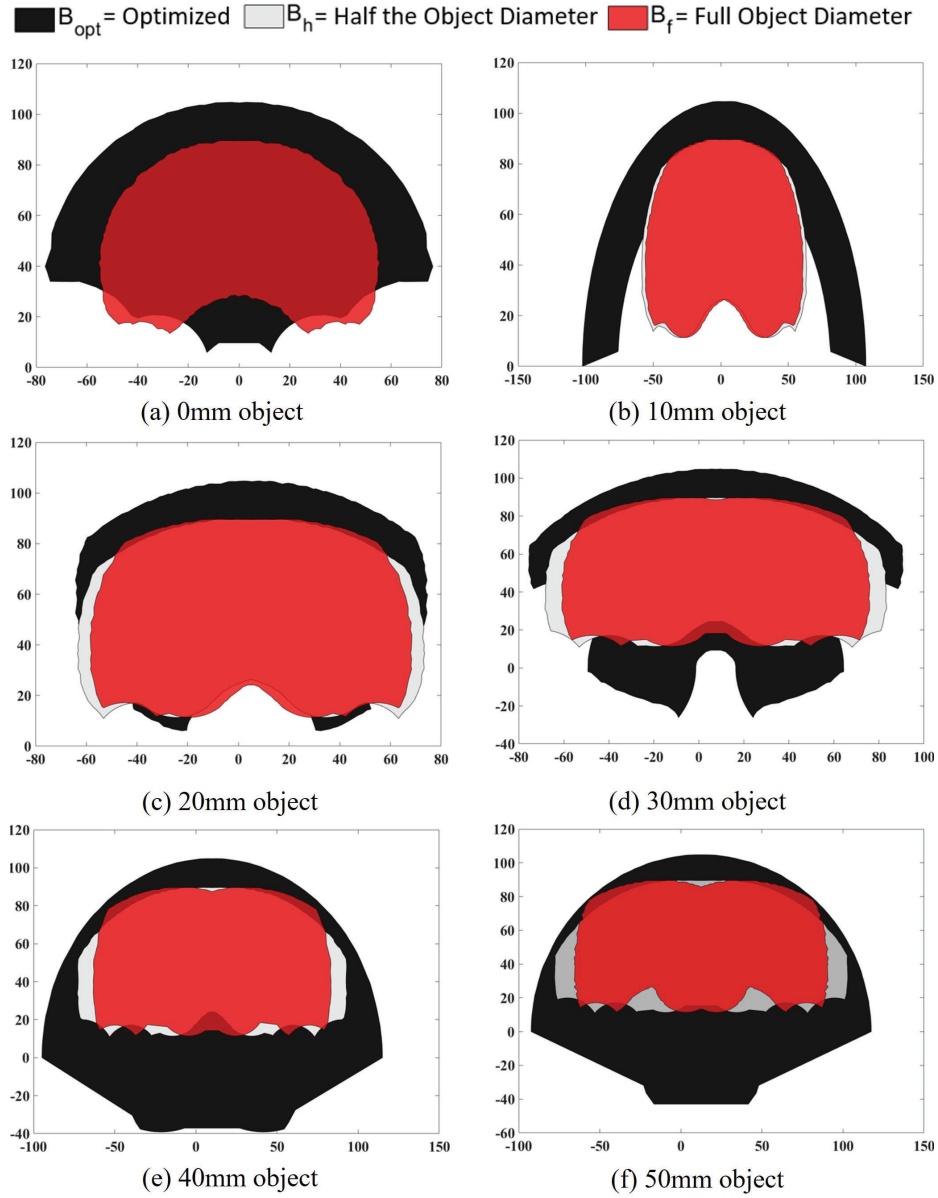


Figure 9.5: Workspace comparison results for symmetric gripper with three phalanges per finger and different object diameters. Inter-finger distance was: i) optimized (B_{opt}), ii) half the object diameter (B_h), and iii) equal to the full object diameter (B_f).

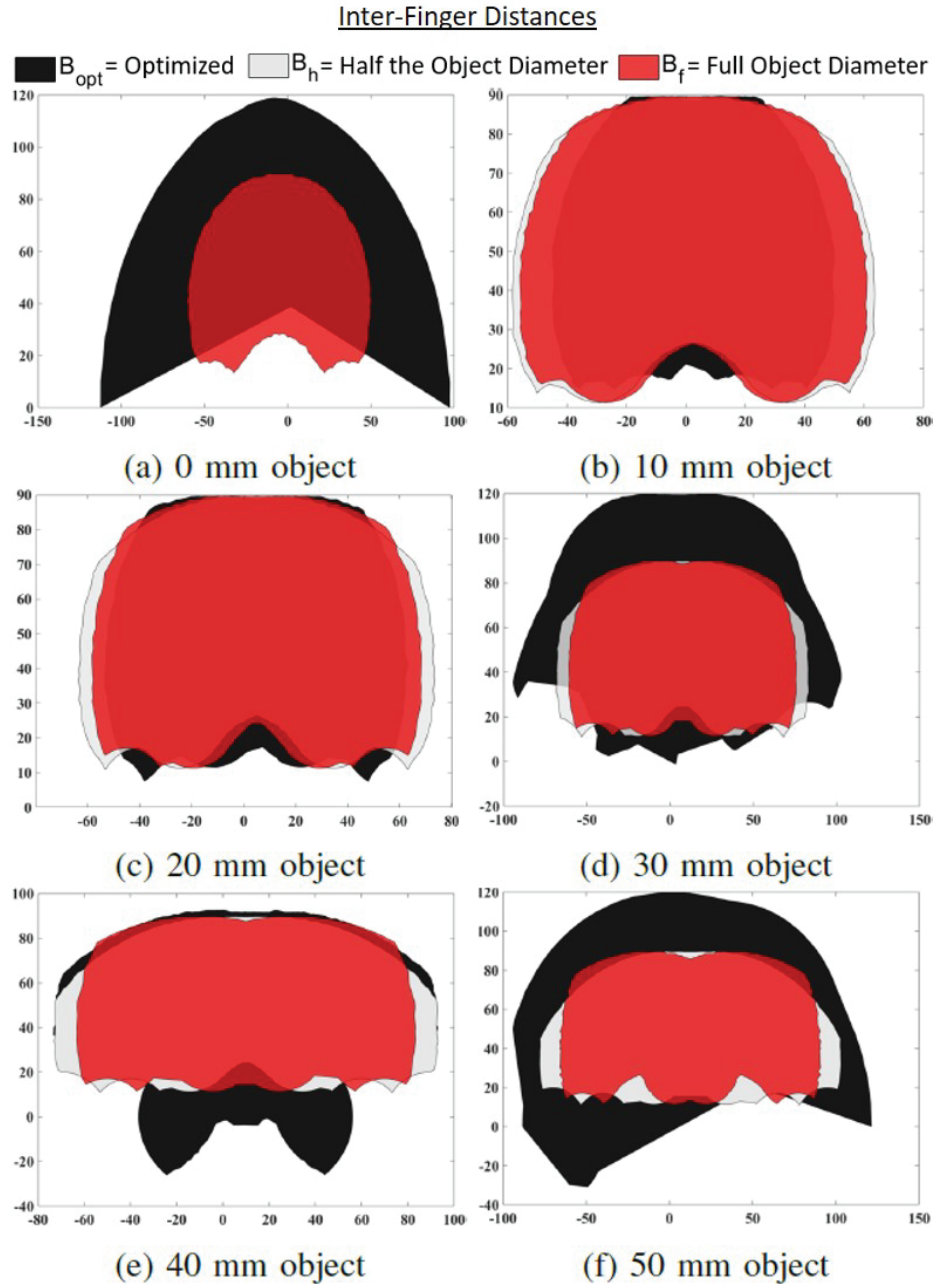


Figure 9.6: Workspace comparison results for asymmetric gripper with three phalanges per finger and different object diameters. Inter-finger distance was: i) optimized (B_{opt}), ii) half the object diameter (B_h), and iii) equal to the full object diameter (B_f).

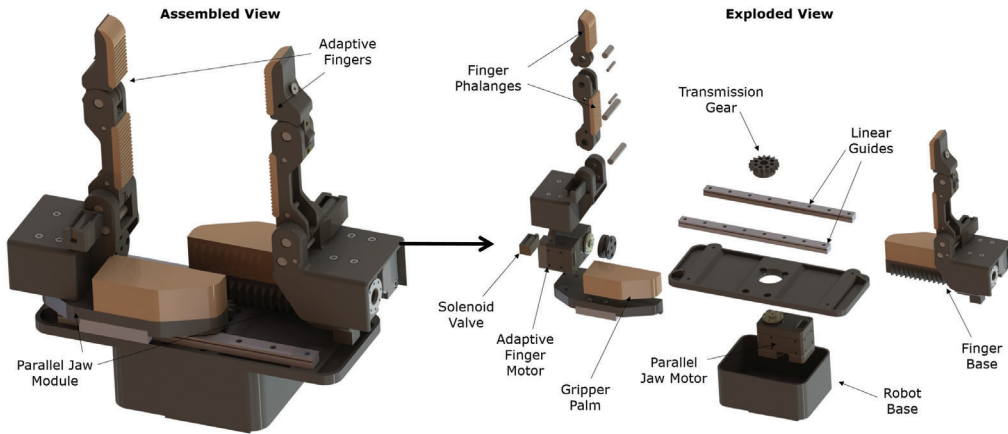


Figure 9.7: The assembled and exploded views of the proposed multi-modal robotic gripper.

different regions of the achievable workspaces when different inter-finger distances are employed. In order to determine the percentage of area that can be covered with a certain inter-finger distance, we computed the ratio of the individual workspace to the union of all workspaces (combined workspace) the value of which was always less than 1. Even though the ratio was higher for optimized workspaces indicating their ability to cover a major section of the union of workspaces, they still couldn't represent the entire union. The results of these comparisons for all the fingers with two and three phalanges are presented in Table 9.1. Also, it can be noticed that in the workspace plots there are gaps and regions that are not connected in some optimized workspaces which are included in workspaces generated by non-optimal inter-finger distances. The hand would lose contact with the object in these regions (under normal circumstances), rendering the manipulative space as a set of non-connected regions. Hence, in order to maximize the dexterous manipulation capability of a two fingered gripper, the distance between the finger base frames should be reconfigurable, enabling the fingers to reach workspace regions generated by varying inter-finger distances. Taking all these into account, the gripper described in Section 9.4 has been designed with reconfigurable finger base frames so as to increase the volume of the manipulation workspace.

9.4 Design

The ideas derived from the dexterous manipulation workspace analysis were employed for the development of a multi-modal robotic gripper that is composed of two different modules: a parallel jaw module and two adaptive robot fingers (as shown in Figure 9.7). A

Table 9.2: Grasping (G) and Manipulation (M) capabilities of the multi-modal gripper for five different spheres employing the adaptive gripper mode (at base widths: 0 mm, 30 mm, 70 mm, and 110 mm) and the parallel jaw mode.

Object	Adaptive (0 mm)		Adaptive (30 mm)		Adaptive (70 mm)		Adaptive (110 mm)		Parallel Jaw	
	G	M	G	M	G	M	G	M	G	M
Marble	Y	Y	Y	Y	Y	Y	Y	Y	Y	N
Golf Ball	Y	Y	Y	Y	Y	Y	Y	Y	Y	N
Racquetball	Y	Y	Y	Y	Y	Y	Y	Y	Y	N
Baseball	Y	Y	Y	Y	Y	Y	Y	Y	Y	N
Softball	Y	Y	Y	Y	Y	Y	Y	Y	Y	N



Figure 9.8: The workspace generated by the gripper was examined for objects of varying diameter that include: a marble (diameter: 16 mm), a golf ball (diameter: 42.7 mm), a racquetball (diameter: 55.3 mm), a baseball (diameter: 73.3 mm), and a softball (diameter: 96 mm).

Dynamixel XM430-W350 motor, two linear guides, and a transmission gear are used to construct the gripper base that creates the parallel jaw module. The two adaptive finger units are mounted on linear rails allowing them to slide to and away from the gripper center thereby allowing the inter-finger distance between the finger bases to vary between 0 mm to 110 mm. The parallel jaw motor in the gripper base is coupled to a rack in the finger units for force transmission. The design of the tendon-driven finger unit is based on the adaptive robot fingers of the Model O gripper of the Yale Open Hand project [198]. Each finger is actuated using a Dynamixel XM430-W350 motor that is enclosed in the

finger unit. A locking mechanism is created using a solenoid valve that allows the fingers to be locked perpendicularly to the base thereby converting the gripper to act as a parallel jaw gripper. This allows the gripper to exert higher grasping forces owing to the lack of post-contact reconfiguration in parallel jaw grippers [18]. When this mechanism is not activated, the finger has a bigger aperture for caging objects more easily, like adaptive grippers [198]. This allows the fingers to conform to the object's surface resulting in a more stable grasp owing to the increase in the number of contact points. Thus, the proposed robotic gripper exploits the advantages of both these grasping modes (adaptive and parallel jaw).

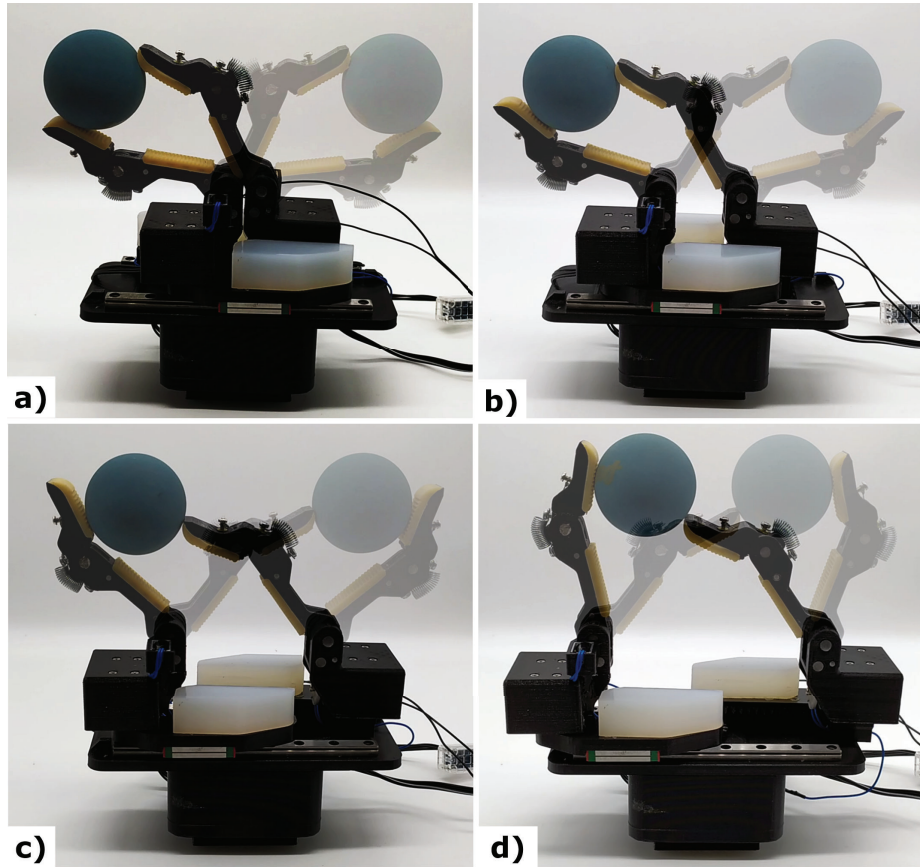


Figure 9.9: Dexterous manipulation of a racquetball when the inter-finger distances are: a) 0 mm, b) 30 mm, c) 70 mm, and d) 110 mm.

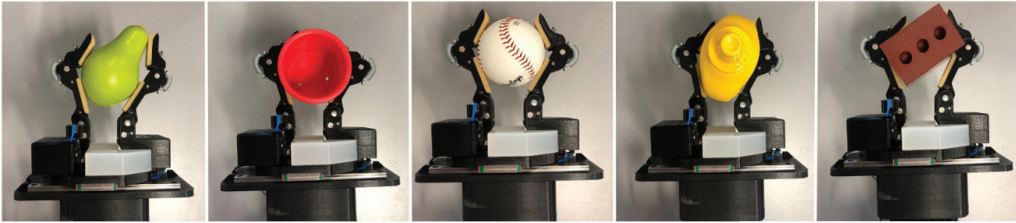
9.5 Results and Discussion

The ability of the proposed gripper to manipulate objects of varying sizes is validated using the object set shown in Figure 9.8. This object set is composed of spherical objects of

Form Closure Grasp (Adaptive Grasp)



Power Grasp (Adaptive Grasp)



Pinch Grasp (Adaptive Grasp)



Pinch Grasp (Parallel Jaw Grasp)

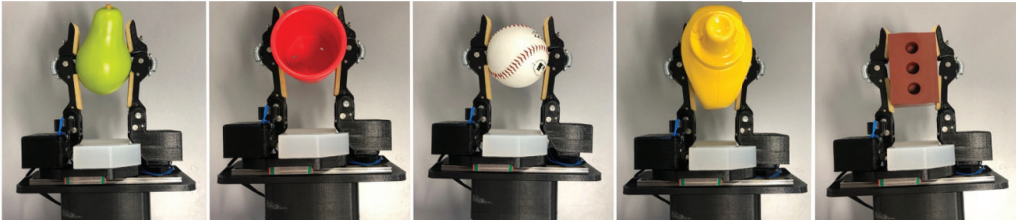


Figure 9.10: Comparison for different types of grasps that are executed with the proposed gripper.

varying texture and diameter ranging from 16 mm (marble) to 96 mm (softball). The results of this experiment are presented in Table 9.2 and show that the gripper can successfully grasp and manipulate the objects while the fingers were locked at various positions with the inter-finger distance varying from 0 mm to 110 mm in the adaptive grasping mode. Although the gripper managed to robustly grasp all the objects using the parallel jaw grasping mode, object manipulation was not feasible. The manipulation workspace for a racquetball at its workspace extremes during different inter-finger distances is presented in Figure 9.9. It shows the variation in workspace shape when the base width is altered from 0 mm through to 110 mm. It clearly demonstrates that the displacement of

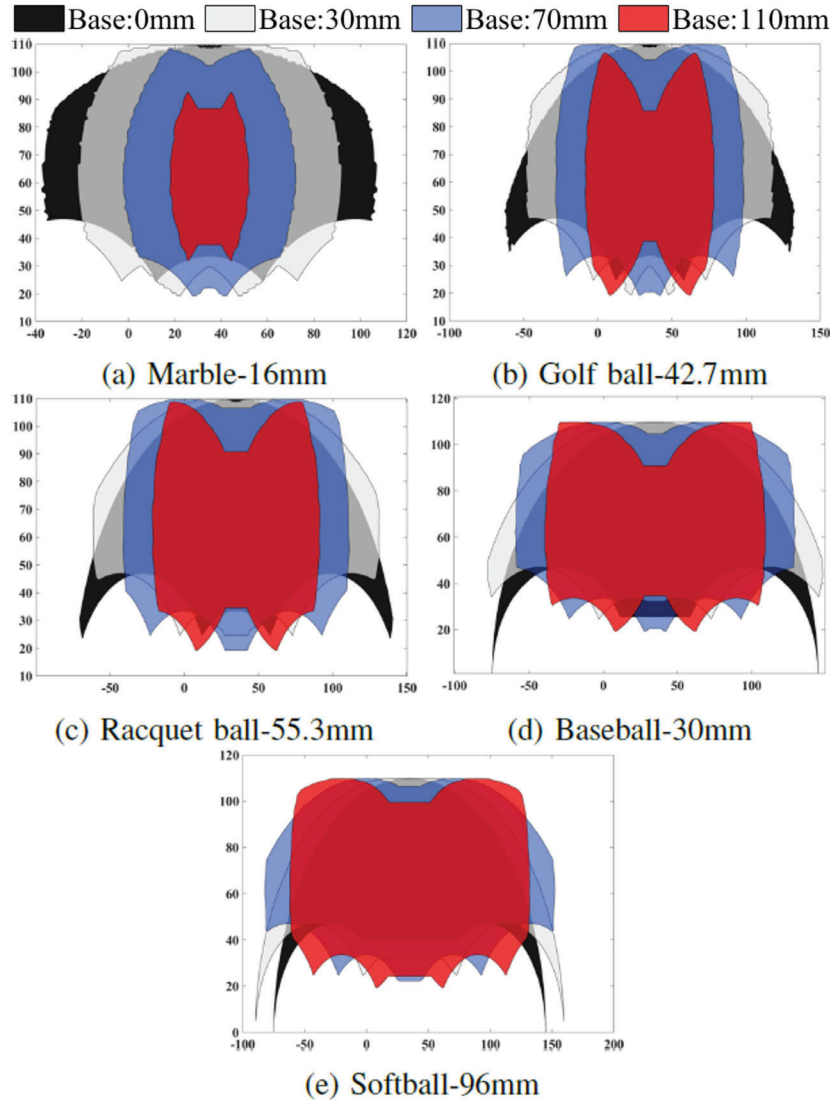


Figure 9.11: Results for the multi-modal robotic gripper with reconfigurable finger bases. Comparison of workspace achieved for spherical objects presented in Figure 9.8 that have different diameters and separated by base width: $B_w = 0$ mm, 30 mm, 70 mm, and 110 mm.

the object is larger when the inter-finger distance is 0 mm and decreases as the inter-finger base distance approaches 110 mm, indicating that the manipulation workspace volume is inversely proportional to the inter-finger distance. The figure clearly shows the variation in workspace shape when the base width is altered from 0 mm through to 110 mm and that all workspaces have unique regions. Hence, the union of the workspaces is always greater than any of the individual workspaces, as shown in Table 9.3. It can also be noted from Table 9.3 that when the phalange ratio is fixed, the optimal workspace is achieved

Table 9.3: Results of the multi-modal robotic gripper with reconfigurable finger bases. The ratio of optimized workspace (WS_{opt}) to the union of all the workspaces ($\bigcup_{i=1}^n WS_i$) generated for spherical objects of varying object diameter at base width $B_w = 0$ mm, 30 mm, 70 mm, and 110 mm.

Object Name	Object Diameter (mm)	$WS_{opt} / \bigcup_{i=1}^n WS_i$			
		$B_w=0$ mm	$B_w=30$ mm	$B_w=70$ mm	$B_w=110$ mm
Marble	16	0.8703	0.8234	0.5107	0.1509
Golf ball	42.7	0.8831	0.7661	0.76	0.4556
Racquet ball	55.3	0.7558	0.8512	0.81	0.5421
Baseball	73.3	0.6201	0.7115	0.745	0.5835
Softball	96	0.5425	0.6254	0.7939	0.7413

Table 9.4: Workspace comparison of the multi-modal gripper with the Barrett hand, the T42 gripper, and the Robotiq 3-fingered adaptive robotic gripper.

Object Name	Object Diameter (in mm)	Planar Manipulation Workspace (in mm ²)			
		Multi-modal	Barrett Hand	T42	Robotiq 3-fingered
Marble	16	9853.25	3132.09	3503.70	662.94
Golf ball	42.7	12373.54	8015.71	6862.21	2527.41
Racquet ball	55.3	14103.66	10056.80	9035.30	3663.85
Baseball	73.3	17888.25	13338.65	9814.61	5626.74
Softball	96	18849.60	16718.32	12522.67	8446.33

only with a lower inter-finger distance. Moreover, the configuration space of the gripper gets limited when trying to manipulate an object that is much bigger than the gripper fingers. If the inter-finger distance is increased, the object can be approached by the distal fingertips from the sides, allowing it to manipulate the object freely. Hence variation of the inter-finger distance is necessary for improving the overall manipulation capability when the ratio of the phalanges is fixed. This can only be achieved by a gripper capable of varying the base-width/inter-finger distance online while maintaining contact with the object, as demonstrated in this study. Figure 9.10 demonstrates the effectiveness of the gripper in executing various types of grasps on a number of objects of varying sizes and shapes using the adaptive and the parallel jaw mode. The manipulation workspace of spherical objects with varying diameters and inter-finger distances are presented in Figure 9.11. The unique vertical and lateral manipulation capability of the gripper is demonstrated in Figure 9.13a and Figure 9.13b. While the gripper can manipulate the objects along a straight line vertically, the lateral movement is along an arc like most grippers resulting in a blind space in the gripper workspace. The multi-modal gripper overcomes

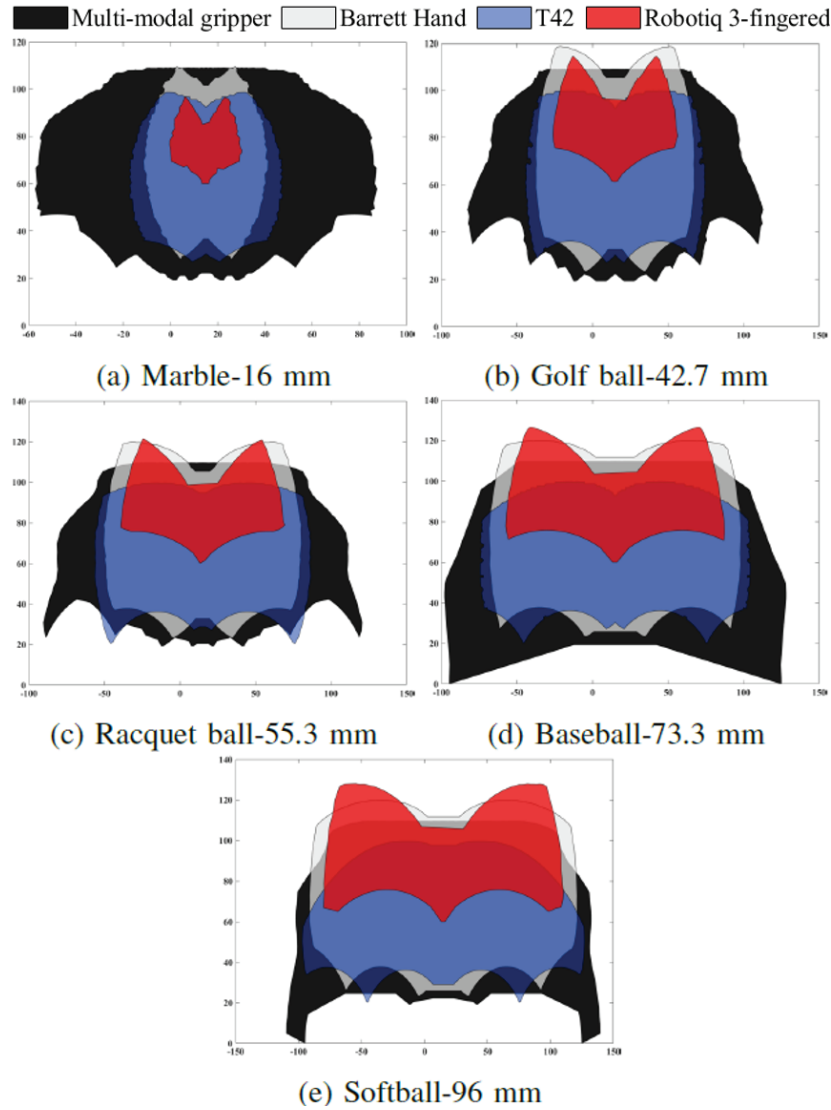
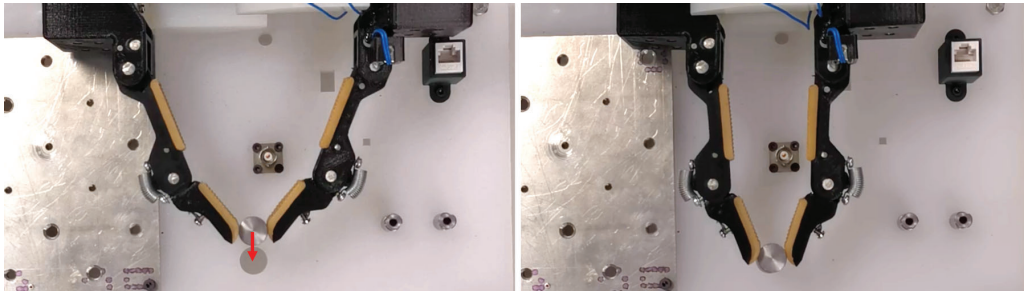


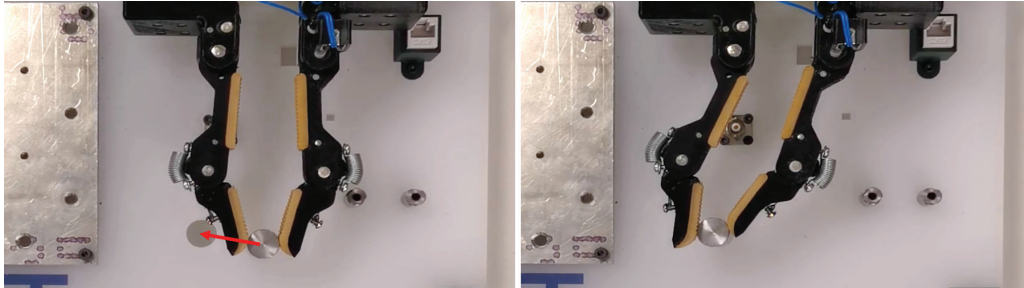
Figure 9.12: Comparison of the workspaces achieved by the multi-modal gripper, the Barrett hand, the T42 gripper, and the Robotiq 3-fingered adaptive robotic gripper for the spherical objects presented in figure 9.8 that have different diameters.

this limitation by combining the vertical and lateral manipulation movements, increasing the overall available manipulation workspace as presented in Figure 9.13c.

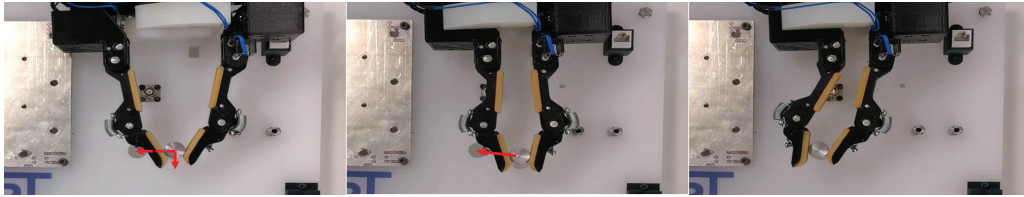
In order to compare the efficiency of the multi-modal gripper against some of the commonly used grippers in literature, the kinematic models of the multi-modal gripper, the Barrett hand, the T42 gripper, and the Robotiq 3-fingered adaptive robotic gripper were prepared in MATLAB and the planar manipulation workspace for the objects presented in Figure 9.8 was generated. The workspace generated by these grippers for the



(a) Vertical Manipulation of a peg



(b) Lateral Manipulation of a peg



(c) Combined Manipulation of a peg to cover blind space in manipulation workspace

Figure 9.13: Demonstration of a vertical and horizontal manipulation capability of the multi-modal gripper while performing a peg in hole task.

various objects can be seen in Figure 9.12 and the results of this simulation calculated in mm^2 are presented in Table 9.4. The workspace generated by the multi-modal gripper is significantly larger compared to the workspaces for the other grippers for the entire set of objects. This can be attributed to the reconfigurable finger bases of the gripper that enable it to adapt to various object sizes and cover a wider range of workspace regions with any given object. This clearly demonstrates the improved manipulation capability of the proposed gripper.

A video presenting experiments conducted with the proposed multi-modal robotic gripper can be found at the following URL:

<https://newdexterity.org/multimodalgripper>

9.6 Conclusion

This chapter proposed a framework for finding the optimal link dimensions and inter-finger distance (for a given object) of robotic grippers that are symmetric or asymmetric with two and three phalanges per finger. The optimization problem was designed so as to maximize the manipulation workspace volume for a wide range of objects by parametrizing the link dimensions and inter-finger distance and searching the design space for the optimal values of these parameters. This was performed using a parallel multi-start search algorithm to solve the multiparametric optimization problem. The optimization provided us with the optimal link ratios for all four gripper configurations examined. The workspace analysis results demonstrate that for a fixed finger dimension, the manipulation workspace is inversely proportional to the distance between the fingers and reaches its maximum volume at zero inter-finger distance. The workspace varied widely in shape and volume for varying link ratios and inter-finger distances. The achievable workspaces had unique regions and some of them had gaps or disconnected regions, indicating that the union of these workspaces is always greater than any individual workspace and that a gripper capable of covering the union of these workspaces is required so as to maximize grasp robustness and improve manipulation performance. Thus, a gripper with a reconfigurable base was designed and developed and its efficiency was experimentally validated. The gripper was fabricated with an optimal link ratio and was mounted on a parallel jaw module that allowed varying the inter-finger distance from zero to 110 mm. The design is equipped with lockable joints that allow transitioning between an adaptive grasping configuration and a parallel jaw grasping configuration. The proposed gripper achieved a great increase in the volume of the achievable manipulation workspace without sacrificing grasping robustness and efficiency. It demonstrated clearly that for a given link ratio, the manipulation workspace is maximum when the inter-finger distance is zero and decreases as the finger bases move away from each other. This can easily be extended to other robotic hands as the parameters and features being optimized here are applicable to all robotic end-effectors.

In terms of potential future work, the framework will be extended to grippers with more phalanges and more fingers. Another key priority would be to check how the inter-finger distance affects the workspace of multi-fingered hand designs. We also intend to identify and optimize other key design parameters.

Part V

Conclusion and Future Directions

Chapter 10

Conclusions and Major Contributions

10.1 Conclusion

This thesis focused on the analysis and evaluation of the dexterity and the grasping and manipulation capabilities of humans and robot hands. To accomplish this, we first investigated the boundaries of the term dexterity by analyzing, evaluating, and classifying the various definitions, classes, and metrics described in the literature with respect to human hands and robotic end-effectors. We then proposed a definition of dexterity that summarises the key attributes of human and robot dexterity. Based on the analysis, we proposed a new modular, affordable, accessible open-source dexterity test that enables the evaluation of human and robot hands alike solely based on their task completion capabilities irrespective of individual design parameters. The dynamic dexterity test rig, standardized objects, benchmarking protocols, and scoring methodology are all open-source and can be used for replicable research and benchmarking under identical conditions. Human trials were performed to validate the proposed evaluation methods and to be used as baseline scores for robotic grippers. Further experiments with robotic grippers and hands revealed a huge disparity in the task completion capabilities and speed (time required for task completion) when compared to the baseline scores.

This highlighted the urgent need for capability maps and taxonomies that can capture and map the task execution capabilities of humans to robotic end-effectors. For this purpose, we created an initial dataset of the various grasping and manipulation strategies employed by the human arm-hand systems for the execution of kitchen tasks from the video analysis of human subjects performing ADLs in home kitchen environments. These unique strategies are captured in a kitchen tasks specific taxonomy. The current

capabilities of various grippers are benchmarked against human performances by performing the same tasks in a kitchen set up at the lab. The abilities and limitations of the current gripper configurations are presented in a capability map. We also derived the major attributes used by humans that need to be translated to the robotic end-effectors for improved dexterity and task performance. An expanded dataset was created by analyzing videos of further subjects performing kitchen tasks over five trials and including the key attributes identified from the initial analysis to the annotation process. The expanded dataset included more than 10,000 entries annotated with 24 attributes for each activity. We performed clustering to analyze this multi-dimensional dataset and identify underlying patterns among the various grasping and manipulation strategies employed by the various subjects. While this initial analysis was able to successfully group activities employing similar strategies, it also reinforced our earlier suggestion that the majority of the tasks in each cluster can be successfully executed using a limited number of grasps and manipulation strategies. Inter-subject variability calculated from the low-dimensional space of the key attributes was used to derive the most efficient strategies that should be transferred to robotic end-effectors for human-robot collaboration as well as highlighting the tasks requiring attention (that require more data to be collected) during further data collection.

This thesis also focused on developing design optimization frameworks and deriving design guidelines for robotic grippers and hands. Initially, we exploited certain limitations in the current design of adaptive grippers such as joint compliance and underactuation that cause uncertainty post-contact and a parasitic reconfiguration, to improve dexterous manipulation through the efficient prediction of contact forces. This was achieved by predicting the forces exerted by the adaptive grippers from their finger reconfiguration profiles. Further, we derived design specifications for robotic grippers based on the analysis and optimization of existing gripper characteristics. In particular, the proposed metrics were used in the formulation of a design optimization framework that improves the manipulation capabilities of grippers based on their workspace analysis. The efficiency of the optimization framework was demonstrated through the design, analysis, and experimental validation of a multimodal robotic gripper with reconfigurable finger bases and lockable joints that exhibits improved manipulation capabilities without sacrificing grasping performance.

The insights from the extensive human trials and robotic experiments performed in this thesis can be employed to derive design specifications for the development of new classes of highly efficient adaptive robotic grippers and hands capable of performing on par with human hands.

10.2 Major Contributions

The major contributions of this PhD are summarised as follows:

A Comprehensive Dexterity test

For the benchmarking of human and robot dexterity, this study presents a

- A standardized dexterity test consisting of a dynamic rig that requires the object to be reoriented and assembled during the approach phase to meet the changes in end position and orientation. This is representative of real life environments such as assembly lines that require dexterous manipulation in a dynamic environment with obstacles.
- Open source standardized test rig, objects, standard operating procedures, and scoring methodology to enable replicable research and benchmarking under identical conditions.
- A dexterity metric that converts the successful task completion (ability) and rate of completion (speed) to a scale of 0 (non-dexterous) to 1 (highly dexterous human-like) irrespective of independent design characteristics of the gripper.
- Baseline scores obtained from extensive human experimentation. Experimental validation of the efficiency of the benchmarking system based on human and robot experiments.

Kitchen Task Specific Dataset and Taxonomy

- The design of a comprehensive dataset of kitchen tasks collected by humans in a home environment.
- The dataset includes high-definition videos recorded from various angles to supplement each other. The detailed dataset contains each of the activities in the video annotated with over 24 attributes.
- The dataset has been analyzed to identify the most commonly employed human task execution strategies and the unique strategies are captured in a taxonomy.
- A capability map that highlights the current abilities and limitations of the robotic grippers in their performance in various kitchen tasks. This is used to identify the current shortcomings in the design and control of robotic end-effectors.
- Clustering techniques to identify underlying patterns of grasping and manipulation strategies employed for the successful execution of a group of tasks.

- Identified optimal strategies that can be transferred directly to robotic end-effectors and identified tasks that require further data collection based on inter-subject variability.
- Derived inputs based on dataset analysis and benchmarking for the development of new classes of robotic grippers and hands that can perform on par with human hands.

Exploiting Post Contact Reconfiguration of Adaptive Robot Grippers

- A methodology that combines Random Forest regression models and motion capture systems to predict the contact forces exerted by an adaptive robot finger in pinch grasps, using its post-contact reconfiguration profile.
- Remove uncertainties in the force exertion during the post-contact phases of adaptive grippers caused by joint compliance and underactuation. Exploit the limitations of underactuated adaptive fingers to increase dexterous manipulation capabilities.

Design Optimization Framework

- A parallel multi-start multiparametric optimization framework was developed to maximize the workspace volume of grippers with varied configurations (symmetric/asymmetric with 2-3 phalanges per finger).
- Analysed the effect of optimal inter-finger distance for a fixed (optimized) finger link ratio on maximizing the dexterous manipulation workspace.
- A multimodal robotic gripper with reconfigurable finger bases capable of varying inter-finger distance while grasping an object, exhibiting increased dexterous manipulation workspace without sacrificing grasping efficiency.
- Validated the efficiency of the gripper in offering an increased manipulation performance without sacrificing grasping efficiency through experiments and comparison against other state of the art grippers.

10.3 Future Directions

The main directions for future work are:

- Translate the key strategies of human dexterity derived from extensive human trials and experiments to autonomous robotic arm-hand system strategies.
- Expand the kitchen task specific dataset by including data of users performing the kitchen tasks with limited grasping and manipulation strategies. For example, tasks executed with one hand, use certain predefined grasps only etc. This will provide further insights into strategies that can be adopted by robotic grippers that have limited grasp variability.
- Capture grasping and manipulation strategies employed by humans in other environments such as performing other ADLs, in a machine shop, assembly lines etc to derive the key attributes and strategies associated with dexterous manipulation in these environments.
- Expand the optimization framework to other multi-fingered hand designs such as anthropomorphic hands.
- Employ the insights from all the aforementioned analyses to derive design specifications for the development of new classes of highly efficient adaptive robotic grippers and hands capable of performing on par with human hands.

Part VI

Appendices

Appendix A

Thesis Outcomes

A.1 Awards

1. **Best Paper Award Winner**, Robot Mechanisms and Design, IEEE International Conference on Intelligent Robots and Systems (IROS), 2021, Prague, Czech Republic.

A.2 Journal Publications

1. **Nathan Elangovan**, Che-ming Chang, Geng Gao, and Minas Liarokapis, “An accessible, open-source dexterity test: Evaluating the grasping and dexterous manipulation capabilities of humans and robots,” *Frontiers in Robotics and AI*, p. 53, 2022. doi: 10.3389/frobt.2022.808154
2. **Nathan Elangovan**, Lucas Gerez, Geng Gao, and Minas Liarokapis, “Improving Robotic Manipulation without Sacrificing Grasping Efficiency: A Multi-Modal, Adaptive Gripper with Reconfigurable Finger Bases.” *IEEE Access*. vol.9, pp.83298-83308. 2021.
3. Che-ming Chang, Lucas Gerez, **Nathan Elangovan**, Agisilaos Zisimatos, and Minas Liarokapis, “On alternative uses of structural compliance for the development of adaptive robot grippers and hands.” *Frontiers in neurorobotics*, vol. 13,p. 91, 2019.

A.3 Conference Publications

1. **Nathan Elangovan**, Che-ming Chang, Ricardo V. Godoy, Felipe Sanches, Ke Wang, Patrick Jarvis, and Minas Liarokapis, “Comparing Human and Robot Performance in the Execution of Kitchen Tasks: Evaluating Grasping and Dexterous Manipulation Skills,” in 2022 IEEE-RAS International Conference on Humanoid Robots (Humanoids), IEEE, Okinawa, Japan, 2022.
2. **Nathan Elangovan**, Lucas Gerez, Geng Gao, and Minas Liarokapis, “A Multi-Modal Robotic Gripper with a Reconfigurable Base: Improving Dexterous Manipulation without Compromising Grasping Efficiency,” IEEE/RSJ International Conference on Intelligent Robots and Systems (IROS), IEEE, Prague, Czech Republic, 2021, pp. 6124-6130.
3. **Nathan Elangovan**, Geng Gao, Che-ming Chang, and Minas Liarokapis, “A modular, accessible, affordable dexterity test for evaluating the grasping and manipulation capabilities of robotic grippers and hands,” in 2020 IEEE International Symposium on Safety, Security, and Rescue Robotics(SSRR), IEEE, Abu Dhabi, United Arab Emirates, 2020, pp. 304–310.
4. Gal Gorjup, Anany Dwivedi, **Nathan Elangovan**, and Minas Liarokapis, “An intuitive, affordances oriented telemanipulation framework for a dual robot arm hand system: On the execution of bimanual tasks,” in 2019 IEEE/RSJ International Conference on Intelligent Robots and Systems (IROS), IEEE, Macau, China, 2019, pp. 3611–3616.
5. **Nathan Elangovan**, Anany Dwivedi, Lucas Gerez, Che-ming Chang, and Minas Liarokapis, “Employing imu and aruco marker based tracking to decode the contact forces exerted by adaptive hands,” in 2019 IEEE-RAS 19th International Conference on Humanoid Robots (Humanoids), IEEE, Toronto, ON, Canada, 2019, pp. 525–530.
6. Che-ming Chang, Lucas Gerez, **Nathan Elangovan**, Agisilaos Zisimatos, and Minas Liarokapis, “Unconventional uses of structural compliance in adaptive hands,” in 2019 28th IEEE International Conference on Robot and Human Interactive Communication (RO-MAN), IEEE, New Delhi, India, 2019, pp. 1–7.
7. Geng Gao, Anany Dwivedi, **Nathan Elangovan**, Yige Cao, Lucy Young, and Minas Liarokapis, “The new dexterity adaptive, humanlike robot hand,” in IEEE In-

ternational Conference on Robotics and Automation (ICRA). Montreal, Canada, 2019, pp. 6124-6130.

Appendix B

Annotation Guide for Grasping and Manipulation Tasks Executed in Kitchen Environments

B.1 Instructions for Annotating Each Video

Step1: Create a separate spreadsheet for each trial. Each trial has recordings of the same scene from multiple angles. Cam1 - POV, Cam3 - Side angle. While most of the information can be annotated from Cam1 recording, supplementary information (like posture, is the user bending, shoulder movement etc) needs to be derived from other camera angles. Only one spreadsheet should be created per trial.

Step2: Sheets to be named with House/kitchen number, trial number, task name. Eg., H4T1_DishLoading refers to House/kitchen 4, Trial 1, loading the dishwasher.

Step3: Fill all columns in the excel sheet using the following set of instruction specifications.

- If a task lasts less than 1 second, do not record the task.
- If the task is not performed by “Hands”, do not record the activity. Eg. Users closing the drawer with legs, pushing a door with their elbows etc.

Column 1 Kitchen task name: Select one of the 10 kitchen tasks from the dropdown menu. For example, Breakfast, Unloading dishwasher).

Column 2 Video number: Enter the Trial/video number from the video file(1a ,2a, 3a).

Column 3 Task Type: Determine the actual activity from the dropdown list that contains 13 predetermined category (“Pick” , “Lift”, “Place”). If none of the items in the list describe the activity aptly, populate your own description for this activity. If an object grasp is changed during the activity, select “convert grasp”.

Column 4 Start time: Time stamp when activity started.

Column 5 End time: Time stamp when activity ended.

Column 6 Duration: Duration for the activity is auto generated from column 4 and 5.

B.1.1 Object Attributes

Column 7 Objects picked: Check if a single object is grasped or multiple objects are being grasped.

Column 8 Object location:

Low	If the object is located much below waist height requiring the user to bend/lower in order to reach the object. Eg., plates in dishwasher rack, lower shelf of fridge
Level	Object is around waist high and can easily be grasped from a neutral position. Eg. object on kitchen counter, stove top etc.
High	Object over chest high, requires the arm to be raised or shoulder movement to reach the object. Eg. a can in the top shelf of a pantry

Column 9 Object orientation:

Isolated	The object is isolated and can be approached/grasped from all direction
Clutter	If the object is surrounded by a lot of items restricting identification and grasps
On top	If the object is on top of other objects/pile restricting the grasp to be approached from one or more sides
Buried	If other objects are lying over the object, that has to be moved to access the particular object
Irrelevant	The object is not being grasped or manipulated (non-prehensile). Eg. pushing a pantry door, pressing a button etc.

Column 10 Approach of the arm: Check the angle/direction the arm takes to approach the object and select one of the options from the list below.

Column 11 Object shape: Select the shape of the object from drop down menu.

Cylindrical	Canned beans, pringles can, bottles, door handles, handles of pots etc.
Boxes	Cereal box, Jello box, salt box and other grocery boxes
Sphere	Oranges, apples
Flat	Includes objects like plates, lids, spoons, buttons, doors etc
Deformable	Can be used to classify soft deforming items like cleaning cloth, tissue
Other	If the object is irregularly shaped, annotate as other

Column 12 Object type: Choose between one the types of objects listed.

Column 13 Object size:

Small	Small objects such as strawberries, lids, cutlery, glasses, etc.
Medium	Canned foods, pots/pans, regular groceries, etc.
Large	Large can of milk, a rice bag, big fruits such as watermelons, etc.
Irrelevant	The object is not being grasped or manipulated (non-prehensile). Eg. pushing a pantry door, pressing a button etc.

Column 14 Object weight:

Light	Lightweight objects like cutlery, strawberry, empty cups/glasses etc.
Medium	This could include pots/pans, canned foods, groceries etc.
Heavy	Heavy objects like a large can of milk, a rice bag, a heavy pan etc.
Irrelevant	The object is not being grasped or manipulated (non-prehensile). Eg. pushing a pantry door, pressing a button etc.

Column 15 Hands no.: Check if the subject uses 1 hand or both hands for completing a given activity.

- If 1 hand no need to specify which hand. Populate the cell with “One hand”. If the subject moves an object from one hand to another, it is still classified as “One hand”. Example: An user picking a glass with left hand, moving the object to right hand, and placing it down with right hand.
- If the subjects are using both hands to execute a single task, we call it bimanual and populate the details for what each hand is doing under bimanual(left) and bimanual(right). Example: Holding a bottle and opening the lid. Holding a strawberry with one hand and cutting it with the other.

- If both hands are used for carrying separate activities, populate separate rows for left (parallel left) and right (parallel right) hands. Example: carrying a plate in one hand and glasses in the other. Moving an object with the left hand to place another object in a dishwasher.

B.1.2 Grasp Attributes

Column 16 Grasp Classification: Determine the hand pose is Power/Intermediate/Precision.

- Power: Firm grasp against palm/pad. Finger manipulation not feasible. Requires arm movement to manipulate object.
- Precision: Objects can be manipulated easily with fingers. Not held against the palm. Fingertips/pad involved in grasp.
- Intermediate: Grasp involves equal proportion of power and precision. Involves firm grasps involving fingers holding objects against the side of another finger.

Column 17 Thumb:

- Abduction - Thumb out of plane from palm/fingers enabling it to oppose the fingers. It can be seen how the thumb has been rotated (to various degree) out of plane from the palm to oppose the fingers to enable stable grasps.
- Adduction - Thumb in same plane with palm. As shown in the images below, the thumb is in the same plane as the palm and cannot oppose the fingers.

Column 18 Grasp type: Select the appropriate grasp type from Figure "GraspTaxonomy" that matches with the video execution. If the grasp type does not represent any described in the Taxonomy, choose "Unknown". In case of view occlusion, check for nearby non-occluded frames. If still not possible, mark as "Unknown".

Opposition type:

- Palm: When the object is held firmly against the palm. Commonly observed in power grasp. Objects can only be moved using arm motion in this configuration.
- Pad: The objects are stabilised against finger pads.






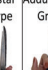



















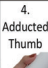

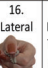
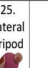


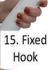



Opp.	Power					Intermediate					Precision					Side
	Palm		Pad			Side			Pad							
Thumb Abducted	1. Large Diameter 	2. Small Diameter 	31. Ring 	28. Sphere 3 Finger 	18. Extension Type 	26. Sphere 4 finger 	19. Distal Type 	23. Adduction Grip 	21. Tripod Variation 	9. Thumb Index Finger 	8. Thumb 2 Finger 	7. Thumb 3 Finger 	6. Thumb 4 Finger 	20. Writing Tripod 		
	3. Medium Wrap 	10. Power Disk 								24. Tip Pinch 	14. Tripod 	27. Quadpod 	12. Precision Disk 			
	11. Power Sphere 									33. Inferior Pincer 			13. Precision Sphere 			
													22. Parallel Extension 			
Thumb Adducted	17. Index Finger Extension 	4. Adducted Thumb 	5. Light Tool 					16. Lateral 	25. Lateral Tripod 		Non-Prehensile 34. Lift  35. Push 					
	15. Fixed Hook 	30. Palmar 					29. Stick 	32. Ventral 								

Figure B.1: Grasp Taxonomy used to classify the various grasps employed by the human hand adapted from [38].

- **Side:** The objects are stabilised entirely by finger sides or between finger pads & side of a finger.

Odd cases:

- **Non-prehensile:** If the object is not being grasped properly and being moved by touching it. Example: pushing buttons, closing doors by pushing on the surface.
- **Multiple grasps:** When multiple objects are being grasped simultaneously.
- **Partial grasp:** involves cases when the object is not completely grasped/stabilised. Examples: partial hook using 2-3 fingers to open cabinet door using handle.

B.1.3 Manipulation attributes

Determine the manipulation type using the following steps.

1. Is the hand (fingers, palm, or back of hand) in contact with the object?
 - a) If there is no contact between the hand and the object , do not record the activity.
 - b) If there is contact proceed to question 2.
2. Is the object being held (grasped) by the user restricting the object partially or fully?
 - a) If the object is not restricted by the hand, select non-prehensile. Proceed to question 3. Eg. object is being pushed by the finger or held on palm.
 - b) If the object motion is restricted fully or partially in the hand by grasping it using fingers and palm. Proceed to question 4.

Non-prehensile:

3. Check if the object is in motion/stationary during the execution of the task.
 - a) If object is stationary, select no motion (NM)
 - Select 4, if the contact is fixed. eg. holding a plate on your palm, pressing down a piece of bacon (while your other hand cuts it) etc.

- Select 5, otherwise.
- b) If the object moves during task execution, select:
 - i. Not within hand ,if the object is moving external to the hand.
 - Select 8, if the contact point between the hand/finger and object remains constant. Eg. pushing a button the contact point between fingertip and button remains constant. Other examples include pushing the door with palm, sliding an object by pushing it with the back of the palm.
 - Select 9, if the contact changes during the activity. Eg. When the palm is used to clear the cereal spilled on the counter top, the hand slides over the counter. The hand does not grasp anything, but the contact point between the hand and the counter changes continuously. Another example is rolling a dough ball using your palm.
 - ii. Within hand - if the object moves within the hand/fingers.
 - Select 12, if the contact point between the hand/finger and object remains constant. Eg. flipping the oven switch on/off using the side of your fingers.
 - Select 13, if the contact changes during the activity. Turning the knob by rolling the fingers over the knob (not holding the knob). In this case, the knob makes contact with multiple points on the finger during the task.

Prehensile:

4. Check if the object is in motion/ stationary during the execution of the task.
 - a) If object is stationary, select no motion (NM).
 - select 6, if the contact is fixed. eg. holding a bottle using a large cylindrical grasp with the left hand (while other hand opens the cap)
 - Select 7, otherwise.
 - b) If the object moves during task execution, select:
 - i. Not within hand, if the object is moving external to the hand.
 - Select 10, if the contact point between the hand/finger and object remains constant. This is the most commonly employed manipulation type. Eg. Grasping the fridge door handle and pulling it open.

The contact points between the hand and door handle remain constant throughout the execution of this task. Other examples include firmly grasping a plate and lowering it in the dishwasher, Grasping a pot handle and positioning it on the stove top etc.

- Select 11, if the contact changes during the activity. Eg. When the hand grasps a cylindrical food wrapped in cover firmly, and slides the cover away. In this case, the contact point between the hand and the cylindrical food changes continuously. Another example is pinching a yoghurt sachet at the end, and squeezing it all the way to the opening to push out all the contents. Again, the grasp remains constant, but the contact point moves from one end of the sachet to the other.

ii. Within hand - if the object moves within the hand/fingers.

- Select 14, if the contact point between the hand/finger and object remains constant. Eg. Picking and turning small food items using tongs. The fingers hold the tongs at the same contact points while the tong moves(opens and closes) within hand. Another example would be using chopsticks.
- Select 15, if the contact changes during the activity. Eg. Twisting a salt grinder requires the bottle to be twisted multiple times. In this case, the finger grasps the bottle and completes the first rotation/twist. Then regrasps the bottle at different set of points (fingers continuously change contact points on the object until task is complete).

Odd cases:

- In-hand stabilised manipulation 16: Holding down an object and manipulating a part of the object using the same hand. Eg. when the user stabilises the milk can by holding its handle while twisting the cap using the index and thumb fingers to open it.
- Compound manipulation 17: Manipulate a wide number of objects of varying shapes and sizes that each require a different grasp type in a single task.
- Grasp conversion manipulation 18: Move the manipulated object from one grasp type to another during the execution of a task. Eg. moving a cup grasped in a

large diameter power grasp type to a precision disk type grasp while picking and placing a cup from the counter onto a dishwasher without losing contact with the manipulated object.

Column 20 Movement direction: Identify the movement direction from the drop down menu. For example, picking a cup from the dishwasher will have “Lift” in movement direction.

Column 21 Bending: Determine whether the subject is Bending his body/back during the execution of the task. Levels can be chosen from drop down menu.

Column 22 Shoulder movement: Determine the level of movement in the shoulder during the execution of the grasping/manipulation from the dropdown menu.

Column 23 Dishes: Determine whether the dishes are wet/dry from the video.

Column 24 Washes Hands: Determine if the subject washes hands.

B.2 Guideline Annotation Sheet

Sample annotation sheet can be downloaded from the following link:

www.newdexterity.org/kitchendataset

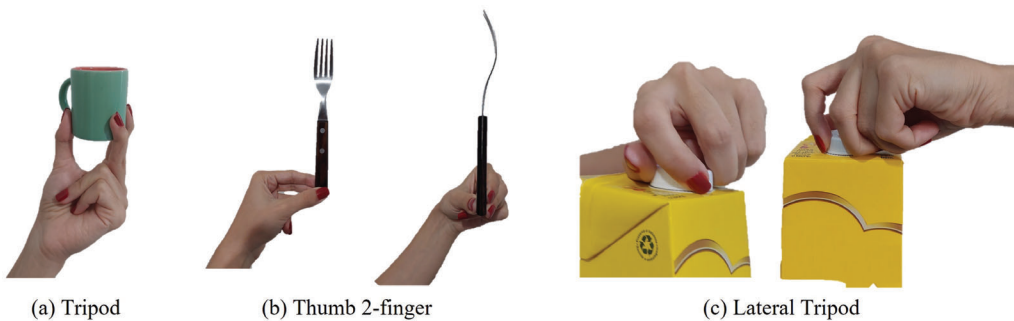


Figure B.2: Demonstration of differences between: a) tripod, b) thumb 2-fingered, and c) lateral tripod.

B.3 Clarification on common grasps

- **Tripod vs Thumb 2-fingered:** In a Tripod grasp, the object is held between 3 fingers exerting force (with finger pads) on the object from 3 different directions. While for Thumb 2 fingers, the object is restricted by forces from 2 directions (The thumb from one side and the other 2 fingers opposing it).
- **Lateral tripod:** In a Lateral Tripod grasp, the object is held between 3 fingers (with 2 finger pads and 1 finger side) exerting force on the object from 3 different directions.
- **Lateral Pinch:** In lateral pinch, the object motion is restricted between one finger pad and the side of another finger as shown.
- **Extension type vs Palmar:** For Extension type, the thumb is rotated to oppose the rest of the fingers. And the object is restricted between the thumb and the fingers. For Palmar: Unlike the extension type, the thumb is not rotated to oppose the rest of the fingers. The thumb is in the same plane as the palm.

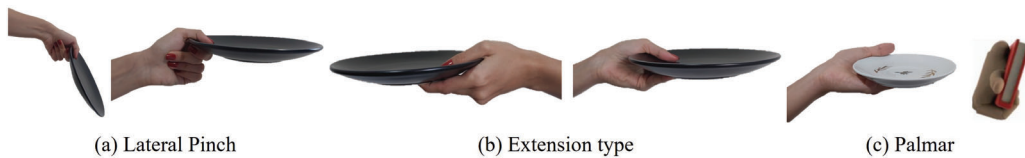


Figure B.3: Demonstration of differences between: a)lateral pinch, b) extension type, and c) palmar.

- **Power Sphere:** Not restricted to spherical objects. Object motion is completely restricted by grasping the object between the finger pads(wrapping around object) and palm. Object can only be moved with arm motion and not finger movements.
- **Precision sphere:** not restricted to spherical objects. The Object is restricted by finger pads(a major portion of the finger wraps around the object). Not held against palm. If the object was restricted against palm, the grasp should be classified as Power sphere.

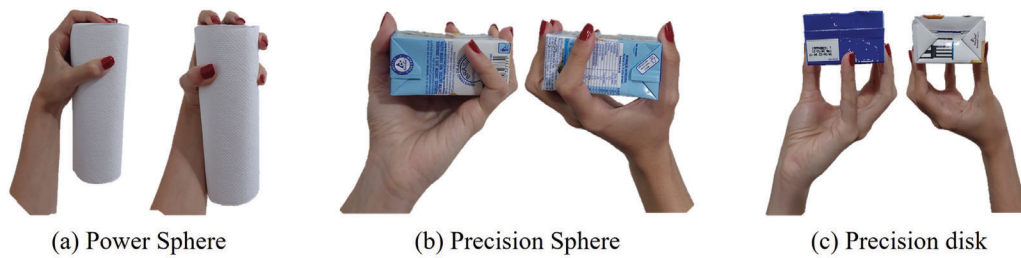


Figure B.4: Demonstration of differences between: a) power sphere, b) precision sphere, and c) precision disc.

- **Precision disc:** not restricted to cylindrical objects. The Object is restricted by finger pads (in most cases only by the distal finger pads and the fingers do not wrap around the object). Not held against palm. If the object was restricted against palm, the grasp should be classified as Power disk.
- **Non-prehensile:** If the object is not being grasped properly and being moved by touching it. Example: pushing buttons, closing doors by pushing on the surface.
- **Multiple grasps:** When multiple objects are being grasped simultaneously.
- **Partial grasp:** involves cases when the object is not completely grasped/stabilised. Examples: partial hook using 2-3 fingers to open cabinet door using handle.

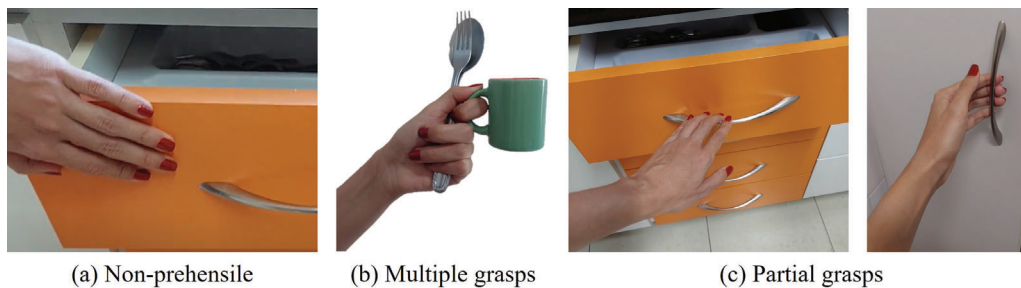


Figure B.5: Demonstration of odd grasps executed by humans is shown. Subfigure a) presents a non-prehensile grasp, subfigure b) presents a multi-object grasp, while subfigure c) presents partial grasps.

References

- [1] Charles Bell. *The hand: its mechanism and vital endowments, as evincing design*. Vol. 4. Bell & Daldy, 1865.
- [2] Aristoteles, David M Balme, and Allan Gotthelf. *Aristotle's "De Partibus Animalium I": And "De Generatione Animalium I"(with Passages from II. 1-3)*. Clarendon Press, 1972.
- [3] Aldo Faisal, Dietrich Stout, Jan Apel, and Bruce Bradley. "The manipulative complexity of Lower Paleolithic stone toolmaking". In: *PloS one* 5.11 (2010), e13718.
- [4] John R Napier. "The prehensile movements of the human hand". In: *The Journal of bone and joint surgery. British volume* 38.4 (1956), pp. 902–913.
- [5] Antonio Bicchi. "Hands for dexterous manipulation and robust grasping: A difficult road toward simplicity". In: *IEEE Transactions on robotics and automation* 16.6 (2000), pp. 652–662.
- [6] Mary W Marzke. "Tool making, hand morphology and fossil hominins". In: *Philosophical Transactions of the Royal Society B: Biological Sciences* 368.1630 (2013), p. 20120414.
- [7] Tracy L Kivell. "Evidence in hand: recent discoveries and the early evolution of human manual manipulation". In: *Philosophical Transactions of the Royal Society B: Biological Sciences* 370.1682 (2015), p. 20150105.
- [8] Ian M Bullock, Raymond R Ma, and Aaron M Dollar. "A hand-centric classification of human and robot dexterous manipulation". In: *IEEE transactions on Haptics* 6.2 (2012), pp. 129–144.
- [9] Lovchik C.S and Myron A Diftler. "The robonaut hand: A dexterous robot hand for space". In: *Proceedings 1999 IEEE international conference on robotics and automation (Cat. No. 99CH36288C)*. Vol. 2. IEEE. 1999, pp. 907–912.

- [10] Jose L Pons, Eduardo Rocon, Ramón Ceres, Dominiek Reynaerts, B Saro, S Levin, and W Van Moorleghe. “The MANUS-HAND dextrous robotics upper limb prosthesis: mechanical and manipulation aspects”. In: *Autonomous Robots* 16.2 (2004), pp. 143–163.
- [11] Hong Liu, Ke Wu, Peter Meusel, Nikolaus Seitz, Gerd Hirzinger, MH Jin, YW Liu, SW Fan, T Lan, and ZP Chen. “Multisensory five-finger dexterous hand: The DLR/HIT Hand II”. In: *Intelligent Robots and Systems, 2008. IROS 2008. IEEE/RSJ International Conference on*. IEEE. 2008, pp. 3692–3697.
- [12] Geng Gao, Anany Dwivedi, Nathan Elangovan, Yige Cao, Lucy Young, and Minas Liarokapis. “The New Dexterity adaptive, humanlike robot hand”. In: *IEEE International Conference on Robotics and Automation*. 2019.
- [13] Geng Gao, Jayden Chapman, Saori Matsunaga, Toshisada Mariyama, Bruce MacDonald, and Minas Liarokapis. “A Dexterous, Reconfigurable, Adaptive Robot Hand Combining Anthropomorphic and Interdigitated Configurations”. In: *2021 IEEE/RSJ International Conference on Intelligent Robots and Systems (IROS)*. IEEE, pp. 7209–7215.
- [14] Raymond R Ma, Lael U Odhner, and Aaron M Dollar. “A modular, open-source 3D printed underactuated hand”. In: *Robotics and Automation (ICRA), 2013 IEEE International Conference on*. IEEE. 2013, pp. 2737–2743.
- [15] Lael U Odhner, Leif P Jentoft, Mark R Claffee, Nicholas Corson, Yaroslav Tenzler, Raymond R Ma, Martin Buehler, Robert Kohout, Robert D Howe, and Aaron M Dollar. “A compliant, underactuated hand for robust manipulation”. In: *The International Journal of Robotics Research* 33.5 (2014), pp. 736–752.
- [16] Lael U Odhner and Aaron M Dollar. “Dexterous manipulation with underactuated elastic hands”. In: *2011 IEEE International Conference on Robotics and Automation*. IEEE. 2011, pp. 5254–5260.
- [17] Sangbae Kim, Cecilia Laschi, and Barry Trimmer. “Soft robotics: a bioinspired evolution in robotics”. In: *Trends in biotechnology* 31.5 (2013), pp. 287–294.
- [18] Che-Ming Chang, Lucas Gerez, Nathan Elangovan, Agisilaos Zisimatos, and Minas Liarokapis. “On Alternative Uses of Structural Compliance for the Development of Adaptive Robot Grippers and Hands”. In: *Frontiers in Neurorobotics* 13 (2019), p. 91.

- [19] Minas Liarokapis and Aaron M Dollar. “Learning the post-contact reconfiguration of the hand object system for adaptive grasping mechanisms”. In: *2017 IEEE/RSJ International Conference on Intelligent Robots and Systems (IROS)*. IEEE. 2017, pp. 293–299.
- [20] Minas Liarokapis and Aaron M Dollar. “Post-contact, in-hand object motion compensation for compliant and underactuated hands”. In: *IEEE International Symposium on Robot and Human Interactive Communication (RO-MAN)*. 2016, pp. 986–993.
- [21] Raymond R Ma and Aaron M Dollar. “On dexterity and dexterous manipulation”. In: *2011 15th International Conference on Advanced Robotics (ICAR)*. IEEE. 2011, pp. 1–7.
- [22] Françoise Poirier. “Dexterity as a valid measure of hand function: a pilot study”. In: *Occupational therapy in health care* 4.3-4 (1988), pp. 69–83.
- [23] Lev P Latash and Mark L Latash. “A new book by NA Bernstein: “On dexterity and its development””. In: *Journal of motor behavior* 26.1 (1994), pp. 56–62.
- [24] Colleen G Canning, Louise Ada, and Nicholas J O’Dwyer. “Abnormal muscle activation characteristics associated with loss of dexterity after stroke”. In: *Journal of the neurological sciences* 176.1 (2000), pp. 45–56.
- [25] Allison M Okamura, Niels Smaby, and Mark R Cutkosky. “An overview of dexterous manipulation”. In: *Proceedings 2000 ICRA. Millennium Conference. IEEE International Conference on Robotics and Automation. Symposia Proceedings (Cat. No. 00CH37065)*. Vol. 1. IEEE. 2000, pp. 255–262.
- [26] RH Sturges. “A quantification of machine dexterity applied to an assembly task”. In: *The International Journal of Robotics Research* 9.3 (1990), pp. 49–62.
- [27] Catherine Backman, Stacy Cork Deborah Gibson, and Joy Parsons. “Assessment of hand function: the relationship between pegboard dexterity and applied dexterity”. In: *Canadian Journal of Occupational Therapy* 59.4 (1992), pp. 208–213.
- [28] Joshua Yong, Joy C MacDermid, and Tara Packham. “Defining dexterity—Untangling the discourse in clinical practice”. In: *Journal of Hand Therapy* 33.4 (2020), pp. 517–519.
- [29] Charles A Klein and Bruce E Blaho. “Dexterity measures for the design and control of kinematically redundant manipulators”. In: *The international journal of robotics research* 6.2 (1987), pp. 72–83.

- [30] Raúl Suárez, Jordi Cornella, and Máximo Roa Garzón. *Grasp quality measures*. Citeseer, 2006.
- [31] Sarosh Patel and Tarek Sobh. “Manipulator performance measures-a comprehensive literature survey”. In: *Journal of Intelligent & Robotic Systems* 77.3 (2015), pp. 547–570.
- [32] Minas V Liarokapis, Panagiotis K Artemiadis, and Kostas J Kyriakopoulos. “Quantifying anthropomorphism of robot hands”. In: *2013 IEEE International Conference on Robotics and Automation*. IEEE. 2013, pp. 2041–2046.
- [33] Minas V Liarokapis, Panagiotis K Artemiadis, and Kostas J Kyriakopoulos. “Functional anthropomorphism for human to robot motion mapping”. In: *2012 IEEE RO-MAN: The 21st IEEE International Symposium on Robot and Human Interactive Communication*. IEEE. 2012, pp. 31–36.
- [34] Luigi Biagiotti, Fabrizio Lotti, Claudio Melchiorri, and Gabriele Vassura. “How far is the human hand? a review on anthropomorphic robotic end-effectors”. In: (2004).
- [35] Joseph T Belter and Aaron M Dollar. “Performance characteristics of anthropomorphic prosthetic hands”. In: *2011 IEEE International Conference on Rehabilitation Robotics*. IEEE. 2011, pp. 1–7.
- [36] Jianshu Zhou, Xiaojiao Chen, Ukyoung Chang, Jui-Ting Lu, Clarisse Ching Yau Leung, Yonghua Chen, Yong Hu, and Zheng Wang. “A soft-robotic approach to anthropomorphic robotic hand dexterity”. In: *Ieee Access* 7 (2019), pp. 101483–101495.
- [37] Mark R Cutkosky. “On grasp choice, grasp models, and the design of hands for manufacturing tasks”. In: *IEEE Transactions on robotics and automation* 5.3 (1989), pp. 269–279.
- [38] Thomas Feix, Javier Romero, Heinz-Bodo Schmiedmayer, Aaron M Dollar, and Danica Kragic. “The grasp taxonomy of human grasp types”. In: *IEEE Transactions on human-machine systems* 46.1 (2015), pp. 66–77.
- [39] A Kapandji. “Clinical test of apposition and counter-apposition of the thumb”. In: *Annales de chirurgie de la main: organe officiel des societes de chirurgie de la main* 5.1 (1986), pp. 67–73.
- [40] Ana Huamán Quispe, Heni Ben Amor, and Henrik I Christensen. “A taxonomy of benchmark tasks for robot manipulation”. In: *Robotics Research*. Springer, 2018, pp. 405–421.

- [41] Sergio Garrido-Jurado, Rafael Muñoz-Salinas, Francisco José Madrid-Cuevas, and Manuel Jesús Marién-Jiménez. “Automatic generation and detection of highly reliable fiducial markers under occlusion”. In: *Pattern Recognition* 47.6 (2014), pp. 2280–2292.
- [42] Gary Bradski. “The openCV library.” In: *Dr. Dobb’s Journal: Software Tools for the Professional Programmer* 25.11 (2000), pp. 120–123.
- [43] Gal Gorjup, Geng Gao, Anany Dwivedi, and Minas Liarokapis. “Combining compliance control, cad based localization, and a multi-modal gripper for rapid and robust programming of assembly tasks”. In: *2020 IEEE/RSJ International Conference on Intelligent Robots and Systems (IROS)*. IEEE. 2020, pp. 9064–9071.
- [44] Che-Ming Chang, Jayden Chapman, Ke Wang, Patrick Jarvis, and Minas Liarokapis. “On Wearable, Lightweight, Low-Cost Human Machine Interfaces for the Intuitive Collection of Robot Grasping and Manipulation Data”. In: *International Conference on Robotics and Automation* (2022).
- [45] Raymond R Ma, Lael U Odhner, and Aaron M Dollar. “Dexterous manipulation with underactuated fingers: Flip-and-pinch task”. In: *2012 IEEE International Conference on Robotics and Automation*. IEEE. 2012, pp. 3551–3552.
- [46] Hui-Mei Chen, Christine C Chen, I-Ping Hsueh, Sheau-Ling Huang, and Ching-Lin Hsieh. “Test-retest reproducibility and smallest real difference of 5 hand function tests in patients with stroke”. In: *Neurorehabilitation and neural repair* 23.5 (2009), pp. 435–440.
- [47] Emily L Lawrence, Isabella Fassola, Inge Werner, Caroline Leclercq, and Francisco J Valero-Cuevas. “Quantification of dexterity as the dynamical regulation of instabilities: comparisons across gender, age, and disease”. In: *Frontiers in neurology* 5 (2014), p. 53.
- [48] *Normal Range of Motion Reference Values*, in: *The Electronic Textbook of Hand Surgery*. URL: <http://www.eatonhand.com/nor/nor002.htm> (visited on 01/12/2018).
- [49] John M Hollerbach. *Workshop on the Design and Control of Dexterous Hands*. Tech. rep. Massachusetts Institute of Technology, Cambridge Artificial Intelligence Laboratory, 1982.
- [50] Frank C Park and Roger W Brockett. “Kinematic dexterity of robotic mechanisms”. In: *The International Journal of Robotics Research* 13.1 (1994), pp. 1–15.

- [51] Zexiang Li, JF Canny, and Shankar S Sastry. “On motion planning for dextrous manipulation”. In: *The problem formulation* (1989), pp. 775–80.
- [52] Antonio Bicchi and Alessia Marigo. “Dexterous grippers: Putting nonholonomy to work for fine manipulation”. In: *The International Journal of Robotics Research* 21.5-6 (2002), pp. 427–442.
- [53] Sing Bing Kang and Katsushi Ikeuchi. “Toward automatic robot instruction from perception-mapping human grasps to manipulator grasps”. In: *IEEE transactions on robotics and automation* 13.1 (1997), pp. 81–95.
- [54] Matthew T Mason and J Kenneth Salisbury Jr. “Robot hands and the mechanics of manipulation”. In: (1985).
- [55] G Morris and L Haynes. “Robotic assembly by constraints”. In: *Proceedings. 1987 IEEE International Conference on Robotics and Automation*. Vol. 4. IEEE. 1987, pp. 1507–1515.
- [56] Aaron Bloomfield, Yu Deng, Jeff Wampler, Pascale Rondot, Dina Harth, Mary McManus, and Norman Badler. “A taxonomy and comparison of haptic actions for disassembly tasks”. In: *IEEE Virtual Reality, 2003. Proceedings*. IEEE. 2003, pp. 225–231.
- [57] Domenico Prattichizzo and Jeffrey C Trinkle. “Grasping”. In: *Springer handbook of robotics*. Springer, 2016, pp. 955–988.
- [58] Landsmeer J.M.F. “Power grip and precision handling”. In: *Annals of the rheumatic diseases* 21.2 (1962), p. 164.
- [59] Noriko Kamakura, Michiko Matsuo, Harumi Ishii, Fumiko Mitsuboshi, and Yoriko Miura. “Patterns of static prehension in normal hands”. In: *The American journal of occupational therapy* 34.7 (1980), pp. 437–445.
- [60] Thea Iberall. “Human prehension and dexterous robot hands”. In: *The International Journal of Robotics Research* 16.3 (1997), pp. 285–299.
- [61] Thea Iberall. “Grasp Planning from Human Prehension.” In: *IJCAI*. Vol. 87. 1987. Citeseer. 1987, pp. 1153–1157.
- [62] Ian M Bullock, Joshua Z Zheng, Sara De La Rosa, Charlotte Guertler, and Aaron M Dollar. “Grasp frequency and usage in daily household and machine shop tasks”. In: *IEEE transactions on haptics* 6 (2013), pp. 296–308.
- [63] J Daniel Morrow and Pradeep K Khosla. “Manipulation task primitives for composing robot skills”. In: *Proceedings of International Conference on Robotics and Automation*. Vol. 4. IEEE. 1997, pp. 3354–3359.

- [64] Javier Felip, Janne Laaksonen, Antonio Morales, and Ville Kyrki. “Manipulation primitives: A paradigm for abstraction and execution of grasping and manipulation tasks”. In: *Robotics and Autonomous Systems* 61.3 (2013), pp. 283–296.
- [65] P Wright, James W Demmel, and Mark Nagurka. “The dexterity of manufacturing hands”. In: *Robotics Research, DSC* 14 (1989), pp. 157–163.
- [66] Thomas H Speeter. “Primitive based control of the Utah/MIT dextrous hand”. In: *Proceedings. 1991 IEEE International Conference on Robotics and Automation*. IEEE Computer Society. 1991, pp. 866–867.
- [67] Pierre Tournassoud, Tomas Lozano-Perez, and Emmanuel Mazer. “Regrasping”. In: *International Conf. Robotics and Automation*. IEEE. 1987, pp. 1924–1928.
- [68] Li Han and Jeffrey C Trinkle. “Dextrous manipulation by rolling and finger gaiting”. In: *Proceedings. 1998 IEEE International Conference on Robotics and Automation (Cat. No. 98CH36146)*. Vol. 1. IEEE. 1998, pp. 730–735.
- [69] Daniela Rus. “Dexterous rotations of polyhedra”. In: *Proceedings 1992 IEEE International Conference on Robotics and Automation*. IEEE Computer Society. 1992, pp. 2758–2759.
- [70] David L Brock. “Enhancing the dexterity of a robot hand using controlled slip”. In: *Proceedings. 1988 IEEE International Conference on Robotics and Automation*. IEEE. 1988, pp. 249–251.
- [71] Antonio Bicchi and Raffaele Sorrentino. “Dexterous manipulation through rolling”. In: *Proceedings of 1995 IEEE International Conference on Robotics and Automation*. Vol. 1. IEEE. 1995, pp. 452–457.
- [72] Fabian Heinemann, Steffen Puhlmann, Clemens Eppner, José Elvareiz-Ruiz, Marianne Maertens, and Oliver Brock. “A taxonomy of human grasping behavior suitable for transfer to robotic hands”. In: *2015 IEEE International Conference on Robotics and Automation (ICRA)*. IEEE. 2015, pp. 4286–4291.
- [73] David Paulius, Yongqiang Huang, Jason Meloncon, and Yu Sun. “Manipulation motion taxonomy and coding for robots”. In: *2019 IEEE/RSJ International Conference on Intelligent Robots and Systems (IROS)*. IEEE. 2019.
- [74] John M Elliott and KJ Connolly. “A classification of manipulative hand movements”. In: *Developmental Medicine & Child Neurology* 26.3 (1984), pp. 283–296.
- [75] Charlotte E Exner. “In-hand manipulation skills”. In: *Development of hand skills in the child* (1992), pp. 35–45.

- [76] Lael U Odhner, Raymond R Ma, and Aaron M Dollar. “Precision grasping and manipulation of small objects from flat surfaces using underactuated fingers”. In: *2012 IEEE International Conference on Robotics and Automation*. IEEE. 2012, pp. 2830–2835.
- [77] Joe Falco, Jeremy Marvel, and Elena Messina. *A roadmap to progress measurement science in robot dexterity and manipulation*. US Department of Commerce, National Institute of Standards and Technology, 2014.
- [78] Fabio Bonsignorio and Angel P. Del Pobil. “Toward Replicable and Measurable Robotics Research [From the Guest Editors]”. In: *IEEE Robotics and Automation Magazine* 22.3 (2015), pp. 32–35. ISSN: 10709932. DOI: 10.1109/MRA.2015.2452073.
- [79] Joe Falco and Elena Messina. “Performance Metrics and Test Methods for Robotic Hands”. In: *DRAFT NIST Special Publication 1227* October (2018), p. 65. DOI: 10.6028/NIST.SP.1227-draft. URL: <https://doi.org/10.6028/NIST.SP.1227-draft>.
- [80] Jeffrey Mahler, Rob Platt, Alberto Rodriguez, Matei Ciocarlie, Aaron Dollar, Renaud Detry, Maximo A. Roa, Holly Yanco, Adam Norton, Joe Falco, Karl Van Wyk, Elena Messina, Jurgen Juxi Leitner, Doug Morrison, Matt Mason, Oliver Brock, Lael Odhner, Andrey Kurenkov, Matthew Matl, and Ken Goldberg. “Guest Editorial Open Discussion of Robot Grasping Benchmarks, Protocols, and Metrics”. In: *IEEE Transactions on Automation Science and Engineering* 15.4 (2018), pp. 1440–1442. ISSN: 15455955. DOI: 10.1109/TASE.2018.2871354.
- [81] Berk Calli, Aaron Walsman, Arjun Singh, Siddhartha Srinivasa, Pieter Abbeel, and Aaron M Dollar. “Benchmarking in manipulation research: The YCB object and model set and benchmarking protocols”. In: *arXiv preprint arXiv:1502.03143* (2015).
- [82] Kayla Matheus and Aaron M Dollar. “Benchmarking grasping and manipulation: Properties of the objects of daily living”. In: *2010 IEEE/RSJ International Conference on Intelligent Robots and Systems*. IEEE. 2010, pp. 5020–5027.
- [83] Thomas Feix, Ian M Bullock, and Aaron M Dollar. “Analysis of human grasping behavior: Object characteristics and grasp type”. In: *IEEE transactions on haptics* 7.3 (2014), pp. 311–323.

- [84] Berk Calli, Arjun Singh, Aaron Walsman, Siddhartha Srinivasa, Pieter Abbeel, and Aaron M Dollar. “The ycb object and model set: Towards common benchmarks for manipulation research”. In: *2015 international conference on advanced robotics (ICAR)*. IEEE. 2015, pp. 510–517.
- [85] Jürgen Leitner, Adam W Tow, Niko Sünderhauf, Jake E Dean, Joseph W Durham, Matthew Cooper, Markus Eich, Christopher Lehnert, Ruben Mangels, Christopher McCool, et al. “The ACRV picking benchmark: A robotic shelf picking benchmark to foster reproducible research”. In: *2017 IEEE International Conference on Robotics and Automation (ICRA)*. IEEE. 2017, pp. 4705–4712.
- [86] Mauricio Matamoros, Caleb Rascon, Sven Wachsmuth, Alexander William Moriarty, Johannes Kummert, Justin Hart, Sammy Pfeiffer, Matthijs van der Brugh, and Maxime St-Pierre. *RoboCup@Home 2019: Rules and Regulations (draft)*. http://www.robocupathome.org/rules/2019_rulebook.pdf. 2019.
- [87] Clemens Eppner, Sebastian Höfer, Rico Jonschkowski, Roberto Martián-Martián, Arne Sieverling, Vincent Wall, and Oliver Brock. “Lessons from the amazon picking challenge: Four aspects of building robotic systems.” In: *Robotics: science and systems*. 2016.
- [88] Geng Gao, Gal Gorjup, Ruobing Yu, Patrick Jarvis, and Minas Liarokapis. “Modular, Accessible, Sensorized Objects for Evaluating the Grasping and Manipulation Capabilities of Grippers and Hands”. In: *IEEE Robotics and Automation Letters* 5.4 (2020), pp. 6105–6112.
- [89] Berk Calli, Aaron Walsman, Arjun Singh, Siddhartha Srinivasa, Pieter Abbeel, and Aaron M Dollar. “Benchmarking in manipulation research: Using the Yale-CMU-Berkeley object and model set”. In: *IEEE Robotics & Automation Magazine* 22.3 (2015), pp. 36–52.
- [90] Boling Yang, Patrick E Lancaster, Siddhartha S Srinivasa, and Joshua R Smith. “Benchmarking Robot Manipulation With the Rubik’s Cube”. In: *IEEE Robotics and Automation Letters* 5.2 (2020), pp. 2094–2099.
- [91] Nikolaus Correll, Kostas E Bekris, Dmitry Berenson, Oliver Brock, Albert Causo, Kris Hauser, Kei Okada, Alberto Rodriguez, Joseph M Romano, and Peter R Wurman. “Analysis and observations from the first amazon picking challenge”. In: *IEEE Transactions on Automation Science and Engineering* 15.1 (2016), pp. 172–188.

- [92] Nathan Koenig and Andrew Howard. “Design and use paradigms for gazebo, an open-source multi-robot simulator”. In: *2004 IEEE/RSJ International Conference on Intelligent Robots and Systems (IROS)(IEEE Cat. No. 04CH37566)*. Vol. 3. IEEE. 2004, pp. 2149–2154.
- [93] Marc G Bellemare, Yavar Naddaf, Joel Veness, and Michael Bowling. “The arcade learning environment: An evaluation platform for general agents”. In: *Journal of Artificial Intelligence Research* 47 (2013), pp. 253–279.
- [94] Greg Brockman, Vicki Cheung, Ludwig Pettersson, Jonas Schneider, John Schulman, Jie Tang, and Wojciech Zaremba. “Openai gym”. In: *arXiv preprint arXiv:1606.01540* (2016).
- [95] Wei Qian, Zeyang Xia, Jing Xiong, Yangzhou Gan, Yangchao Guo, Shaokui Weng, Hao Deng, Ying Hu, and Jianwei Zhang. “Manipulation task simulation using ROS and Gazebo”. In: *2014 IEEE International Conference on Robotics and Biomimetics, IEEE ROBIO 2014* (2014), pp. 2594–2598. DOI: 10.1109/ROBIO.2014.7090732.
- [96] Linxi Fan, Yuke Zhu, Jiren Zhu, Zihua Liu, Orien Zeng, Anchit Gupta, Joan Creus-Costa, Silvio Savarese, and Li Fei-Fei. “Surreal: Open-source reinforcement learning framework and robot manipulation benchmark”. In: *Conference on Robot Learning*. 2018, pp. 767–782.
- [97] Adithyavairavan Murali, Tao Chen, Kalyan Vasudev Alwala, Dhiraj Gandhi, Lerrel Pinto, Saurabh Gupta, and Abhinav Gupta. “PyRobot: An Open-source Robotics Framework for Research and Benchmarking”. In: (2019). eprint: 1906.08236. URL: <http://arxiv.org/abs/1906.08236>.
- [98] Michael Beetz, M Lorenz, and Moritz Tenorth. “CRAM — A Cognitive Robot Abstract Machine for Everyday Manipulation in Human Environments”. In: *Intelligent Robots and Systems* (2010), pp. 1012–1017.
- [99] Brian Yang, Dinesh Jayaraman, Jesse Zhang, and Sergey Levine. “REPLAB: A reproducible low-cost arm benchmark for robotic learning”. In: *Proceedings - IEEE International Conference on Robotics and Automation 2019-May* (2019), pp. 8691–8697. ISSN: 10504729. DOI: 10.1109/ICRA.2019.8794390.
- [100] Michael Ahn, Henry Zhu, Kristian Hartikainen, Hugo Ponte, Abhishek Gupta, Sergey Levine, and Vikash Kumar. “ROBEL: Robotics Benchmarks for Learning with Low-Cost Robots”. In: *CoRL 2019* (2019). arXiv: 1909.11639. URL: <http://arxiv.org/abs/1909.11639>.

- [101] Darpa. *DARPA Robotics Challenge Finals: Rules and Course - IEEE Spectrum*. Accessed: 2021-12-22. 2015.
- [102] Adam Jacoff and Elena Messina. “Urban search and rescue robot performance standards: Progress update”. In: *Unmanned Systems Technology IX*. Vol. 6561. International Society for Optics and Photonics. 2007, p. 65611L.
- [103] World Robot summit. “Real Space Rules & Regulations 2020”. In: (2021). URL: https://wrs.nedo.go.jp/wrs2020/challenge/download/Rules/DetailedRules%7B%5C_%7DPartner%7B%5C_%7DEN.pdf.
- [104] Darpa. “DARPA Robotics Challenge (DRC)”. In: <https://www.darpa.mil/program/darpa-robotics-challenge> (2020). Accessed: 2020-08-10.
- [105] NIST. “Robotic Hand Grasping and Manipulation”. In: <http://rhgm.org/activities/education/competition.html> (2020). Accessed: 2020-08-10.
- [106] NIST. “Robotic Grasping and Manipulation Competition @ IROS 2019”. In: https://rpal.cse.usf.edu/competition/{_}iros2019/ (2019). Accessed: 2020-08-10.
- [107] NIST. “IROS 2020 Grasping and Manipulation Competition: Manufacturing Track-Task Rules Background”. In: *url = https://www.nist.gov/el/intelligent-* (2020). Accessed: 2022-01-24.
- [108] Robocup. “RoboCup@Home – Where the best domestic service robots test themselves”. In: <https://athome.robocup.org/> (2020). Accessed: 2020-08-10.
- [109] Mauricio Matamoros, Caleb Rascon, Sven Wachsmuth, Alexander William Moriarty, Johannes Kummert, Justin Hart, Sammy Pfeiffer, Matthijs van der Brugh, and Maxime St-Pierre. *RoboCup@Home 2019: Rules and Regulations (draft)*. http://www.robocupathome.org/rules/2019_rulebook.pdf. Accessed: 2021-08-10. 2019.
- [110] World Robot summit. *Partner Robot Challenge (Real Space) | Service Robotics Category | World Robot Challenge | World Robot Summit*. URL: <https://wrs.nedo.go.jp/en/wrs2020/challenge/service/partner.html> (visited on 04/04/2022).

- [111] Carlos Hernández Corbato, Mukunda Bharatheesha, Jeff Van Egmond, Jihong Ju, and Martijn Wisse. “Integrating different levels of automation: Lessons from winning the amazon robotics challenge 2016”. In: *IEEE Transactions on Industrial Informatics* 14.11 (2018), pp. 4916–4926.
- [112] Yu Sun, Joe Falco, Máximo A Roa, and Berk Calli. “Research challenges and progress in robotic grasping and manipulation competitions”. In: *IEEE robotics and automation letters* 7.2 (2021), pp. 874–881.
- [113] Lafayette. “Dexterity Tests | Human Evaluation by Lafayette Instrument Company”. In: <https://lafayetteevaluation.com/listing/dexterity-tests> (2021). Accessed:2021-03-26.
- [114] Rehabmart. “Dexterity Test | Purdue Pegboard Test | Manual Dexterity | Fine Motor Skills”. In: https://www.rehabmart.com/category/manipulation/dexterity_tests.htm (2021). Accessed:2021-03-26.
- [115] Katie E Yancosek and Dana Howell. “A narrative review of dexterity assessments”. In: *Journal of Hand Therapy* 22.3 (2009), pp. 258–270.
- [116] Michael A Saliba, Alistaire Chetcuti, and Matthew J Farrugia. “Towards the rationalization of anthropomorphic robot hand design: Extracting knowledge from constrained human manual dexterity testing”. In: *International Journal of Humanoid Robotics* 10.02 (2013), p. 1350001.
- [117] Matthew J Farrugia and Michael A Saliba. “Optimisation of anthropomorphic robot hand design through human manual dexterity testing”. In: *VDI BERICHTE* 1956 (2006), p. 147.
- [118] Dorit H Aaron and Caroline W Stegink Jansen. “Development of the Functional Dexterity Test (FDT): construction, validity, reliability, and normative data”. In: *Journal of Hand Therapy* 16.1 (2003), pp. 12–21.
- [119] Lorrie A Buddenberg and Chris Davis. “Test–retest reliability of the Purdue Pegboard Test”. In: *American Journal of Occupational Therapy* 54.5 (2000), pp. 555–558.
- [120] Ying-Chih Wang, Rick Wickstrom, Sheng-Che Yen, Jay Kapellusch, and Kimberly A Grogan. “Assessing manual dexterity: Comparing the workability rate of manipulation test with the Minnesota manual dexterity test”. In: *Journal of Hand Therapy* 31.3 (2018), pp. 339–347.

- [121] William P Lundergan, Elizabeth J Soderstrom, and David W Chambers. “Tweezer dexterity aptitude of dental students”. In: *Journal of Dental Education* 71.8 (2007), pp. 1090–1097.
- [122] Ying-Chih Wang, Susan R Magasi, Richard W Bohannon, David B Reuben, Heather E McCreath, Deborah J Bubela, Richard C Gershon, and William Z Rymer. “Assessing dexterity function: a comparison of two alternatives for the NIH Toolbox”. In: *Journal of Hand Therapy* 24.4 (2011), pp. 313–321.
- [123] Wesley S Roeder. *Roeder Manipulative Aptitude Test*. Lafayette instrument, 1967.
- [124] Erman Çakıt, Behice Durgun, and Oya Cetik. “Assessing the relationship between hand dimensions and manual dexterity performance for Turkish dental students”. In: *Advances in physical ergonomics and human factors*. Springer, 2016, pp. 469–479.
- [125] George K Bennett. *Hand-tool dexterity test*. Psychological Corporation, 1965.
- [126] Keith L Doty, Claudio Melchiorri, Eric M Schwartz, and Claudio Bonivento. “Robot manipulability”. In: *IEEE Transactions on Robotics and Automation* 11.3 (1995), pp. 462–468.
- [127] Tsuneo Yoshikawa. “Manipulability of robotic mechanisms”. In: *The international journal of Robotics Research* 4.2 (1985), pp. 3–9.
- [128] Nikolaus Vahrenkamp, Tamim Asfour, Giorgio Metta, Giulio Sandini, and Rüdiger Dillmann. “Manipulability analysis”. In: *IEEE-RAS International Conference on Humanoid Robots* (2012), pp. 568–573. ISSN: 21640572. DOI: 10.1109/HUMANOIDS.2012.6651576.
- [129] Masaki Togai. “An application of the singular value decomposition to manipulability and sensitivity of industrial robots”. In: *Siam journal on algebraic discrete methods* 7.2 (1986), pp. 315–320.
- [130] Clément M Gosselin. “The optimum design of robotic manipulators using dexterity indices”. In: *Robotics and Autonomous systems* 9.4 (1992), pp. 213–226.
- [131] Jihong Lee. “Study on the manipulability measures for robot manipulators”. In: *IEEE International Conference on Intelligent Robots and Systems* 3 (1997), pp. 1458–1465.

- [132] Imed Mansouri and Mohammed Ouali. “The power manipulability A new homogeneous performance index of robot manipulators”. In: *Robotics and Computer-Integrated Manufacturing* 27.2 (2011), pp. 434–449. ISSN: 07365845. DOI: 10.1016/j.rcim.2010.09.004. URL: <http://dx.doi.org/10.1016/j.rcim.2010.09.004>.
- [133] Krishna C Gupta. “On the nature of robot workspace”. In: *The International journal of robotics research* 5.2 (1986), pp. 112–121.
- [134] Gianni Castelli, Erika Ottaviano, and Marco Ceccarelli. “A fairly general algorithm to evaluate workspace characteristics of serial and parallel manipulators”. In: *Mechanics based design of structures and machines* 36.1 (2008), pp. 14–33.
- [135] Jingzhou Yang, Karim Abdel-Malek, and Yunqing Zhang. “On the workspace boundary determination of serial manipulators with non-unilateral constraints”. In: *Robotics and Computer-Integrated Manufacturing* 24.1 (2008), pp. 60–76.
- [136] Richard E Stamper, Lung-Wen Tsai, and Gregory C Walsh. “Optimization of a three DOF translational platform for well-conditioned workspace”. In: *Proceedings of international conference on robotics and automation*. Vol. 4. IEEE. 1997, pp. 3250–3255.
- [137] Lisandro J Puglisi, Roque J Saltaren, Hector A Moreno, Pedro F Cárdenas, Cecilia Garcia, and Rafael Aracil. “Dimensional synthesis of a spherical parallel manipulator based on the evaluation of global performance indexes”. In: *Robotics and Autonomous Systems* 60.8 (2012), pp. 1037–1045.
- [138] Alok Kumar and Ken J Waldron. “The workspaces of a mechanical manipulator”. In: *Journal of Mechanical Design* 103.3 (1981), pp. 665–672.
- [139] Franziska Zacharias, Christoph Borst, and Gerd Hirzinger. “Capturing robot workspace structure: representing robot capabilities”. In: *2007 IEEE/RSJ International Conference on Intelligent Robots and Systems*. Ieee. 2007, pp. 3229–3236.
- [140] Joe Falco, Karl Van Wyk, and Elena Messina. “Performance metrics and test methods for robotic hands”. In: *NIST, Tech. Rep. DRAFT NIST Special Publication* 1227 (2018).
- [141] Valerio. Ortenzi, Marco Controzzi, Francesca Cini, Jurgen Leitner, Matteo Bianchi, Maximo A. Roa, and Peter Corke. “Robotic manipulation and the role of the task in the metric of success”. In: *Nature Machine Intelligence* 1.8 (2019), pp. 340–346. ISSN: 2522-5839. DOI: 10.1038/s42256-019-0078-4. URL: <http://dx.doi.org/10.1038/s42256-019-0078-4>.

- [142] Minas V Liarokapis and Aaron M Dollar. “Learning task-specific models for dexterous, in-hand manipulation with simple, adaptive robot hands”. In: *2016 IEEE/RSJ International Conference on Intelligent Robots and Systems (IROS)*. IEEE. 2016, pp. 2534–2541.
- [143] Lael U Odhner and Aaron M Dollar. “Stable, open-loop precision manipulation with underactuated hands”. In: *The International Journal of Robotics Research* 34.11 (2015), pp. 1347–1360.
- [144] IROS. “Different Approaches, the Same Goal: Autonomous Object Manipulation”. In: <https://manipulation-iros-workshop.github.io/> (2020). Accessed: 2020-08-10.
- [145] Nathan Elangovan, Geng Gao, Che-Ming Chang, and Minas Liarokapis. “A Modular, Accessible, Affordable Dexterity Test for Evaluating the Grasping and Manipulation Capabilities of Robotic Grippers and Hands”. In: *2020 IEEE International Symposium on Safety, Security, and Rescue Robotics (SSRR)*. IEEE. 2020, pp. 304–310.
- [146] Nathan Elangovan, Che-Ming Chang, Geng Gao, and Minas Liarokapis. “An accessible, open-source dexterity test: Evaluating the grasping and dexterous manipulation capabilities of humans and robots”. In: *Frontiers*, 2022, p. 53.
- [147] Victor Gonzalez, Jennifer Rowson, and Alaster Yoxall. “Development of the variable dexterity test: Construction, reliability and validity”. In: *International journal of therapy and rehabilitation* 22.4 (2015), pp. 174–180.
- [148] Gaurav Saraf and Dhananjay Singh Bisht. “Novel Dexterity Kit Concept Based on a Review of Hand Dexterity Literature”. In: *Innovative Product Design and Intelligent Manufacturing Systems* (2020), pp. 81–89.
- [149] L Noël, M-C Blancher, J-P Kempf, A Bodin, S Facca, H Khalifa-Dubert, and P Liverneaux. “The “peg test”: a novel technique for dexterity evaluation in hand immobilized with a splint”. In: *Chirurgie de la main* 30.6 (2011), pp. 385–392.
- [150] Nadine Wilson, Emma Hough, Anita Hamilton, Michele Verdonck, and Ross Clark. “Development and test-retest reliability assessment of a low-cost, 3D printed tool for assessing different aspects of hand dexterity”. In: *Journal of Hand Therapy* (2021).
- [151] Amazon Robotics Challenge. “Amazon robotics challenge 2016”. In: <https://www.amazonrobotics.com/> (2016). Accessed: 2020-01-24.

- [152] NIST. “IROS 2020 Grasping and Manipulation Competition: Manufacturing Track”. In: <https://www.nist.gov/el/intelligent-systems-division-73500/iros-2020-robotic-grasping-and-manipulation-competition> (2020). Accessed: 2022-01-24.
- [153] Peter F Edemekong, Deb L Bomgaars, and Shoshana B Levy. “Activities of daily living (ADLs)”. In: (2017).
- [154] Nadina B Lincoln and John RF Gladman. “The extended activities of daily living scale: a further validation”. In: *Disability and rehabilitation* (1992).
- [155] Redwan Alqasemi, Sebastian Mahler, and Rajiv Dubey. “Design and construction of a robotic gripper for activities of daily living for people with disabilities”. In: *2007 IEEE 10th International Conference on Rehabilitation Robotics*. IEEE. 2007, pp. 432–437.
- [156] Dae-Jin Kim, Ryan Lovelett, and Aman Behal. “An empirical study with simulated ADL tasks using a vision-guided assistive robot arm”. In: *2009 IEEE International Conference on Rehabilitation Robotics*. IEEE. 2009, pp. 504–509.
- [157] Thomas Rühr, Jürgen Sturm, Dejan Pangercic, Michael Beetz, and Daniel Cremers. “A generalized framework for opening doors and drawers in kitchen environments”. In: *2012 IEEE International Conference on Robotics and Automation*. IEEE. 2012, pp. 3852–3858.
- [158] Kimitoshi Yamazaki, Yoshiaki Watanabe, Kotaro Nagahama, Kei Okada, and Masayuki Inaba. “Recognition and manipulation integration for a daily assistive robot working on kitchen environments”. In: *2010 IEEE international conference on robotics and biomimetics*. IEEE. 2010, pp. 196–201.
- [159] Laura Petrich, Jun Jin, Masood Dehghan, and Martin Jagersand. “A Quantitative Analysis of Activities of Daily Living: Insights into Improving Functional Independence with Assistive Robotics”. In: *arXiv* (2021).
- [160] Moritz Tenorth, Jan Bandouch, and Michael Beetz. “The TUM kitchen data set of everyday manipulation activities for motion tracking and action recognition”. In: *2009 IEEE 12th International Conference on Computer Vision Workshops, ICCV Workshops*. IEEE. 2009, pp. 1089–1096.
- [161] Sebastian Stein and Stephen J McKenna. “Combining embedded accelerometers with computer vision for recognizing food preparation activities”. In: *Proceedings of the 2013 ACM international joint conference on Pervasive and ubiquitous computing*. 2013, pp. 729–738.

- [162] Alireza Fathi, Yin Li, and James M Rehg. “Learning to recognize daily actions using gaze”. In: *European Conference on Computer Vision*. Springer. 2012, pp. 314–327.
- [163] Nathan Elangovan, che-ming Chang, Ricardo V. Godoy, Felipe Sanches, Ke Wang, Patrick Jarvis, and Minas Liarokapis. “Comparing Human and Robot Performance in the Execution of Kitchen Tasks: Evaluating Grasping and Dexterous Manipulation Skills”. In: *2022 IEEE-RAS International Conference on Humanoid Robots (Humanoids), IEEE, Okinawa, Japan, 2022*. IEEE. Okinawa, Japan, 2022.
- [164] Anil K Jain and Richard C Dubes. *Algorithms for clustering data*. Prentice-Hall, Inc., 1988.
- [165] John T Hancock and Taghi M Khoshgoftaar. “Survey on categorical data for neural networks”. In: *Journal of Big Data* 7.1 (2020), pp. 1–41.
- [166] Laurens Van der Maaten and Geoffrey Hinton. “Visualizing data using t-SNE.” In: *Journal of machine learning research* 9.11 (2008).
- [167] Gordana Ivosev, Lyle Burton, and Ron Bonner. “Dimensionality reduction and visualization in principal component analysis”. In: *Analytical chemistry* 80.13 (2008), pp. 4933–4944.
- [168] Aristidis Likas, Nikos Vlassis, and Jakob J Verbeek. “The global k-means clustering algorithm”. In: *Pattern recognition* 36.2 (2003), pp. 451–461.
- [169] Trupti M Kodinariya and Prashant R Makwana. “Review on determining number of Cluster in K-Means Clustering”. In: *International Journal* 1.6 (2013), pp. 90–95.
- [170] Martin Ester, Hans-Peter Kriegel, Jörg Sander, Xiaowei Xu, et al. “A density-based algorithm for discovering clusters in large spatial databases with noise.” In: *kdd*. Vol. 96. 34. 1996, pp. 226–231.
- [171] Erich Schubert, Jörg Sander, Martin Ester, Hans Peter Kriegel, and Xiaowei Xu. “DBSCAN revisited, revisited: why and how you should (still) use DBSCAN”. In: *ACM Transactions on Database Systems (TODS)* 42.3 (2017), pp. 1–21.
- [172] David L Davies and Donald W Bouldin. “A cluster separation measure”. In: *IEEE transactions on pattern analysis and machine intelligence* 2 (1979), pp. 224–227.

- [173] Peter J Rousseeuw. “Silhouettes: a graphical aid to the interpretation and validation of cluster analysis”. In: *Journal of computational and applied mathematics* 20 (1987), pp. 53–65.
- [174] Tadeusz Caliński and Jerzy Harabasz. “A dendrite method for cluster analysis”. In: *Communications in Statistics-theory and Methods* 3.1 (1974), pp. 1–27.
- [175] Raphael Deimel and Oliver Brock. “A novel type of compliant and underactuated robotic hand for dexterous grasping”. In: *The International Journal of Robotics Research* 35.1-3 (2016), pp. 161–185.
- [176] Daniel M Aukes, Barrett Heyneman, John Ulmen, Hannah Stuart, Mark R Cutkosky, Susan Kim, Pablo Garcia, and Aaron Edsinger. “Design and testing of a selectively compliant underactuated hand”. In: *The International Journal of Robotics Research* 33.5 (2014), pp. 721–735.
- [177] Minas Liarokapis and Aaron M Dollar. “Deriving dexterous, in-hand manipulation primitives for adaptive robot hands”. In: *2017 IEEE/RSJ International Conference on Intelligent Robots and Systems (IROS)*. IEEE. 2017, pp. 1951–1958.
- [178] Agisilaos G Zisimatos, Minas V Liarokapis, Christoforos I Mavrogiannis, and Kostas J Kyriakopoulos. “Open-source, affordable, modular, light-weight, underactuated robot hands”. In: *Intelligent Robots and Systems (IROS 2014), 2014 IEEE/RSJ International Conference on*. IEEE. 2014, pp. 3207–3212.
- [179] George P Kontoudis, Minas V Liarokapis, Agisilaos G Zisimatos, Christoforos I Mavrogiannis, and Kostas J Kyriakopoulos. “Open-source, anthropomorphic, underactuated robot hands with a selectively lockable differential mechanism: Towards affordable prostheses”. In: *2015 IEEE/RSJ International Conference on Intelligent Robots and Systems (IROS)*. IEEE. 2015, pp. 5857–5862.
- [180] Aaron M Dollar and Robert D Howe. “The SDM hand as a prosthetic terminal device: a feasibility study”. In: *2007 IEEE 10th International Conference on Rehabilitation Robotics*. IEEE. 2007, pp. 978–983.
- [181] Mahmoud Tavakoli and Aníbal T de Almeida. “Adaptive under-actuated anthropomorphic hand: ISR-SoftHand”. In: *2014 IEEE/RSJ International Conference on Intelligent Robots and Systems*. IEEE. 2014, pp. 1629–1634.
- [182] Lionel Birglen and Clément M. Gosselin. “Kinetostatic analysis of underactuated fingers”. In: *IEEE Transactions on Robotics and Automation* 20.2 (2004), pp. 211–221.

- [183] Hamed Khakpour and Lionel Birglen. “Numerical analysis of the grasp configuration of a planar 3-DOF linkage-driven underactuated finger”. In: *Journal of Computational and Nonlinear Dynamics* 8.2 (2013), p. 021010.
- [184] Lionel Birglen, Thierry Laliberté, and Clément M Gosselin. *Underactuated Robotic Hands*. Vol. 40. Springer Science & Business Media, 2008.
- [185] Mathieu Baril, Thierry Laliberté, Clément Gosselin, and François Routhier. “On the Design of Mechanically Programmable Underactuated Anthropomorphic Robotic and Prosthetic Grippers”. In: *Volume 4: 36th Mechanisms and Robotics Conference, Parts A and B* 135. December 2013 (2012), p. 85.
- [186] Dalibor Petković, Nenad D. Pavlović, Žarko Čojbašić, and Nenad T. Pavlović. “Adaptive neuro fuzzy estimation of underactuated robotic gripper contact forces”. In: *Expert Systems with Applications* 40.1 (2013), pp. 281–286.
- [187] Kamal Mohy El Dine, Jose Sanchez, Juan Antonio Corrales Ramón, Youcef Mezouar, and Jean-Christophe Fauroux. “Force-Torque Sensor Disturbance Observer using Deep Learning”. In: 2018.
- [188] Matei Ciocarlie and Peter Allen. “Data-driven Optimization for Underactuated Robotic Hands”. In: *International Conference on Robotics and Automation*. 2010, pp. 1292–1298.
- [189] Cosimo Della Santina, Cristina Piazza, Giorgio Grioli, Manuel G Catalano, and Antonio Bicchi. “Toward dexterous manipulation with augmented adaptive synergies: The pisa/iit soffhand 2”. In: *IEEE Transactions on Robotics* 34.5 (2018), pp. 1141–1156.
- [190] Cosimo Della Santina, Cristina Piazza, Gaspare Santaera, Giorgio Grioli, Manuel Catalano, and Antonio Bicchi. “Estimating contact forces from postural measures in a class of under-actuated robotic hands”. In: *2017 IEEE/RSJ International Conference on Intelligent Robots and Systems (IROS)*. IEEE. 2017, pp. 2456–2463.
- [191] *How the i-limb works | Touch Bionics*. URL: <http://touchbionics.com/products/how-i-limb-works> (visited on 02/27/2019).
- [192] Nathan Elangovan, Anany Dwivedi, Lucas Gerez, Che-Ming Chang, and Minas Liarokapis. “Employing IMU and ArUco marker based tracking to decode the contact forces exerted by adaptive hands”. In: *2019 IEEE-RAS 19th International Conference on Humanoid Robots (Humanoids)*. IEEE. 2019, pp. 525–530.

- [193] Vladimir N. Vapnik. *The Nature of Statistical Learning Theory*. Berlin, Heidelberg: Springer-Verlag, 1995. ISBN: 0-387-94559-8.
- [194] Tin Kam Ho. “Random decision forests”. In: *Proceedings of the third international conference on Document analysis and recognition*. Vol. 1. 1995, pp. 278–282.
- [195] Leo Breiman. “Random forests”. In: *Machine learning, Springer* 45.1 (2001), pp. 5–32.
- [196] Matei Ciocarlie, Fernando Mier Hicks, and Scott Stanford. “Kinetic and dimensional optimization for a tendon-driven gripper”. In: *2013 IEEE International Conference on Robotics and Automation*. IEEE. 2013, pp. 2751–2758.
- [197] Raymond R Ma, Adam Spiers, and Aaron M Dollar. “M 2 Gripper: Extending the Dexterity of a Simple, Underactuated Gripper”. In: *Advances in reconfigurable mechanisms and robots II*. Springer, 2016, pp. 795–805.
- [198] Raymond Ma and Aaron Dollar. “Yale openhand project: Optimizing open-source hand designs for ease of fabrication and adoption”. In: *IEEE Robotics & Automation Magazine* 24.1 (2017), pp. 32–40.
- [199] Woojin Chung, Changju Rhee, Youngbo Shim, Hyungjin Lee, and Shinsuk Park. “Door-opening control of a service robot using the multifingered robot hand”. In: *IEEE Transactions on Industrial Electronics* 56.10 (2009), pp. 3975–3984.
- [200] Federico Vicentini, Nicola Pedrocchi, Manuel Beschi, Matteo Giussani, Nicolò Iannacci, Paolo Magnoni, Stefania Pellegrinelli, Loris Roveda, Enrico Villagrossi, Mehrnoosh Askarpour, et al. “PIROS: Cooperative, safe and reconfigurable robotic companion for cnc pallets load/unload stations”. In: *Bringing Innovative Robotic Technologies from Research Labs to Industrial End-users*. Springer, 2020, pp. 57–96.
- [201] Jefferson Coelho, Justus Piater, and Roderic Grupen. “Developing haptic and visual perceptual categories for reaching and grasping with a humanoid robot”. In: *Robotics and Autonomous Systems* 37.2-3 (2001), pp. 195–218.
- [202] R Garcíea-Rodriéguez, M Villalva-Lucio, and V Parra-Vega. “Dexterous Dynamic Optimal Grasping of a Circular Object subject to Gravity with Soft-fingertips”. In: *IFAC-PapersOnLine* 48.19 (2015), pp. 220–225.

- [203] Asad Ali Shahid, Loris Roveda, Dario Piga, and Francesco Braghin. “Learning Continuous Control Actions for Robotic Grasping with Reinforcement Learning”. In: *2020 IEEE International Conference on Systems, Man, and Cybernetics (SMC)*. IEEE. 2020, pp. 4066–4072.
- [204] Matei Ciocarlie and Peter Allen. “Data-driven optimization for underactuated robotic hands”. In: *2010 IEEE International Conference on Robotics and Automation*. IEEE. 2010, pp. 1292–1299.
- [205] R. Cabas, L. M. Cabas, and C. Balaguer. “Optimized design of the underactuated robotic hand”. In: *Proceedings 2006 IEEE International Conference on Robotics and Automation, 2006. ICRA 2006*. 2006, pp. 982–987.
- [206] R Saravanan, S Ramabalan, N Godwin Raja Ebenezer, and C Dharmaraja. “Evolutionary multi criteria design optimization of robot grippers”. In: *Applied Soft Computing* 9.1 (2009), pp. 159–172.
- [207] R Venkata Rao and Gajanan Waghmare. “Design optimization of robot grippers using teaching-learning-based optimization algorithm”. In: *Advanced Robotics* 29.6 (2015), pp. 431–447.
- [208] Huixu Dong, Ehsan Asadi, Chen Qiu, Jiansheng Dai, and I-Ming Chen. “Geometric design optimization of an under-actuated tendon-driven robotic gripper”. In: *Robotics and Computer-Integrated Manufacturing* 50 (2018), pp. 80–89.
- [209] Rituparna Datta, Shikhar Pradhan, and Bishakh Bhattacharya. “Analysis and design optimization of a robotic gripper using multiobjective genetic algorithm”. In: *IEEE Transactions on Systems, Man, and Cybernetics: Systems* 46.1 (2015), pp. 16–26.
- [210] Aaron M Dollar and Robert D Howe. “Joint coupling design of underactuated hands for unstructured environments”. In: *The International Journal of Robotics Research* 30.9 (2011), pp. 1157–1169.
- [211] Christine L MacKenzie and Thea Iberall. *The grasping hand*. Elsevier, 1994.
- [212] Won Suk You, Young Hun Lee, Gitae Kang, Hyun Seok Oh, Joon Kyue Seo, and Hyouk Ryeol Choi. “Kinematic design optimization for anthropomorphic robot hand based on interactivity of fingers”. In: *Intelligent Service Robotics* 12.2 (2019), pp. 197–208.
- [213] Raymond R Ma and Aaron M Dollar. “Linkage-based analysis and optimization of an underactuated planar manipulator for in-hand manipulation”. In: *Journal of Mechanisms and Robotics* 6.1 (2014).

- [214] Michael T Leddy and Aaron M Dollar. “Stability Optimization of Two-Fingered Anthropomorphic Hands for Precision Grasping with a Single Actuator”. In: *2019 International Conference on Robotics and Automation (ICRA)*. IEEE. 2019, pp. 451–457.
- [215] Walter G Bircher and Aaron M Dollar. “Design principles and optimization of a planar underactuated hand for caging grasps”. In: *2019 International Conference on Robotics and Automation (ICRA)*. IEEE. 2019, pp. 1608–1613.
- [216] Nathan Elangovan, Lucas Gerez, Geng Gao, and Minas Liarokapis. “Improving Robotic Manipulation Without Sacrificing Grasping Efficiency: A Multi-Modal, Adaptive Gripper With Reconfigurable Finger Bases”. In: *IEEE Access* 9 (2021), pp. 83298–83308.
- [217] Peter I Corke. “A robotics toolbox for MATLAB”. In: *IEEE Robotics & Automation Magazine* 3.1 (1996), pp. 24–32.
- [218] Herbert Edelsbrunner and Ernst P Mücke. “Three-dimensional alpha shapes”. In: *ACM Transactions on Graphics (TOG)* 13.1 (1994), pp. 43–72.